IMMUNE FINGERPRINTING IN ACUTE SEVERE SEPSIS

Matthew Philip Govier Morgan

Thesis presented for the degree of

Doctor of Philosophy

December 2014

Institute of Infection and Immunity

Cardiff University

Dedication

I dedicate this work to my wife Alison and my parents Carole and Jef. They have been a constant source of support, encouragement, and inspiration not only in writing this thesis, but also throughout my life. Thank you mum, dad and my love. To my two daughters, Evie and Amelia, thanks for reminding me of what is important in life when I had forgotten and for colouring in all over my paperwork.

Acknowledgements

I would like to thank my supervisors, Dr Matthias Eberl and Professor Judith Hall, for their support, encouragement, and guidance throughout my study. I am also extremely grateful to Professor Bernhard Moser and Dr Tamas Szakmany who were a constant source of advice and knowledge.

I would like to thank Dr Ann Kift-Morgan for her expert help with cytokine analysis and Dr Martin Davey for his technical expertise and guidance. I am grateful to everyone in the Cardiff Institute of Infection & Immunity who have helped me with this work.

Many thanks to Cardiff University's biostatisticians Dr Robert Hills and Dr Anthony Wilkes for their invaluable guidance in planning and assisting with the statistical analysis of these data. I am also very grateful to Dr Peter Morgan from the Cardiff Business School for his help in the production and interpretation of the neural network and decision tree models.

I would like to thank the external examiners, Prof Mervyn Singer and Prof Derek Doherty, and the Chair of my viva voce**,** Prof Nicholas Topley for their valuable comments that have improved this work in many ways.

Finally, I appreciate the invaluable contributions of the intensive care community including doctors, nurses, database managers, and most importantly, patients. Without the selfless generosity shown by both healthy volunteers and patients, this study would simply not have been possible.

Summary

Sepsis kills more people than car accidents, breast cancer, and bowel cancer combined. The key areas integral for ensuring improvements in the care of sepsis patients include improved risk stratification, better microorganism identification techniques, and a reduction in the burden of second-hit nosocomial infections. This work addresses each of these key areas in turn, with the ultimate aim of improving patient care through applied translation research.

Firstly, this work will combine small-scale yet complex immunological data with new statistical modelling techniques to form a new approach to microbe identification based on “immune fingerprints”. This new approach will allow discrimination between Gram-positive and Gram-negative infecting organisms using a small set of immune markers suitable for development into point-of-care technology. These immune fingerprints will also be used to improve the diagnosis of sepsis and provide risk stratification models.

Secondly, this thesis will offer new insights into immunosuppression that may impact upon current and future clinical trials. Specifically, it will suggest that aminobisphosphonates may help in the treatment of sepsis related-immunosuppression and that sepsis neutrophils gain the ability to act as antigen presenting cells.

Publications and presentations

Publications

2014

Eberl, M., Friberg, I. M., Liuzzi, A. R., Morgan, M. P. & Topley, N. Pathogen-Specific Immune Fingerprints during Acute Infection: The Diagnostic Potential of Human γδ T cells. *Frontiers in Immunology* **5,** 572 (2014).

Davey, M., **Morgan M. P**., Liuzzi A. R., Tyler C. J., Khan A. W. M., Szakmany T., Hall J. E., Moser B., and Eberl M. Microbe-specific unconventional T cells induce human neutrophil differentiation into antigen cross-presenting cells. *The Journal of Immunology* **193**, 3704–3716 (2014).

2013

Welton J., Morgan M. P., Martí S., Stone M. D., Moser B., Sewell A. K., Turton J., and Eberl, M. Monocytes and γδ T cells control the acute-phase response to intravenous Zoledronate: Insights from a phase IV safety trial. *J Bone Miner Res* **28**, 464–471 (2013).

2012

Wise, M. P., Morgan, M. P. & Saayman, A. G. Duration of antibiotic therapy in bacteraemia. *Crit Care* **16**, 403 (2012).

Oral presentations

2014

The Annual γδ T cell meeting, University of Chicago, USA.

UK Critical Care Research Forum annual meeting, Cardiff, UK.

2013

Intensive Care National Audit and Research Centre Annual Meeting, London, UK.

Intensive Care Society State of the Art Meeting, London, UK.

2012

Intensive Care Society State of the Art Meeting, London, UK.

Poster presentations

2012

"The role of γδ T cells in sepsis", International γδ T cell Meeting, Freiberg, Germany.

Prizes

2013 Intensive Care Society free research paper winner, UK.

2012 Welsh Intensive Care Society research prize-winner, UK.

2012 Microbiology and Infection Translational Research Group prizewinner, UK.

2012 Welsh Intensivists in Training research prizewinner, UK.

2011 Welsh Intensive Care Society Travel Scholarship winner, UK.

Public engagement work

Professional delegate representative at the World Sepsis Day Government Reception, House of Commons, London, UK, 2012, 2013 and 2014.

List of abbreviations

APACHE	Acute Physiology And Chronic Health Evaluation
APC	Antigen Presenting Cell
AUC	Area Under The Receiver Operating Characteristic Curve
BAL	Bronchoalveolar Lavage
BMI	Body Mass Index
BPM	Beats Per Minute
BTN3	Butyrophilin 3
CAP	Community-Acquired Pneumonia
CARS	Compensatory Anti-Inflammatory Response Syndrome
CI	Confidence Interval
CM	Central memory
CMV	Cytomegalovirus
CRP	C-Reactive Protein
CVP	Central Venous Pressure
DAMPs	Danger-Associated Molecular Patterns
ECA	Anti-Enterobacteriaceae Common Antigen Monoclonal Antibody
EDTA	Ethylenediaminetetraacetic Acid
ELISA	Enzyme-Linked Immunosorbent Assay
EM	Effector memory
EM-RA	Effector memory RA
ESBL	Extended spectrum beta-lactamases
FACS	Fluorescence-Activated Cell Sorting
FDA	Food And Drug Administration
FLT-3L	FMS-like tyrosine kinase 3 ligand
FSA	Forward Scatter Area
FSH	Forward Scatter Height
GM-CSF	Granulocyte‑macrophage colony‑stimulating factor

HA-1A	Anti-endotoxin Monoclonal Antibody
HMB-PP	(E)-4-Hydroxy-3-Methylbut-2-Enyl Pyrophosphate
ICU	Intensive Care Unit
IL	Interleukin
LPS	Lipopolysaccharide
Lumazine	6,7-Dimethyl-8-D-Ribityllumazine
MACS	Magnetic-Activated Cell Sorting
MAIT	Mucosal-Associated Invariant T
MALDI-TOF	Matrix Assisted Laser Desorption/Ionization
MAP	Mean Arterial Blood Pressure
MFI	Mean Fluorescence Intensity
MHC	Major Histocompatibility Complex
MRSA	Methicillin Resistant Staphylococcus Aureus
MyD88	Myeloid differentiation primary response gene 88
NET	Neutrophil extracellular trap
NFκB	Nuclear factor kappa-light-chain-enhancer of activated B cells
NHS	National Health Service
NICE	The National Institute For Health And Care Excellence
NKT	Natural Killer T
PAMP	Pathogen-Associated Molecular Patterns
PBMC	Peripheral Blood Mononucleated Cell
PBS	Phosphate Buffered Saline
PCR	Polymerase Chain Reaction
PCT	Procalcitonin
PD1	Programmed Cell Death Protein 1
PDL-1	Programmed Death-Ligand 1
PMA	Phorbol Myristate Acetate
PMH	Past Medical History
proADM	Proadrenomedullin
PRR	Host Pathogen Recognition Receptors

ROC	Receiver Operator Curve
ROS	Reactive Oxygen Species
SBP	Systolic Blood Pressure
$ScvO_2$	Central Venous Oxygen Saturation
SD	Standard Deviation
SE	Standard Error
SEM	Standard Error Of The Mean
sensePCT	Kryptor Procalcitonin
SIRS	Systemic Inflammatory Response Syndrome
SNNS	Stuttgart Neural Network Simulator
SOFA	Sequential Organ Failure Assessment
SSC	Surviving Sepsis Campaign
TLR	Toll-Like Receptor
Treg	Regulatory T cells
TRIF	TIR-domain-containing adapter-inducing interferon-β
UK	United Kingdom
VAP	Ventilator-Associated Pneumonia
VRE	Vancomycin Resistant Enterococcus Species
VSE	Vancomycin Sensitive Enterococcus Species

Table of contents

List of figures

List of tables

CHAPTER 1

INTRODUCTION

Chapter 1 Introduction

1.1. Clinical sepsis

Measured using any chosen metric, sepsis is a devastating condition for patients, their families, and society. Responsible for more deaths than breast cancer and traffic accidents combined, sepsis kills over 39,000 people a year in the United Kingdom alone[1,2]. Globally it accounts for 60-80% of all deaths, killing over 6 million children every year in the developing world[1,3]. As a medical condition, it is more deathly than a stroke, killing a third of all patients with the severe form of the illness[3,4]. It is responsible for a third of admissions to the intensive care unit (ICU) and costs the economy of the United States $17 billion pounds annually[4-6]. For patients that do survive, many will carry a substantial burden of continued physical and psychological ill health, with return to work rates of less than 65%[5-7]. Despite these facts, historically both public and professional knowledge of this condition has been poor. This has been accompanied by low rates of proportional research funding and low prioritisation of associated research outputs. Thankfully, partially due to the work of the Global Sepsis Alliance, these shortcomings are changing. The start of this research project coincided with the launch of the first World Sepsis Day in 2011. Three years later, the political situation in the United Kingdom has changed dramatically with the development of guidelines from The National Institute for Health and Care Excellence (NICE) in progress, new data capture across the National Health Service (NHS) and the formation of an all-party parliamentary group to champion the cause. This thesis will help address the other essential component needed to realise improvements in sepsis care; quality, applied, translational scientific research.

1.1.1. Definitions

The first formal definition of sepsis resulted from a meeting of an international consensus panel in 1992 held in Chicago[7-9]. This concluded that sepsis was a systemic inflammatory response (SIRS) to infection with severe sepsis being present where there was associated organ dysfunction and septic shock, defined as the presence of hypotension refectory to adequate fluid resuscitation. The two subsequent updates in 2003 and 2012 provided more detail on the definitions of SIRS, expanded its criteria significantly, and asserted that the suspicion of infection alone was sufficient to make

the initial diagnosis[8-10]. The most recent 2012 definition of sepsis from the Surviving Sepsis Campaign (SSC) is:

"the presence (probable or documented) of infection together with systemic manifestations of infection. Severe sepsis is defined as sepsis plus sepsis-induced organ dysfunction or tissue hypoperfusion".

Whilst the broadening of the entry criteria in the 2012 SSC guidelines may be beneficial for patient care, it does pose a challenge for the research community in ensuring consistency across patient populations. Many patients fulfilling the SIRS criteria with a suspicion of infection will subsequently have negative diagnostic tests for infectious organisms[10,11]. This will leave the classification of this patient in a state of flux for research interpretation purposes.

1.1.2. Causes

In the developed world, respiratory infection is responsible for over half of all cases of sepsis. The majority of the remaining infections are due to intra-abdominal pathology or urinary tract infections. In the developing world, although respiratory illness still predominates the aetiological factors, it plays a less substantial role compared to the alternative pathologies (Figure 1.1).

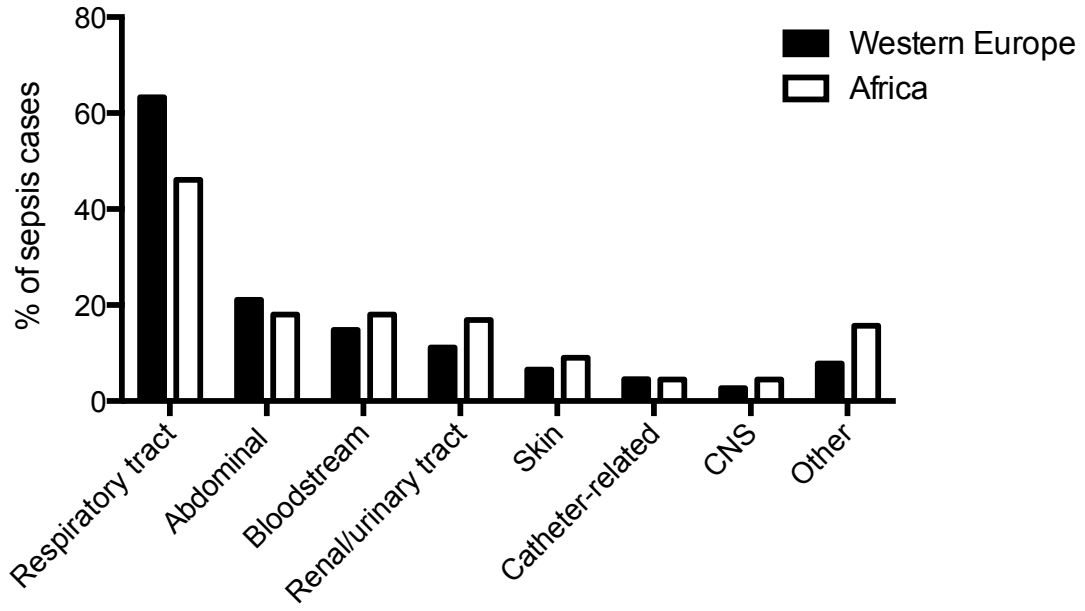

Figure 1.1 Sources of sepsis in patients from Western Europe and Africa. Shown above are the proportions of different sources of sepsis in patients in both Western Europe and Africa. Data are not mutually exclusive and therefore total percentages may be greater than 100%. These data have been adapted from [11].

Although fungal and viral infections are also causative factors in many sepsis deaths, bacterial pathogens predominate. *Staphylococcus aureus* and *Streptococcus pneumonia* are the common Gram-positive species considered causative with *Escherichia coli*, *Klebsiella* species, and *Pseudomonas aeruginosa* dominating the Gram-negative group[4,11]. This pattern is shown in Figure 1.2. There is debate regarding the relative contribution by each of these different organism types. One large multicentre study found a predominance of Gram-positive infections causing sepsis[4,11] whilst the more recent large epidemiological study looking at intensive care patients found 62% of patients to have Gram-negative infections compared with only 47% with Gram-positive infections[a 11]. This balance is likely to be heavily influenced by local population characteristics, organism virulence factors, and other health care structure variables in the studied region.

[a] This total is greater than 100% due to mixed infections.

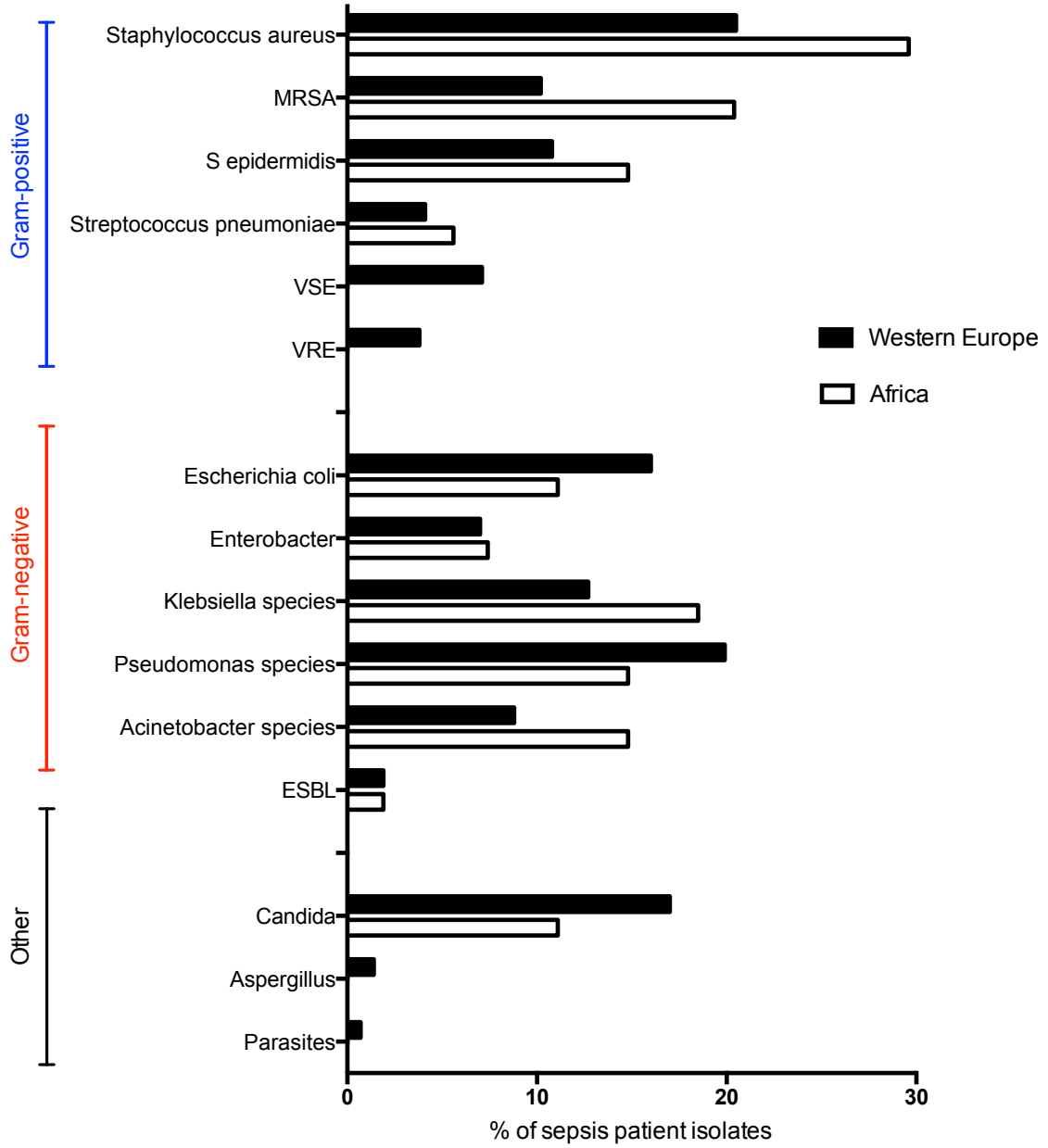

Figure 1.2 Causative organisms in sepsis patients in Western Europe and Africa. Shown above are the proportions of different causative organisms in sepsis patients in both Western Europe and Africa divided by Gram status. Data are not mutually exclusive and therefore total percentages may be greater than 100%. These data have been adapted from[11,12]. MRSA, Methicillin-resistant *Staphylococcus aureus*; VSE, vancomycin sensitive Enterococcus; VRE, vancomycin resistant Enterococcus; ESBL, extended spectrum beta-lactamases.

1.1.3. Treatments

Following the association between TNF-α levels and the pathogenesis of sepsis in the 1980s[12], the pharmaceutical industry has invested heavily in a range of immunotherapy agents targeted at treatments for sepsis patients. Most of these agents have been directed towards three main areas of pathophysiology: dysregulated coagulation, host responses (including complement and proinflammatory activation) and mechanisms of microbial

virulence (pathogen-associated molecular patterns (PAMPs) and host pathogen recognition receptors (PRRs)). The most high profile of these drugs was activated protein C (Xigris), initially approved for use by the Food and Drug Administration (FDA) in 2001 based on the results of the PROWESS trial[13,14]. Although initially heavily endorsed by the 2003 SSC guidelines through close industry links[13,15], a subsequent negative trial[15,16] led the intensive care community to reappraise the use of this therapy. This process eventually led to the withdrawal of Xigris by the FDA amid much public criticism of the initial process that had led to its widespread adoption[16,17]. Sadly, this picture of initial hope in a new therapeutic intervention followed by negative clinical trials has plagued the field of sepsis therapy. Table 1.1 details many such treatments that have now been shown to be ineffective. Whilst there remain some therapies under investigation, the tenants of modern sepsis treatment rely upon three simple yet considered (by international guidelines) effective interventions: antibiotic use, source control, and supportive critical care.

Table 1.1 Interventions used to treat sepsis classified by their currently known efficacy.

Treatments shown to be ineffective	**Promising treatments still under evaluation**	**Treatments that feature in major international guidelines**
Activated protein C	Alkaline phosphatase	Early appropriate antibiotic therapy
Anti-thrombin III recombinant human tissue factor pathway inhibitor (Tifacogin)	Beta-blockers	Early source control
Anti-tumour necrosis factor monoclonal antibody	GM-CSF	Supportive critical care bundles
Anti-tumour necrosis factor receptor antagonist	Immunoglobulin	
Bradykinin antagonist (Deltibant)	Interferon gamma	
ECA (anti-*Enterobacteriaceae* common antigen monoclonal antibody)	TLR-4 antagonist (e5564)	

Growth hormone		
HA-1A (anti-endotoxin monoclonal antibody)		
Interleukin-1 receptor antagonist		
N-acetyl cysteine		
Nitric oxide inhibitors		
Plasma exchange or coupled filtration adsorption		
Selenium		
Statins		
TAK 242 (TLR-4 antagonist)		
Talactoferrin		

The table above shows many of the published interventions that have been subjected to clinical trials, are currently in trials or are promoted by major international guidelines for the treatment of sepsis. Interventions classed as ineffective either failed to meet their primary endpoint or were stopped early due to increased mortality[17].

1.1.3.1. The evidence for antibiotic use in sepsis

Although early, aggressive and appropriate antibiotics form the cornerstone of national and international guidelines on the treatment of sepsis[2,9], there remains evidential uncertainty of the role that they play in reducing mortality. Although the pathophysiological basis of microbial killing resulting from antibiotic use has been known for decades[18], sepsis is a disease causing mortality through a patient's response to infection rather than simply presence of microbial agents directly. Therefore, scientific evidence of pathogen killing is insufficient to infer clear mortality benefits that may result. Multiple studies focusing on patient outcomes have been published showing a higher mortality in patients where antibiotics have been delayed or were deemed inappropriate [19-25]. However, all of these are methodologically flawed retrospective studies unable to compensate for unmeasured cofounders that may play an important part in such a diverse condition. Due to the lack of ethical clinical equipoise required to perform a double-blind randomised placebo controlled clinical trial in this area, few studies are able to produce a high grade of evidence. One study has used an innovative approach to this problem, using a quasi-experimental, before and after observational cohort study of aggressive versus conservative antimicrobial treatment[26].

Interestingly, this showed a negative association between mortality and early, aggressive broad-spectrum antibiotic use. Summarising more than 50 trials of early, aggressive broad-spectrum antibiotics use in sepsis (20 of which showed no positive association between this intervention and mortality) McGregor[27] summarises the current state of the evidence by stating that:

"there is little evidence for or against recommendations regarding aggressive empiric therapy with broad-spectrum antibiotics".

This underlines the importance of using more directed approaches to antibiotic use, specifically aimed at those patients who actually do have infection and not simply sterile SIRS. Furthermore, targeting the correct individual microbial pathogen in non-mixed infections, rather than using a one-size-fits-all approach of empirical antibiotics, may help power studies that show mortality reductions. In order to realise the evidence for antibiotics, the background noise concerning inappropriate antibiotic use needs to be silenced. This is especially true in a world of increasing antimicrobial resistance[28,29].

Despite these uncertainties, early, appropriate antibiotic use remains the cornerstone of sepsis treatment with one study showing an increased mortality of 7.6% for each hour that this intervention is delayed[30,31]. However, the ideal initial choice of agents is open to debate and relies greatly upon local microbiological surveillance data as well as patient characteristics. However, the prediction of local resistance patterns and likely causative organisms is known to be difficult with as many as 1 in 5 patients receiving inappropriate initial antibiotics[30,32]. Early source control relies upon early source identification, another challenge that can be difficult to meet early in a patient's presentation with sepsis. Many patients are diagnosed with an incorrect source of infection where effective source control would thus not be possible[32,33].

1.1.3.2. The evidence in care bundles in sepsis

Providing supportive critical care encompasses packages of interventions that have some degree of an evidence-base when applied across the critically ill patient population as a whole[33,34]. The most robust elements of this package include lung protective ventilation, blood glucose control, maintenance of the patient's bed at a 45-degree angle, antithrombotic prophylaxis, nutritional support, and care within a multidiscipline dedicated critical care team. The SSC guidelines include additional

suggested interventions within their bundles of care. The most widely applied of these is their approach to initial resuscitation largely based on a goal-directed therapy paradigm promoted by a controversial single-centre study[34,35].

Despite many international authorities continuing to promote the use of these above measures thought to be beneficial in the form of bundles of care, the most current evidence does not support many of these practices. Even those measures universally applied in critical care practice, such as the use of a 45 degree head-up tilt in ventilated patients to reduce levels of Ventilator-Associated Pneumonia (VAP), when considered objectively may fail to deliver patient benefits[36]. In VAP specifically, the use of a 45 degree head-up tilt has even been shown to be detrimental in basic scientific studies [37]. The patient centred outcome of this practice will be further elucidated on completion of the on-going Gravity-VAP (Ventilator-Associated Pneumonia) Trial (ClinicalTrials.gov Identifier: NCT01138540).

The questioning of established convention has also occurred in the management of sepsis following the publication of two major international randomised controlled trials[35,38]. Both the US based ProCESS and the more recent Australian ARISE studies have questioned many of the accepted interventions featuring in the SSC 6 hour bundle, most notably the use of central venous pressure (CVP) and central venous oxygen saturation ($ScvO_2$). The former 24 hour bundle has already been removed and now in light of these studies questioning the utility of CVP and $ScvO_2$ monitoring as part of an early resuscitation strategy, many are calling for this to be reflected in the current guidelines[28,39]. In response, the SSC released a statement on 1st October 2014 to address these issues stating that they will continue to recommend CVP and $ScvO_2$ monitoring as they have not been demonstrated to be associated with any adverse outcomes. However, they state that:

"in light of the evidence from the ProCESS and ARISE trials, the SSC guidelines committee will immediately review the evidence and assess whether the guidelines need to be updated now".

1.1.4. Outcomes

Whilst the mortality rates in sepsis have improved greatly from as high as 80% in series published 30 years ago[40,41], it remains far higher when compared with many other common pathologies[40,42]. Many researchers feel that increased awareness and training amongst staff along with better supportive treatment and aggressive initial antibiotic use have reduced mortality in severe sepsis to around 20-30%[6,42]. However, the long-term morbidity associated with this condition is substantial with return-to-work rates as low as 60%[6,43,44]. Many survivors will develop severe psychological symptoms and others will suffer debilitating chronic pain. Even 10 years following an initial illness, survivors have been shown to have a reduced cardiovascular reserve, poor lung function, and persistent muscle waisting[6,43-45].

The organism class responsible for infection has been shown to play a role in determining the mortality of patients with sepsis[46,47]. However, there are variations in both the magnitude and the direction of the differences shown between Gram-positive and Gram-negative infections. The largest of these studies, with over 5 retrospective electronic records analysed retrospectively of patients from the United States, attributed a mortality of 30.4% to sepsis caused by Gram-positive organisms and 23.3% for Gram-negative organisms. However, the highest mortality by organism type in this cohort was 36.3% in anaerobic microbes that were formed from a subclass of the Gram-negative species[48]. A European study of 3000 patients with sepsis showed an unadjusted hospital mortality rate of 37.6% in Gram-positive infections compared with 35.3% in Gram-negative infections[46]. A much smaller study of 436 patients, which controlled for appropriate antibiotic use, conversely showed an unadjusted hospital mortality rate of 50% in Gram-positive infections compared with a higher rate of 52.3% in Gram-negative infections[47].

As well as the associations between Gram status and mortality, individual organism species can also help to explain differences in patient mortality [46,47]. After adjustment for an organism's class and other important cofounders, Labelle et al have shown there to be a hierarchal mortality rate associated with different organism types within Gram-positive and Gram-negative subgroups. Overall, whilst patients with Gram-positive infections were shown to have a mortality rate of 50%, having a methicillin susceptible *Staphylococcus aureus* had a raw mortality rate of just 30% with an odds ratio of 0.3

after adjustment using linear regression analysis compared with other organism types. However, the larger study by Ani et al, although not adjusted for co-founders or appropriate antibiotic use, showed methicillin susceptible *Staphylococcus* aureus as having the highest mortality rate compared with all other Gram-positive and Gram-negative species[48].

In fact, after the adjustments for the organism class and type, the site of infection also appears to play a key role in differential patient survival [46,49]. These mortality differences found through comparison of sources can be as much as a 50% increase in absolute mortality rates in ischemic bowel sepsis compared with urosepsis from obstructive uropathy.

With the knowledge that patterns of microbial classes differ between different infectious sources[48], simply basing a mortality prediction on an organism type may act as a surrogate for the likely source of infection. This may help explain some of the variation shown in the literature comparing organism class and species. The extent of analysis variation shown in these studies expose many of the difficulties inherent in retrospective analysis of a syndrome characterised by a number of individual disease entities across a hugely variable cohort of patients. In conjunction with local microbial resistance patterns, the variable use and timing of appropriate antibiotics further complicates research in this area.

1.2. The cellular immune response in sepsis

The early determinants of the host response to infection lie predominantly with the innate immune system, orchestrated by several important effector cell types.

1.2.1. Monocytes

Cells emerging from the monocyte-macrophage lineage, often found tissue resident in end-organ systems, play a key role in phagocytosis of pathogens and mounting a rapid response through activation of pattern recognition receptors. The subsequent release of proinflammatory mediators, most notably interleukin(IL)-6, TNF-α, IL-1β and IL-10, is accompanied by the release of a broad range of cytokines, chemokines and free radicals which promote cell migration, adhesion and tissue inflammation[50]. A key example of this functional ability occurs in Gram-negative infections through binding of microbial

lipopolysaccharide (LPS) to monocyte toll-like receptor 4(TLR4)/CD14 complex mediated by myeloid differentiation primary response gene 88 (MyD88) and TIR-domain-containing adapter-inducing interferon-β (TRIF) dependent pathways, stimulating the production of intracellular nuclear factor kappa-light-chain-enhancer of activated B cells (NFκB) and hence the phenotypical and function changes that result[51]. Conversely, Gram-positive microbes, with their peptidoglycan and lipoteichoic acid cell walls, classically were considered to act independently through TLR2 receptors but increasing evidence now points towards crossover in the activation of divergent TLRs by both Gram-positive and Gram-negative species and their associated PAMPs[52]. Furthermore, human monocytes can be divided into two subsets based on their expression of CD14 and the immunoglobulin receptor CD16. Those $CD14^{+}CD16^{-}$-monocytes represent the majority of peripheral circulating monocytes whilst the $CD14^{+}CD16^{+}$ monocytes produce the higher levels of proinflammatory cytokines and lower levels of IL-10[53].

1.2.2. Neutrophils

The innate immune response in sepsis is heavily reliant on neutrophils for regulatory processes, phagocytosis and direct antimicrobial killing. The regulatory aspects of the neutrophil response are dependent upon cytokines, chemokines, and leukotrienes whilst antimicrobial killing occurs in response to neutrophil peptide, protease, and oxidant production. Dysregulation of neutrophils during sepsis has been demonstrated in a range of models, including studies showing a reduced ability for neutrophil migration to the appropriate sites of infection[54] and an inadequate functional response following neutrophil stimulation by PAMPS including LPS[55]. Inappropriate neutrophil migration to non-pathological sites, most notably the lungs[56], has been shown to result in immune-related pathology[57] and contribute towards the pathophysiology of multi-organ failure in sepsis[58]. The mechanisms implicated in these changes include impaired neutrophil chemotaxis mediated through TLR and cytoskeletal alterations[59] and more recently the detrimental role that continued late neutrophil extracellular trap (NET) formation may have on a balanced immune response in sepsis[60,61].

1.2.3. Lymphocytes

$CD4^{+}$ T cell subsets play an important role in the regulation of the immune response in sepsis. Whilst initially promoting a T_{H1} IFN-γ dominant response, there is an increasingly recognised role for other important T_H cell subsets including T_{H17} [62] and

regulatory T cells[63] (Tregs) in the control of an infective response. The secretion of IL-23 and IL-1 by antigen presentation cells help promote IL-17 producing T_{H17} subsets that in turn form a balancing link between the adaptive and innate immune system[64,65]. This T_{H17} role seems especially important in combating extracellular bacteria such as *Staphylococcus aureus*[66]. There are strong signals linking increased levels of Treg cells in peripheral blood of patients with sepsis and immunosuppression although the exact role of this subset of T cells remains contentious[67,68]. Changes in the distribution of $CD8^+$ effector cytotoxic T cells have also been shown to occur during the early phases of sepsis. In combination with increased levels of Tregs, lymphocyte changes are linked to the anti-inflammatory phenotype observed in many sepsis patients[69].

1.2.4. γδ T cells

γδ T cells expressing a Vγ9/Vδ2 T cell receptor are unique to humans and primates and represent only a minor population in the peripheral circulation; yet they expand dramatically in many infections and may exceed all other lymphocyte populations within days[70]. This is arguably the most impressive expansion of any human immune cell and indicates a fundamental role for these cells in acute disease. With respect to antigen selectivity and recognition, Vγ9/Vδ2 T cells differ fundamentally from other human or non-human γδ T cells, and from 'conventional' αβ T cells. They occupy a unique niche in microbial recognition as they are directly activated by (*E*)-4-hydroxy-3-methyl-but-2-enyl pyrophosphate (HMB-PP), an essential metabolite in the majority of Gram-positive (*Bacillus*, *Clostridium*, *Mycobacterium*) and Gram-negative bacteria (*E. coli*, *Klebsiella*, *Pseudomonas*, *Salmonella*)[71]. Although the exact mechanism of this non-major histocompatibility complex (MHC) dependant recognition of HMB-PP is not fully understood, it is known to involve HMB-PP binding through the B30.2 intracellular domain of butyrophilin 3 (BTN3)[72,73]. The innate-like capacity of Vγ9/Vδ2 T cells to recognize HMB-PP offers a simple means to respond to numerous pathogens, by targeting a vital metabolic route shared by these organisms. Notable exceptions of medical relevance are the Gram-positive bacteria *Enterococcus*, *Staphylococcus*, and *Streptococcus* and Gram-negative *Legionella* that cause considerable disease but fail to stimulate γδ T cells due to the absence of HMB-PP in their metabolism. It has been demonstrated that stimulation of human γδ T cells has implications for both pathogen clearance and development of microbe-specific immunity[74]. However, if triggered at the

wrong time or the wrong site, especially in vulnerable individuals with severe infection, this reaction may lead to inflammation-related damage and affect patient outcomes[74]. γδ T cell responses may act as relevant biomarkers for differential diagnosis of patients with acute infection but also may contribute to risk modelling as predictors of morbidity and mortality.

1.3. Immunosuppression in sepsis

Although host responses to infection have been studied extensively for decades[75,76], the concept of a transition to a hypoimmune status following initial recovery from sepsis is a relatively new concept. Combined with the failure to realise mortality improvements by addressing the proinflammatory cytokine storm in the initial period of sepsis, there is great interest in immunotherapy directed towards this contrary process[75,77]. Although addressing immunosuppression has been shown to bring mortality benefits in cancer patients by reducing immunosuppression related infections[77,78], it has not yet been shown to be an effective intervention for reducing sepsis deaths. These deaths resulting from immunosuppression in sepsis generally occur later in the disease process and are due to either a failure to control the initial infective insult or the acquisition of a second-hit nosocomial low virulence infection.

1.3.1. Models of immunosuppression

The accepted paradigm of a period of hyperimmune inflammatory storm only subsequently followed by a hypoimmune phase has been questioned by many in recent times[78,79]. Most notably, data from the associated conditions of trauma and burns has shown that immune suppression can occur as early as 2 hours following an initial insult[79,80]. A landmark study examining splenocytes of patients that died from sepsis has shown simultaneous alterations in both pro and anti-inflammatory pathways suggesting a far more complex picture of converging dysregulation across these two domains[80,81]. This complexity is further confounded by using artificial timescales to time illness start by a patient's presentation point to hospital. Clinicians meeting a patient for the first time are actually seeing only a snapshot in a pathophysiological process that may have been occurring for many days previously. Imposition of these false time points must have major implications for trials on novel therapies in sepsis where the definition of a zero time point is highly variable (Figure 1.3).

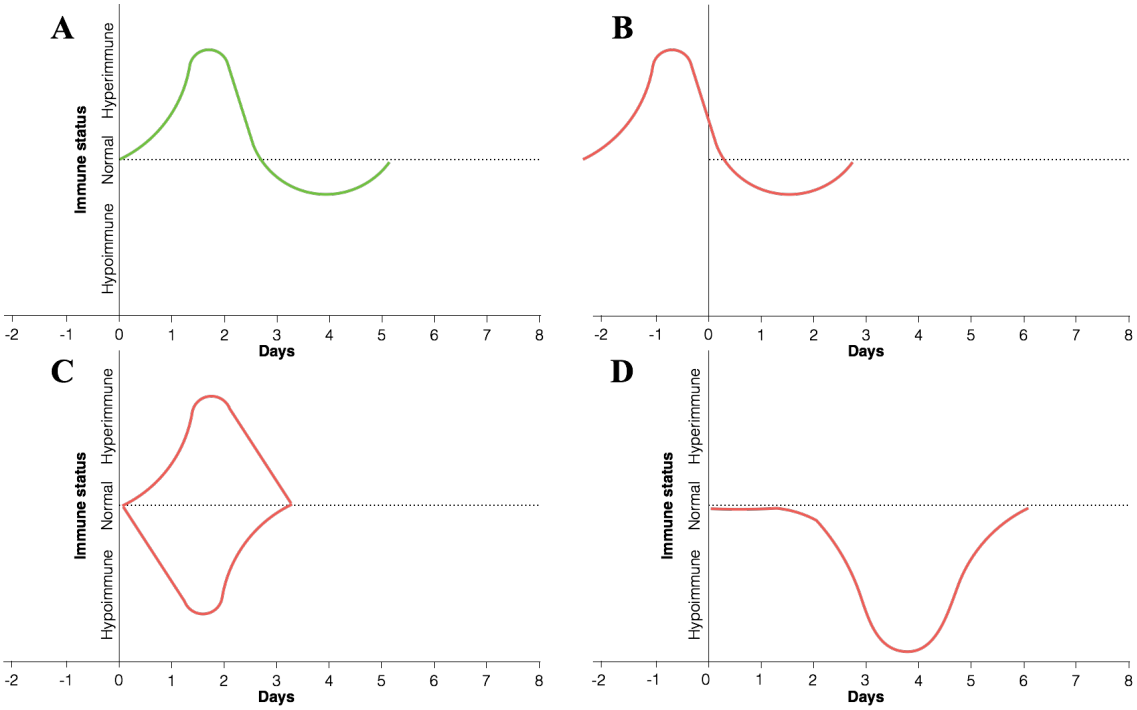

Figure 1.3 Models of immunosuppression. The figure above illustrates four example models of immunosuppression possible in patients presenting with sepsis. (A) The classical picture of a sepsis timescale showing a period of hyperimmune activity on admission to hospital followed by a gradual transition to a hypoimmune, immunosuppressed status. Figure adapted from [81,82]. (B) This shows how the model may differ when a patient presents late to hospital having already transitioned through the hyperimmune phase. (C) Demonstrates simultaneous hyper and hypoimmune status thereby complicating any simplistic targeting of sepsis interventions by disease category alone. (D) Shows a predominant hypoimmune patient response where the classical proinflammatory cytokine storm is completely absent.

1.3.2. Mechanisms and monitoring of immunosuppression

The general mechanisms leading to sepsis related-immunosuppression fall into one of three main categories; cell death and apoptosis, cellular anergy and cellular reprogramming[82,83]. Thus a patient may be found to have low absolute numbers of live immune cells, many of which either no longer respond to PAMPs or else respond in ways that no longer ensure effective pathogen clearance (Figure 1.4). Described in these terms as a complex interconnected dysfunctional system, developing an effective monitor of this process is difficult. It has now been broadly accepted that monocyte cell surface HLA-DR is a useful surrogate marker of sepsis related-immunosuppression[83,84]. Using this single maker has helped to reduce the complexity of these mechanistic changes into a relatively simple to measure, quantitative metric. Monocyte HLA-DR has formed part of the entry criteria into clinical trials on interventions designed to reduce sepsis related-immunosuppression [80,84] as well acted as an endpoint in many pilot studies in this field[78,80]. Although alternative reactive measures are currently being

investigated, including the ability of cells to produce cytokines against set standard microbial PAMPs, these techniques are not yet reproducible nor practical.

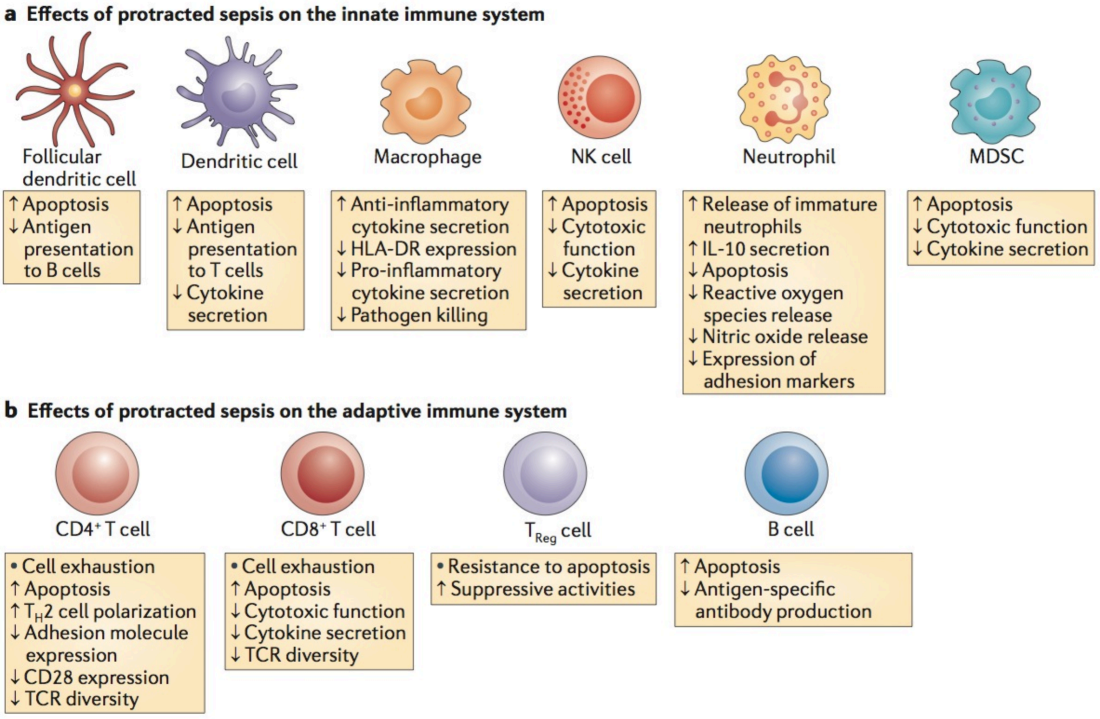

Figure 1.4 Typical immunosuppression changes in sepsis according to cell type. The figure above shows the typical findings in different cell types found in patients with severe sepsis. Taken from [78]. The schema above outlines how a patient may be found to have a low absolute number of live immune cells, many of which either no longer respond to PAMPs or else respond in ways that no longer ensure effective pathogen clearance

1.3.3. Immunosuppression treatments

One advantage of describing such a complex mechanistic system underpinning sepsis related-immunosuppression is the abundant availability of different therapeutic targets (Figure 1.5). Treatment trials thus far have been directed at either using recombinant cytokines (including IL-17, IFN-γ, GM-CSF and G-CSF) or else blocking key inhibitory receptors implicated in sepsis related-immunosuppression (most notably programmed cell death protein 1 (PD1) and programmed death-ligand 1 (PDL-1)). Although many of the in vitro and ex vivo studies using PD1 show initial promise in sepsis models[85,86], none have yet been shown to meet a clinically relevant primary endpoint in patients. However, the PD-1/PD-L1 Pathway Study on Septic Patients has now been completed, the results of which should be available soon (ClinicalTrials.gov Identifier:NCT01161745). It will have to be seen whether this study and the most recent

GM-CSF trial (NCT01653665), due to meet its recruitment target in April 2015, will change this trend of negative sepsis trials.

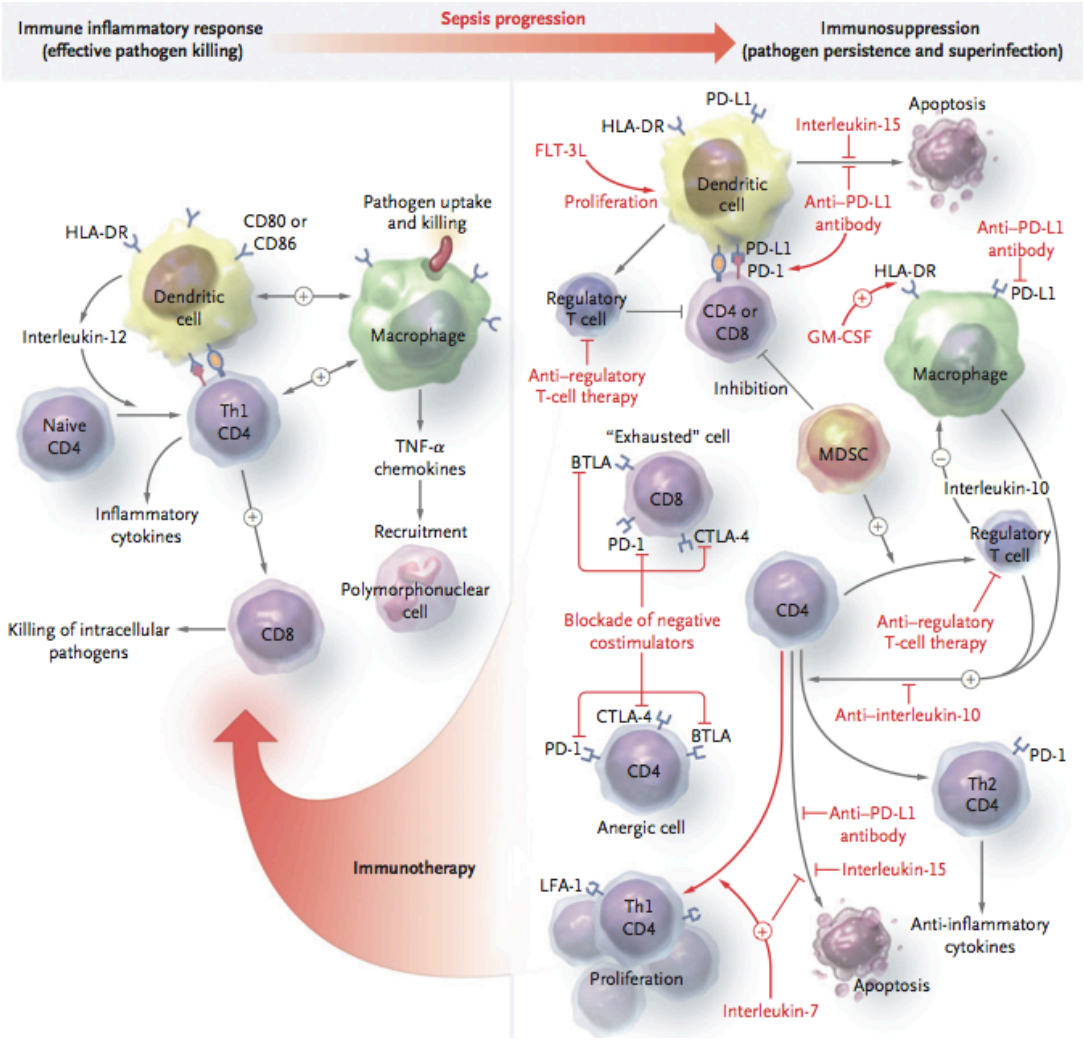

Figure 1.5 Possible targets for treatments aimed at sepsis-related immunosuppression.

The above shows the possible targets for addressing deficits resulting in sepsis related-immunosuppression (taken from [78,87]). Given the complexity of the immune response in sepsis, there are numerous potential targets for therapeutic intervention in immunosuppression. Those highlighted here include positive treatment with recombinant IL-15, IL-7, FMS-like tyrosine kinase 3 ligand (FLT-3L) and granulocyte‐macrophage colony‐stimulating factor (GM‐CSF). However, alternative strategies include receptor blockade with PD-L1 specific antibodies, IL-10 antibodies and anti-Treg treatments. GM‐CSF increases monocyte and macrophage HLA‐DR expression with the aim of increasing cell activation following microbial stimulation. IL-15 similarly acts on $CD4^+$ and $CD8^+$ T cells to reduce apoptosis but importantly also has positive effects on both dendritic and natural killer cells. IL-7 has shown promise in non-sepsis related immunosuppression by improving T cell activation, elevating cell adhesion molecules and hence may improve T cell trafficking to sites of infection. FLT-3L has been shown to increase the number of functional dendritic cells in a number of locations including the lung and spleen following infection. PD1‐specific antibodies may restore the functions of $CD4^+$ and $CD8^+$ cells and hence indirectly improve monocyte and macrophage stimulation. They block the stimulation of PD-L1, resulting in less T cell anergy, apoptosis and lower levels of IL-10. The strong association between IL-10 and mortality in sepsis has led many to suggest that blocking the immune responses induced by IL-10 will be beneficial in sepsis related immunosuppression. The changes induced are primarily due to the ability of IL-10 to supress macrophage activation and inhibit neutrophil phagocytic and bactericidal activity. The role of Tregs in sepsis is controversial and their activity has been considered both beneficial and detrimental at different time points. However, suppression of Treg activity has been linked to improved survival in poly-microbial sepsis models [88,89].

1.4. "Immune fingerprints" in infection

With the increasingly efficient yet complex technological innovation that has flooded the biotechnology field over the last 10 years, the approach to results analysis has been largely side-lined[87,90]. The genetic revolution brought such a paradigm shift in the sheer amount of data needing analysis, that new statistical techniques were forced to the forefront. The steadier creep of big data into the world of immunology has not necessitated a Big Bang approach to data analysis. However, with the advent of multiplex enzyme-linked immunosorbent assay (ELISA) and multi-colour flow cytometry becoming readily accessible to many medical research projects, the sheer amount of data produced from even the most simple of projects is now not suitable for analysis using traditional statistical tools. Indeed, the entire field of hypothesis-driven research is slowly being eroded by data-driven research, the outputs of which are re-assimilated with existing knowledge only after the event of discovery rather than preceding it[90,91]. Diagnostic medicine needs to embrace these new tools, utilising powerful new predictive techniques that allow multiple combinations of biomarkers to form robust models that can impact upon patient care. This is true especially in the field of sepsis research, where single biomarkers studied in isolation have been the traditional direction of travel. With the inherent complexity of the host-pathogen interaction, it is no wonder that simply relying upon these isolated biomarkers cannot lead to rapid advances in diagnostics. Further still, the failure of new therapeutic agents has illustrated the importance of patient stratification, a process that is possible only when the complexity of the immune response is compensated for by new tools that allow a multiple biomarker, non-linear approach to prediction.

1.4.1. The concept

Immune fingerprints in general can be considered as the immune responses that a disease process leaves in its host through its pathophysiology. Using statistical techniques that deal efficiently with non-linear complexity, these fingerprints can be used to predict many aspects of the causative disease. The most obvious use would be to simply recognise the presence of a specific disease. In this case, it could be exploited to differentiate between sepsis and SIRS caused by pathology such as pancreatitis for example. Here through the measurement of both cellular and humoral immunological parameters, a predictive model could be formed to aid in the diagnostic process. This

concept could be taken further to predict the impending disease severity and hence the likely mortality outcome from sepsis.

Although using the new term "immune fingerprints", this is largely what current biomarker identification projects are already doing but without exploiting a combination of biomarkers using modern modelling techniques. However, the real benefit of this approach is revealed when it is used to predict what infecting organism is responsible for sepsis. Historical microbial identification approaches (including microscopy and culture) as well as more modern polymerase chain reaction (PCR) based approaches, simply detect what microbes are present in a given sample. This is appropriate in specimens that should remain sterile such as blood. However, with bacteraemia rates as low as 15% in the leading causes of sepsis in the Western world, community-acquired pneumonia, detecting pathogens directly will only help in a fraction of cases[91,92]. Furthermore, when testing specimens with high non-pathogenic microbial loads (such as bronchoalveolar lavage (BAL) fluid), positive species detection leads to difficult interpretation of what may be normal and what is pathogenic. The immune fingerprinting approach exploits a patient's own immune response to infection to identify not what microbes are present, but rather what microbes are causing disease. This can therefore avoid the issues surrounding low bacteraemia rates and simultaneously deal with specimens that have high commensal bacteria loads.

1.4.2. Statistical approaches and artificial neural networks

In order to fully realise the benefits of immune fingerprinting, non-linear statistical approaches that can deal efficiently with multiple biomarkers are required. Although traditional techniques, such as multiple regression, can be used for these purposes, they are not well suited to an immune dataset typical of sepsis, with three main shortcomings[92,93]. Firstly, the numbers of observations required for effective analysis is largely related to the number of independent variables. With modern analysis techniques, the number of variables produced is substantial compared with the relatively small number of patient subjects in a typical clinical study. Secondly, traditional techniques mostly need the assumption of linearity between the dependent and the independent variables. In complex interdependent immunological systems, this linearity is often not present. Finally, multiple regressions can only apply to studies using between-subject designs. When analysing patient cohorts with multiple outcome

measures (survival, infecting organism type, disease type), a within-subject design may be required and can reduce resources.

For these reasons, alternative statistical approaches have been developed in recent years. Many are now applied to fields of research entirely devolved from those in which they were initially developed. Artificial neural networks belong to a group of modelling techniques termed artificial intelligence or machine learning methods. They have been used in fields as diverse as chemical kinetic modelling and onion plant production planning[93,94]. In the medical literature, they have recently been applied to the search for cancer biomarkers due to their characteristics of dealing effectively with large datasets with multiple non-linear variables[8,94]. However, they remain in an early stage of development and thus some of the more advanced functions, including their ability to automatically reduce the number of variables needed to form a robust prediction, are not yet present.

Artificial neural networks are ideally suited to classification problems where a large number of complex input variables form the basis of a prediction about a relatively small number of output possibilities. The network exploits interconnected processing elements, termed neurones, acting in efficient, parallel, yet modular means modelled on the human brain. These interconnected elements are organised into three distinct layers, an input, an output and a hidden layer. The input layer deals effectively with all types of predictor variables including non-linear continuous, binary data and zero-inflated data typical of medical research studies. The output layer contains the outcomes of any prediction and may include binary or categorical data. Between the input and the output layers, there is the so-called hidden layer that is a series of artificially constructed nodes which allows the model to deal with non-linearity and perform complex functions to model predictions accurately. In a supervised artificial neural network, the model is told of the correct output result for each test item and then differentially weights the input variables according to how this allows the overall model to perform on average across the total dataset. This weighting is achieved using a weight matrix applied to the connections between each layer. In order for this iterative adjustment to be accurate, it is repeated a greater number of times than the total number of samples in the dataset using a technique analogous to bootstrapping with repeated random sampling from the parent dataset. This entire process is thus called a feed-forwards supervised artificial

neural network model, with typical values of 2 hidden layers and 3000 bootstrapped iterations. As an example, a household burglar alarm system can be considered (Figure 1.6). It has three variables in the input layer; a binary glass-breaking sensor, a non-linear sound sensor and a linear movement sensor. The two possibilities in the output layer are to sound the house alarm or not. The system may operate well using all three input variables at maximum until a new kitten arrives in the house. At this point, a supervised feed-forward artificial neural network could be trained by putting the cat in the house and informing the alarm that no real threat was present. The alarm will thus learn what are the expected normal levels of inputs to each of the sensors in its system. The network would therefore reduce the value on the movement and the sound sensor on the weight matrix for that layer. Ideally, the system will then need to be trained with a real intruder in the house, at which point it would increase the weight on the glass breaking sensor to directly sound the alarm on the output layer.

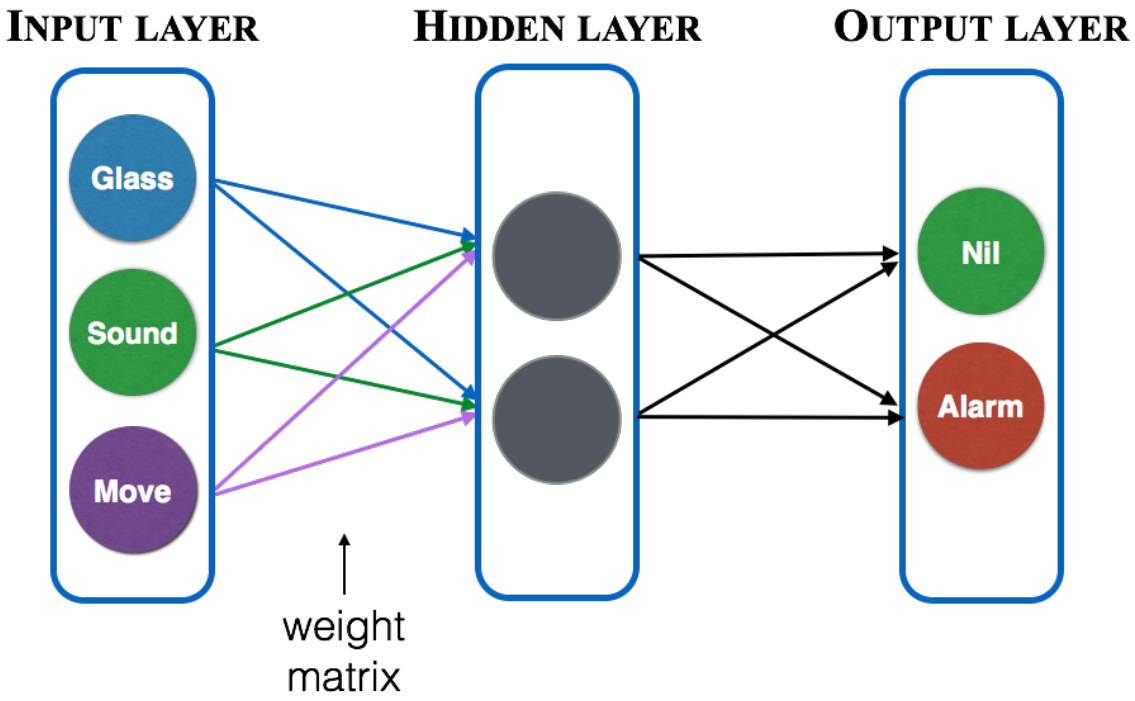

Figure 1.6 An example of an artificial neural network using a house alarm system. The input layer uses a glass break binary sensor, a non-linear sound sensor and a linear movement sensor. The weight matrix is adjusted to deal with background movement from a pet that is introduced to the home by reducing the sensitivity of the movement and sound aspect of the alarm system. The output layer allows the house alarm to be sounded should a certain threshold be reached as dictated by a complex non-linear function determined by a hidden layer.

One major shortcoming with neural network design at present is its inability to suggest removal of particular variables to make models more efficient and practical. Whilst traditional techniques such as logistic regression can focus on key predictors required

for sufficient prediction power, artificial neural networks effectively deal with large variable numbers without the ability to dispose of those variables that add little to prediction power. Although this may not pose an issue in the world of economics where systems use data collated for other purposes, in medicine where simply measuring variables comes with a financial and human cost, it is essential that a technique is efficient with consumables, time and money. This will be explored and solved in Chapter 4. The additional disadvantages of this modelling technique will be explored and illustrated using the models produced in 3.4.5.3 Application of neural networks

1.5. The Scope of this thesis

Overall, this thesis will use small-scale yet complex basic science data, new statistical modelling techniques, and a new approach to microbe identification to shed light on the complexities of sepsis-related critical illness. It aims to ultimately improve patient care and improve scientific understanding through exploration of host responses, microbe identification, and immunosuppression in a cohort of the sickest patients in hospital with this devastating disease. Its outputs will suggest new concepts in risk stratification of first-hit infections, proof-of-concept for the development of a new technology to detect causative organisms and finally bring new insights into immunosuppression that may impact upon current and future clinical trials. This thesis will deliver these elements in the following sections:

Chapter 3 will describe the early immunological changes in severe sepsis patients and use an immune fingerprinting approach to predict survival, disease type, and infecting organism subtype. It will exploit new machine learning approaches to predictive modelling and use a customised programming script to reduce the numbers of variables required to form a robust yet efficient model.

Chapter 4 will explore the links between monocyte immunological changes and sepsis related-immunosuppression including the use of a bisphosphonate as a potential new therapeutic intervention. It will demonstrate gain-of-function rather than loss-of-function changes in sepsis neutrophils showing that they can act as antigen presenting cells.

CHAPTER 2

MATERIALS AND METHODS

Chapter 2 Materials and Methods

2.1. Ethics and consent

This study's design, management, and analysis were conducted according to the principles declared in The World Medical Association's Declaration of Helsinki. All patient sampling were approved through the South East Wales Research Ethics Committee (reference number 10WSE/421, protocol reference 3.4 9/12/2010, amendment 3.5 24/05/2011) and registered with the UK Clinical Research Network (Cellular and biochemical investigations in sepsis, ID 11231). A waiver of consent system was used where patients were unable to provide informed consent due to the nature of their critical illness. In these cases, permission was sought from the next of kin as a consultee. Informed consent was subsequently obtained when the patient regained capacity. If consent was subsequently withdrawn at any time, all remaining samples and data were destroyed. In cases where the patient died before regaining capacity, the initial consultee's approval would stand. This process was overseen by the research team's clinical lead Dr Szakmany.

2.2. Patient recruitment

Patients admitted to the ICU at The Royal Glamorgan Hospital, Llantrisant were recruited into the study by the research team's clinical lead Dr. Szakmany using the inclusion and exclusion criteria shown in Table 2.1. Patients that had been admitted to the hospital prior to ICU admission for greater than 48 hours were excluded as were patients admitted from another outside care institution. Patients recruited to the SIRS arm of the study fulfilled the SIRS and organ failure criteria shown in Table 2.1 but were not receiving antibiotics nor suspected of having an infection. Healthy controls were:

- Normally fit and well.
- Not suffering from an acute or chronic inflammatory illness (e.g. severe asthma or rheumatoid arthritis).
- Not taking immunosuppressant medications.

Table 2.1 Recruitment criteria for sepsis and SIRS patients.

Inclusion criteria	Exclusion criteria
Age > 18 years. Within 24 hours of the presumed onset of the infective illness. The patient will require arterial cannulation as part of their standard care.	Currently pregnant, breastfeeding or females in whom a pregnancy test has not been performed. Patient unlikely to survive for the duration of the study period. Post-cardiac arrest patients. Underlying impairment of higher function that would make it impossible for informed consent to be given upon recovery (e.g. severe learning disability).
Diagnosis of severe sepsis or septic shock: a) 3 of 4 SIRS criteria: i) Temperature >38°C or <36°C. ii) Heart rate >90 BPM. iii) Respiratory rate > 20/min or $PaCO_2$ < 32 mmHg or need for ventilation. iv) White cell count > 12,000 or <4000 cells/$^+$ or >10% band forms in whole blood. b) Known or suspected bacterial infection requiring antimicrobial therapy. c) Organ dysfunction (one of the following): i) Circulatory (one of the following): • SBP <90 mmHg for 1 hour despite adequate volume	Severe immune deficiency including AIDS diagnosis, use of anti-rejection drugs or high dose corticosteroid treatment >10 mg prednisolone equivalent per day. Child-Pugh grade 3 or greater liver failure.

replacement. • MAP <70 mmHg for 1 hour despite adequate volume replacement. ii) Respiratory (one of the following): • PaO_2:FiO_2 ratio <250 mmHg in the presence of other organ failure. • PaO_2:FiO_2 ratio <200 mmHg in primary pulmonary failure. iii) Renal • Urine output <0.5 ml/kg/hr for 1 hour despite adequate volume replacement. iv) Haematological: • Platelet count <80,000 cells per mm^3. v) Metabolic (one of the following): • Unexplained acidosis with pH <7.3 or BE <-5. • Lactate >1.5 normal upper limit for laboratory.	

These criteria follow the definitions in the SSC 2008[8,95] in place during the study period. Patients fulfilling the criteria above without a "known or suspected bacterial infection requiring antimicrobial therapy" were recruited into the SIRS arm of the study.

2.3. Sample and data collection

2.3.1. Main sepsis patient study

A day 1 sample of 40 ml of peripheral blood was taken from an arterial line during the first 24 hours of infective illness. 2000 units of heparin were added to the whole blood before it was transported to the laboratory on ice. A second sample was collected on day 5 if the patient was still on the ICU. All clinical data were exported from the electronic

health record system Intellivue (Phillips). Missing data were collected manually using paper records.

2.4. Microbiology

2.4.1. Main sepsis patient study

Microbiological data were captured using the hospital's electronic microbiology patient database. The main organism causing sepsis was defined as the presence of a positive microbiological or viral result in any sample taken from 72 hours preceding recruitment to 72 hours following admission to the ICU. The microbiological techniques used in the study hospital for diagnostics included standard microscopy and culture, viral PCR studies, and urine *Legionella* antigen testing. Advanced bacterial identification systems such as PCR or Matrix Assisted Laser Desorption/Ionization (MALDI-TOF) based techniques were not used.

One independent intensive care doctor and one independent microbiologist were consulted to confirm that any given positive result would be appropriate when considering the clinical context and other supporting clinical results. This was adjudicated with full access to patients' clinical notes, electronic clinical results and a discussion with the clinical consultant intensivist responsible for the patients' care. Culture results considered as non-relevant or contaminations were excluded from further analysis. Patients with no relevant positive results were classed as culture-negative. Infections were then grouped into Gram-positive and Gram-negative species.

2.5. Reagents

A list of solution-based reagents used can be found in Table 2.2. All reagents were kept under the conditions specified by the manufacturer and added constituents filtered using a 0.22 μm pore size hydrophilic polyethersulfone membrane filter. All soluble mediators used can be found in Table 2.3. All soluble reagents were stored at -70 ℃, defrosted, and underwent a minimum number of freeze/thaw cycles through aliquoting. Stock tests were performed on new batches before use in experiments.

Table 2.2 Composition of solution based reagents.

Reagent	Constituents
Complete RPMI medium	RPMI-1640 (Invitrogen) plus: 2 mM L-glutamine 1% sodium pyruvate 50 mg/ml penicillin/streptomycin 10% foetal calf serum
FACS buffer	PBS plus: 2% *v/v* foetal calf serum (Invitrogen) 0.04% *v/v* sodium azide (Fisher Scientific)
MACS buffer	PBS plus: 5 mM EDTA 2% *v/v* foetal calf serum

All solution based reagents used including their constituent parts.

Table 2.3 Details of soluble reagents.

Reagent	Source
Brefeldin A	Sigma
HMB-PP	A gift from Dr Hassan Jomaa, Justus-Liebig. University Giessen, Germany
Salmonella abortus equi ultra-pure LPS	Sigma
Zoledronate	Aclasta/Zometa; Novartis

All soluble agents used including their procurement source.

2.6. Leukocyte isolation from blood

An outline of the cellular subset isolations with representative purities is shown in Figure 2.1.

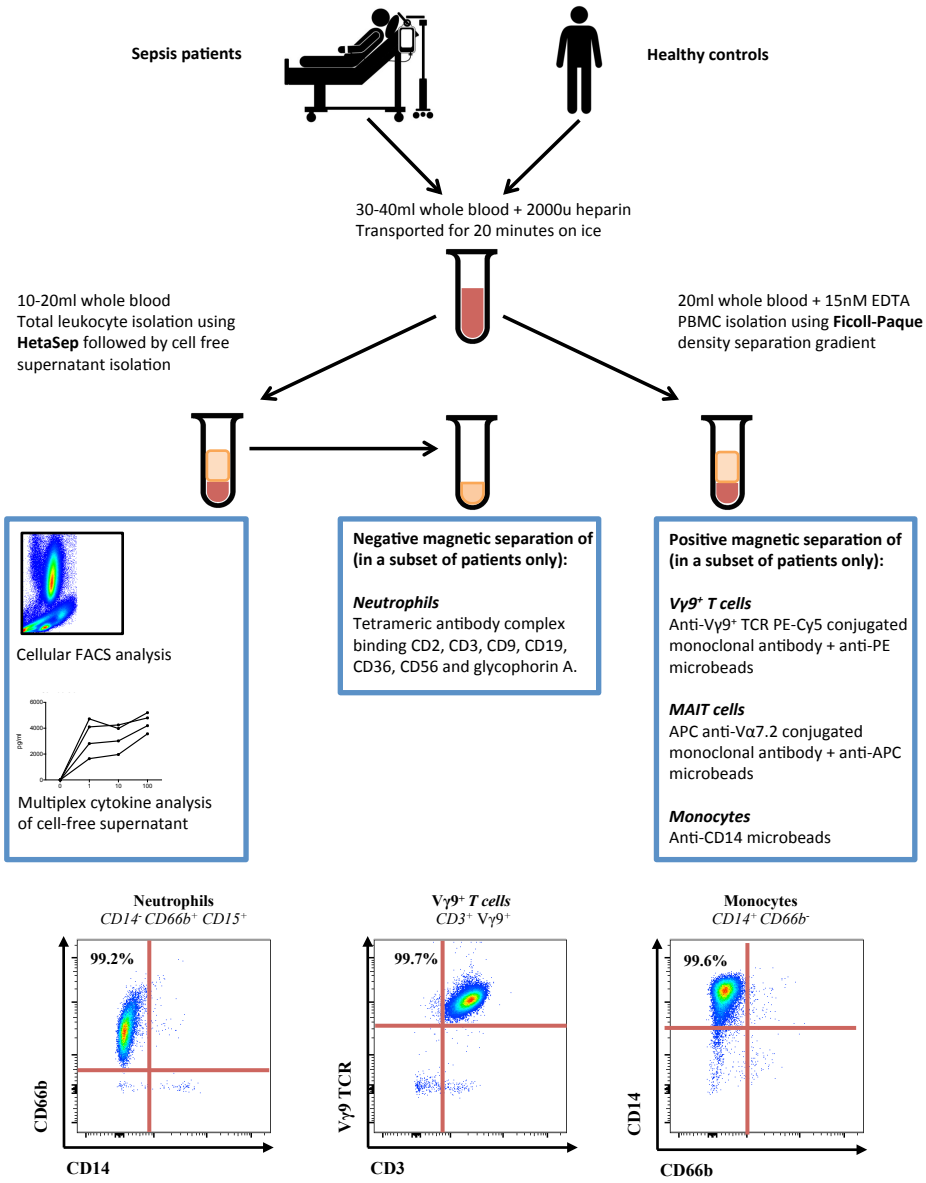

Figure 2.1 An outline of cellular subset isolation from sampled blood. The above is illustrative of all of the cellular subsets isolation during the study. Only a subset of samples was used for each isolation as outlined in **Figure 3.1** and **Figure 3.2**. The resulting purities shown are illustrative and were gated on live, non-doublet cells. PBMCs, Peripheral Blood Mononucleated Cells.

2.6.1. Total leukocyte isolation

2 ml of HetaSep (Stemcell Technologies) was added to 10 ml of blood and centrifuged at 100 *g* for 6 minutes. The plasma and leukocyte layer was then removed with a Pasteur pipette and centrifuged at 500 *g* for 10 minutes. The cell free supernatant was removed, aliquoted and stored at -70°C. The remaining cell pellet was washed with phosphate buffered saline (PBS) (Invitrogen) before being centrifuged at 120 *g* for 10 minutes to remove remaining platelets. The cell pellet was then re-suspended in PBS

and cells counts performed using a haemocytometer. The suspension was re-centrifuged at 500 *g* for 10 minutes and the pellet re-suspended in PBS at a final concentration of 2 x 10^7 cells/ml.

2.6.2. Peripheral blood mononuclear cells isolation

Venous blood from healthy volunteers was added to 20 units/ml of heparin and 15 mM of Ethylenediaminetetraacetic acid (EDTA) (Fisher Scientific UK). 20 ml of whole blood was then layered onto 20 ml of Ficoll-Paque (Axis-Shield, Norway) and centrifuged at 690 *g*, at 18°C for 20 minutes with minimal low acceleration and no brake. The mononuclear cell layer formed was removed with a Pasteur pipette and washed twice with PBS with centrifugation at 400 *g* and 4°C for 8 minutes. The cell pellet was re-suspended in fluorescence-activated cell sorting (FACS) buffer for evaluation by flow cytometry or medium for cellular assays.

2.6.3. Neutrophil isolation following total leukocyte isolation

Neutrophils (>99% $CD14^-$ $CD66b^+$ $CD15^+$; monocyte contamination <0.1%) were purified from whole blood by HetaSep sedimentation as in 2.6.1 followed by negative selection using the EasySep neutrophil enrichment kit (Stemcell Technologies). The gating strategy shown in

was used to identify neutrophils followed by the additional purity markers shown in

. The total leukocytes were resuspended at 5 x 10^7 cells/ml in magnetic-activated cell sorting (MACS) buffer with 50 µl/ml of the negative selection tetrameric antibody complex binding CD2, CD3, CD9, CD19, CD36, CD56 and glycophorin A at 4°C for 10 minutes. 100 µl/ml dextran-coated magnetic particles were then added after mixing and incubated at 4°C for 10 minutes. The suspension was then made up to 2.5 ml with MACS buffer before being inserted into an EasySep magnet for 5 minutes. Using a continuous motion with the magnet surrounding the solution, the desired fraction was then poured into a new container and the process repeated with a resulting purity >99%.

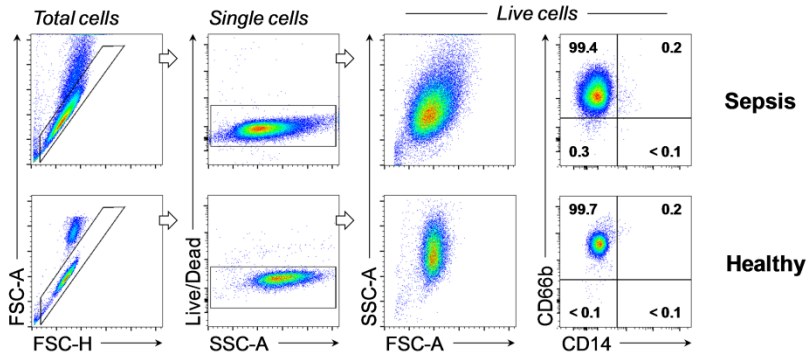

Figure 2.2 Purity gating used in neutrophil antigen presentation cell (APC) assays. For functional assays, neutrophils were isolated by negative selection from the blood of healthy donors or patients with sepsis, using the EasySep neutrophil enrichment kit that depletes all other human blood cells by specifically targeting CD2, CD3, CD9, CD19, CD36, CD56 and glycophorin A (Stemcell Technologies). Purities were confirmed by the percentage of cells expressing CD66b but lacking CD14. FACS plots are representative of 5 sepsis patients and 15 healthy donors.

2.6.4. Vγ9$^+$ T cell and monocyte isolation from peripheral blood mononucleated cells (PBMCs)

The resulting PBMCs from 2.6.2 were re-suspended in 1 ml MACS buffer and blocked with 1% human normal immunoglobulin (Kiovig; Baxter) for 10 minutes on ice. 2.5 µl of anti-Vγ9$^+$ TCR PE-Cy5 conjugated monoclonal antibody (1:400) (Immu360; Beckman-Coulter) was then added for 15 minutes on ice in the dark. Following incubation, the cells were washed with MACS buffer and re-suspended in 400 µl of MACS buffer. 80 µl of anti-PE microbeads (1:5) (Miltenyi Biotec) were then added for 15 minutes at 4°C in the dark. The cells were washed with MACS buffer and re-suspended at 2 ml. LS columns (Miltenyi Biotec) were then used as per the manufacturer's instructions to perform magnetic separation of Vγ9$^+$ T cells resulting in a purity of >98% by using this positive selection method. The pass-through fraction lacking Vγ9$^+$ T cells was used to purify monocytes with anti-CD14 microbeads (Miltenyi Biotec) resulting in a purity of >98%.

2.6.5. MAIT cell isolation from PBMCs

For isolation of MAIT cells, PBMCs were prepared as in 2.6.2 and the cells suspended in 500 µl of MACS buffer. 10 µl of APC anti-Vα7.2 antibody (1:50) (Miltenyi Biotec) was then added for 15 minutes on ice in the dark. Following incubation, the cells were washed with MACS buffer and re-suspended in 400 µl of MACS buffer. 80 µl of anti-APC microbeads (1:5) (Miltenyi Biotec) were then added for 15 minutes at 4°C in the dark. The cells were washed with MACS buffer and re-suspended at 2 ml. LS columns (Miltenyi Biotec) were then used as per the manufacturer's instructions to perform

magnetic separation of MAIT cells resulting in a purity of >98% by using this positive selection method.

2.7. Flow cytometry

2.7.1. Cell-surface marker staining

A pellet of 2 x 10^6 cells was stained by adding 3 µl live/dead stain (fixable Aqua; Invitrogen) and incubated at room temperature for 15 minutes in the dark. Following incubation, the cells were washed with PBS and re-suspended in FACS buffer. Cells were then blocked for non-specific antigen binding with 1% human normal immunoglobulin (Kiovig; Baxter) before the cells were incubated for 15 minutes on ice in the dark. The cells were then washed again with FACS buffer and cocktails of surface marker monoclonal antibodies were added with appropriate isotype controls for 20 minutes on ice in the dark. The full range of monoclonal antibodies used is shown in Table 2.4. All antibodies were titrated before use and their corresponding isotype used at an equivalent concentration to the parent antibody.

Table 2.4 Fluorochrome conjugated antibodies used for cell-surface flow cytometry.

Antigen	Conjugate	Clone	Isotype	Company	Final dilution
CCR7	PE-Cy7	G043H7	Rat IgG2a, κ	BD Biosciences	1:100
CD3	Pacific blue	UCHT1	Mouse IgG1, κ	BD Biosciences	1:100
CD4	APC-H7	SK3	Mouse IgG1, κ	BD Biosciences	1:60
CD8	APC	RPA-T8	Mouse IgG1, κ	BD Biosciences	1:40
CD8	PE-Cy7	SK1	Mouse IgG1, κ	BD Biosciences	1:200
CD8	PE	HIT8a	Mouse IgG1, κ	Pharmingen	1:40
CD11b	PE	D12	Mouse IgG2a, κ	BD Biosciences	1:20
CD14	PE-Cy7	61D3	Mouse IgG1, κ	eBioscience	1:160
CD14	PB	M5E2	Mouse IgG1, κ	BD Biosciences	1:40
CD15	APC	HI98	Mouse IgM, κ	BD Biosciences	1:5
CD16	FITC	3G8	Mouse IgG1, κ	Pharmingen	1:20
CD25	APC-H7	M-A251	Mouse IgG1, κ	BD Biosciences	1:20
CD25	PE-Cy7	M-A251	Mouse IgG1, κ	BD Biosciences	1:40
CD27	FITC	M-T271	Mouse IgG1, κ	BD Biosciences	1:40
CD27	PE-Cy5	1A4LDG5	Mouse IgG1, κ	Coulter	1:40
CD40	PE	mAB89	Mouse IgG1, κ	Beckman Coulter	1:20
CD45RA	APC	HI100	Mouse IgG1, κ	eBioscience	1:10
CD62L	PE-Cy5	DREG-56	Mouse IgG1, κ	Pharmingen	1:15
CD64	APC-H7	G10F5	Mouse IgG1, κ	Pharmingen	1:60
CD69	FITC	FN50	Mouse IgG1, κ	BD Biosciences	1:20
CD80	FITC	2D10.4	Mouse IgM, κ	eBioscience	1:5
CD83	PE	HB15e	Mouse IgM, κ	Pharmingen	1:5
CD86	FITC	2331; FUN1	Mouse IgG1, κ	BD Biosciences	1:40
HLA-A2	FITC	BB7.2	Mouse IgG2b, κ	Serotec	1:20
HLA-ABC	PE	W6/32	Mouse IgG2a, κ	eBioscience	1:10
HLA-DR	APC-H7	L243	Mouse IgG1, κ	BD Biosciences	1:40
HLA-DR	PE	G46-6	Mouse IgG2a, κ	Pharmingen	1:20
$V\gamma9^{+}$	PE-Cy5	Immu360	Mouse IgG1, κ	Beckman Coulter	1:400
Vδ2	PE	B6.1	Mouse IgG1, κ	BD Biosciences	1:100

All antibodies used in this study for cell-surface staining including their respective antigen, conjugate, clone, isotype control, company source and final dilution used.

2.7.2. Intracellular cytokine staining

10 μg/ml brefeldin A (Sigma) was added to cell cultures 5 hours before harvesting. Positive controls were stimulated with 50 ng/ml phorbol myristate acetate (PMA) and 1

μg/ml ionomycin (Sigma). Cells were then stained with the live/dead stain as above and for surface marker expression. After two washes with PBS, the cells were incubated with 100 μl of fixation buffer (eBioscience) for 15 minutes at room temperature in the dark. Cells were subsequently washed once with PBS and once with permeabilization buffer (eBioscience). Cells were re-suspended in 50 μl of a cocktail containing permeabilization buffer and fluorochrome conjugated monoclonal antibodies shown in Table 2.5 for 15 minutes at room temperature in the dark. After two washes, the cells were resuspended in 100 μl of FACS buffer and analysed using flow cytometry.

Table 2.5 Fluorochrome conjugated antibodies used for intracellular flow cytometry.

Antigen	Conjugate	Clone	Isotype	Company	Final dilution
IFN-γ	FITC	B27	Mouse IgG1	BD Biosciences	1:100
TN	APC	6401.1111	Mouse IgG1	BD Biosciences	1:20

All antibodies used in this study for intracellular staining including their respective antigen, conjugate, clone, isotype control, company source and final dilution used.

2.7.3. Analysis

Cells were acquired on an eight-colour FACSCanto II (BD Biosciences) and analysed with FlowJo (TreeStar). Variations in baseline MFI measurements were compensated for by using 8 peak sphero rainbow calibration particles (Spherotech). Single cells of interest were gated based on their appearance in side scatter and forward scatter area/height, exclusion of live/dead staining and surface staining: $CD3^-$ $CD14^-$ $CD15^+$ neutrophils, $CD3^-$ $CD14^+$ $CD15^-$ monocytes and $CD3^+$ $CD14^-$ $CD15^-$ T cells. T cell subsets were identified as $CD3^+$ $CD4^+$ $CD8^-$ helper T cells, $CD3^+$ $CD4^-$ $CD8^+$ cytotoxic T cells and $CD3^+$ $V\gamma9^+$ or $CD3^+$ $V\delta2^+$ $V\gamma9^+$ T cells. Full details of the gating procedures can be found in Figure 2.3.

Naïve subsets in $CD4^+$ and $CD8^+$ T cells were characterised as $CD45RA^+/CCR7^+$ cells, central memory (CM) as $CD45RA^-/CCR7^+$ cells, effector memory (EM) as $CD45RA^-/CCR7^-$ cells and effector memory RA (EM-RA) as $CD45RA^+/CCR7^-$ according to the classification by Sallusto et al., 1999[96].

Vγ9^{+} cells were classed as naïve CD45RA^{+}/CD27^{+}, CM CD45RA^{-} /CD27^{+}, EM CD45RA^{-}/CD27^{-} and EM-RA CD45RA^{+}/CD27^{-} subtypes, based on the definition by Dieli et al., 2003[97].

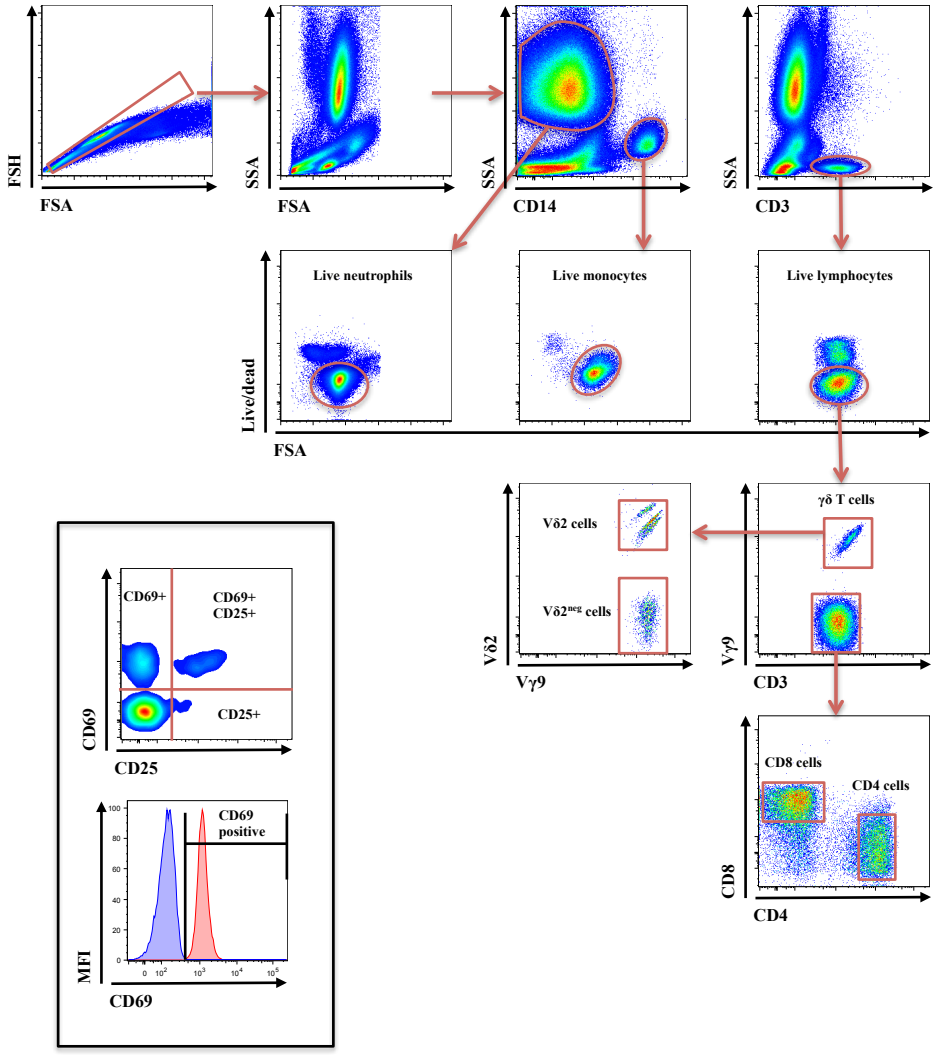

Figure 2.3 Gating strategy used throughout the immunophenotyping study. The gating used generally consisted of excluding non-single cells before lineage identification followed by dead cell analysis. Isotype gating or MFI values were then used to measure discrete cell-surface or intracellular markers.

2.7.3.1. Quality control in FACS analysis

Systems for the reduction of both inter and intra-user variations were employed to ensure consistency of analysis. A single person performed all the cell staining, flow cytometry acquisition and subsequent analysis using batch tested and controlled reagents. The same flow cytometer was used for the duration of the project with the manufacturer's recommended cytometer set-up and tracking analysis standardisation performed before acquisition of each batch of samples. Voltages, compensations and

gates were chosen to maximise separation between different cell populations into discrete units. The strict use of appropriate isotype controls allowed consistent gating, compensated for variations in background fluorescence or channel overspills. In addition, to ensure consistent readings across the duration of the study, 8 peak sphero rainbow calibration particles (Spherotech) were used before each batch of sample acquisitions. These allowed a set mean fluorescence intensity (MFI) for each of the 8 colour channels to be targeted on each acquisition cycle in a reliable and reproducible manner due to the inherent stability of the entrapped fluorochrome in the bead particles as shown by Perfetto et al[98]. The sample compensation and voltages of each laser channel was adjusted on each acquisition cycle to target these standardised MFIs.

2.8. ELISA based techniques

2.8.1. Single ELISA

Plasma procalcitonin (PCT) and proadrenomedullin (proADM) were kindly measured by Thermo Fisher Scientific at their laboratory in Hennigsdorf, Germany. The standard automated PCT analysis was carried out with the Liaison® system and is termed PCT throughout this study. The highly sensitive procalcitonin analysis was carried out using the Kryptor® and is termed sensePCT throughout this study. Further discussion relating to these two analysis techniques can be found in 3.4.5.2.

2.8.2. Multiplex biological assays

Cell-free plasma samples were analysed on a SECTOR Imager 600 for TNF-α, GM-CSF, IFN-γ, IL-1β, IL-2, IL-6, IL-10, IL-12p70 and CXCL8 (IL-8), using the ultra-sensitive human proinflammatory 9-plex kit (Meso Scale Discovery). This technology uses electrochemiluminescence detection based on amine-reactive N-hydroxysuccinimide esters. These are coupled to the primary amine groups of proteins to form stable amide bonds and bound to a carbon electrode plate surface. These pre-formed "Sulfo-TAG" labels are used in pre-configured multi-spot plates that simultaneously measure the above 9 cytokines across a wide dynamic range with high sensitivity and specificity. Emission is recorded at 620 nm from the $Ru(bpy)_3^{2+}$ bound group and the results analysed using the provided MSD Discovery Workbench software version 4.0. The 25μL plasma samples were measured with the supplied reagents according to the manufacturer's protocol and all fell between the upper and lower

detection limit of the calibration curve formed by the supplied controls for each cytokine. The lower limit of detection was classed as 2.5 standard deviations above the level of background emission. To eliminate any residual batch variation, all samples were measured on a single batch of 96-well multi-spot plates in duplicate and the resulting mean value used for analysis.

2.9. Production of activated Vγ9$^+$ T cell supernatant

Vγ9$^+$ T cells isolated as in 2.6.4 were suspended at 0.5 million/ml in complete RPMI-1640 culture medium in a 24-well flat bottom culture plate (Nunc plates; Thermo Scientific). 10 nM of HMB-PP was then added for 24 hours in an incubator maintained at 37°C with a humidified environment containing 5% CO_2. Following incubation, the plate was centrifuged at 400 *g* for 3 minutes and the resulting supernatant was removed, filtered using a 0.22 μM pore sized hydrophilic polyethersulfone membrane (Millipore) and stored at – 70°C. Activation of the Vγ9$^+$ T cells was confirmed by elevated levels (>50% positivity) of cell surface expression of CD69 and CD25 on FACS analysis compared with isotype controls. These levels were confirmed as being greatly above the corresponding values in the baseline non-stimulated cells.

2.10. Production of activated MAIT cell supernatant

MAIT cells isolated as shown in 2.6.5 were suspended at 0.5 million/ml in complete RPMI-1640 culture medium in a 24-well flat bottom culture plate (Nunc plates; Thermo Scientific). 6 μl of Dynabeads® Human T-Activator CD3/CD28 (Life Technologies) containing 0.25 million beads in a 1:2 bead-to-cell ratio were then added for 24 hours in an incubator maintained at 37°C with a humidified environment containing 5% CO_2. Following incubation, the plate was centrifuged at 400 *g* for 3 minutes and the resulting supernatant was removed, filtered using a 0.22 μM pore size hydrophilic polyethersulfone membrane (Millipore) and stored at – 70°C. Activation of the MAIT cells was confirmed by elevated levels (>50% positivity) of cell surface expression of CD69 and CD25 on FACS analysis compared with isotype controls. These levels were confirmed as being greatly above the corresponding values in the baseline non-stimulated cells.

2.11. Co-cultures of Vγ9$^+$ T cells and monocytes

Purified monocytes were added at 2 million/ml in complete RPMI medium in a variety of conditions including in the presence of Zometa 10 μM, ultra-pure LPS 100 ng/ml and Vγ9$^+$ cell supernatant 1:4. These were cultured for 18 hours before analysis of cytokine production was performed.

2.12. Antigen presentation assays with sepsis neutrophils

M1-specific CD8$^+$ T cells were generated by stimulating PBMCs with 0.1 nM M1p58-66 peptide (kindly provided by P. Romero, University of Lausanne, Switzerland). After 3 days, 40 U/mL of IL-2 was added. Cells were re-stimulated after 10–14 days in the presence of irradiated (40 Gy) PBMCs. Resting cells with 25–45% M1p58-66–specific cells were used for assays, as determined by tetramer staining (kindly provided by A. Sewell, Cardiff University, United Kingdom). M1(p58-66) specific CD8$^+$ T cell lines were >95% pure, as confirmed by tetramer staining (Figure 2.4). Sepsis patients recruited were rapidly typed for their HLA-A2 status using FACS analysis, gated on neutrophils using whole blood lysed using 0.2% hypotonic saline. Samples that were HLA-A2$^+$ compared with isotype controls were subsequently used in the remainder of the experiment. Fresh neutrophils from these HLA-A2$^+$ sepsis patients were incubated with 0.01-1 μM recombinant influenza M1 protein for 18 hours or cultured in medium for 17 hours before addition of 0.1 μM M1(p58-66) peptide for a further 1 hour. In each case, following extensive washing, neutrophils were incubated with HLA-A2$^+$ peptide-specific CD8$^+$ T cells at a ratio of 1:1. After 1 hour, 10 μg/ml brefeldin A (Sigma) was added and cultures were incubated for a further 4 hours. Activation of M1(p58-66) positive CD8$^+$ T cells was assessed by intracellular cytokine staining with the relevant controls and analysed by flow cytometry. Expanded M1-specific CD8$^+$ T cells were kindly provided by W. Khan, Cardiff University, United Kingdom.

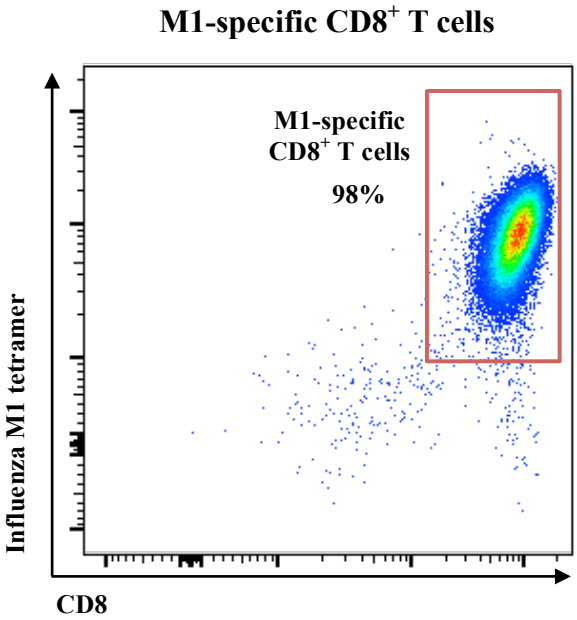

Figure 2.4 Flow cytometric purity of M1-specfic CD8$^+$ T cells

After the exclusion of dead cells and doublets, gating on Influenza M1p58-66 tetramer$^+$ and CD8$^+$ cells was used to ensure a high purity in the responder cell population.

2.13. Statistical methods

2.13.1. Basic statistical analyses

Statistical analyses were performed using SPSS 19.0, GraphPad Prism 6.0 and R version 3.0.2. All variables were tested for normal distributions visually and using the Shapiro-Wilk test. Nonparametric variables were log-transformed where required. Descriptive statistics are expressed as medians with interquartile ranges unless stated otherwise. Tests of significance used in Chapter 3 are shown in Table 2.6. The statistical analyses used in Chapter 4 are outlined in Table 2.7

Although non-parametric tests could be employed in place of transformation, the differences acquired in the initial comparisons were used to inform the formation of combination models through linear regression and predictive modelling. Therefore, the capture of any potential significant differences was of prime importance and any artifactual differences would be subsequently excluded through the production of non-linear, non-parametric modelling.

Table 2.6 Statistical tests used in Chapter 3.

Comparison	Statistical test
Healthy/sepsis/SIRS	One-way ANOVA, non-assumption of equal variability and Tukey's correction for multiple comparisons.
Sepsis died/sepsis survived	Multiple t tests with Holm-Sidak method for correction for multiple comparisons.
Culture-negative/Gram-positive / Gram-negative	One-way ANOVA, non-assumption of equal variability and Tukey's correction for multiple comparisons.

Outline of the statistical tests used in the main immunophenotyping chapter in different comparator groups.

Table 2.7 Statistical tests used in Chapter 4.

Comparison	Statistical test
Monocyte cytokine responses to LPS stimulation	Analysis is based on a repeated measures two-way ANOVA with Dunnett's correction for multiple comparisons based on a reference group of medium cultured cells. The use of Dunnett's correction here is due to the reference of a control group.
Osteoporosis patient data analysis	Data were analysed using a matched Friedman test due to the non-parametric nature of the data with the reference group as day 0 and Dunn's correction for multiple comparisons.
Antigen presentation data	Data were analysed by one or two-way ANOVA with Dunnett's post-hoc testing. The use of Dunnett's correction here is due to the reference of a control group. Where no control group was used, Bonferroni's post-hoc testing was used. Any paired data were analysed using Mann-Whitney tests
Sepsis subset data	Smaller data subsets used here were analysed using Kruskal-Wallis tests and Dunn's multiple comparison tests and paired data using Mann-Whitney tests.

Outline of statistical tests used in the immunosuppression analyses in different comparator groups.

2.13.2. Regression analyses

Predictive biomarkers were assessed using linear regression; statistically significant ($p < 0.05$) variables from univariate analyses were included in multiple regression analyses based on forward selection or all variables included with backward selection as indicated.

2.13.3. Receiver operator curve analyses

Discrimination between binary groups was assessed using the area under the receiver operating characteristic curve (AUC). Comparisons between different AUC values resulting from different receiver operating curves were compared using a nonparametric approach. The receiver operating curve analysis was also used to calculate cut-off sensitivity and specificity values. The resulting models from multiple regression and machine learning analyses were used to produce predicted values for combinations of biomarkers. These values were then used to form additional combination receiver operating curves. All distributions shown in figures relate to the mean and standard error of the mean unless otherwise stated.

2.13.4. Machine learning algorithms

The production of neural networks for combination biomarker prediction utilised the Neural Networks in R using the Stuttgart Neural Network Simulator (SNNS) version 0.4. Unless otherwise stated this used 2 hidden nodes with a 10% training: testing set split and 3000 maximum training iterations. Further details are given in 3.3.1.4, “Fingerprint prediction models”. Decision trees were produced using Recursive Partitioning and Regression Tree package (rpart) version 4.1-8 the full script of which can be found in 3.3.1.4, “Fingerprint prediction models”.

2.14. The contribution of data by others

There have been important contributions by others that have enabled this work to synthesize and make sense of a complex story. Dr Ann Kift-Morgan carried out the multiplex cytokine analysis discussed in Chapter 3. Dr Joanne Welton contributed work related to the osteoporosis patient data in Chapter 4 and Dr Martin Davey contributed data related to the in vivo neutrophil analysis in Chapter 4

CHAPTER 3

CHARACTERISATION OF IMMUNE RESPONSES IN SEPSIS

Chapter 3 Characterisation of immune responses in sepsis

3.1. Introduction

Accurate prediction forms a cornerstone of modern medicine. Prediction leads not only to medical diagnostics but also to outcome forecasting as demonstrated in Chapter 1, both of which are essential to the delivery of evidence-based treatments to the right patients, at the right times[99-101]. Whilst medical diagnostics have advanced since the age of relying purely upon a patient's history and examination, it still depends upon on a small number of poorly performing biomarkers often considered in isolation[99,100,102,103]. This is divorced from the understanding of health being a complex integration of multiple systems with reciprocal change and interconnected results.

This chapter aims to not only identify new biomarkers that may be useful in the diagnosis of sepsis, the prediction of death or the prediction of an infecting organism type, but also importantly to combine a number of biomarkers using novel statistical techniques. In combination, biomarkers that have historically been of little use clinically may produce accurate prediction models that impact upon patient care.

However, before this process can start, the immunological changes that occur in sepsis and related conditions will firstly be described. These changes will be considered from clinical, cellular and humoral immunology perspectives in a range of patients classified by disease type, survival, and infecting organism subgroups.

Whilst this descriptive approach is essential for the formation of predictive models, it has several shortcomings. Most notably, this approach will be unable to draw conclusions about the mechanistic basis for any descriptive changes shown in different subgroups. This chapter must rely upon peer-reviewed, published evidence to explore what these underlying mechanisms may be. However, it is hoped that this process of description can form the initial part of a journey towards developing mechanistic theories that underpin an eventual understanding of this complex, devastating disease. Furthermore, even before a complete understanding is achieved, descriptive changes

can be applied pragmatically to help advance patient care through resulting predictive models.

3.2. Aims

- Describe the early clinical, cellular and humoral immunological changes in:
  (a) Acute severe sepsis patients.
  (b) Acute severe SIRS patients.

- Perform comparative analysis between these groups including healthy controls.

- Describe sub-group differences in sepsis patients according to:
  (a) Patient survival.
  (b) Infecting organism subtype.

- Form statistical models to accurately predict patient diagnosis, outcome, and infecting organism subtype in sepsis. These models should take into consideration the practical aspects of developing point-of-care diagnostic tests used in a clinical environment.

3.3. Results

Figure 3.1 summarises the total number of sample sets used in the different aspects of the study for patients with sepsis. A similar outline is provided in Figure 3.2 for SIRS patients and healthy controls.

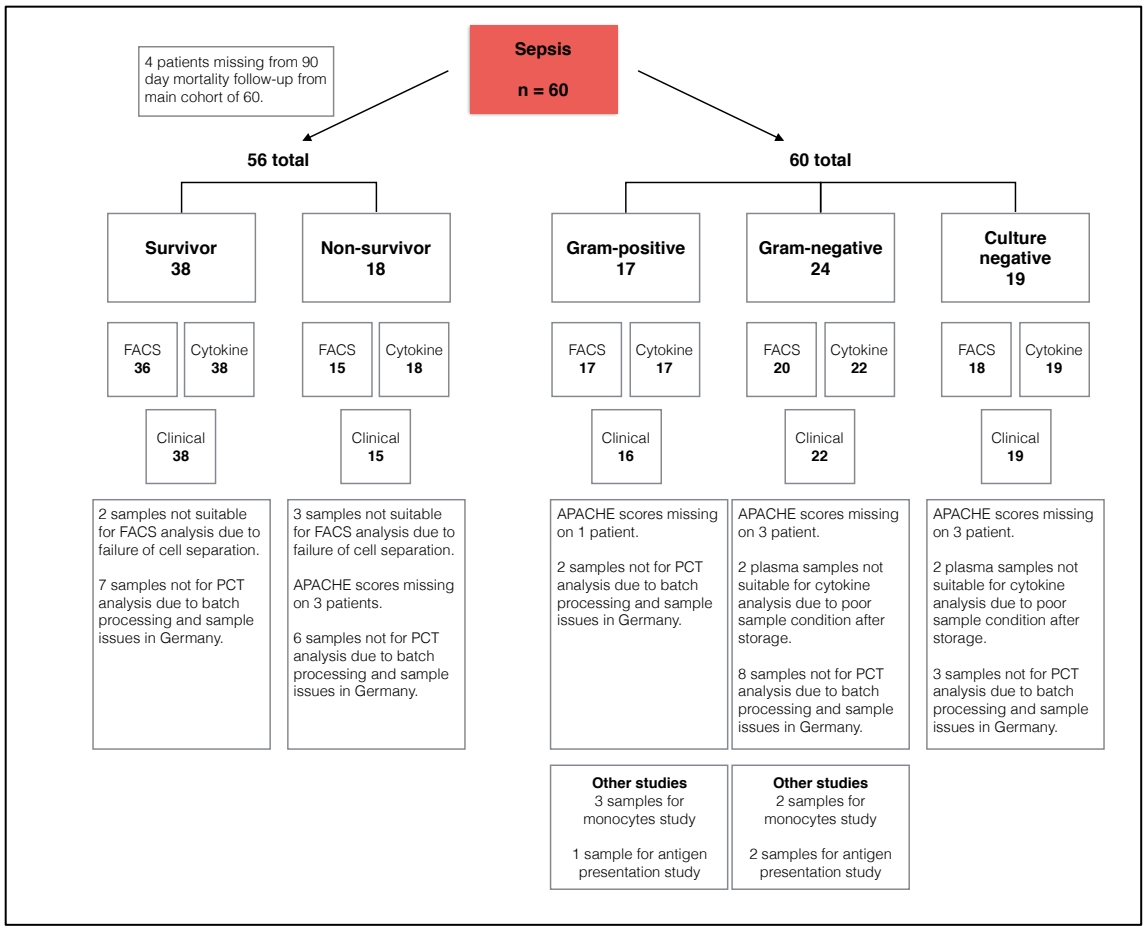

Figure 3.1 Overview of sample flow in recruited sepsis patients.

The above outlines the numbers of samples processed and analysed in sepsis patients recruited into the main study. Where there are discrepancies in the number of samples taken forward, an explanation is given in the free text areas. It shows further breakdowns of survival and organism class along with the use of these samples in subsequent experiments.

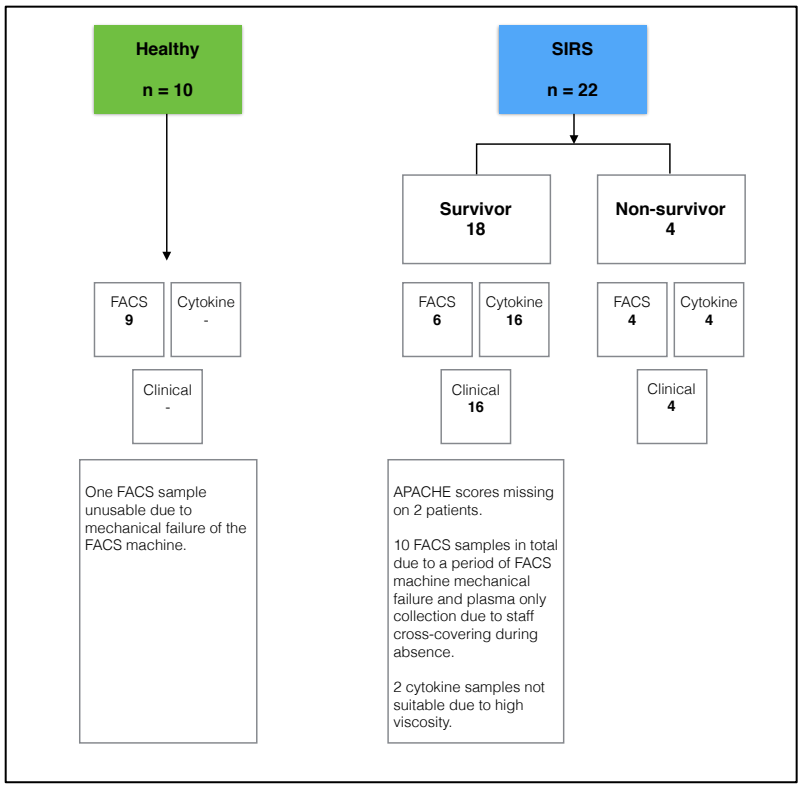

Figure 3.2 Overview of sample flow in recruited healthy control and SIRS patients.

The above outlines the numbers of samples processed and analysed in healthy controls and SIRS patients recruited into the main study. Where there are discrepancies in the number of samples taken forward, an explanation is given in the free text areas.

3.3.1. Immune differences according to survival status

In order to study differential immune responses between survivors and non-survivors at 90 days, data from 56 of the patients recruited with severe sepsis on day 1 of their admission to ICU were analysed. Using clinical and microbiological data collection, multi-colour flow cytometry and multiplex ELISA, differences that may exist between these groups were analysed. The groups were well matched with similar ages, gender distributions, and body mass index (BMI) measurements with no significant differences in the sites of pathology (Table 3.1).

Table 3.1 Baseline characteristics of sepsis patients according to survival status at 90 days.

	Sepsis lived	**Sepsis Died**
Total number of patients	38	18
Age (median (quartiles)) years	60 (50-73)	63 (60-71)
Male gender (%)	50	50
BMI (median (quartiles))	27.5 (23.8-35.0)	21.3 (25.0-37.5)
Site of pathology (%)		
Abdominal	14 (36.8)	8 (44.4)
Respiratory	15 (39.5)	6 (33.3)
Soft tissue	5 (13.2)	2 (11.1)
Urinary tract	4 (10.5)	2 (11.1)

The table shows intergroup differences in the age, gender, BMI, or site of pathology of patients in each respective group.

3.3.1.1. Clinical differences

Clinical measures of immune status are a key feature of a patient's initial investigations when admitted to ICU with severe sepsis. These include a differential white cell count and biomarkers such as C-reactive protein (CRP). Figure 3.3 shows no significant differences in these measures at either day 1 or day 5 of a patient's admission with severe sepsis. Furthermore, whilst the eventual outcome between both groups is radically different, initial organ failure scores used to assess disease severity show no differences at either day 1 or day 5 (Figure 3.4). These scoring systems include the Acute Physiology and Chronic Health Evaluation II (APACHE) score capturing the worse value in twelve physiological parameters during the first 24-hours of critical care

admission, and the Sequential Organ Failure Assessment (SOFA) score based on a six component, organ-based calculation measured throughout a patient's stay. Further details of these scoring systems can be found in Appendix 1: Scoring systems used in critical care.

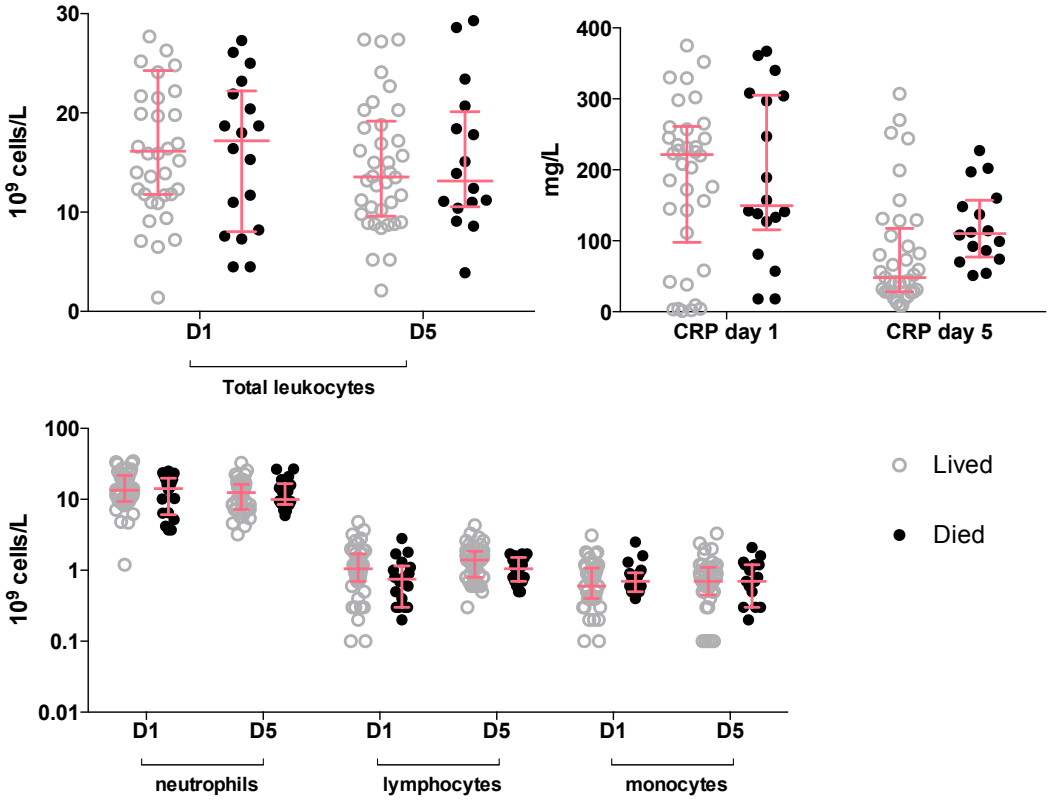

Figure 3.3 Differences in standard clinical immune parameters between sepsis survivors and non-survivors. Differences in commonly measured clinical immune parameters are shown between sepsis survivors and non-survivors at both day 1 and day 5 time points. These include peripheral blood total leukocyte, neutrophil, lymphocyte and monocyte counts, as well as plasma CRP level. Day 1 survivors n = 38, day 5 survivors n = 37, day 1 non-survivors n = 18, day 5 non-survivors n = 16.

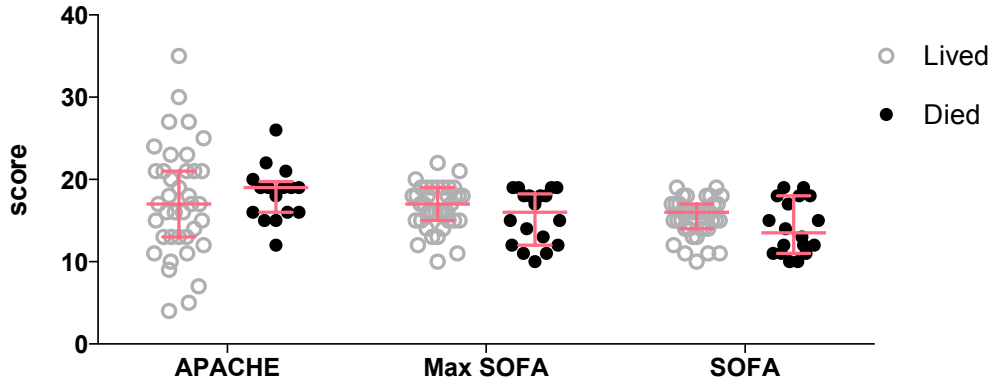

Figure 3.4 Differences in severity of illness scores between sepsis survivors and non-survivors.

Severity of illness scores in sepsis survivors and non-survivors are shown including APACHE and SOFA scores. The maximum SOFA score was the highest recorded during a patient's ICU admission excluding periods following active withdrawal of treatment. Survivors n = 38, non-survivors n = 15 for APACHE and 18 for SOFA and max SOFA scores.

3.3.1.2. Cellular immunology

By examining the immune response in more detail using multi-colour flow cytometry, subtle differences can be shown in patients that ultimately die from sepsis. Whilst the basic clinical immune characterisation failed to show differences in differential white cell counts, Figure 3.5 shows minor significant differences in $CD3^+$ T cells as a percentage of total cells. These changes were not compensated by statistically significant reciprocal increases in the other cell subsets measured. There were further trends in subdivisions of $CD3^+$ T cells, with a higher percentage of $V\gamma9^+$ T cells in survivors although this was not statistically significant.

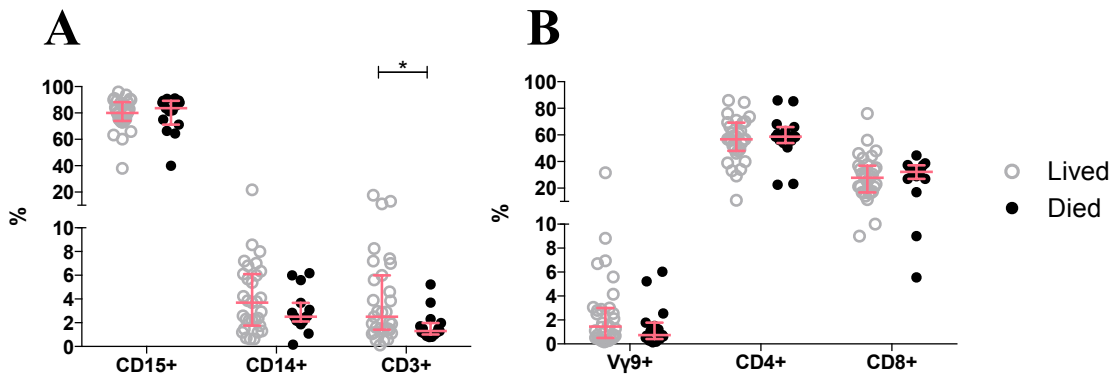

Figure 3.5 Differences in immune cell types analysed by flow cytometry in sepsis survivors and non-survivors. The main cell lineages observed in peripheral blood are shown in sepsis survivors and non-survivors. (A) Shows the differential leukocyte split into $CD15^+$ neutrophils, $CD14^+$ monocytes and $CD3^+$ lymphocytes. (B) Shows how the $CD3^+$ subpopulations are further sub-divided in $V\gamma9^+$ T cells, $CD4^+$ T cells, and $CD8^+$ T cells in these differing groups. Survivors n = 36, non-survivors n = 15. Numbers in specific gates may vary due to low subset number.

Whilst neutrophil influx and activation is a major component of the pathophysiology of sepsis, there were few differences in the patterns of activation in survivors and non-survivors (Figure 3.6). However, rapidly elevated levels of cell-surface CD80 on neutrophils, likely due to translocation, were seen in survivors pointing towards new gain-of-function abilities in these neutrophils. This also fits with a trend of increased CD86 also required for antigen presentation cell (APC)-like functions.

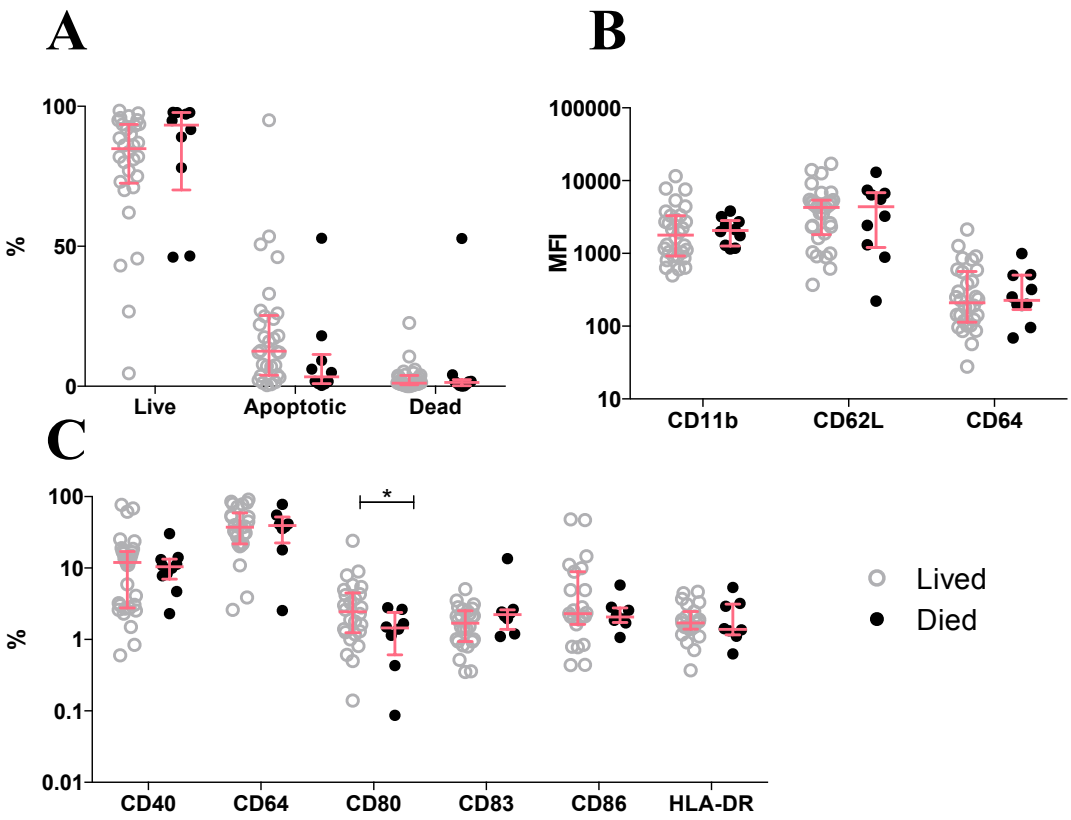

Figure 3.6 Differences in neutrophil survival and cell-surface markers in sepsis survivors and non-survivors. (A) Neutrophil survival analysis using aqua staining of gated single neutrophils in sepsis survivors and non-survivors. (B) Cell-surface expression levels of classical neutrophil activation markers CD11b, CD62L, and CD64 in sepsis survivors and non-survivors measured in mean fluorescence intensity (MFI). (C) Levels of cell-surface markers CD40, CD64, CD80, CD83, CD86, and HLA-DR on neutrophils from sepsis survivors compared with non-survivors measured in percentage of positive expression compared with isotype controls. Survivors n = 36, non-survivors n =12. Numbers in specific gates may vary due to low subset number.

Sepsis monocytes showed a similar pattern of APC-related cell-surface protein expression differences in survivors and non-survivors including elevated levels of HLA-DR and CD86 in survivors (Figure 3.7). In addition, there was a small yet significant increase in CD64 on monocytes in non-survivors.

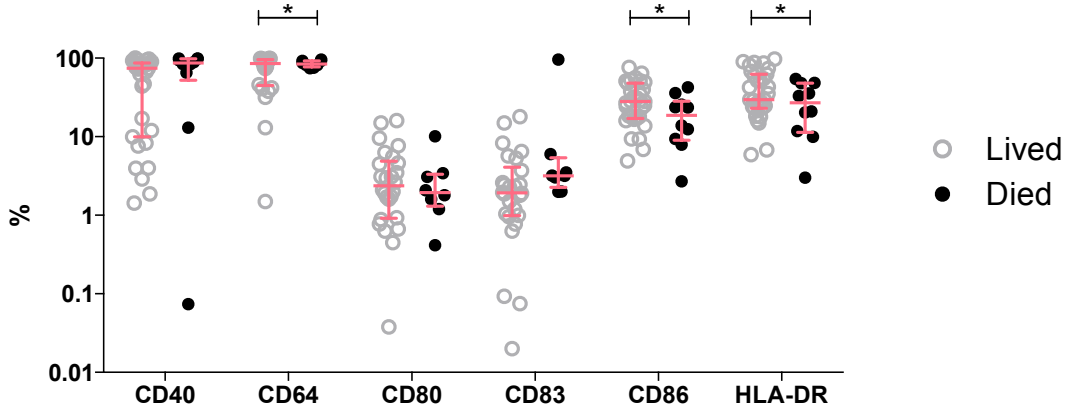

Figure 3.7 Differences in monocyte cell-surface markers seen in sepsis survivors and non-survivors.

Levels of cell-surface markers CD40, CD64, CD80, CD83, CD86, and HLA-DR on monocytes from sepsis survivors and non-survivors measured in percentage of positive expression compared with isotype controls. Survivors n = 35, non-survivors n = 13. Numbers in specific gates may vary due to low subset number.

It can also be seen in Figure 3.8 that although there is a trend for increased cell activation across the lymphocyte subtypes, there are no significant differences.

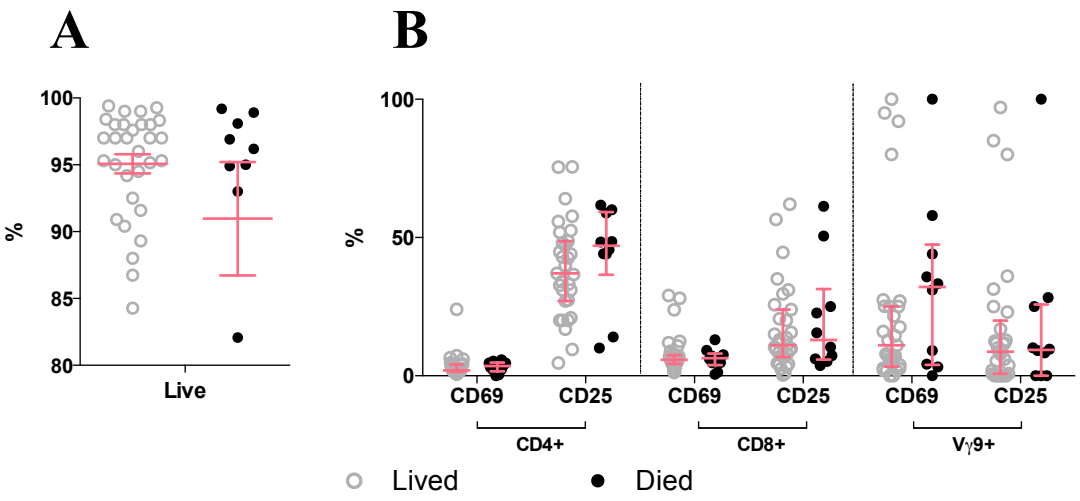

Figure 3.8 Survival and activation markers in $CD3^+$ T cells and their subtypes in survivors and non-survivors. (A) $CD3^+$ T cell death analysed according to aqua staining on $CD3^+$ gated cells. (B) Cell-surface activation makers CD25 and CD69 expressed on $CD4^+$, $CD8^+$, and $V\gamma9^+$ T cells in sepsis survivors compared with non-survivors. All values are measured in percentage of positive expression compared with isotype controls. Survivors n = 31, non-survivors n = 9. Numbers in specific gates may vary due to low subset number.

Finally, the subset markers on both $V\gamma9^+$ and $V\gamma9^-$ $CD3^+$ T cells as well as more generalised memory markers for lymphocytes were examined (Figure 3.9 and Figure 3.10). Again, no significant differences were found in these divisions when considering survival as an outcome.

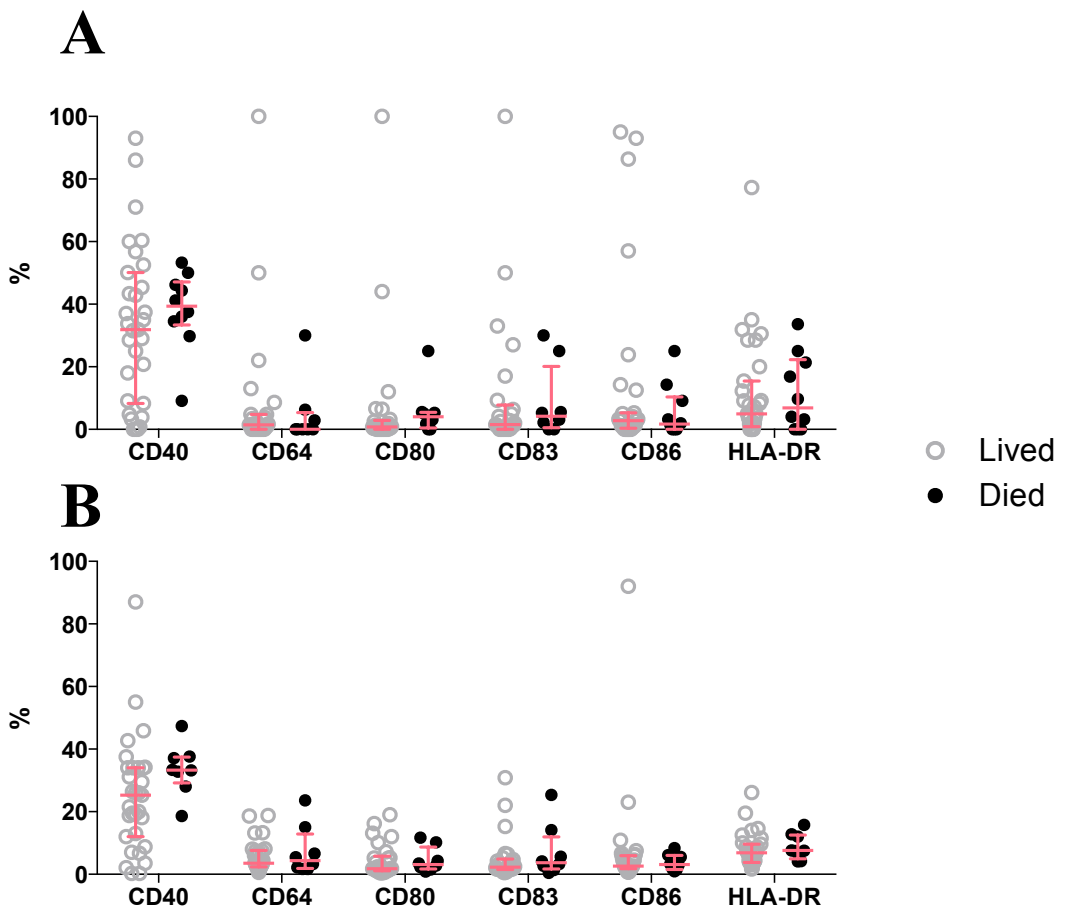

Figure 3.9 Cell-surface markers on Vγ9^{+} and Vγ9^{-} CD3^{+} T cells in sepsis survivors and non-survivors. (A) Vγ9^{+} T cell and (B) Vγ9^{-} T cell expression of cell-surface markers CD40, CD64, CD80, CD83, CD86, and HLA-DR on sepsis survivors compared with non-survivors. All values are measured in percentage of positive expression compared with isotype controls. Survivors n = 31, non-survivors n = 9. Numbers in specific gates may vary due to low subset number.

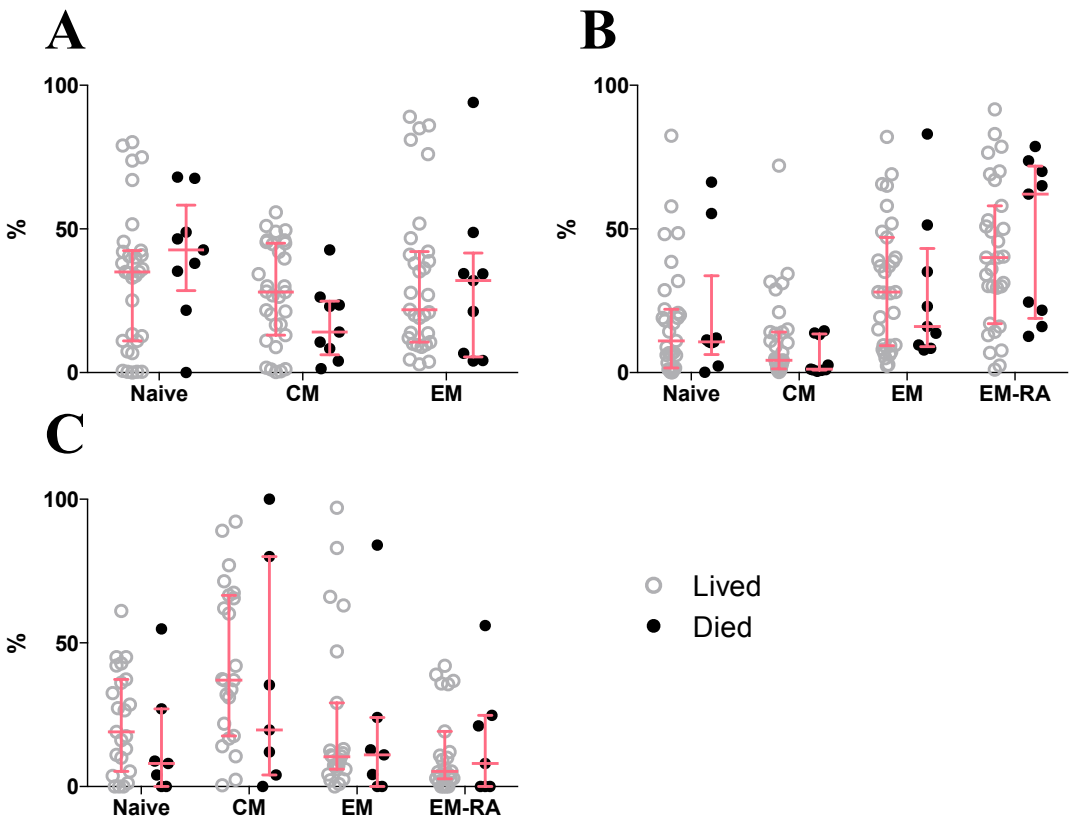

Figure 3.10 Memory subsets of CD4$^+$, CD8$^+$, and Vγ9$^+$ T cells in survivors and non-survivors. (A) CD4$^+$, (B) CD8$^+$ and (C) Vγ9$^+$ cell divisions of memory subsets. Naïve subsets in CD4$^+$ and CD8$^+$ T cells were characterised as CD45RA$^+$/CCR7$^+$ cells, central memory (CM) as CD45RA$^-$/CCR7$^+$ cells, effector memory (EM) as CD45RA$^-$/CCR7$^-$ cells and effector memory RA (EM-RA) as CD45RA$^+$/CCR7$^-$ according to the classification by Sallusto et al., 1999[96].Vγ9$^+$ cells were classed as naïve CD45RA$^+$/CD27$^+$, central memory CD45RA$^-$/CD27$^+$, effector memory CD45RA$^-$/CD27$^-$ and effector memory RA CD45RA$^+$/CD27$^-$ subtypes, based on the definition by Dieli et al., 2003[97]. Survivors n = 31, non-survivors n = 9. Numbers in specific gates may vary due to low subset number.

3.3.1.3. Cytokine analysis

To gain a complete picture of the immunological differences seen in these two populations, the humoral aspects of the immune response need to be considered as well as the cellular components. By using stored plasma from these patients, multiplex cytokine analysis was performed on day 1 and 5 of ICU admission.

It is clear that survivors showed a greater proinflammatory cytokine response to sepsis at an early time point (Figure 3.11). Procalcitonin measured using the sensitive assay variation as well as IL-6 and GM-CSF were significantly elevated in survivors compared with non-survivors. These cytokines are known to rise quickly following systemic infection whilst others, such as IL-2, may need a cascade of secondary signals to produce a maximal response. Therefore, IL-2 was not found to be elevated until day 5

(Figure 3.12). At this later time point, greater levels of the ultra-sensitive Kryptor procalcitonin analysis (sensePCT), pro-ADM, GM-CSF, IFN-γ and IL-2 were associated with non-survivors, perhaps indicating the presence of continued, unresolved infection or second-hit infections.

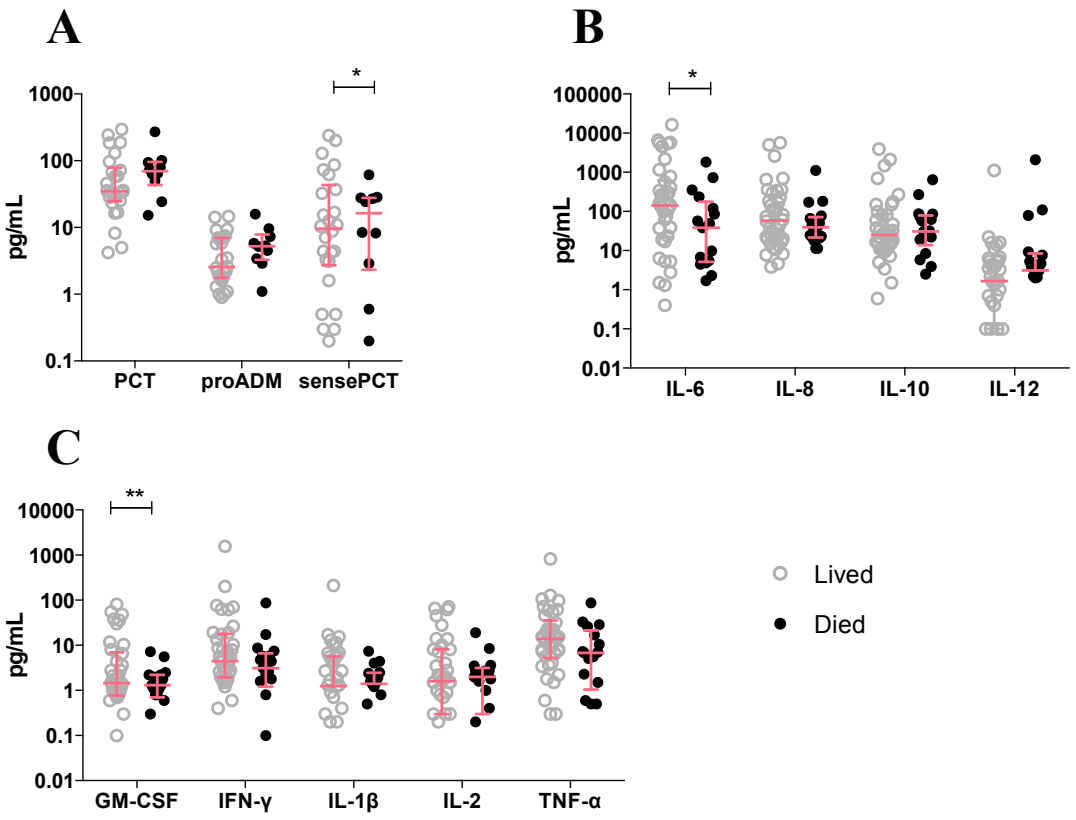

Figure 3.11 Day 1 differences in plasma cytokine levels in sepsis survivors and non-survivors.

Cytokines are divided according to their relative level of magnitude in pg ranges. (A) Levels of procalcitonin (PCT), proadrenomedullin (proADM), and the sensitive Kryptor procalcitonin assay (sensePCT) in sepsis survivors compared with non-survivors. (B) Levels of IL-6, IL-8, IL-10 and IL-12 in sepsis survivors compared with non-survivors. (C) GM-CSF, IFN-γ, IL-1β, IL-2 and TNF-α levels in sepsis survivors compared with non-survivors. Survivors n = 31 (A) and 38 (B & C), non-survivors n = 12 (A) and 18 (B & C).

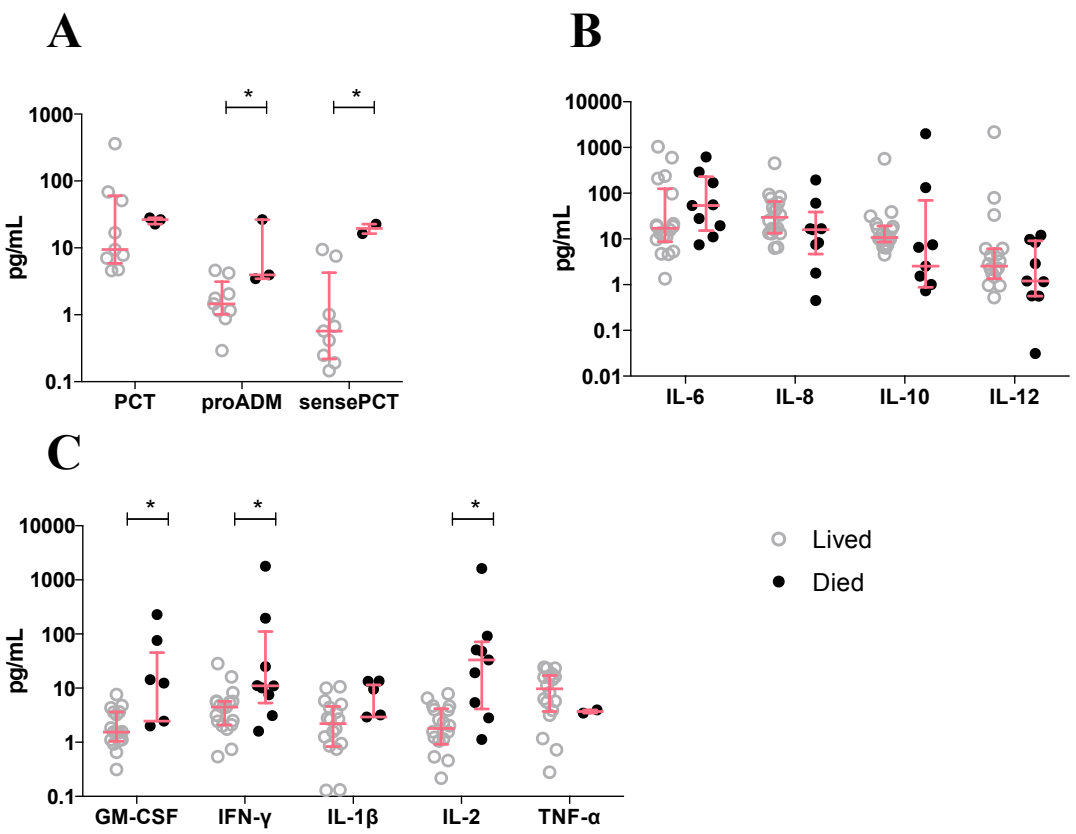

Figure 3.12 Day 5 differences in plasma cytokine levels seen in survivors and non-survivors.

Cytokines are divided according to their relative level of magnitude in pg ranges. (A) Levels of procalcitonin (PCT), proadrenomedullin (proADM), and the sensitive Kryptor procalcitonin assay (sensePCT) in sepsis survivors compared with non-survivors. (B) Levels of IL-6, IL-8, IL-10 and IL-12 in sepsis survivors compared with non-survivors. (C) GM-CSF, IFN-γ, IL-1β, IL-2 and TNF-α levels in sepsis survivors compared with non-survivors. Survivors n = 9 (A) and 21 (B & C), non-survivors n = 3 (A) and 9 (B&C).

3.3.1.4. Fingerprint prediction models

Using the immune differences so far identified, it appears possible to select single markers to produce a diagnostic test that distinguishes survivors from non-survivors such as PCT, IL-6, and GM-CSF. However, given the complexity, variation, and subtlety of these differences, the sensitivity, specificity, and usefulness of such a single marker would be limited. Indeed this has been found to be the case in many of the newer identified biomarkers[99,102-104]. However, using a combination of small signals to predict the likelihood of patient survival would be a more robust and ultimately more physiologically plausible technique considering the complexity of a system of this nature.

Whilst all of the markers that showed statistical differences could be combined, ideally a resulting model should be practical as well as accurate. Such analysis needs to be possible not only in a laboratory setting but also at the point-of-care as a useful diagnostic test to rapidly impact on patient survival in the real world. Statistical techniques that reduce the numbers of variables used to form predictive models can thus be used for this purpose.

In Table 3.2, all significant variables identified in the preceding analysis were entered into a binary logistic model with backward conditioning. These included IL-6, sensePCT, GM-CSF, CD3%, $CD14^+CD86\%$, $CD14^+HLA\text{-}DR\%$, $CD14^+CD64\%$, $CD15^+CD80\%$. This model can identify the most suitable measures that correctly differentiate between the binary outcomes of survival and non-survival. In this case, a model was produced that included just two variables (day 1 $CD3^+$ percentage and day 1 GM-CSF level) that could be used to predict patient survival. Using this model and applying it to the existing dataset allowed the generation of a receiver operator curve (ROC) to further investigate the clinical usefulness of this prediction. This model provided an AUC of 0.77 (95% confidence intervals of 0.66 – 0.89) for the prediction of patient death calculated at day 1 shown in Figure 3.13.

Table 3.2 Predictor variables for patient survival selected using binary logistic regression with backwards conditioning.

	B	S.E.	Wald	df	Sig.	Exp(B)	CI lower	CI upper
CD3%	-.534	.249	4.593	1	.032	.587	.287	-.534
D1 GM-CSF	-.190	.131	2.092	1	.148	.827	.521	-.190
Constant	.739	.669	1.219	1	.270	2.094		

All significant variables were entered into this model of patient survival using binary logistic regression with backwards conditioning at $p < 0.05$. The remaining significant variables in the prediction model at this level were day 1 $CD3^+$ cell percentage from total cells measured by flow cytometry and day 1 level of plasma GM-CSF measured by ELISA.

Whilst this model gives an AUC that is comparable to many diagnostic tests used in medicine today[102-104], new statistical methods can further improve upon this approach. Neural network models allow complex non-linear relationships to be effectively modelled for not only binary but also multinomial outputs. However, the ability to "prune" these networks to reduce the number of variables required for accurate modelling is poorly developed. Therefore, by using a script designed to progress

through all permutations of an incremental number of defined variables, models could be compared using their relative AUC values. Table 3.3 demonstrates that using a combination of just three variables (IL-6, sensePCT, CD3%) neural networking could produce a prediction model able to distinguish patient survival at day 1 with an AUC value of 0.90 (95% confidence intervals of 0.78 – 0.99). The highlighted row is suggested as the most practical combination of variables that may be taken forwards for development into a point-of-care test. The practical results from the requirement to measure just two key cytokines along with one cell lineage percentage achievable reliably, at speed and for a low cost. This resulting model is shown in Figure 3.13 and the script written to perform this calculation shown in Appendix 3: R script. As outlined in 2.13.4 Machine learning algorithms, this analysis uses 2 hidden nodes and 3000 bootstrapped maximum iteration. Although there is no theoretical limit on the number of hidden layers in a typical back-propagation network, there are typically between 1 and 2. The AUCs generated were preferable where 2 hidden nodes were used (data not shown).

Table 3.3 Predictor variables for patient survival selected using neural network modelling.

Number of variables	Combination	AUC
8	IL-6, sensePCT, GM-CSF, CD3%, $CD14^+$CD86%, $CD14^+$HLA-DR%, $CD14^+$CD64%, $CD15^+$CD80%	0.99
7	IL-6, sensePCT, CD3%, $CD14^+$CD86%, $CD14^+$HLA-DR%, $CD14^+$CD64%, $CD15^+$CD80%	0.99
6	IL-6, sensePCT, CD3%, $CD14^+$HLA-DR%, $CD14^+$CD64%, $CD15^+$CD80%	0.98
5	IL-6, sensePCT, CD3%, $CD14^+$CD64%, $CD15^+$CD80%	0.97
4	IL-6, CD3%, $CD14^+$CD64%, $CD15^+$CD80%	0.96
3	IL-6, sensePCT, CD3%	0.90
2	IL-6, $CD14^+$HLA-DR%	0.87

All significant variables were modelled using a feed-forward neural network model with 2 hidden nodes and 3000 maximum iteration. The table shows the best AUC values for each number of possible variable combinations. The highlighted combination of IL-6, sensePCT (Kryptor assay) and $CD3^+$ cell percentage from total cells was most favourable given the AUC value and the practical advantages of a small variable number for development into a point-of-care test.

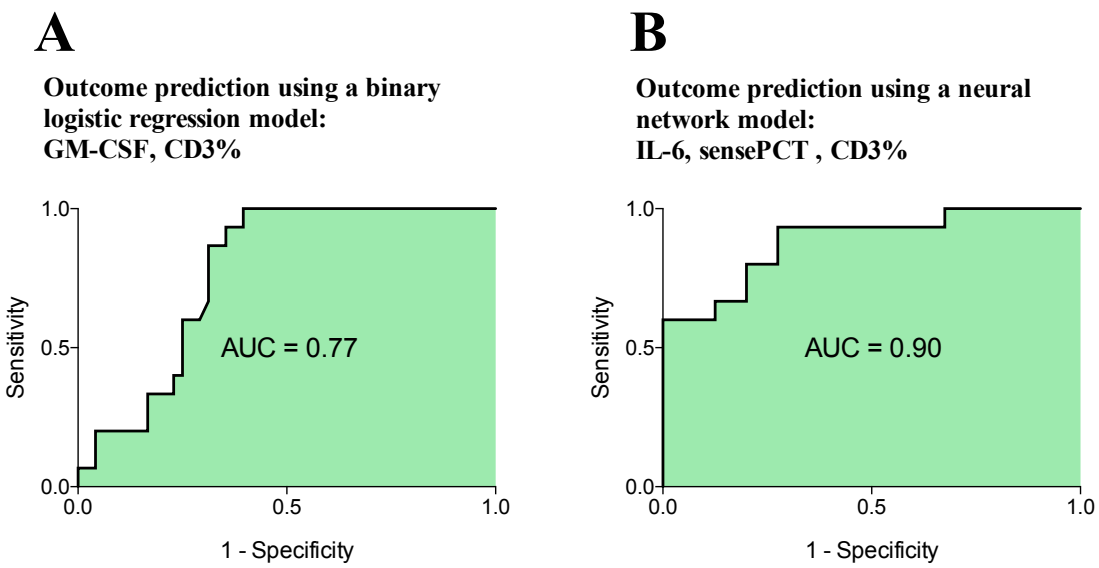

Figure 3.13 ROC curves for prediction of patient survival using logistic regression and neural network modelling. Using the variables sets previously selected, ROC curves were constructed using the predicted probabilities from each model's output. (A) Shows a binary logistic regression model with 2 predictor variables (day 1 plasma GM-CSF and $CD3^+$ cell percentage from total cells) with an AUC of 0.77. (B) Uses a neural network model with 3 predictor variables (day 1 plasma IL-6, day 1 sensePCT (Kryptor assay), and $CD3^+$ cell percentage from total cells showing an AUC value of 0.90 for patient survival.

Following production of the neural network model, a decision tree was constructed (Figure 3.14) using the same variable set for further validation. Whilst the linear nature of the decision tree limits its ability to perform to the same degree of accuracy as the neural network model, it does allow cut-off values to be suggested. Through the process of decision tree production, the three input variables have been automatically reduced to two due to model saturation. The sensitivities shown in this tree are representative of the total sensitivity for that outcome whilst the specificities relate to the individual specificities of each branch.

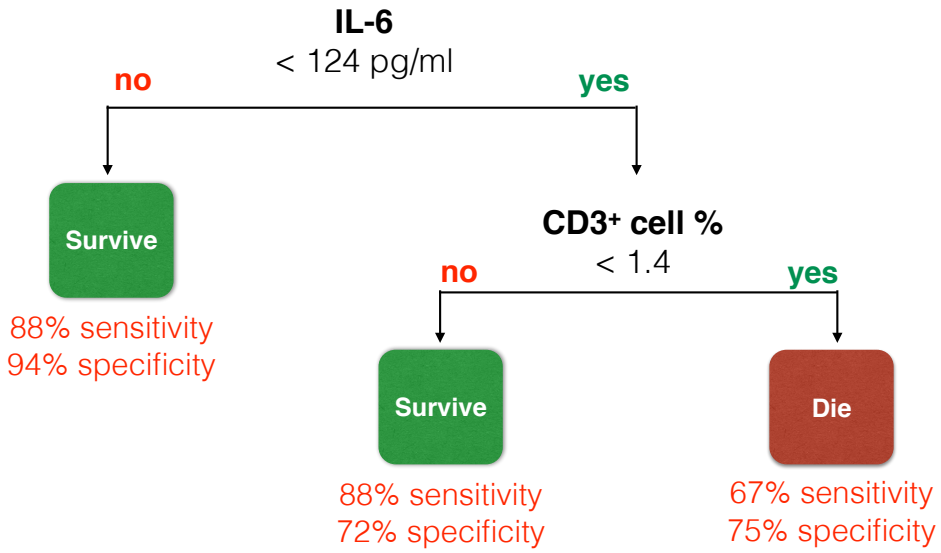

Figure 3.14 A decision tree model for prediction of patient survival.

Using the variable sets previously selected, a decision tree model was constructed without forced pruning. The resulting variables included in the decision trees were automatically chosen according to the ability to discriminate based on the illustrated cut-off values. In this example the $CD3^+$ cell percentage from total cells plus day 1 IL-6 concentrations were required. The sensitivities relate to the overall sensitivity for that diagnostic category in all branches whilst the specificity relates to branch specific values, as is the nature of decision tree analyses.

3.3.2. Immune differences seen in sepsis and SIRS

The differentiation between patient survival and non-survival has already been considered. This chapter will now consider the ability of immunophenotyping to distinguish between the states of health, sepsis and SIRS. The baseline characteristics for these different patient groups are shown in Table 3.4, demonstrating a lower age in the SIRS population compared with sepsis patients. Despite these age differences, other indices including the severity of illness scores were uniform across the groups. However, the sites of pathology did differ between patients with sepsis and SIRS as described in Table 3.4.

Table 3.4 Baseline characteristics in patients with sepsis, SIRS, and healthy controls.

	Sepsis	SIRS	Healthy
Total number of patients	60	22	10
Age (median (quartiles)) years	63 (54-71)*	44 (34-65)*	57 (54-63)
Male gender (%)	50.9	76.5	50.0
BMI (median (quartiles))	27.5 (24.7-35.7)	31.5 (22.5-31.6)	27.6 (24.2-29.1)
ICU mortality (%)	9 (15.0)	2 (9.1)	-
Hospital mortality (%)	14 (23.3)	4 (18.1)	-
90-day mortality (%)	18 (32.1)	4 (18.1)	-
Site of pathology (%)*			
Abdominal	22 (36.7)	6 (27.3)	
Cardiac	0	1 (4.5)	
Trauma	0	4 (18.2)	
Respiratory	23 (38.3)	6 (27.3)	
Soft tissue	9 (15.0)	2 (9.1)	
Urinary tract	6 (10.0)	1 (4.5)	
Other	0	2 (9.1)	

The table shows intergroup differences in the age, gender, BMI, ICU mortality, and sites of pathology of patients in each respective group. 90-day hospital mortality related to 56 sepsis patients for which 90 days follow-up was possible as shown in the previous section.

3.3.2.1. Clinical differences

No standard clinical immune investigations measured were able to distinguish between sepsis and SIRS apart from an elevated CRP on day 1 in the sepsis group (Figure 3.15). However, by day 5 there was a subgroup of SIRS patients that also displayed an elevated CRP therefore limiting the usefulness of this marker after the initial stages of a patient's presentation. Again, the distribution of severity of illness scores was broadly similar between both groups allowing an unbiased comparison of other parameters to occur (Figure 3.16).

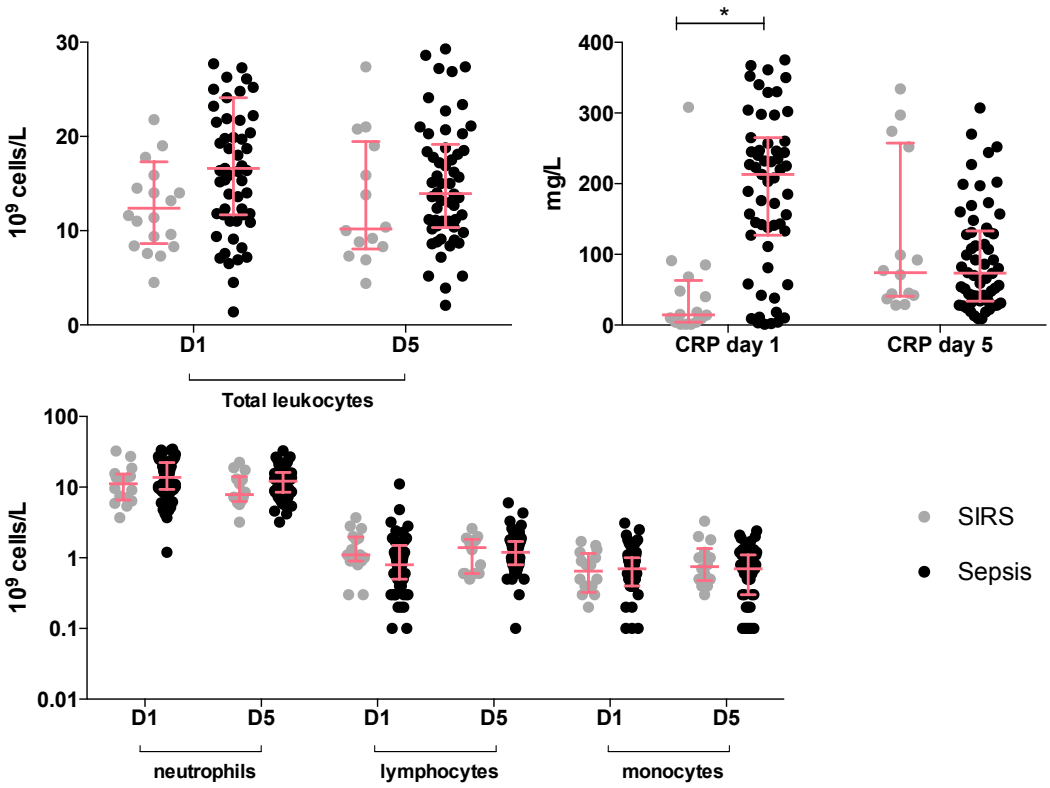

Figure 3.15 Differences in standard clinical immune parameters between sepsis and SIRS patients.

Differences in commonly measured clinical immune parameters are shown between sepsis and SIRS patients at both day 1 and day 5 time points. These include peripheral blood total leukocyte, neutrophil, lymphocyte and monocyte counts, as well as plasma CRP level. Sepsis day 1 n = 60, day 5 = 57, SIRS day 1 = 20 (CRP n = 16), day 5 = 14.

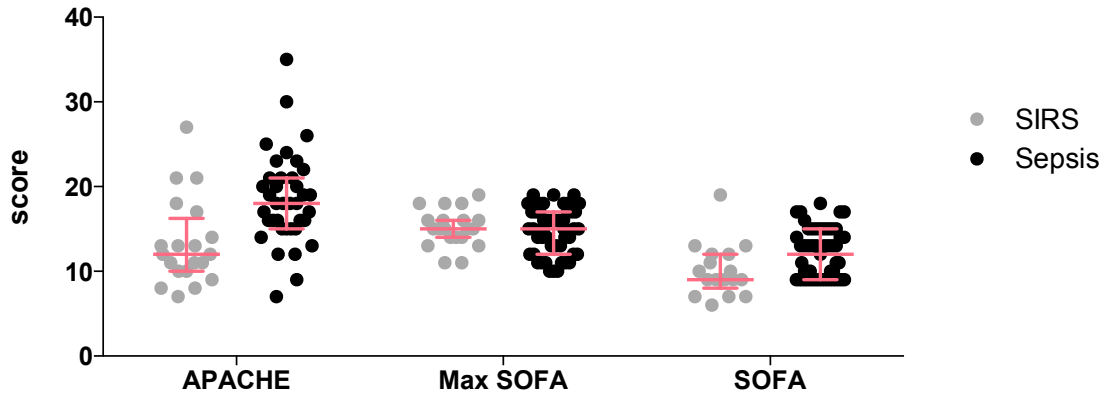

Figure 3.16 Differences in severity of illness scores between sepsis and SIRS patients. Severity of illness scores in sepsis and SIRS patients are shown including APACHE and SOFA scores. The maximum SOFA score was the highest recorded during a patient's ICU admission excluding periods following active withdrawal of treatment. Sepsis n = 57 APACHE, n = 60 SOFA & max SOFA, SIRS n = 20 APACHE, n = 22 SOFA and max SOFA.

3.3.2.2. Cellular immunology

Examining the detailed cellular changes using flow cytometry revealed many trends and some significant differences between these three groups. There were trends in increased $CD3^+$ and $V\gamma9^+$ T cells in healthy controls compared with both sepsis and SIRS patients (Figure 3.17). However, the large variations in healthy controls for these indices made any comparisons of this nature underpowered.

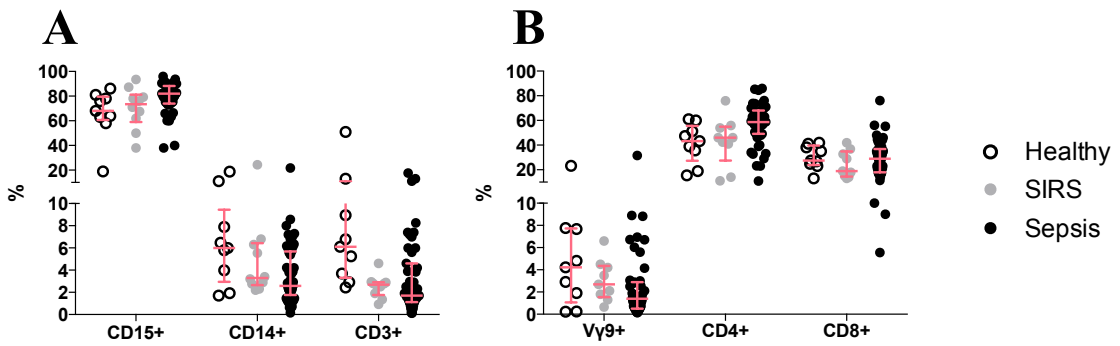

Figure 3.17 Differences in immune cell types analysed by flow cytometry in healthy controls, patients with sepsis and SIRS. The main cell lineages observed in peripheral blood are shown in healthy controls, patients with sepsis and SIRS. (A) Shows the differential leukocyte split into $CD15^+$ neutrophils, $CD14^+$ monocytes and $CD3^+$ lymphocytes. (B) Shows how the $CD3^+$ subpopulations are further sub-divided in $V\gamma9^+$ T cells, $CD4^+$ T cells, and $CD8^+$ T cells in these differing groups. Healthy n = 9, sepsis n = 55, SIRS n = 10.

When neutrophil markers were considered, there were a number of significant differences that are described in Figure 3.18. Firstly, the numbers of dead neutrophils were greater in sepsis compared with SIRS patients although this included a number of outliers. The adhesion molecule CD62L as well as the activation marker CD64 were increased in patients with sepsis. CD40, known to interact with platelets in sepsis, was also increased on sepsis neutrophils along with the APC marker CD86[104].

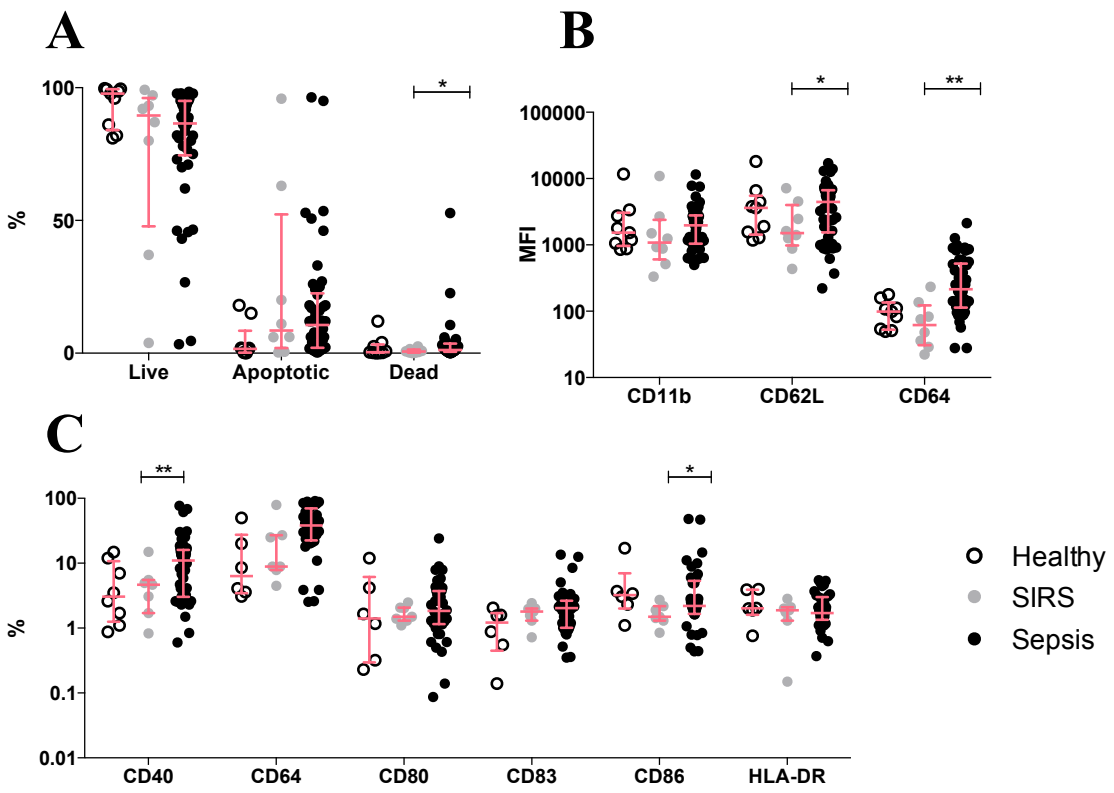

Figure 3.18 Differences in neutrophil survival and cell-surface markers in healthy controls, patients with sepsis and SIRS. (A) Neutrophil survival analysis using aqua staining of gated single neutrophils in healthy controls, sepsis and SIRS patients. (B) Cell-surface expression levels of classical neutrophil activation markers CD11b, CD62L, and CD64 in healthy controls, sepsis, and SIRS patients measured in MFI. (C) Levels of cell-surface markers CD40, CD64, CD80, CD83, CD86 and HLA-DR on neutrophils from healthy controls, sepsis and SIRS patients compared with non-survivors measured in percentage of positive expression compared with isotype controls. Healthy n = 9, sepsis n = 53, SIRS n = 10.

The significant results on monocytes included decreased CD40 seen in both sepsis and SIRS patients when compared with healthy controls (Figure 3.19). Furthermore, an early and profound decrease in cell-surface HLA-DR was observed in both sepsis and SIRS patients compared with healthy controls. This has been observed by others and usually has been interpreted as a sign of immunosuppression[1,2,105-107].

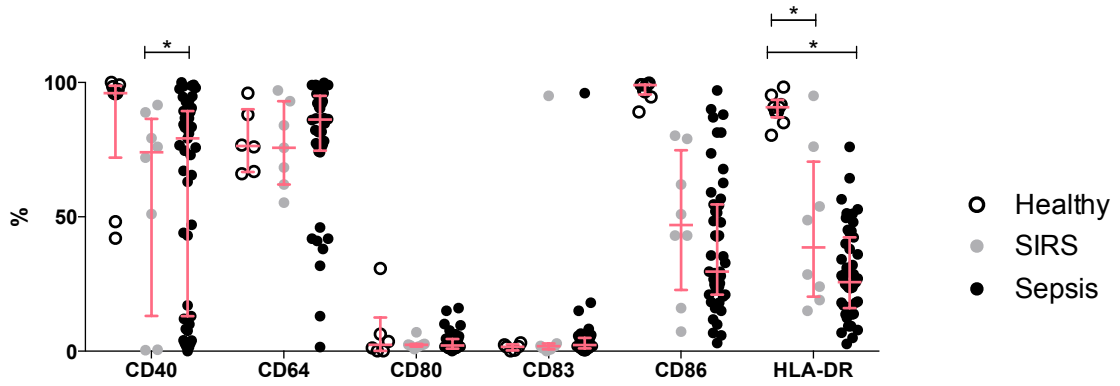

Figure 3.19 Differences in monocyte cell-surface markers seen in healthy controls, sepsis, and SIRS patients. Levels of cell-surface markers CD40, CD64, CD80, CD83, CD86 and HLA-DR on monocytes from healthy controls, sepsis and SIRS patients measured in percentage of positive expression compared with isotype controls**.** Healthy n = 9, sepsis n = 53, SIRS n = 9.

Whilst the percentage of $CD3^+$ T cells has been shown to be lower in both sepsis and SIRS patients (Figure 3.17), the numbers of these $CD3^+$ T cells that were apoptotic are greatly increased in sepsis patients compared with SIRS patients as shown in Figure 3.20. Furthermore, the activation of $V\gamma9^+$ T cells in sepsis patients as measured by CD69 was significantly increased in sepsis compared with SIRS patients. There was also a trend in the activation marker CD25 on both $V\gamma9^+$ and $CD8^+$ cells although these did not reach statistical significance.

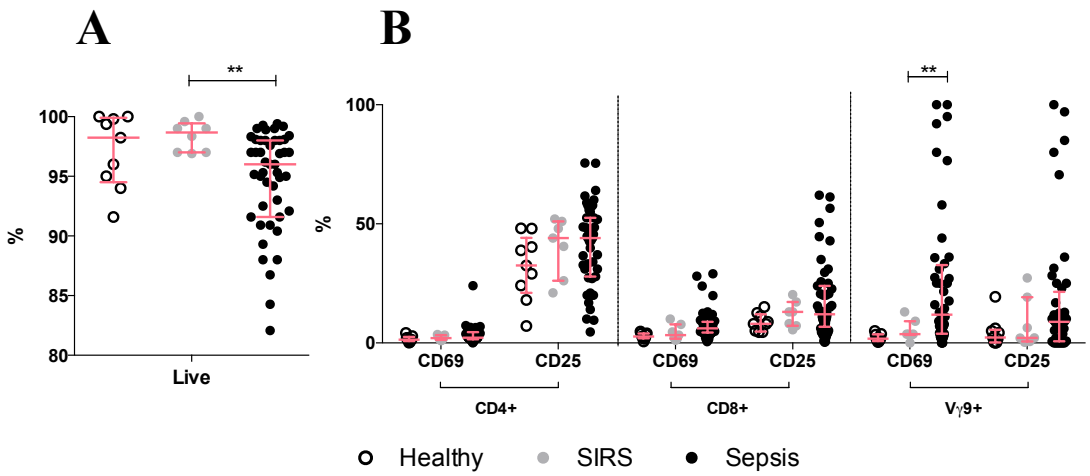

Figure 3.20 Survival and activation markers in CD3$^+$ T cells and their subtypes in healthy controls, patients with sepsis and SIRS. (A) CD3$^+$ T cell death analysed according to aqua staining on CD3$^+$ gated cells. (B) Cell-surface activation makers CD25 and CD69 expressed on CD4$^+$, CD8$^+$, and Vγ9$^+$ T cells in healthy controls, sepsis, and SIRS patients. All values are measured in percentage of positive expression compared with isotype controls**.** Healthy n = 9, sepsis n = 45, SIRS n = 9.

Vγ9^{+} T cells also demonstrated higher levels of CD86 and HLA-DR in sepsis patients as shown in Figure 3.21, findings that were not replicated with Vγ9^{-} CD3^{+} T cells.

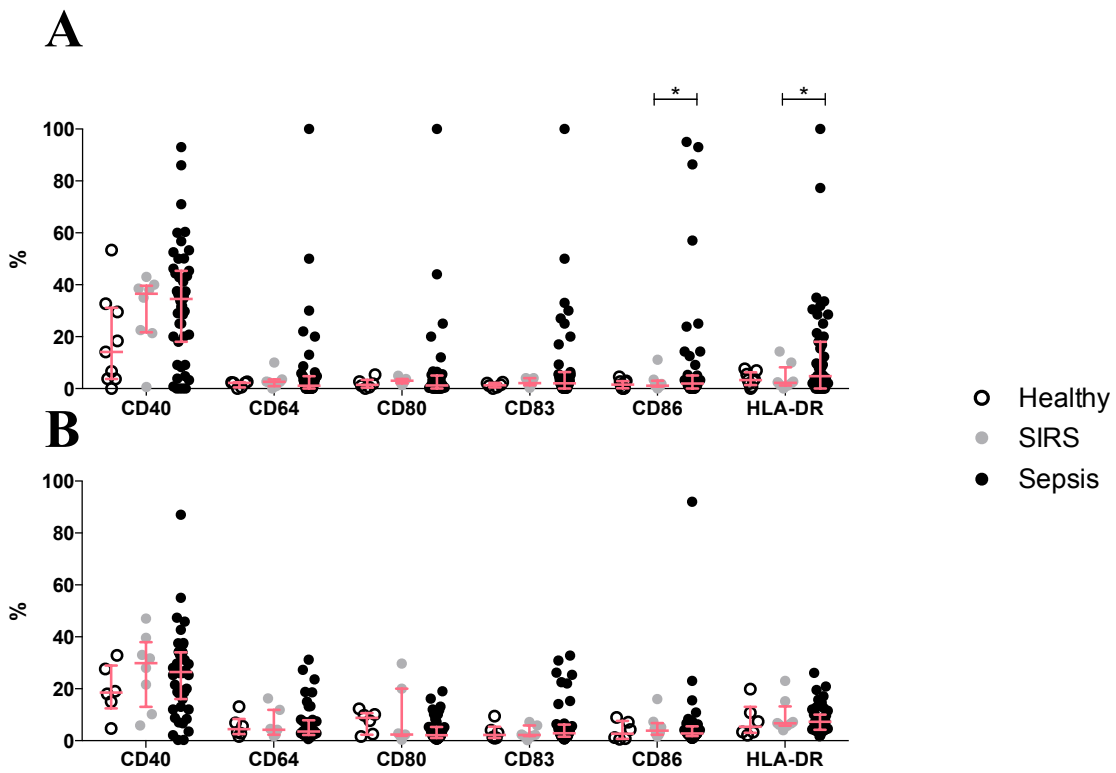

Figure 3.21 Cell-surface markers on Vγ9^{+} and Vγ9^{-} CD3^{+} T cells in healthy controls, patients with sepsis and SIRS. (A) Vγ9^{+} T cell and (B) Vγ9^{-} T cell expression of cell-surface markers CD40, CD64, CD80, CD83, CD86, and HLA-DR in healthy controls, sepsis, and SIRS patients. All values are measured in percentage of positive expression compared with isotype controls. Healthy n = 9, sepsis n = 45, SIRS n = 9.

Finally, an analysis of memory cell subsets showed increased numbers of naïve cells in both CD4^{+} and CD8^{+} populations whilst Vγ9^{+} cell subsets showed no significant differences (Figure 3.22).

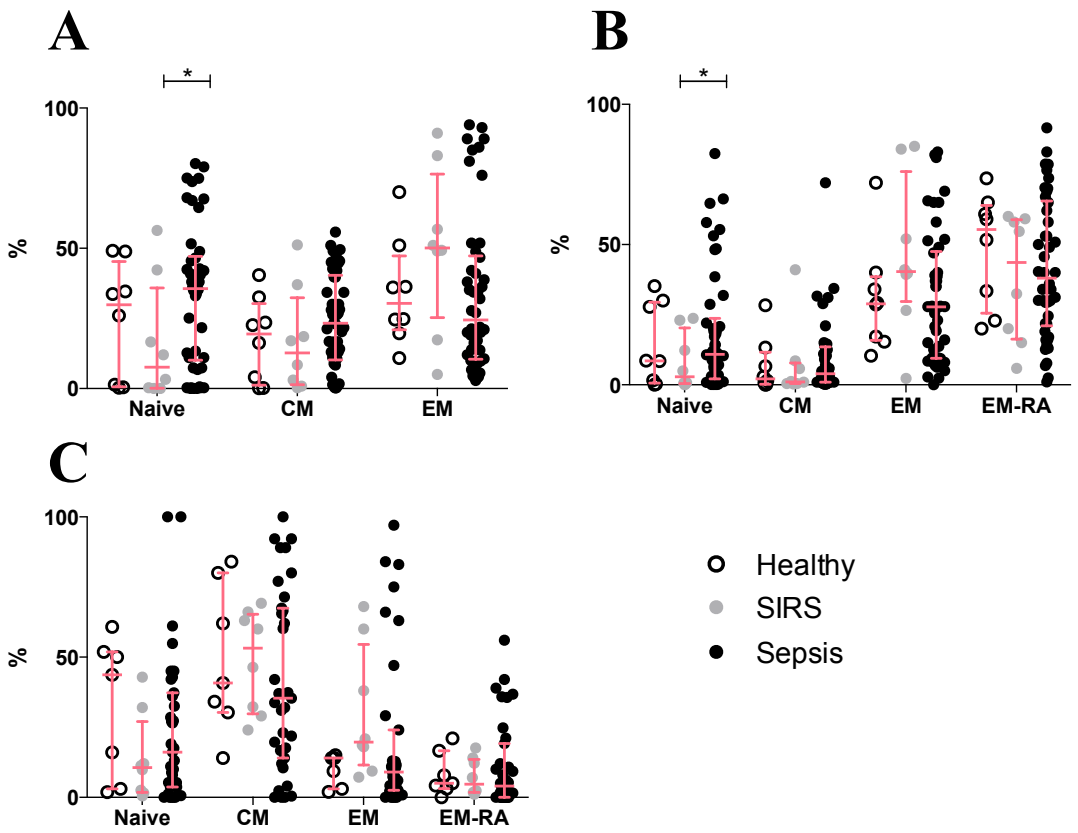

Figure 3.22 Memory subsets of CD4$^+$, CD8$^+$, and Vγ9$^+$ T cells in in healthy controls, patients with sepsis and SIRS. (A) CD4$^+$, (B) CD8$^+$ and (C) Vγ9$^+$ cell divisions of memory subsets. (A) CD4$^+$, (B) CD8$^+$ and (C) Vγ9$^+$ cell divisions of memory subsets. Naïve subsets in CD4$^+$ and CD8$^+$ T cells were characterised as CD45RA$^+$/CCR7$^+$ cells, central memory (CM) as CD45RA$^-$/CCR7$^+$ cells, effector memory (EM) as CD45RA$^-$/CCR7$^-$ cells and effector memory RA (EM-RA) as CD45RA$^+$/CCR7$^-$ according to the classification by Sallusto et al., 1999[96].Vγ9$^+$ cells were classed as naïve CD45RA$^+$/CD27$^+$, central memory CD45RA$^-$/CD27$^+$, effector memory CD45RA$^-$/CD27$^-$ and effector memory RA CD45RA$^+$/CD27$^-$ subtypes, based on the definition by Dieli et al., 2003[97]. Healthy n = 9, sepsis n = 45, SIRS n = 9.

3.3.2.3. Cytokine analysis

Figure 3.23 shows the day 1 cytokine analysis of patients with sepsis compared with SIRS. Here clear differences emerged in the classical proinflammatory cytokines including increased levels of IL-6, TNF-α, and IFN-γ in sepsis compared with SIRS patients. However, significant differences in recently described biomarkers were also demonstrated including procalcitonin, sensitive procalcitonin and proadrenomedullin. Furthermore, an increased IL-2 was shown in sepsis patients contradicting previous studies that described lower levels in this group[108,109].

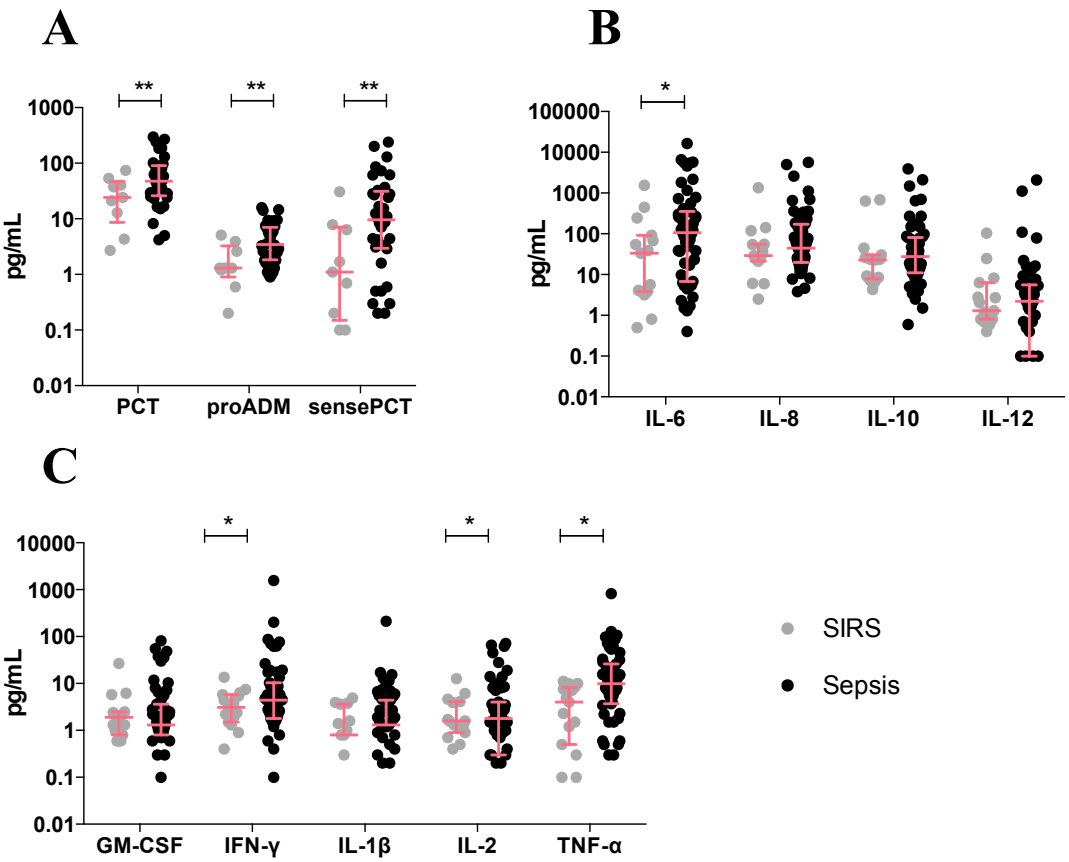

Figure 3.23 Day 1 differences in plasma cytokine levels in sepsis and SIRS patients. Cytokines are divided according to their relative level of magnitude in pg ranges. (A) Levels of procalcitonin (PCT), proadrenomedullin (proADM) and the sensitive Kryptor procalcitonin assay (sensePCT) in sepsis and SIRS patients. (B) Levels of IL-6, IL-8, IL-10, and IL-12 sepsis and SIRS patients. (C) GM-CSF, IFN-γ, IL-1β, IL-2 and TNF-α levels in sepsis and SIRS patients. Sepsis samples n = 46 (A) and 58 (B&C), SIRS n = 20.

3.3.2.4. Fingerprint prediction models

Due to the large number of significant differences between groups of patients with sepsis and SIRS, a binary logistic regression model (Table 3.5) comparing these groups resulted in a very good AUC (Figure 3.24, A). The model was unable to reduce the number of variables required to an amount either practical or useful in a point-of-care test. However, using a pruned neural network, the relative increases in AUC for the given complexity of additional variable numbers could be compared (shown in Table 3.6). The combination of TNF-α, IL-2, $V\gamma9^+$ CD69% and $CD3^+$ live% highlighted still produced a ROC curve with an AUC of 0.93 (Figure 3.24, B) whilst providing a more practical implementation of these findings.

Table 3.5 Predictor variables for patient disease type (sepsis or SIRS) selected using binary logistic regression with backwards conditioning.

	B	S.E.	Wald	df	Sig.	Exp(B)	CI lower	CI upper
$CD15^+$ CD62L MFI	-.001	.001	1.922	1	.166	.999	.998	1.000
$CD15^+$ CD64 MFI	.010	.006	2.565	1	.109	1.010	.998	1.023
CD3%	.725	.380	3.634	1	.057	2.065	.980	4.351
$CD4^+$ naive	-.129	.065	3.907	1	.048	.879	.773	.999
CRP	-.025	.010	5.948	1	.015	.975	.955	.995
IFN-γ	-.206	.128	2.612	1	.106	.813	.633	1.045
IL-2	.737	.345	4.558	1	.033	2.090	1.062	4.112
PCT	-.057	.032	3.106	1	.078	.945	.887	1.006
sensePCT	.142	.087	2.657	1	.103	1.152	.972	1.366
TNF-α	-.517	.231	5.031	1	.025	.596	.379	.937
Urea	-.350	.172	4.120	1	.042	.705	.503	.988
V $\gamma 9^+$ CD69%	-.069	.042	2.710	1	.100	.934	.860	1.013
V$\gamma 9^+$ CD86%	-.114	.057	4.027	1	.045	.892	.798	.997
Constant	-54.061	33.18	2.654	1	.103	.000		

All significant variables were entered into this model of patient survival using binary logistic regression with backwards conditioning at $p < 0.05$. The remaining 13 significant variables in the prediction model at this level are shown in the first column.

Number of variables used	Combination	AUC
5	IL-2, urea, $V\gamma9^+$ CD69%, $CD3^+$ live%, $CD15^+$CD62LMFI	1
4	TNF-α, IL-2, $V\gamma9^+$ CD69%, $CD3^+$ live%	0.93
3	TNF-α, $V\gamma9^+$ CD69%, $CD3^+$ live%	0.91
2	TNF-α, $V\gamma9^+$ CD69%,	0.86

Table 3.6 Predictor variables for patient disease type (sepsis or SIRS) selected using neural network modelling.

All significant variables were modelled using a feed-forward neural network model with 2 hidden nodes and 3000 maximum iteration. The table shows the best AUC values for each number of possible variable combinations. The highlighted combination of plasma TNF-α level, plasma IL-2 level, $V\gamma9^+$ T cell CD69 positive cell percentage and $CD3^+$ T cell percentage from total cells was most favourable given the AUC value and the practical advantages of a small variable number for development into a point-of-care test.

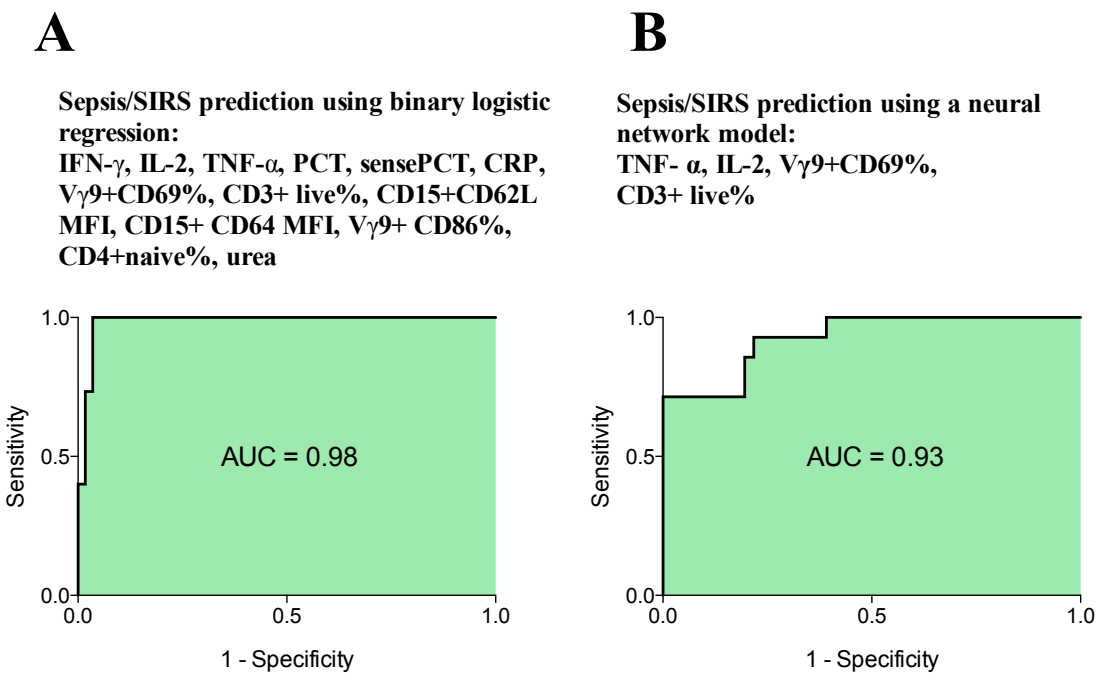

Figure 3.24 ROC curves for prediction of patient disease type (sepsis or SIRS) using logistic regression and neural network modelling. Using the variables sets previously selected, ROC curves were constructed using the predicted probabilities from each model's output. (A) Shows a binary logistic regression model with all 13 significant predictor variables with an AUC of 0.98. (B) Uses a neural network model with 4 day 1 predictor variables (plasma TNF-α level, plasma IL-2 level, $V\gamma9^+$ T cell CD69 positive percentage and $CD3^+$ cell percentage from total cells showing an AUC value of 0.93 for patient disease type.

Following production of the neural network model, a decision tree was constructed (Figure 3.25) using the same variable set for further validation. This tree is significant more complex than the previous related to patient outcome due to the multiple cut-off levels of IL-2 needed to produce a robust model. It is standard to produce decision models with a binary branching pattern as shown below.

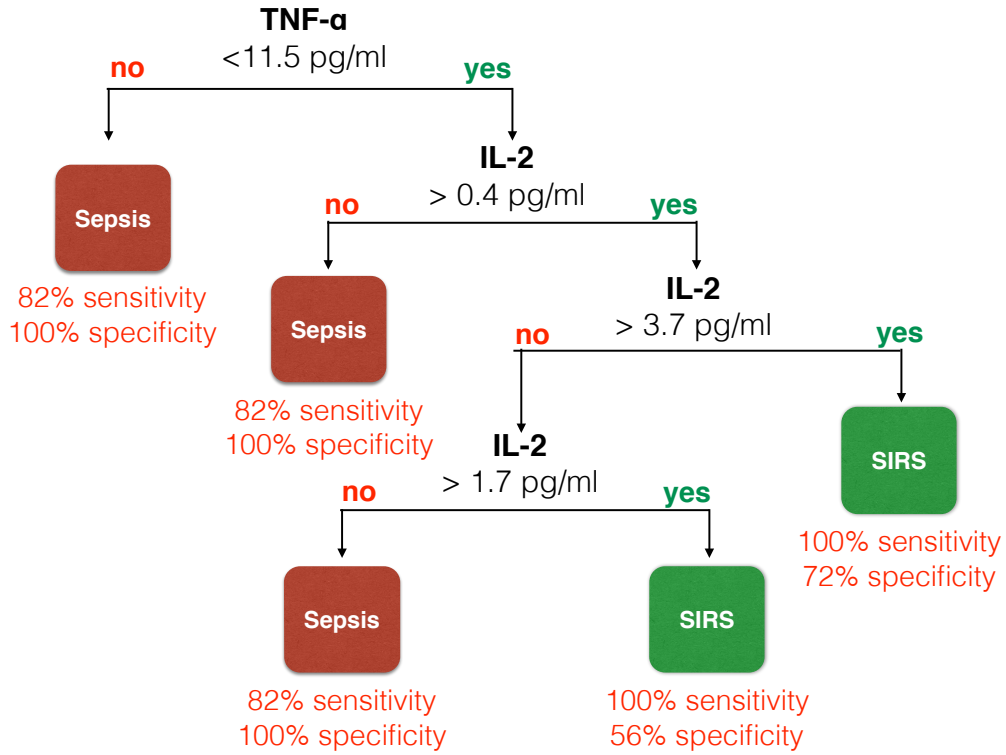

Figure 3.25 A decision tree model for prediction of sepsis vs. SIRS.

Using the variable sets previously selected, a decision tree model was constructed without forced pruning. The resulting variables included in the decision trees were automatically chosen according to the ability to discriminate based on the illustrated cut-off values. In this example the day 1 plasma TNF-α and IL-2 concentrations were required. The multiple branches of IL-2 are shown to illustrate the different categories of IL-2 concentrations used to divide the populations. The sensitivities relate to the overall sensitivity for that diagnostic category in all branches whilst the specificity relates to branch specific values, as is the nature of decision tree analyses.

3.3.3. Immune differences according to infecting organism type

The final division of patients into discrete categories will examine the immune-fingerprints left by different infecting organism types in patients with severe sepsis. It is this application of immune fingerprinting that is most novel and has the greatest ability to significantly impact on the care of critically ill patients.

This chapter aims to identify the Gram-status of an organism causing sepsis by interpreting a patient's own immune response to that infection. This method overcomes many of the inherent disadvantages of using microbiological culture or PCR-based identification techniques. It will identify not simply what microbes can be grown in culture from a sample, but importantly what microbes are causing disease. This should thus be able to compensate for sample contamination, non-pathogenic microbes and culture-negative sepsis patient samples.

Table 3.7 shows that apart from the site of pathology, there were no significant differences between the organism subgroups of patients with sepsis.

Table 3.7 Baseline characteristics in patients according to infective organism group.

	Gram-negative	**Gram-positive**	**Culture-negative**
Total number of patients	24	17	19
Age (median (quartiles)) years	63 (54-73)	63 (53-69)	64 (52-77)
Male gender (%)	40.9	57.1	47.3
BMI (median (quartiles))	24.2 (22.3-29.9)	27.1 (25.6-34.7)	34.9 (25.2-42.6)
ICU mortality (%)	2 (8.3)	4 (23.5)	3 (15.8)
Hospital mortality (%)	8 (33.3)	5 (29.4)	3 (15.8)
90-day mortality (%)	9 (37.5)	6 (35.3)	3 (15.8)
Site (%)*			
Abdominal	10 (41.7)	5 (29.4)	7 (36.9)
Respiratory	7 (29.2)	7 (41.1)	9 (47.4)
Soft tissue	1 (4.2)	5 (29.4)	3 (15.8)
Urinary tract	6 (25.0)	0 (0.0)	0 (0.0)

The table shows intergroup differences in the age, gender, BMI, and sites of pathology of patients in each respective group.

3.3.3.1. Clinical differences

The day 1 and day 5 clinical blood results according to infecting organism subgroup are shown in Figure 3.26. There were no significant differences seen in any of these standard immune parameters routinely relied upon in clinical practice. Furthermore, the similar patterns of organ failure scores between groups shown in Figure 3.27 allowed us to fairly compare any identified biomarkers as a true measure of organism differences rather than simply a surrogate for the severity of illness. Further clinical details are shown in Appendix 2: Further data, Table 0.9 to Table 0.12.

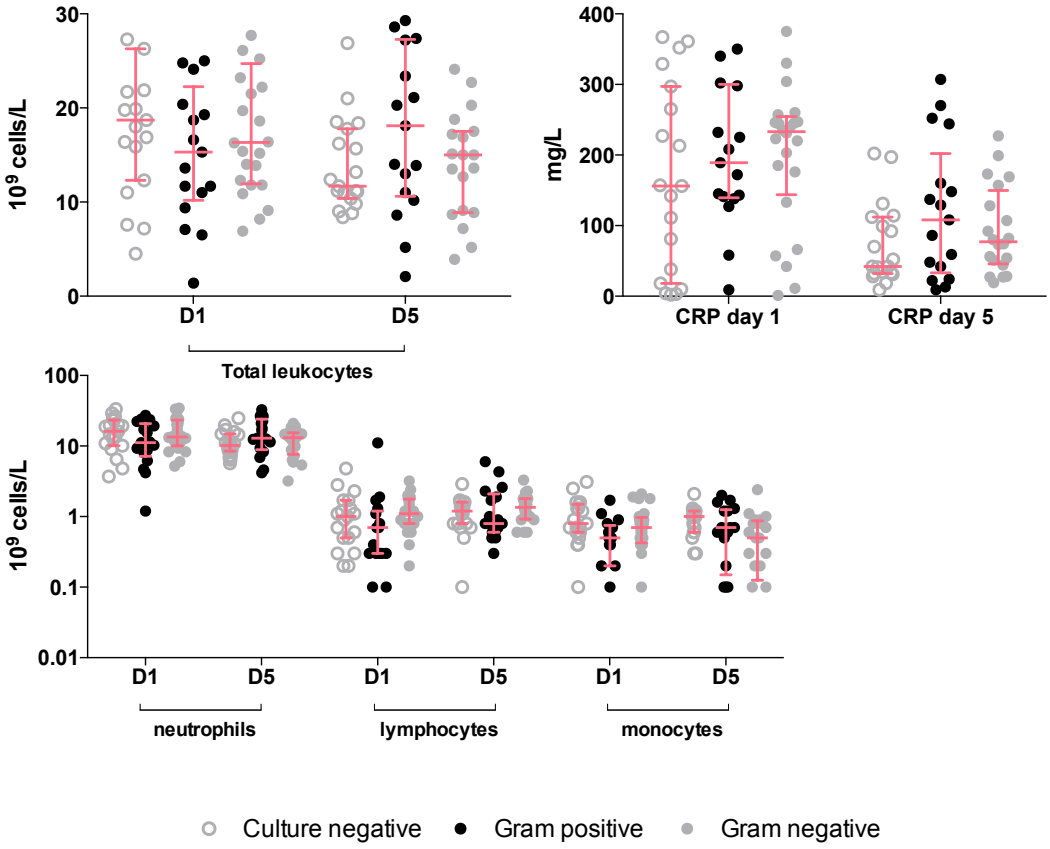

Figure 3.26 Differences in standard clinical immune parameters between sepsis patient infective groups. Differences in commonly measured clinical immune parameters are shown between sepsis patients in different infective groups at both day 1 and day 5 time points. These include peripheral blood total leukocyte, neutrophil, lymphocyte and monocyte counts, as well as plasma CRP level. Culture-negative day 1 & 5 n = 19, Gram-positive day 1 & 5 n = 17, Gram-negative day 1 = 24, day 5 n = 20.

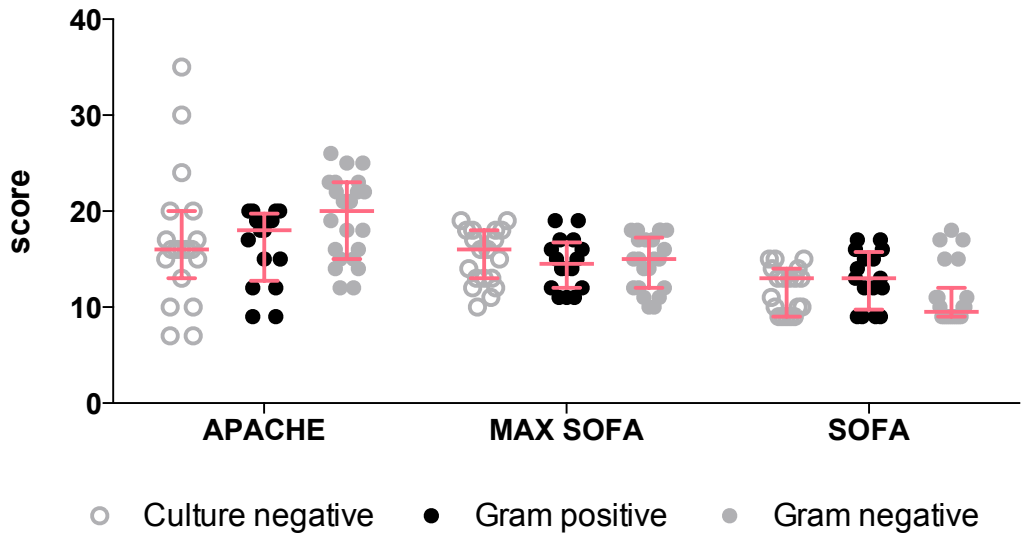

Figure 3.27 Differences in severity of illness scores between sepsis patients with different infective organisms. Severities of illness scores in sepsis patients of differing infectious groups are shown including APACHE and SOFA scores. The maximum SOFA score was the highest recorded during a patient's ICU admission excluding periods following active withdrawal of treatment. Culture-negative n = 19, Gram-positive n = 16, Gram-negative n =22 (APACHE), n = 24 (SOFA % max SOFA).

A full list of the microbiological findings and outcome for these patients is shown in Table 3.8.

Table 3.8 Microbiological findings and source of infection in sepsis patients.

Study ID	Culture result	Gram status	Outcome	Source	Associated experiments
SEP001	-	Culture-negative	Lived	Respiratory	
SEP002	*Klebsiella oxytoca*	Gram-negative	Lived	Abdominal	
SEP003	-	Culture-negative	Lived	Abdominal	
SEP004	*Staphylococcus aureus*	Gram-positive	Died	Respiratory	
SEP005	*Escherichia coli*	Gram-negative	Lived	Abdominal	
SEP006	-	Culture-negative	Died	Abdominal	
SEP007	*Streptococcus pneumoniae*	Gram-positive	Lived	Respiratory	
SEP008	-	Culture-negative	Lived	Abdominal	
SEP009	-	Culture-negative	Lived	Abdominal	
SEP010	*Staphylococcus aureus*	Gram-positive	Lived	Respiratory	
SEP011	*Escherichia coli*	Gram-negative	Died	Abdominal	
SEP012	*Enterococcus faecalis*	Gram-positive	Died	Abdominal	
SEP013	*Pseudomonas aeruginosa*	Gram-negative	Lived	Respiratory	
SEP014	-	Culture-negative	Lived	Respiratory	
SEP015	*Enterococcus faecalis*	Gram-positive	Lived	Abdominal	
SEP016	*Haemophilus influenzae*	Gram-negative	Lived	Respiratory	
SEP017	*Staphylococcus aureus*	Gram-positive	Lived	Respiratory	
SEP018	*Enterococcus faecalis*	Gram-	Died	Abdominal	

		positive			
SEP019	*Enterobacter cloacae*	Gram-negative	Died	Abdominal	
SEP020	-	Culture-negative	Died	Abdominal	
SEP021	-	Culture-negative	Died	Soft tissue	
SEP022	*Escherichia coli*	Gram-negative	Lived	Urinary tract	
SEP023	*Proteus*	Gram-negative	Died	Urinary tract	
SEP024	-	Culture-negative	Lived	Soft tissue	
SEP025	*Escherichia coli*	Gram-negative	Died	Urinary tract	
SEP026	*Escherichia coli*	Gram-negative	Died	Urinary tract	
SEP027	*Streptococcus pneumoniae*	Gram-positive	Lived	Respiratory	Monocyte rescue
SEP028	*Dermabacter hominis*	Gram-positive	Lived	Abdominal	Monocyte rescue
SEP029	-	Culture-negative	Lived	Abdominal	
SEP030	*Escherichia coli*	Gram-negative	Died	Abdominal	Monocyte rescue
SEP031	*Streptococcus pyogenes*	Gram-positive	Lived	Soft tissue	
SEP032	*Staphylococcus aureus*	Gram-positive	Died	Soft tissue	
SEP033	*Staphylococcus aureus*	Gram-positive	Lived	Soft tissue	
SEP034	*Morganella morganii*	Gram-negative	Died	Abdominal	
SEP035	*Stenotrophomonas maltophilia*	Gram-negative	Lived	Respiratory	
SEP036	-	Culture-negative	Lived	Respiratory	
SEP037	-	Culture-negative	Lived	Respiratory	

SEP038	*Streptococcus pneumoniae*	Gram-positive	Died	Respiratory	Monocyte rescue
SEP039	-	Culture-negative	Lived	Respiratory	
SEP040	*Haemophilus influenzae*	Gram-negative	Lived	Soft tissue	Monocyte rescue
SEP041	-	Culture-negative	Lived	Respiratory	
SEP042	*Proteus*	Gram-negative	Died	Abdominal	
SEP043	-	Culture-negative	Lived	Respiratory	
SEP044	*Enterobacter cloacae*	Gram-negative	Lived	Urinary tract	
SEP045	-	Culture-negative	Lived	Respiratory	
SEP046	*Klebsiella oxytoca*	Gram-negative	Lived	Abdominal	
SEP047	*Pseudomonas sp*	Gram-negative	Lived	Respiratory	
SEP048	*Escherichia coli*	Gram-negative	Lived	Abdominal	
SEP049	*Escherichia coli*	Gram-negative	Lived	Respiratory	
SEP050	-	Culture-negative	Lived	Abdominal	
SEP051	*Staphylococcus epidermidis*	Gram-positive	Lived	Soft tissue	APC assay
SEP052	*Streptococcus pneumoniae*	Gram-positive	Died	Respiratory	
SEP053	*Haemophilus influenzae*	Gram-negative	Lived	Respiratory	
SEP054	*Klebsiella pneumonia*	Gram-negative	Lived	Respiratory	APC assay
SEP055	*Staphylococcus aureus*	Gram-positive	Lived	Soft tissue	
SEP056	*Escherichia coli*	Gram-negative	Died	Urinary tract	APC assay
SEP057	-	Culture-	Lived	Respiratory	

		negative			
SEP058	*Enterococcus faecalis*	Gram-positive	Lived	Abdominal	
SEP059	-	Culture-negative	Lived	Soft tissue	
SEP060	*Enterobacter asburiae*	Gram-negative	Lived	Abdominal	

The table above outlines the microbiological findings, agreed source of infection and patient outcome at 90 days. The single organism specified and source of infection was adjudicated by an independent microbiologist with full access to the patient's clinical notes, electronic clinical results and in conjunction with the clinical consultant intensivist responsible for the patient's care. The Gram status of the organism was recorded according to the classification used in UK Standards for Microbiology Investigations. Any associated experiments performed with these samples are listed in the final column. APC assay = antigen presentation cell assay.

3.3.3.2. Cellular immunology

Whilst the classical clinical divisions into neutrophils, monocytes, and lymphocytes did not reveal any significant differences between these subgroups, the levels of $V\gamma9^+$ T cells were significantly higher in Gram-negative infections compared with both Gram-positive and culture-negative patients (Figure 3.28). Furthermore, culture-negative patients had a lower percentage of $V\delta2^+$ cells amongst all $V\gamma9^+$ T cells (data not shown).

Whilst there were trends in other cellular parameters differences between these subgroups, most notably CD40 and HLA-DR expression on monocytes, there were no further significant differences identified (Figure 3.29 to Figure 3.33).

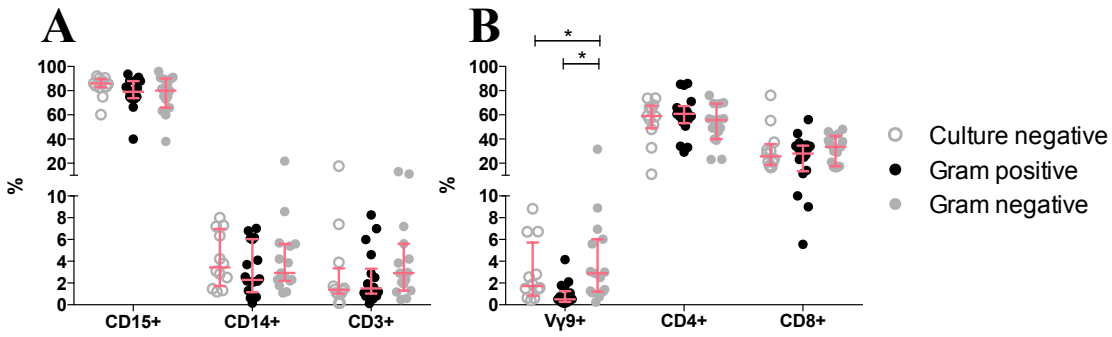

Figure 3.28 Differences in immune cell types analysed by flow cytometry in sepsis patients with different infecting organisms. The main cell lineages observed in peripheral blood are shown in sepsis patients with different causative organisms. (A) Shows the differential leukocyte split into $CD15^+$ neutrophils, $CD14^+$ monocytes and $CD3^+$ lymphocytes. (B) Shows how the $CD3^+$ subpopulations are further sub-divided in $V\gamma9^+$ T cells, $CD4^+$ T cells, and $CD8^+$ T cells in these differing groups. Culture-negative n = 18, Gram-positive n = 17, Gram-negative n = 20. Some counts may be variable depending on the subsequent gating of sub-sets.

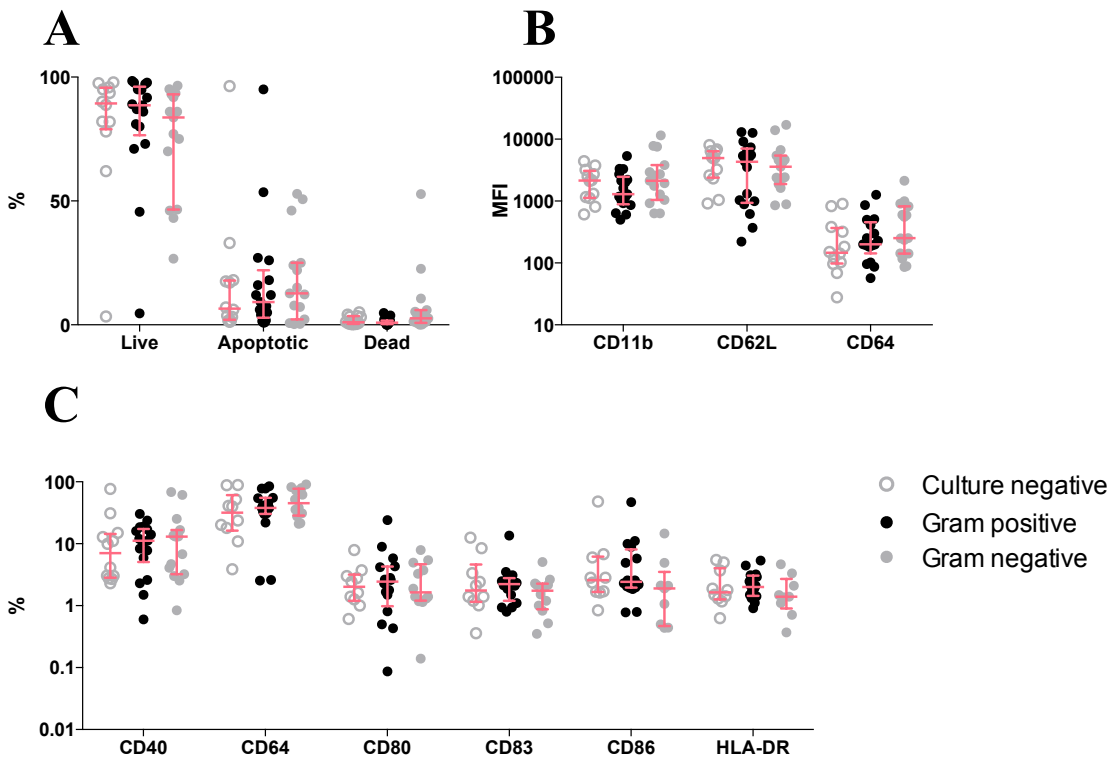

Figure 3.29 Differences in neutrophil survival and cell-surface markers in sepsis patients with different infective organism types. (A) Neutrophil survival analysis using aqua staining of gated single neutrophils in sepsis patients with different infective organism types. (B) Cell-surface expression levels of classical neutrophil activation markers CD11b, CD62L, and CD64 in sepsis patients with different infective organism types measured in MFI. (C) Levels of cell-surface markers CD40, CD64, CD80, CD83, CD86, and HLA-DR on neutrophils from sepsis patients with different infective organism types measured in percentage of positive expression compared with isotype controls. Culture-negative n = 18, Gram-positive n = 17, Gram-negative n = 18. Some counts may be variable depending on the subsequent gating of sub-sets.

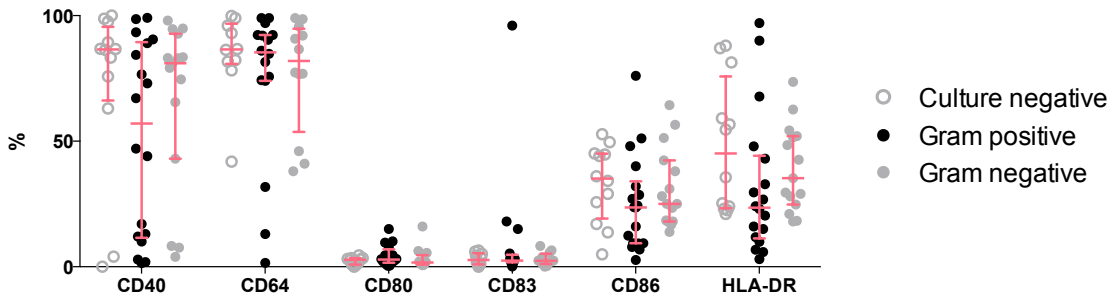

Figure 3.30 Differences in monocyte cell-surface markers seen in sepsis patients with different infecting organism types. Levels of cell-surface markers CD40, CD64, CD80, CD83, CD86, and HLA-DR on monocytes from sepsis patients with different infecting organism types measured in percentage of positive expression compared with isotype controls**.** Culture-negative n = 18, Gram-positive n = 17, Gram-negative n = 18. Some counts may be variable depending on the subsequent gating of sub-sets.

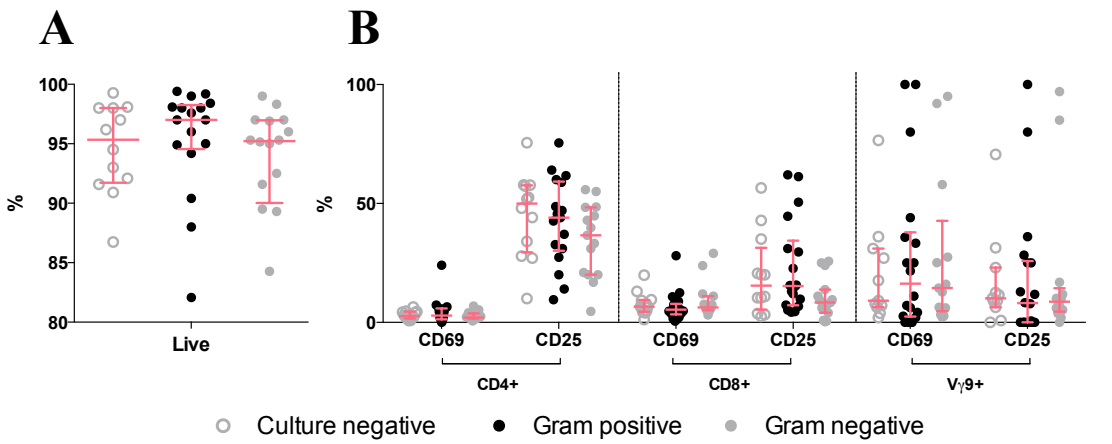

Figure 3.31 Survival and activation markers in CD3$^+$ T cells and their subtypes in sepsis patients with different infective organism types. (A) CD3$^+$ T cell death analysed according to aqua staining on CD3$^+$ gated cells. (B) Cell-surface activation makers CD25 and CD69 expressed on CD4$^+$, CD8$^+$, and Vγ9$^+$ T cells in in sepsis patients with different infective organism types. All values are measured in percentage of positive expression compared with isotype controls**.** Culture-negative n = 12, Gram-positive n = 17, Gram-negative n = 16. Some counts may be variable depending on the subsequent gating of sub-sets.

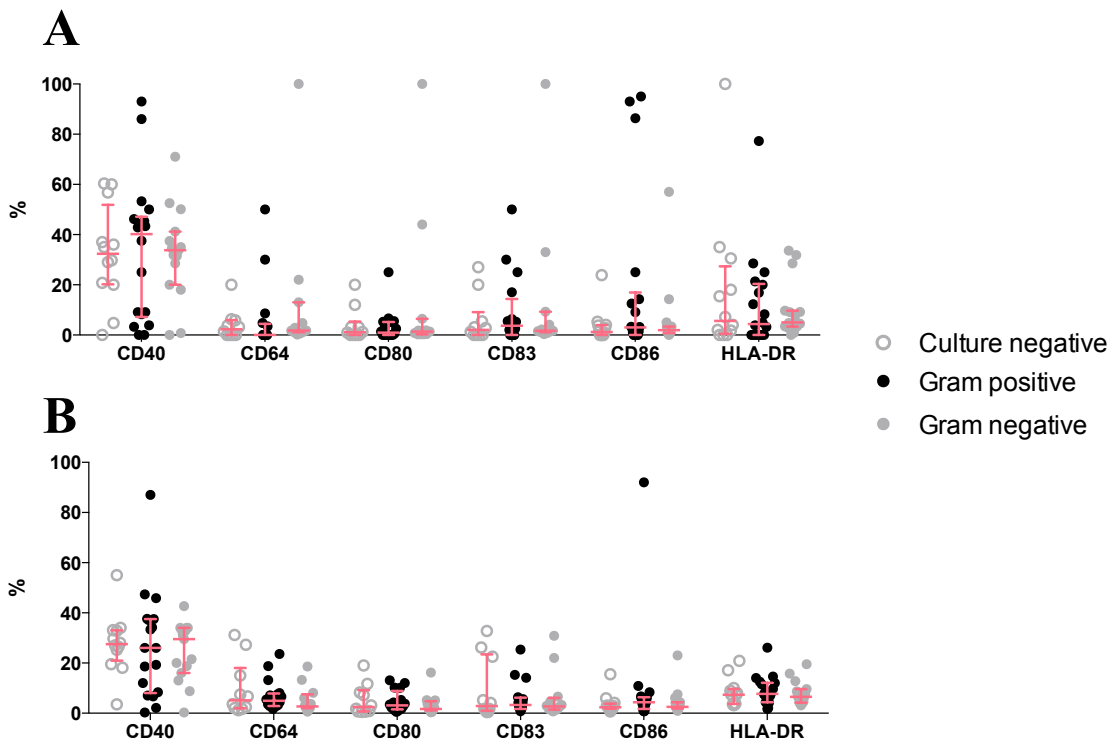

Figure 3.32 Cell-surface markers on Vγ9^{+} and Vγ9^{-} CD3^{+} T cells in sepsis patients with different infecting organism types. (A) Vγ9^{+} T cell and (B) Vγ9^{-} T cell expression of cell-surface markers CD40, CD64, CD80, CD83, CD86, and HLA-DR in in sepsis patients with different infecting organism types. All values are measured in percentage of positive expression compared with isotype controls**.** Culture-negative n = 12, Gram-positive n = 17, Gram-negative n = 16. Some counts may be variable depending on the subsequent gating of sub-sets.

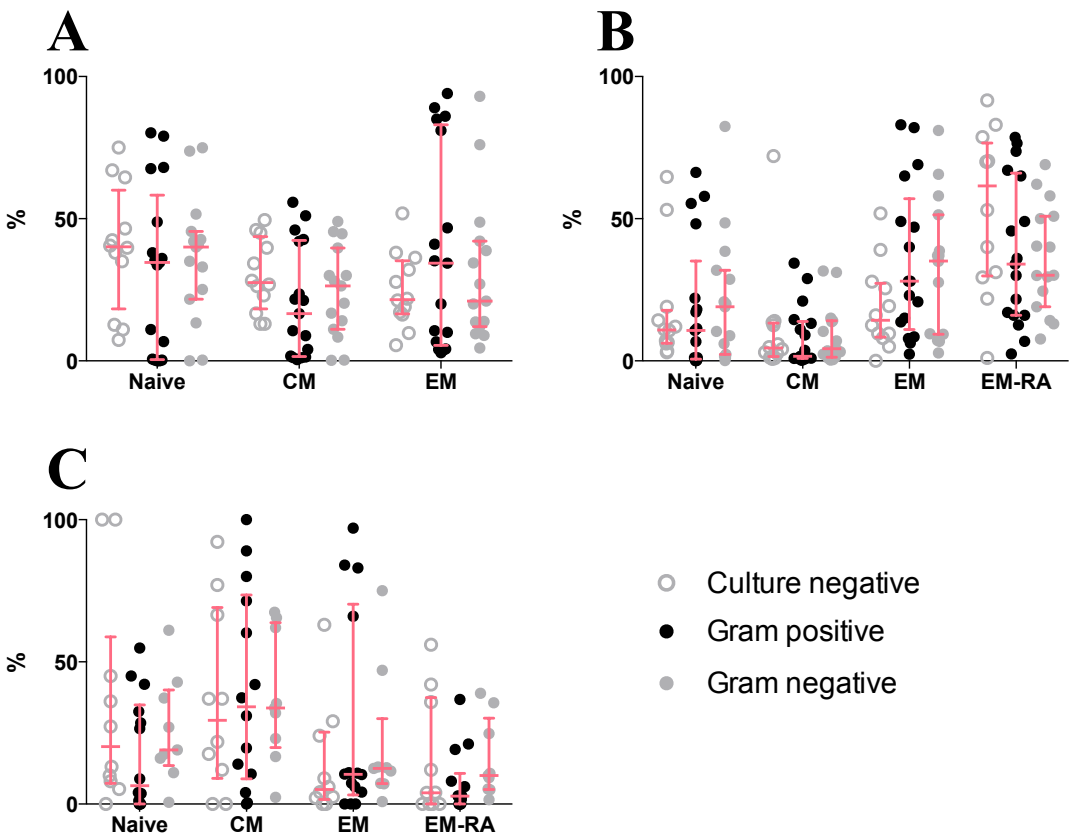

Figure 3.33 Memory subsets of CD4$^+$, CD8$^+$, and Vγ9$^+$ T cells in sepsis patients with different infecting organism types. (A) CD4$^+$, (B) CD8$^+$ and (C) Vγ9$^+$ cell divisions of memory subsets. (A) CD4$^+$, (B) CD8$^+$ and (C) Vγ9$^+$ cell divisions of memory subsets. Naïve subsets in CD4$^+$ and CD8$^+$ T cells were characterised as CD45RA$^+$/CCR7$^+$ cells, central memory (CM) as CD45RA$^-$/CCR7$^+$ cells, effector memory (EM) as CD45RA$^-$/CCR7$^-$ cells and effector memory RA (EM-RA) as CD45RA$^+$/CCR7$^-$ according to the classification by Sallusto et al., 1999[96].Vγ9$^+$ cells were classed as naïve CD45RA$^+$/CD27$^+$, central memory CD45RA$^-$/CD27$^+$, effector memory CD45RA$^-$/CD27$^-$ and effector memory RA CD45RA$^+$/CD27$^-$ subtypes, based on the definition by Dieli et al., 2003[97]. Culture-negative n = 12, Gram-positive n = 17, Gram-negative n = 16. Some counts may be variable depending on the subsequent gating of sub-sets.

3.3.3.3. Cytokine analysis

By analysing the humoral aspects of sepsis immunity, some clear differences emerged. Figure 3.34 shows that levels of both TNF-α and IL-1β were raised in Gram-negative infections compared with Gram-positive or culture-negative patients. Furthermore, it was shown that IL-2 was lower in culture-negative patients, mirroring that of the non-infective SIRS patients earlier in Figure 3.23.

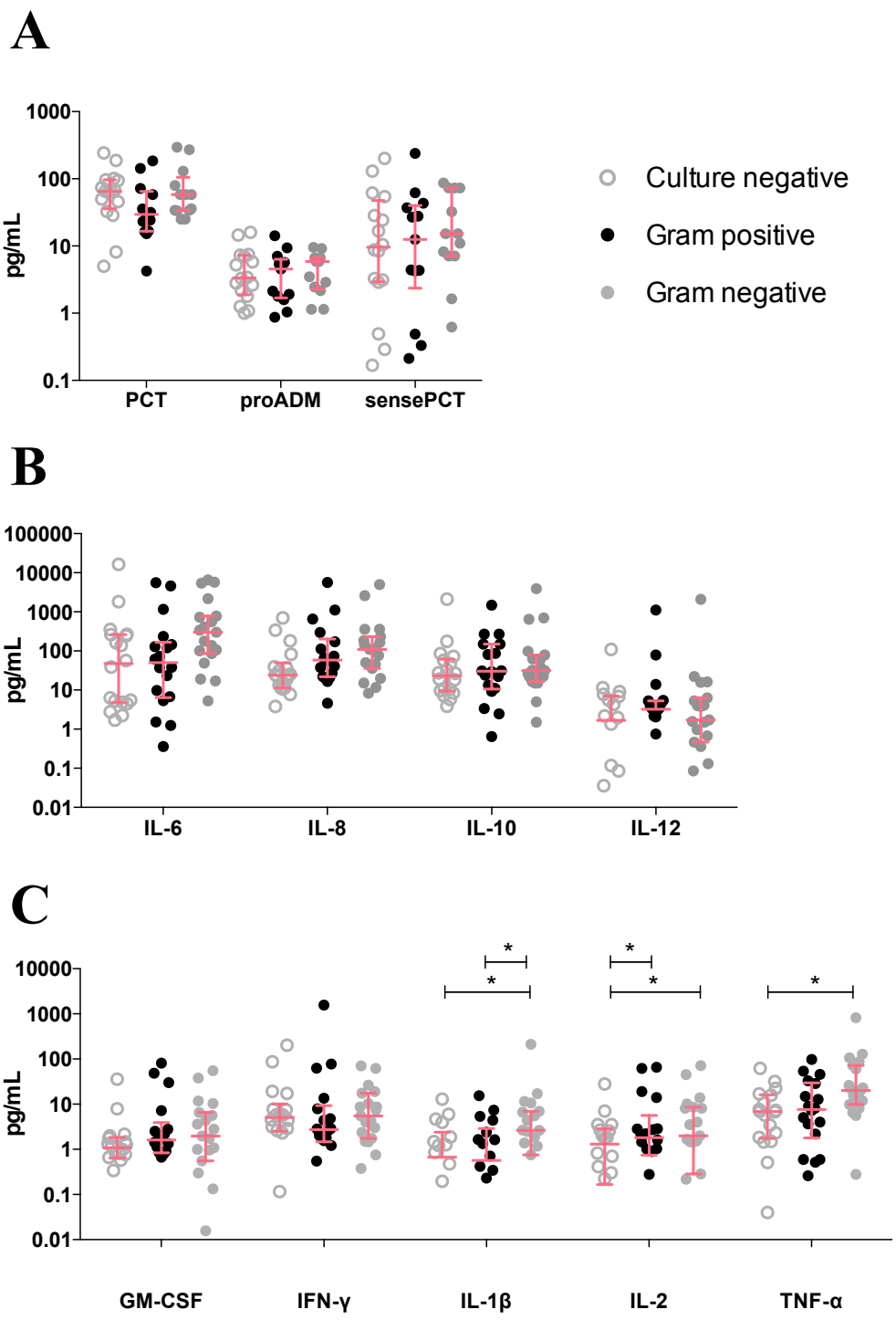

Figure 3.34 Day 1 differences in plasma cytokine levels in sepsis patients with different infecting organism types. Cytokines are divided according to their relative level of magnitude in pg ranges. (A) Levels of procalcitonin (PCT), proadrenomedullin (proADM) and the sensitive Kryptor procalcitonin assay (sensePCT) in sepsis patients with different infecting organism types. (B) Levels of IL-6, IL-8, IL-10, and IL-12 sepsis patients with different infecting organism types. (C) GM-CSF, IFN-γ, IL-1β, IL-2 and TNF-α levels in sepsis patients with different infecting organism types. Culture-negative n = 19 (16 for PCT), Gram-positive n = 17 (15 for PCT), Gram-negative n = 22 (14 for PCT).

3.3.3.4. Fingerprint prediction models

Unlike previous groupings, logistic regression was not able to accurately predict the outcome of a patient's culture results using the significant differences outlined above (data not shown). However, using a neural network model discussed previously, it is now possible to accurately predict the infecting organism group by using a combination of 4 markers highlighted in Table 3.9. This simple combination would allow a point-of-care diagnostic test to produce a ROC curve shown in Figure 3.35 with an AUC for organism prediction of 0.94. This would include determining Gram-positive, Gram-negative or culture-negative patient status.

Table 3.9 Predictor variables for sepsis infecting organism subtype selected using neural network modelling.

Combination	AUC
IL-1β, IL-2, TNF-α, Vγ9$^+$%	0.94
IL-1β, IL-2, Vγ9$^+$%	0.91
IL-1β, IL-2, TNF-α	0.73
IL-2, Vγ9$^+$%	0.89

All significant variables were modelled using a feed-forward neural network model with 2 hidden nodes and 3000 maximum iteration. The table shows the best AUC values for each number of possible variable combinations. The highlighted combination of plasma IL-1β level, plasma IL-2 level, plasma TNF-α level, Vγ9$^+$ T cell percentage from the CD3$^+$ gate was most favourable given the AUC value and the practical advantages of a small variable number for development into a point-of-care test.

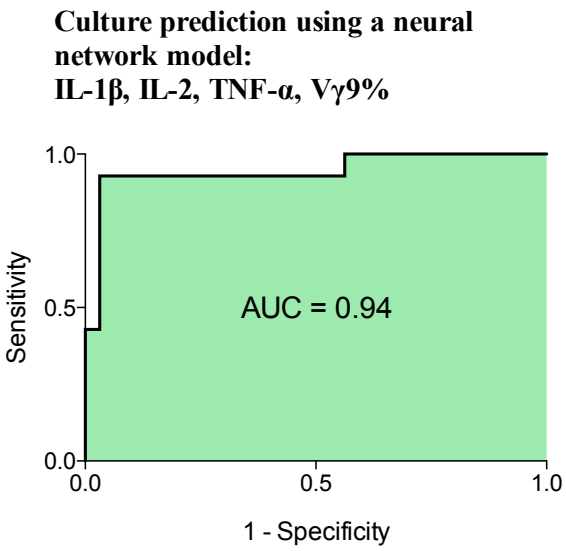

Figure 3.35 ROC curves for prediction of sepsis infecting organism type using neural network modelling.

Using the variables sets previously selected, ROC curves were constructed using the predicted probabilities from the neural network model output. This uses 4 day 1 predictor variables (plasma IL-1β level, plasma IL-2 level, plasma TNF-α level and $V\gamma9^+$ T cell percentage from total lymphocytes, showing an AUC value of 0.94 for infecting organism type.

Following production of the neural network model, a decision tree was constructed (**Figure 3.36**) using the same predictor set for validation.

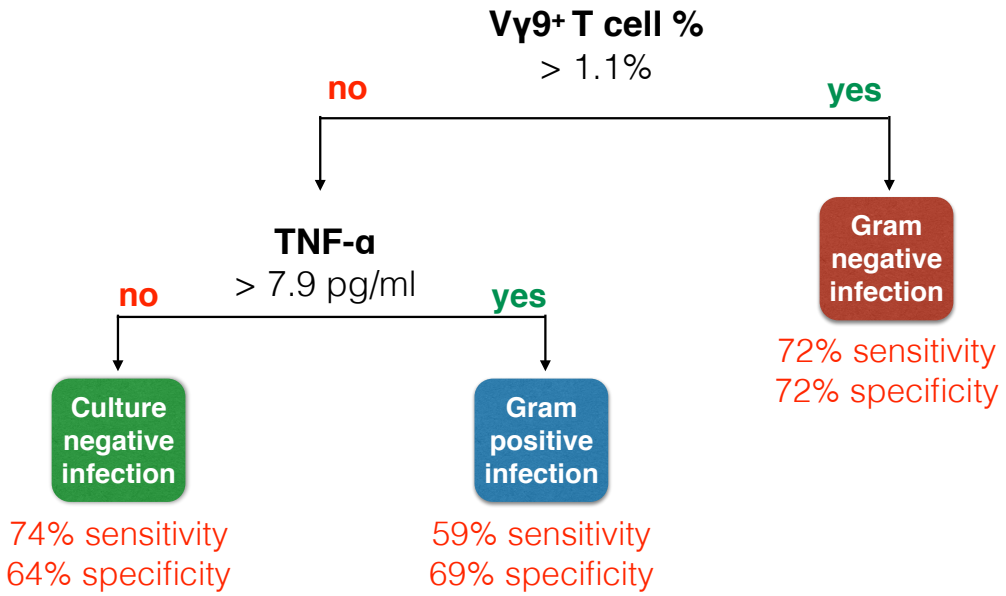

Figure 3.36 A decision tree model for prediction of Gram status of the infecting organism.

Using the variable sets previously selected, a decision tree model was constructed without forced pruning. The resulting variables included in the decision trees were automatically chosen according to the ability to discriminate based on the illustrated cut-off values. In this example the $V\gamma9^+$ cell percentage from $CD3^+$ cells plus day 1 TNF-α concentrations were required. The sensitivities relate to the overall sensitivity for that diagnostic category in all branches whilst the specificity relates to branch specific values, as is the nature of decision tree analyses.

3.4. Discussion

3.4.1. The current state of the art

It has been argued in Chapter 1 that the real advances in the care of patients with sepsis stem from relatively simple, cheap interventions delivered to the right patients at the right times. Early appropriate antibiotic is currently still considered by many to be the most effective weapon against sepsis despite the pharmaceutical industry investing millions of pounds developing complex immunotherapy that has, thus far, failed to deliver[16,108]. However, to fully realise the benefits of these treatments, accurate diagnostics are needed to direct their use[16,110]. This chapter reinforces the emerging view that the utility of many classical medical diagnostics are limited[110,111]. Indeed, it has been suggested that if the stethoscope were submitted for consideration as a piece of medical equipment at today's standards, it would be rejected on the grounds of its poor sensitivity and specificity[111,112].

Just one of the standard clinical measures, CRP, has been shown in this study to be an accurate discriminator in sepsis. However, whilst significant differences were seen between the day 1 level of CRP in patients with sepsis compared with SIRS, the resulting models fail to include CRP in their final selections. Furthermore, these differences in CRP dissipate at day 5, a time-point where a distinction between sepsis and SIRS is most needed in complex patients with multi-system disease.

Finally, even if standard markers were shown to be of use, the implementation of these as diagnostic tools often relies upon single measures considered in isolation. This contradicts the increasing adoption of health and thus disease as an integration of multiple complex systems with significant cross-talk[112,113].

3.4.2. Cross-discipline fertilisation

There is no shortage of studies proclaiming the discovery of a new biomarker useful in sepsis and many other areas of medicine. However, whilst interesting and often based on solid theoretical grounds, these single markers are often time-consuming to measure, expensive to measure and considered in isolation. Indeed, the 13 variables shown in our binary logistic model to distinguish between sepsis and SIRS were all considered, the costs to the health system in delivering these as a point-of-care test would be prohibitive.

Medicine should aim towards the integration of a number of relatively simple markers that, in combination, can model a complex system accurately, cheaply and can be deployed to make a difference to patients at the bedside. However, this approach cannot rely upon the standard statistical concepts in the medical research literature. It needs cross-fertilisation between a diverse range of academic disciplines to produce useful endpoints. Neural network models, although based loosely upon the structure of our nervous system[113-116], were first developed to reduce echoes heard in primitive phone exchanges. Today, they are mostly used in economic forecasting, image compression, and handwriting recognition technology[107,114-116]. The realisation that these systems integrate multiple complex non-linear signals into discrete outputs allowed this study to adapt neural networks to help solve its central problem of prediction. It seems that emerging concepts in fields as diverse as macroeconomics can be successfully applied to help further medical research and ultimately, patients.

3.4.3. Mechanistic basis for descriptive marker differences

The nature of this descriptive study allows models for prediction to be made but limits the ability to describe the underlying mechanisms responsible for any changes seen. However, there are emerging trends in the descriptive data that can be informed by published mechanisms prompting further explorative experiments detailed in Chapter 4.

3.4.3.1. Survival and non-survival mechanisms

The increased CD80 on neutrophils of survivors along with higher HLA-DR and CD86 on monocytes suggest an importance of APC-like functions associated with patient survival. The loss of HLA-DR on monocytes has long been attributed to the CARS syndrome of immunosuppression that may follow sepsis[105,107]. There is also a strong positive association between monocyte HLA-DR levels and patient survival[105,117]. However, it may be that as well as loss-of-function modulation in compensatory anti-inflammatory response syndrome (CARS) (such as a monocyte's ability to act as an APC), immune reprogramming may lead to gain-of-function in other cell subtypes. This will be explored further in Chapter 4. The rapid reversal of a pattern of elevated proinflammatory cytokines seen in survivors at day 1 (higher IL-6, PCT and GM-CSF) into the inverse pattern of higher proinflammatory cytokines seen in non-survivors at day 5 (higher IFN-γ, GM-CSF and IL-2) is intriguing. This may be attributable to a number of published associations including death due to on-going active infection,

development of secondary pathology, or a second-hit infection[117,118]. This also suggests that time-analysis of collections of markers could be used in future studies to help predict the eventual course of a disease[118,119].

The higher levels of day 1 IL-6 seen in survivors on day 1 does warrant further discussion as this contradicts much of the published literature where the reverse relationship is shown[120-122]. Many of those studies have used caecal puncture murine models that have been criticised in recent years[123]. The studies also have small numbers of patients, including those without severe sepsis or septic shock, and so cannot be directly compared to this study. However, the GenIMS study[120] was a large, well-conducted study in humans with over 30% of patients having severe sepsis. That study shows a consistent relationship between 90-day mortality and IL-6 levels at days 1-7 contradicting the present work that shows the inverse relationship at day 1 although a similar pattern at day 5. There are several reasons that may explain this difference. Most notably, the present study has 37.5% of patients that survived with a Gram-negative infection. It has been described in many published in vitro and in vivo works that Gram-negative infections produce higher levels of IL-6 than those of Gram-positive infections [124-126]. However, as the GenIMS study focused on patients with community acquired pneumonia, the rates of Gram-negative infections here in patients that survived were just 2%. In patients with a more balanced cause of sepsis, this relationship between death and elevated IL-6 levels has been questioned in an alternative study[127]. In addition, the relationship between survival and IL-6 at day 5 in this study was shown to have a positive correlation. It is known that sepsis is a disease where time plays an important part in the immune response[128-130], yet the very nature of the disease is that one patient's first day in hospital may differ dramatically in the timescale of that disease process compared with another patient's illness. Indeed, some sepsis studies consider the time zero point as the moment a patient becomes hypotensive[131], while others consider this to be the moment of diagnosis, regardless of how long the patient has been in hospital[132,133]. Whilst the levels of IL-6 are significantly higher in the GenIMS study from day 1, the extent of this difference is far greater by day 5 which the findings of this study conforms to.

Thus the systems in place to admit patients to hospital, admit them to a critical care environment and the very differences in the ability of a population to self-manage at

home before hospital admission may influence dramatically the time point of sampling and hence the absolute and relative values of cytokine levels when considering survival and non-survival. This dynamic time course is thus difficult to compare across disparate groups. However, even with the above explanations, the weight of evidence does question the relation found in this study. Taken along with the timing of sampling being performed only after the admission of a patient into a critical care environment, the utility of prediction survival is diminished and further confirmatory work would be needed before a model of this type could be confidently put into clinical practice.

3.4.3.2. Sepsis and SIRS mechanisms

Examining the differences between healthy controls, sepsis and SIRS patients, it is shown that sepsis induces a greater amount of neutrophil death with higher levels of cell-surface CD62L and CD64 on surviving neutrophils. Sepsis has a number of aetiologies responsible for neutrophil death including necrosis, apoptosis, autophagy, and the recently described NETosis[119,134]. CD62L, essential for interaction with oligosaccharide present on endothelial-cell surface glycoproteins, has been described to shed significantly in sepsis to limit local immune cell adherence thereby reducing microvascular damage[134,135]. CD64 is a very well described marker of neutrophil activation and has been suggested as a biomarker in sepsis[135,136]. The elevated levels of the platelet-interacting CD40 links with the multisystem spectrum of disease caused by sepsis, where platelet dysfunction and disseminated intravascular coagulation frequently coexist. Again, the importance of APC-like function in critical illness can be understood with a rapid and profound decrease in monocyte HLA-DR in both sepsis and SIRS patients compared with healthy controls and elevated CD86 on neutrophils in sepsis. The increased activation of $V\gamma9^+$ T cells seen in sepsis patients (expressed as CD69 levels) is likely attributable to the predominance of Gram-negative (HMB-PP positive) organisms known to induce $V\gamma9^+$ T cell activation. Whilst the observed cytokine pattern is largely typical of sepsis patients, the high IL-2 is contradictory to much of the literature[136,137] and goes against the increased levels of $CD3^+$ T cell death that have been attributed to low IL-2 levels. However, many of these studies sample from patients at a much later time point, again reinforcing the importance of timing. Again, this study finds an elevated level followed by a lower level in sepsis patients is seen at the day 5 time point (data not shown).

Circulating γδ T cells were previously shown to be activated in patients with sepsis[137,138]. However, no study has so far been conducted as to the specific involvement of the Vγ9/Vδ2^{+} subset of peripheral γδ T cells and their activation status in sepsis depending on the nature of the causative pathogen. Our present findings demonstrate higher absolute counts and higher frequencies of Vγ9/Vδ2 T cells among all circulating T cells in infections caused by Gram-negative species compared with Gram-positive microorganisms, in support of their differential responsiveness to distinct groups of pathogens[138,139].

Neutrophil apoptosis, as assessed by gated neutrophils with intermediate loss of cell surface CD16[140], was higher in survivors with sepsis. This generally agrees with the most recent published work showing a negative association between severity of illness and neutrophil apoptosis[141]. However, the work of Marshal and others [142,143] points towards a delay in neutrophil apoptosis in sepsis compared with healthy controls following cell culture. The apparent elevated level of neutrophil apoptosis in sepsis patients compared with healthy controls appears to contradict this view. However, these studies explore the delays in the completion of apoptosis resulting in cell death of neutrophils. Therefore, whilst the time to functional apoptosis and hence cell death is likely to be extended in this study, the overall rates of initiation of neutrophil apoptosis are higher in sepsis patients. Thus whilst taking a snap-shot of a sepsis patient shows a higher percentage of neutrophils expressing cell surface evidence of apoptosis, this does not exclude the functional delays in apoptosis shown by Marshal and others through translocation of NF-κB, caspase-9 and other mitochondrial changes. These can occur alongside cell-surfaces changes indicative of the initiation of the apoptotic response. Therefore, these

"neutrophils are constitutively apoptotic, but they also have the ability to subvert their programmed cell death in response to stimuli from the microenvironment of inflammation."[144]

Therefore, the cell-surface loss of CD16 in these sepsis neutrophils is indicative of their constitutional apoptotic nature. The functional delays in this process are not visible as this study looks only at cell-surface changes and not the NF-κB, caspase-9 and other mitochondrial changes described by Marshal.

3.4.3.3. Infective organism subtype differences

The initial study design was powered specifically to detect differences in $V\gamma9^+$ T cells between Gram-negative and Gram-positive infections. This was largely based around an organism's differential ability to stimulate these cells through HMB-PP expression as described in vivo in peritoneal dialysis patients[139,145]. Whilst it was not possible to show increased levels of activation of these cells, an increased percentage $V\gamma9^+$ T cells in Gram-negative (HMB-PP positive) infections that mirror that study is demonstrated. The increased TNF-α and IL-1β in Gram-negative infections may be due to the influence of LPS[145,146] whilst the lower IL-2 in culture-negative groups parallels the SIRS (non-infective) group. As sepsis is a clinical diagnosis requiring only the "suspicion of infection", the culture-negative group may include patients that in fact do not have an infective aetiology underlying their critical illness.

3.4.4. Implications of resulting models

The production of accurate predictive models does not in itself provide a means to improve patient care. It is the application of these models to the process of care where improvements in morbidity and mortality can be made.

Use of the survival prediction model requiring just three variables (IL-6, sensePCT and $CD3^+$%) may allow a healthcare system with limited resources better target those at the highest risk of death and harm. Patients at high risk of death should be cared for in the critical care environment even if the standard physiological variables that underlie the risk scoring systems fail to identify such patients[146,147].

The ability to distinguish between patients with sepsis and SIRS will become increasingly important, as the use of immune-modulating drugs becomes more widespread[147,148]. The ability to distinguish between non-infective life-threatening inflammatory syndromes, such as acute pancreatitis, and sepsis may allow a reduction in the inappropriate use of broad-spectrum antibiotics. This is essential not only to an individual's risk of multi-resistant organism infection and antibiotic-associated side effects but also to the wider issues surrounding antibiotic resistance[31,148]. In addition, it will help direct clinical to any non-infective diagnoses that may benefit from evidence based intervention directed at that particular pathology.

At this stage, it is possible to distinguish between Gram-positive and Gram-negative infections. As early appropriate antibiotics are considered by many to be the only effective intervention, reducing sepsis mortality by as much as 50%[31,149], this ability may allow personalised, directed antibiotic therapy that is not currently possible. The increasing incidence of community-associated MRSA[149,150] often necessitates the critically ill sepsis patient to receive antibiotics such as Vancomycin that carry inherent risks to this cohort of sick patients. Furthermore, the knowledge of an organism's Gram-type may help direct diagnostics towards sites likely to be the source of such an infection. For example, a test that rapidly identifies a causative Gram-negative organism increases the likelihood of pyelonephritis compared with the cellulitis that has attracted the most attention of the clinical team. A different infective source may thus require a different approach to source control. The uncertainty in the evidence base for antibiotic use discussed in the introduction may be alleviated through studies that correctly target antibiotic use towards patients most likely to benefit, namely those with sensitive organisms. Finally, it is hoped in the future that through exploitation of other immunological markers and greater sample numbers, further sub-categorisation of organisms may be possible. The inclusion of MAIT cell markers may allow differentiation between streptococcal and staphylococcal infections[150,151]. It may eventually be possible to create unique immune-fingerprints for individual organism species such as *Escherichia coli* and MRSA. This could use a system of identification based on Table 3.10.

Table 3.10 A system for bacterial identification using immune fingerprints.

	Non-mevalonate pathway (Vγ9/Vδ2 T cell activation)	**Vitamin B2 synthesis** (MAIT cell activation)
Gram-negative bacteria		
Acinetobacter baumannii	+	+
Chryseobacterium gleum	−	+
Enterobacter cloacae	+	+
Escherichia coli	+	+
Haemophilus influenzae	+	+
Helicobacter pylori	+	+
Klebsiella pneumoniae	+	+
Legionella pneumophila	−	+
Neisseria meningitidis	+	+
Pseudomonas aeruginosa	+	+
Shigella dysenteriae	+	+
Gram-positive bacteria		
Bacillus anthracis	+	+
Clostridium difficile	+	+
Corynebacterium diphtheriae	+	+
Enterococcus faecalis	−	−
Listeria monocytogenes	+	−
Mycobacterium tuberculosis	+	+
Propionibacterium acnes	+	+
Staphylococcus aureus	−	+
Streptococcus pyogenes	−	−
Other bacteria		
Borrelia burgdorferi	−	−
Leptospira interrogans	+	+
Mycoplasma genitalium	−	−
Mycoplasma penetrans	+	−
Treponema pallidum	−	−
Yeasts, fungi		
Aspergillus fumigatus	−	+
Candida albicans	−	+
Crytococcus neoformans	−	+
Saccharomyces cerevisiae	−	+

Using a variety of immune responses microbes can be sub-categorised by Gram-status, HMB-PP status, and their ability to activate MAIT cells. This would allow a granular refining of microbe identification.

3.4.5. Shortcomings in this study

There are two main groups of shortcomings in this study. Firstly, the issues surrounding the study design and conduct. Secondly, issues surrounding the analysis and interpretation of its data.

3.4.5.1. Study design

As discussed, this descriptive study is not best placed to describe underlying mechanisms of any differences identified. However, setting this aside, the nature of this as a pilot study necessitated that a power calculation was performed for a specific purpose. An increase in $V\gamma9^+$ cell frequency of 5% in Gram-negative compared with Gram-positive patients was considered a suitable endpoint. Thus, whilst there are many non-significant trends in the data, the study is highly likely to be underpowered to detect significance in many of these variables. However, as a pilot study it can now be argued that the concept of immune fingerprinting to identify a causative organism's category is possible with larger studies needed to confirm and develop the details of this further.

The diagnosis of sepsis relies upon a combination of measured values and clinical acumen. Specifically the patient needs to have "proven infection or suspicion of infection". However, without a gold standard for "infection", patients classed as culture-negative may in fact be more suitable categorised as patient with non-infective SIRS. Whilst a thorough retrospective case note review was conducted for all patients in the culture-negative category to identify alternative aetiologies, this problem remains in any study of this nature. Additionally, the hospital in which the study was carried out did not use PCR or MALDI-TOF based identification techniques that may have further enhanced the ability to describe causative organisms or delineate the culture-negative group further.

This study also lacks granular detail on the eventual outcome of those patients that died. Although all-cause mortality is reported, this lacks both the timing and mode of death. Ideally, patients that die from causes unrelated to their initial admission with sepsis should be excluded when constructing predictive models of survival. For example, a patient death due to a road traffic accident 30 days following their discharge from hospital could not be considered related or predictable by using an immune fingerprinting approach. Although both the ICU mortality and hospital morality could

be used in this circumstance, 90 day mortality has become an accepted standard on which many trials are based and hence the decision to use this time-point despite the lack of clarity regarding the timing and mode of death.

In addition, when considering survival prediction to guide subsequent levels of care, this should be centred on patient sampling at the initial entry level of care. Rather than sampling patients following admission to the ICU, sampling ideally should occur before hospital admission or in the accident and emergency department. This would allow inclusive sampling of patients that may not have a subsequent ICU admission and would be closer to the desired application of such a test as a point-of-care decision aid to direct future standards of patient care.

3.4.5.2. Analysis

Whilst the baseline characteristics for most groups described were similar, the sites of pathology between sepsis and SIRS patients, as well as between the infecting organisms subgroups, were different. This could lead to the resulting models discriminating not between the identified groups directly, but instead between causative sites of pathology as discussed in the introduction. Future studies could concentrate on specific diseases leading to sepsis, such as community-acquired pneumonia, and apply modelling to the causative organisms alone in this subgroup to help remove any bias from these confounders. Furthermore, this study considers only the spectrum of infections present at a single hospital. The population that this hospital serves is a fairly ethnically restricted group typical of a small Welsh town. Independent validation is required in a multicentre setting to rule out such centre effects which may include genetic, environmental, racial, and comorbidity restricted patterns.

There are clear discrepancies in the measured values of procalcitonin across the two analysis techniques. The two techniques this study employed were the Liaison® system (termed PCT) and the highly sensitive procalcitonin analysis carried out using the Kryptor® system (termed sensePCT). Both have been developed and were processed by Thermo Fisher Scientific directly. The Liaison® system is an enzyme-linked fluorescent immunoassay for the quantitative measurement of PCT performed on the VIDAS system, a multi-parametric immunoassay system produced by bioMérieux. This has a measurement range of 0.09-200 ng/mL with values outside of this range analysed by

serial dilution. However, there does exist both intra-assay and inter-assay variability of 5% as specified by the manufacturer's quality control literature[152]. The Kryptor system uses lateral flow immunoassay principles with monoclonal mouse anti-catacalcin antibody conjugated with colloidal gold (tracer) and a polyclonal sheep anti-calcitonin antibody (solid phase). This is measured on a Thermo Fisher Scientific point-of-care testing system termed the BRAHMS direct Reader. This has a measurement range of 0.1-10ng/ml. In comparison to the Liaison® system the sensitivity was 93% and 88% although the variability can be as high as 20%.

Therefore, although measuring the same entity in this study, the differential analysis methods and ranges used are likely to account for the variability between the two results. However, the sensePCT used in this model is the technique favoured for point-of-care testing by Thermo Fisher Scientific directly. These findings do conform to the published literature on the comparison between these systems[153]. Although Schuetz et al conclude that the systems show good correlation, the relative variability between samples in high measurement values in one subset of the data were as much as 24% with the sensePCT having a lower average value.

3.4.5.3. Application of neural networks

The process of forming predictive modelling has a gold-standard approach to prevent the problem of over-fitting. This process starts with a model formed using a unique "training set" of data. Once the resulting model has been refined using this training set, it is then applied to the "test set" to determine its sensitivity, specificity and ROC curve. This test set should be separated from the data in the training set used to form the model. Without this separation, there is a risk that any model will perform well when formed by and tested against the same set of data. However, when applied to a new set of data or scaled to different populations, this model would becomes less accurate. This is termed over-fitting. However, due to the size of the dataset, it was not possible to separate the data into a testing and training set. Again, any further studies with greater patient numbers should be designed around this gold standard of model production. This is especially true when the final models use markers with a smaller number of observations, as is the case in those models including PCT values gained from a lower number of patients compared with the main study dataset. Although these differences

may be statistically significant, a larger cohort would be needed to validate that this has not occurred simply by nature of chance in a small set of patients.

Neural networks offer many advantages over standard techniques in the field of biomarker prediction. These include the ability to manage complex nonlinear relationships, and detect multiple predictor variable interactions[154]. However, like any model, there are inherent disadvantages that need to be considered alongside such positive aspects. There are issues related to the inclusion of neural networks (and other complex modelling) within viable commercial tools. Neural networks applied to complex human disease may be considered as 'black boxes' that fail to explain or illuminate the nature of causal relationships[155]. This may be especially true when the clinician is expected to make direct patient decisions based upon complex algorithms that are not human comprehensible or open to logical (and regulatory) scrutiny. After production of a model, interpretation of the produced weighting matrix, equivalent to the beta coefficients used in standard linear regression, is difficult. There is no standard method to share or transfer these matrixes and they may include variables due to background noise patterns that the researcher may consider unimportant or clinically insignificant. Thus a model cannot be produced in complete isolation of knowledge relating to the underlying mechanisms although an explicit hypothesis generation approach is not needed in the strictest sense[93]. Once a model is accepted, its integration into a practical device requires high levels of computational power. The communication of results to the end user tends to be a nominal process with little opportunity for human scrutiny. The inclusion of alternative human readable processes, such as the decision trees examples, may help to alleviate some of these issues but will result in loss of many of the advantages from a neural network approach.

CHAPTER 4

IMMUNOSUPPRESSION IN EARLY SEPSIS

Chapter 4 Immunosuppression in early sepsis

4.1. Introduction

It has suggested that profound immune changes occur when patients survive first-hit infection with severe sepsis [151,156]. Sepsis-related immune suppression and the compensatory anti-inflammatory response syndrome (CARS) have been appreciated for some time[156,157]. This spectrum of pathology has been linked to common infections encountered in critical care including ventilator-associated pneumonia (VAP), catheter related infections and reactivation of latent virus infections including herpes simple viruses and cytomegalovirus[84,157]. As a result, the syndrome of CARS is associated with an increased length of hospital stay for patients and worsened long-term outcomes[84,158].

Monocyte cell-surface HLA-DR expression has long been accepted as an objective measure of both the presence and the degree of CARS in sepsis patients[106,158]. Studies have also suggested associations (but not causation) between HLA-DR expression and the ability of monocytes to respond to PAMPs including LPS[84,106]. Most commonly, monocytes with a HLA-DR expression level below 30% have been shown to have an attenuated TNF-α response to LPS. This accompanies a negative relationship between monocyte HLA-DR level and patient outcome measures including 90-day mortality. These factors have focused the minds of the intensive care research community to develop therapeutic strategies which aim to reverse CARS through interventions targeted at improvements in monocyte HLA-DR level. The most notable of these treatments has been the use of recombinant GM-CSF that has been subjected to several small-scale randomised clinical trials [84,159]. However, the primary endpoints in these studies have mainly been an improvement in monocyte HLA-DR level rather than measures that can be directly related to an immune response or patient related outcome.

Despite these strong associations, there have been few mechanistic studies that define the roots of the CARS syndrome. The paper by Adib-Conquy does shed some light on what these mechanisms may include and coins the term monocyte reprogramming rather than immune suppression, arguing that many of the changes seen in CARS may be adaptive rather than simply a loss-of-function[159-161]. Indeed, here it will be argued that CARS does not only herald loss of immune functions but may also include some gain-of-function abilities in neutrophils particularly. The chapter describes how the

reprogrammed monocytes have a limited ability to produce TNF-α in response to LPS whilst the amount of the anti-inflammatory cytokine, IL-10, is increased. Furthermore, they suggest that different subsets of monocytes (CD16 high, CD16 low, CD14 low) have intrinsic levels of responsiveness to LPS with CD16 high monocytes having the highest TNF-α responsiveness with lower IL-10 levels. An example of these subsets is shown in Figure 4.1.

In this chapter, ultra-pure LPS will be used to elicit responses from sepsis monocytes with HLA-DR levels below 30% and compare them with healthy controls. The responsiveness of sepsis monocytes to LPS will then be increased using activated $V\gamma9^+$ T cell supernatant. This supernatant contains many of the cytokines mechanistically appropriate for the reversal of reprogramming identified in other studies[160-162], and has been shown to aid survival and develop APC-like phenotypes in other cell types[162,163]. In addition, using related in vivo studies it will be shown that the licenced bisphosphonate drug Zometa can be used to stimulate $V\gamma9^+$ T cells in vivo in a safe and targeted manner. It may thus be possible to attenuate aspects of the CARS syndrome by using licenced drugs that activate $V\gamma9^+$ T cells in sepsis survivors and hence reduce the burden of subsequent illness that often follows first-hit infections.

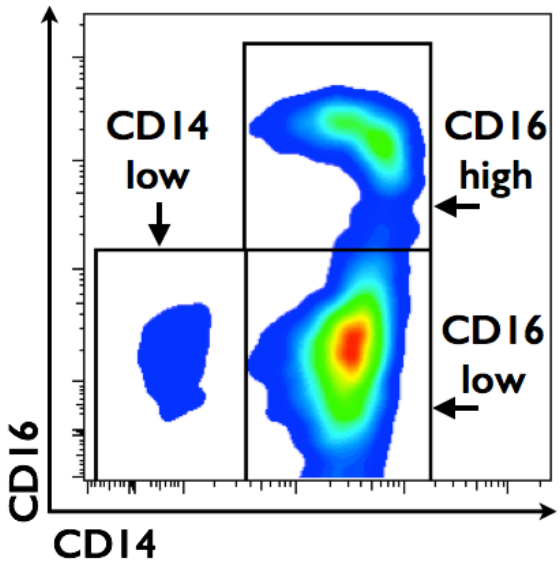

Figure 4.1 Monocyte division into differing subsets. Monocytes can be subdivided into three main distinct groups using the expression of cell-surface CD14 and CD16 based on isotype controls.

Neutrophils are the first cells that are recruited to sites of microbial infection. Although classically viewed as terminally differentiated immune cells, there is emerging evidence that neutrophils represent key components of the effector and regulatory arms of both the innate and adaptive immune system[163,164]. As such, neutrophils secrete an array of immunomodulatory factors affecting the recruitment and effector functions of various cell types and engage in mutual interactions with immune and non-immune cells[164-166].

Most intriguingly, neutrophils directly affect the generation of antigen-specific immune responses, by facilitating monocyte differentiation and DC maturation and by interacting with B cells and T cells[165-167]. Of note, neutrophils patrol the spleen under homeostatic conditions, and in acute inflammatory scenarios co-localise with T cells in the white[167,168] and with B cells in the marginal zone[168,169]. Similarly, neutrophils enter the draining lymph nodes during bacterial and parasitic infections[169-171] where they may influence adaptive immune responses. In mouse models of acute and chronic inflammation, neutrophils have in fact been shown to present antigens directly to both $CD4^+$ and $CD8^+$ T cells[170-175].

In humans, neutrophils with a phenotype consistent with a possible APC function, including surface expression of MHC class II, have been found in diverse inflammatory and infectious scenarios[172-176]. The physiological context underlying a potential differentiation of neutrophils into APCs remains poorly understood, and the

implications for the stimulation of antigen-specific T cell responses are unclear. Previous investigations described the generation of human neutrophils with antigen-presenting features in vitro through the action of cytokines or by crosslinking CD11b[176,177], and in vivo in patients treated with GM-CSF, G-CSF, or IFN-γ[178,179]. These observations were complemented recently by findings in mouse models indicating that neutrophils can differentiate into "neutrophil-DC hybrids" in vitro and in vivo and play a dual protective role by rapidly clearing pathogens and presenting microbial antigens to $CD4^+$ T cells[178,180]. Conversely, neutrophils have also been shown to down modulate responses by activated T cells through the release of arginase and reactive oxygen species (ROS) into the TCR:MHC synapse[180-184], adding to the emergence of distinct neutrophil populations with tailored roles in modulating, dampening and exacerbating immune response. This notwithstanding, direct antigen presentation by neutrophils has thus far not been demonstrated in infected patients. Furthermore, the cellular source of neutrophil-polarizing factors during acute inflammation has not been identified, and the potential contribution of tissue-resident and/or rapidly recruited immune cells in early infection has been overlooked.

Unconventional T cells such as human $V\gamma9^+$ T cells, Natural killer T (NKT) cells and mucosal-associated invariant T (MAIT) cells represent unique sentinel cells with a distinctive responsiveness to self and non-self low molecular weight compounds akin to pathogen-associated (PAMPs) and danger-associated molecular patterns (DAMPs)[181-184]. Unconventional T cells represent a substantial proportion of all T cells in blood (>15%) and mucosal epithelia (>50%), accumulate in many inflamed tissues, and have been implicated in the regulation and pathology of inflammatory and infectious diseases as well as in tumorigenesis[71,181-186]. Given the efficient immune surveillance network constituted by unconventional T cells, it has been suggested that such T cells orchestrate innate and adaptive responses to different stimuli at the site of inflammation where they engage with other components of the inflammatory infiltrate[71,74,185,187]. Recent reports also demonstrated that innate lymphocytes including $V\gamma9^+$ T cells and NKT cells are ideally positioned in lymphoid tissues where they can interact with freshly recruited monocytes and neutrophils in response to blood and lymph-borne pathogens[159,187]. However, the crosstalk of human unconventional T cells and neutrophils has not been studied in detail, and the contribution of different types of unconventional T cells to the host response at early stages of infection remains unclear.

This chapter will conclude by demonstrating that antigen presenting human neutrophils can readily be found during acute sepsis. The presence of such APC-like neutrophils may reflect early responses by unconventional T cells to microbial pathogens as the phenotype and function of sepsis neutrophils can be replicated in vitro upon priming of neutrophils by human $V\gamma9^+$ T cells and MAIT cells. Our findings thus provide a physiological context and a cellular mechanism for the generation of neutrophils with APC function in a broad range of microbial infections.

4.2. Aims

- Explore the association between monocyte cell-surface HLA-DR expression and cytokine responses to LPS.
    (a) Assess whether activation of $V\gamma9^+$ T cells can reverse monocyte reprogramming and hence improve responsiveness of monocytes to LPS.
    (b) Link these findings to in vitro work that may justify the use of a licenced bisphosphonate drug Zometa in future clinical trials of sepsis-related CARS.
- Describe the ability of sepsis neutrophils to act as APC.
    (a) Describe early phenotypic changes in sepsis neutrophils that point towards an APC-like function.
    (b) Perform cross-presentation assays to demonstrate the ability of sepsis neutrophil to act as APCs ex vivo.
    (c) Describe associations between neutrophil APC phenotypes and activated unconventional T cells and link this to published mechanistic ex vivo work.

4.3. Results

The sepsis samples used in this chapter originated from patients enrolled in the main phenotype study covered in Chapter 3 at day 5 of their ICU stay. All purities following magnetic nanoparticle cell isolation were in excess of 98% and the HLA-DR cell-surface expression level on all monocytes used was below 30% using an isotope control. Representative FACS plots of a healthy control and a sepsis patient gated as described in Figure 2.3 is shows in Figure 4.2.

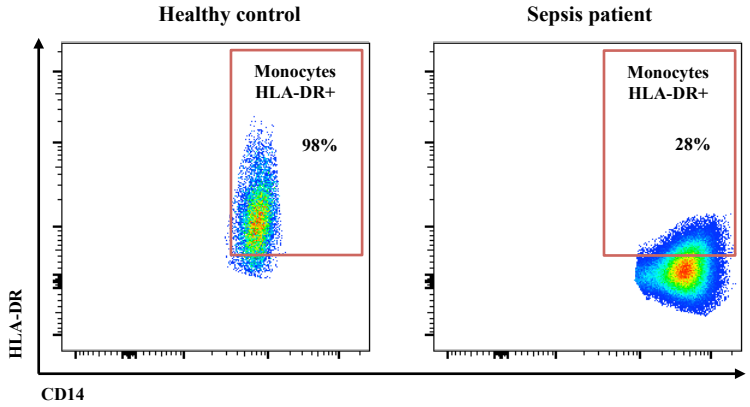

Figure 4.2 Representative FACS plots for monocyte HLA-DR cell-surface expression in healthy controls and sepsis patients.

The level of live monocyte HLA-DR cell-surface expression as a percentage of cells compared with individual isotype controls is shown in healthy controls and sepsis patients. Patients with monocyte HLA-DR levels below 30% were used in the following series of immunosuppression experiments.

4.3.1. Cytokine expression following LPS challenge (n=5)

Despite the isolated sepsis monocytes having a cell-surface HLA-DR level below 30%, their cytokine responsiveness to ultra-pure LPS was highly variable. Two out of the total of five sepsis samples tested resulted in TNF-α levels comparable to healthy controls (Figure 4.3 A and B) when stimulated immediately following isolation. This questions the ability of HLA-DR to act as an accurate surrogate marker for sepsis-related CARS.

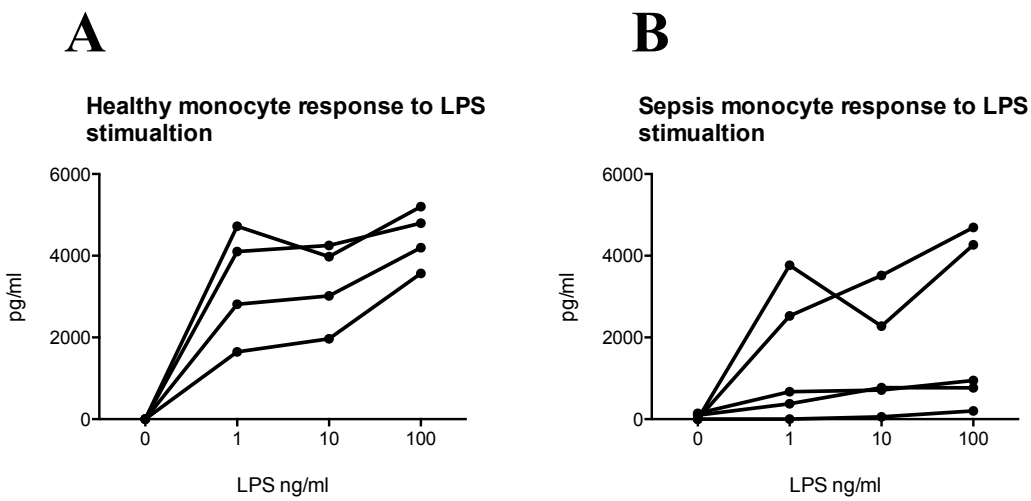

Figure 4.3 Monocyte cytokine production following ultra-pure LPS challenge. (A) Production of ELISA measured TNF-α following ultra-pure LPS challenge in healthy control purified monocytes. (B) Production of ELISA measured TNF-α following ultra-pure LPS challenge in sepsis patients' purified monocytes all with cell-surface HLA-DR levels below 30%. Healthy patients n = 4, sepsis patients n = 5.

Separate samples of isolated monocytes and PBMCs were cultured under a variety of conditions for 20 hours before being stimulated with LPS. Pure monocytes isolated from healthy individuals showed an enhanced TNF-α response to LPS when cultured in the presence of cell-free $V\gamma9^+$ T cell supernatant (Figure 4.4 A). The bisphosphonate Zometa activates $V\gamma9^+$ T cells in the presence of monocytes. Therefore, in Figure 4.4 B, as the PBMC culture includes $V\gamma9^+$ T cells, an enhanced TNF-α response to LPS can be replicated without the need to add extrinsic $V\gamma9^+$ T cell supernatant. The IL-10 cytokine response followed an inverse pattern as would be expected and described by the literature[158,159]. There is a downregulation of IL-10 in the pure monocytes cultured in the presence cell-free $V\gamma9^+$ T cell supernatant shown in Figure 4.4 C. This is again replicated by the use of Zometa to activate $V\gamma9^+$ T cells present in the PBMC culture shown in Figure 4.4 D.

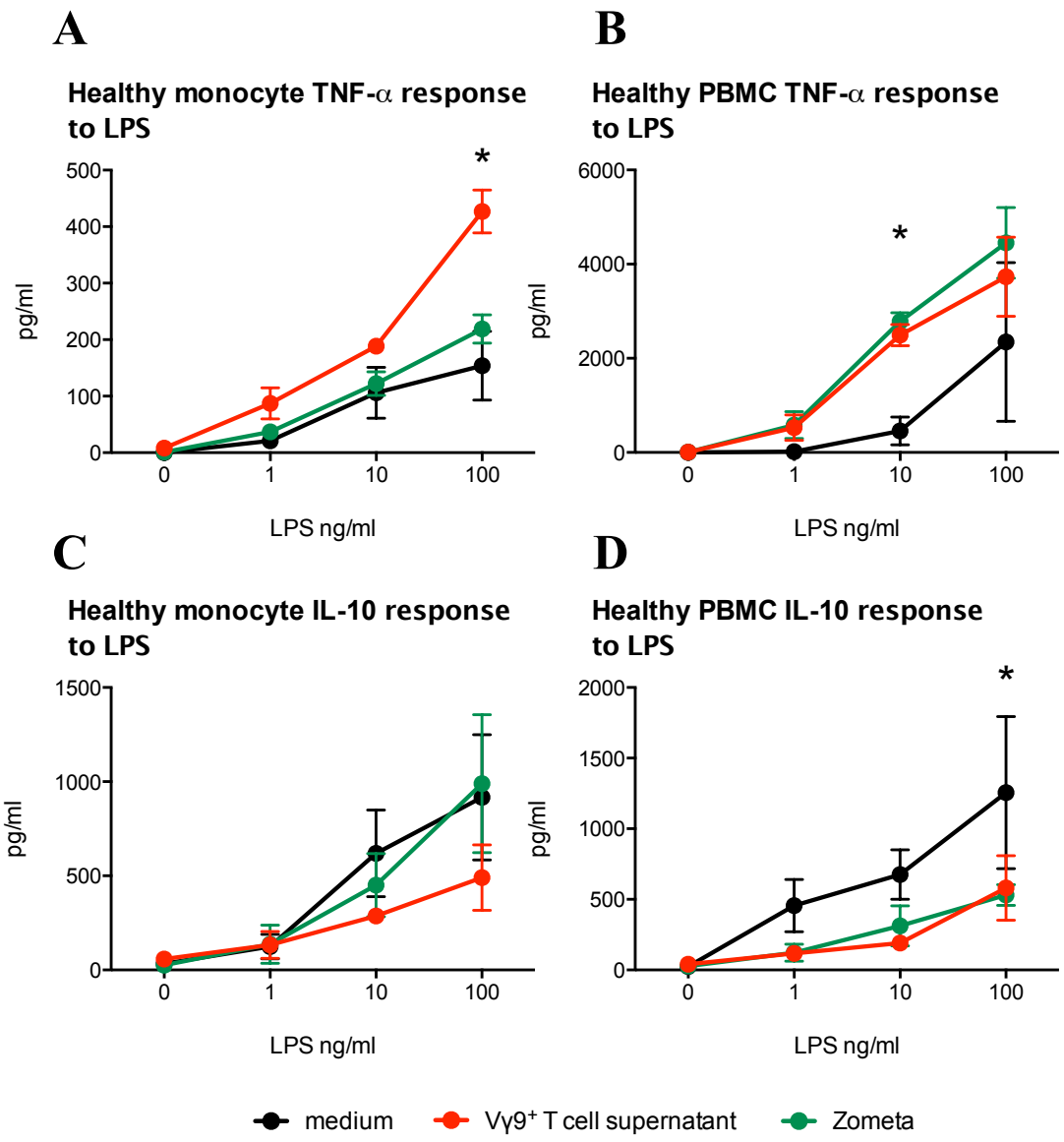

Figure 4.4 Cytokine production following ultra-pure LPS challenge in conditioned healthy monocytes and PBMCs. Production of ELISA measured TNF-α after 20 hours in different culture conditions following ultra-pure LPS challenge in (A) healthy control purified monocytes (B) healthy control PBMCs. Production of ELISA measured IL-10 after 20 hours in different culture conditions following ultra-pure LPS challenge in (C) healthy control purified monocytes (D) healthy control PBMCs. * $p<0.05$. Healthy patients n = 5, sepsis patients n = 5. Analysis is based on a repeated measures two-way ANOVA with Dunnett's correction for multiple comparisons based on a reference group of medium cultured cells.

When these assays are repeated using cells from sepsis patients, a broadly similar pattern is observed in the upregulation of a TNF-α response to LPS when $V\gamma9^+$ T cell supernatant is added to the cultures (Figure 4.5 A). There is a trend in this being replicated using Zometa in PBMC cultures although this does not become statistically significant due to the large variation in responses (Figure 4.5 B). Whilst there is a trend in downregulation of IL-10 in the $V\gamma9^+$ T cell supernatant culture in sepsis monocytes, no similar features are observed in the Zometa treated samples (Figure 4.5 C and D).

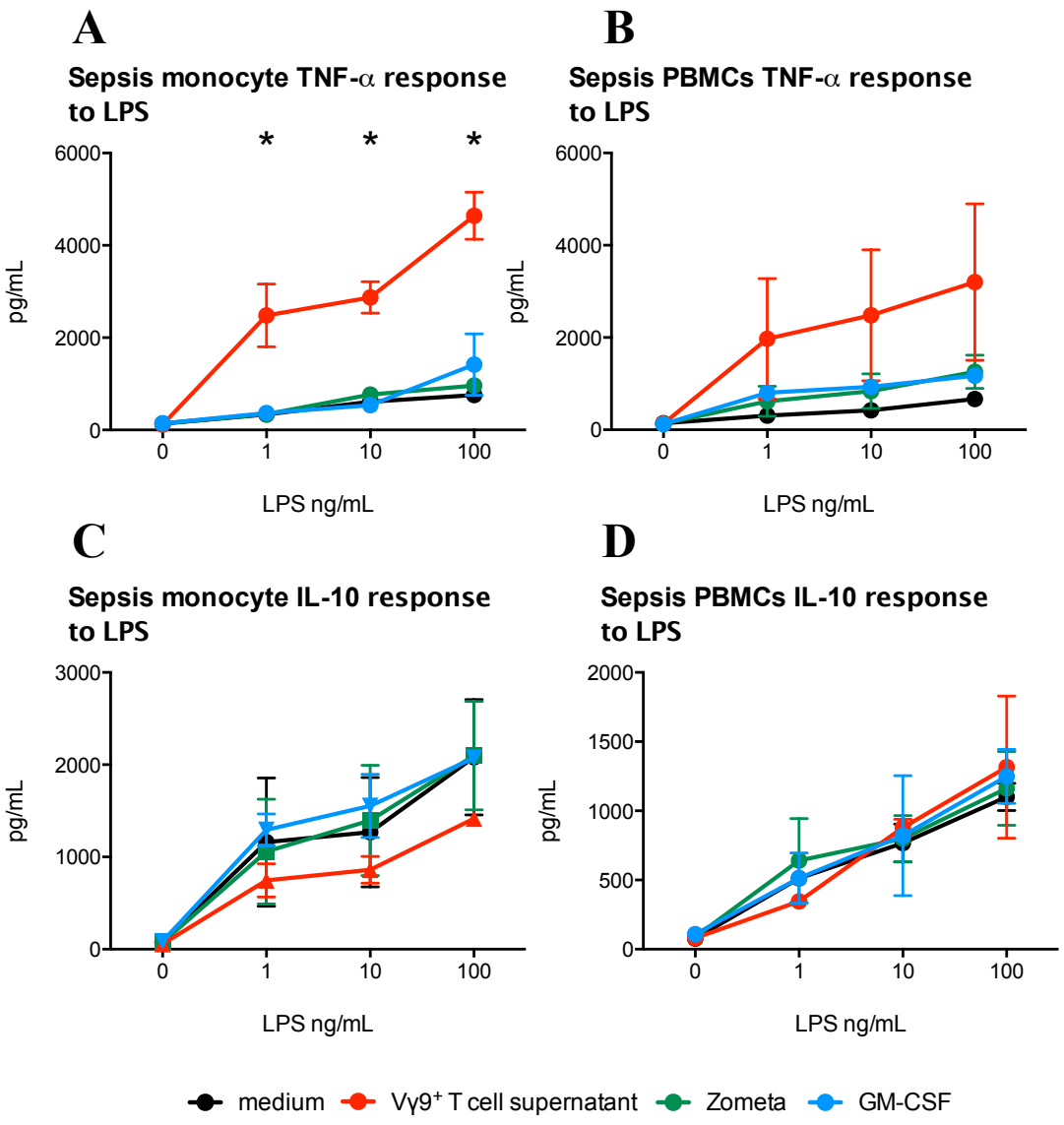

Figure 4.5 Cytokine production following ultra-pure LPS challenge in conditioned sepsis monocytes and PBMCs. Production of ELISA measured TNF-α after 20 hours in different culture conditions following ultra-pure LPS challenge in (A) sepsis purified monocytes with HLA-DR levels below 30% (B) sepsis PBMCs. Production of ELISA measured IL-10 after 20 hours in different culture conditions following ultra-pure LPS challenge in (C) sepsis purified monocytes with HLA-DR levels below 30% (D) sepsis PBMCs. * $p<0.05$. Sepsis patients n = 5. Analysis is based on a repeated measures two-way ANOVA with Dunnett's correction for multiple comparisons based on a reference group of medium cultured cells.

4.3.2. Immune rescue though monocyte subset changes

Although it has been shown that LPS responsiveness could be increased in different culture conditions, this did not seem to be the result of an increased cell-surface expression of monocyte HLA-DR. Figure 4.6 A uses the monocyte divisions outlined in Figure 4.3 to examine cell-surface changes in the different monocyte subsets of CD16 low, CD16 high and CD14 low. It shows little change in the expression of monocyte HLA-DR in any of the monocytes subsets or subgroups. However, when these subset divisions are examined in detail, an increased percentage of the CD16 high monocytes in sepsis patients following treatment with $V\gamma9^{+}$ T cell supernatant are shown (Figure 4.6 B). A representative example of the expansion of this CD16 high subset is shown in Figure 4.7.

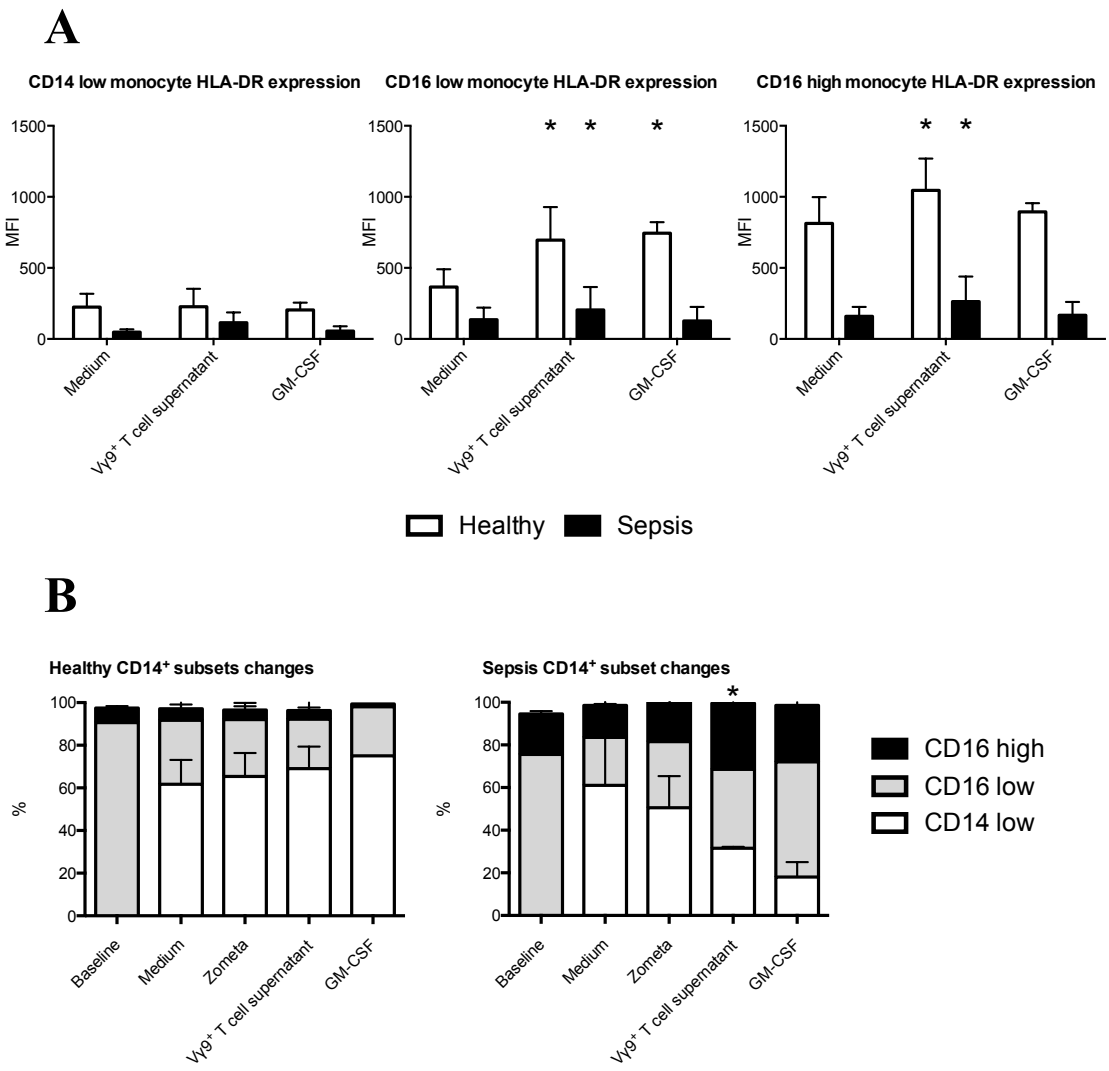

Figure 4.6 Phenotypic changes in sepsis monocytes subgroups under different culture conditions. (A) Alternations in isolated sepsis monocyte HLA-DR cell-surface expression in CD14 low, CD16 low and CD16 high subgroups in different culture conditions. (B) Relative distribution of healthy and sepsis monocyte subgroups in PBMCs following different culture conditions. Healthy patients n = 5, sepsis patients n = 5. Analysis is based on a repeated measures two-way ANOVA with Dunnett's correction for multiple comparisons based on a reference group of medium cultured cells. Comparisons in A were performed independently for healthy controls and sepsis patients.

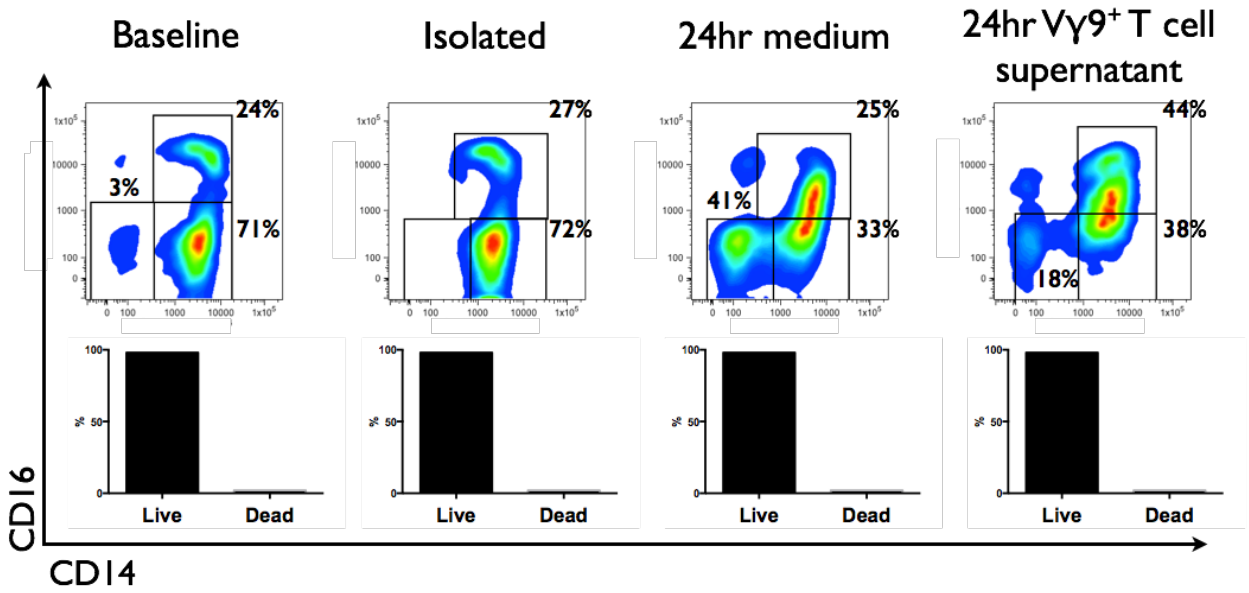

Figure 4.7 An example of subset changes in sepsis monocytes following culture in the presence of Vγ9$^+$ T cell supernatant. Relative changes in the distribution of CD14 low, CD16 low, and CD16 high monocyte subsets in a sepsis patient before positive selection (baseline), following positive selection (isolated) after medium culture controls (medium) and following culture with Vγ9$^+$ T cell supernatant. Cell survival assessed by cell-surface live/dead aqua staining is shown below each FACS plot.

4.3.3. The use of bisphosphonates to rescue monocytes

Although using an artificially produced Vγ9$^+$ T cell supernatant resulted in phenotypic and functional monocyte changes, an intervention of this kind would only be suitable for patients if these responses could be simulated in vivo by the use of safe drugs. The use of Zometa in this experiment suggests that this may be an effective avenue to explore. Therefore, the immune changes that follow when otherwise healthy patients with osteoporosis started taking Zometa were studied. Dr Joanne Welton processed the following samples with all statistical analysis performed by myself. The study cohort comprised of 19 healthy non-smoking adult females with postmenopausal osteoporosis and a bone density T-score of -2.5 or worse at either total spine, total hip, or neck of femur when measured by dual-energy X-ray absorptiometry (DXA). The mean age was 68 years (range 57 to 79 years).

All study participants shown in Figure 4.8, Figure 4.9, Figure 4.10 were bisphosphonates naive and attended outpatient appointments at Cardiff Royal Infirmary for a first-time infusion of 5mg intravenously Zometa (Aclasta). Inclusion criteria included no contraindications to treatment with intravenous bisphosphonates; normal

creatinine clearance levels of >35 mL/min; and normal vitamin D levels of 30 to 100mg/L. Exclusion criteria included a body temperature >38.5°C at first visit; participation in another therapeutic trial within 20 days of consent; history of illness that might compromise participation such as drug or alcohol abuse; hypocalcaemia (<2.2 mmol/L corrected); and current use of oral steroids or other immunosuppressive agents.

There was evidence of $V\gamma9^+$ T cell activation through upregulation of the activation markers CD69 at day 1 and day 3, NKG2D at day 1 and HLA-DR at day 3 (Figure 4.8).

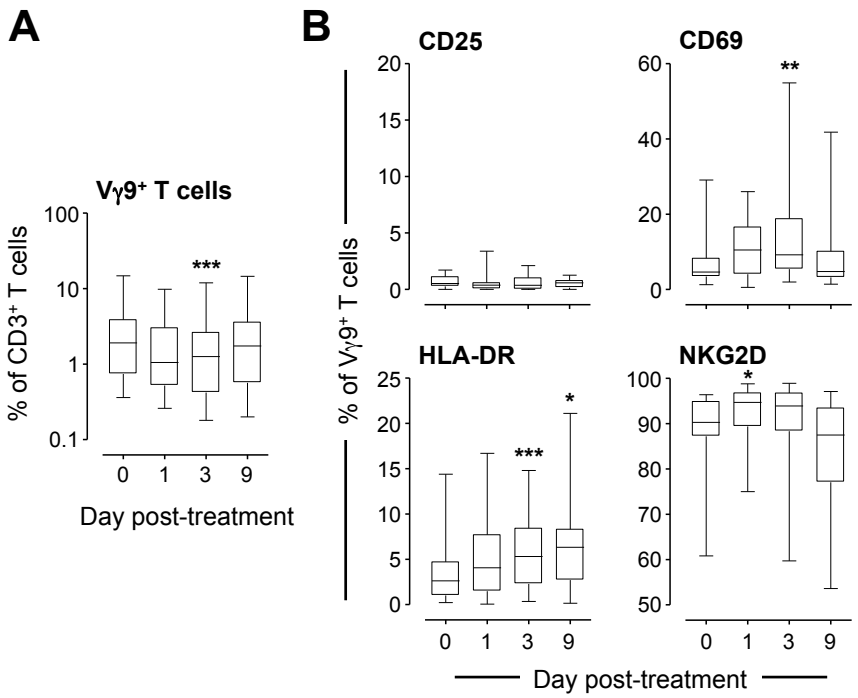

Figure 4.8 Activation of peripheral $V\gamma9^+$ T cells after Zometa treatment. (A) Proportion of $V\gamma9^+$ T cells as percentage of all circulating CD3 T cells; (B) their surface expression of CD25, CD69, HLA-DR, and NKG2D following first-time infusion of 5mg intravenously Zometa (Aclasta). Differences were assessed using Student's t-tests. Dr Joanne Welton processed the following samples with all statistical analysis performed by myself. N = 19. Data were analysed using a matched Friedman test with the reference group as day 0 and Dunn's correction for multiple comparisons.

When examining the resulting cytokine profile following administration of Zometa, they mirrored that typical of in vivo $V\gamma9^+$ T cell activation in PBMCs with significantly higher levels of TNF-α, IFN-γ, GM-CSF and IL-6 following treatment (Figure 4.9).

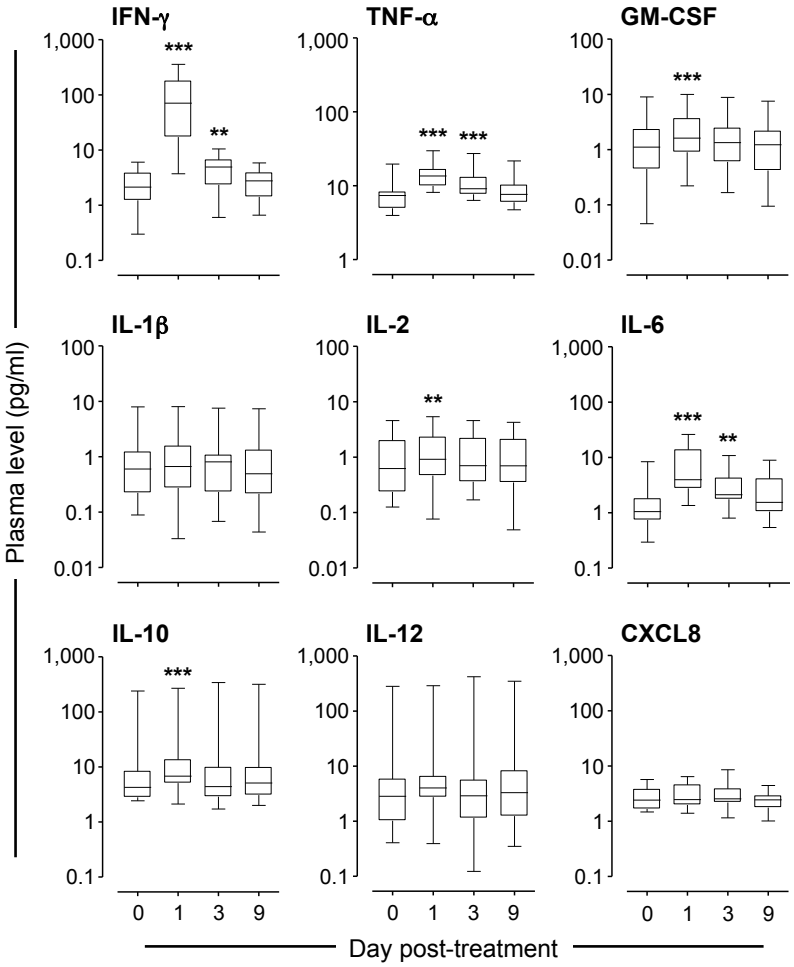

Figure 4.9 Increased plasma cytokines and chemokines after Zometa treatment. Plasma levels of the markers indicated as determined by multiplex ELISA following first-time infusion of 5mg intravenously Zometa (Aclasta). Differences were assessed using Wilcoxon's signed-rank tests for IL-1β, IL-6, IL-10, and IL-12 levels and Student's t tests for all other soluble mediators. Dr Joanne Welton processed the following samples with all statistical analysis performed by myself. N = 19. Data were analysed using a matched Friedman test with the reference group as day 0 and Dunn's correction for multiple comparisons

Furthermore, the use of Zometa appeared to have an effect on monocyte phenotype, both increasing their numbers and upregulation expression of cell-surface CD14, CD40, CD80, and HLA-DR (Figure 4.10).

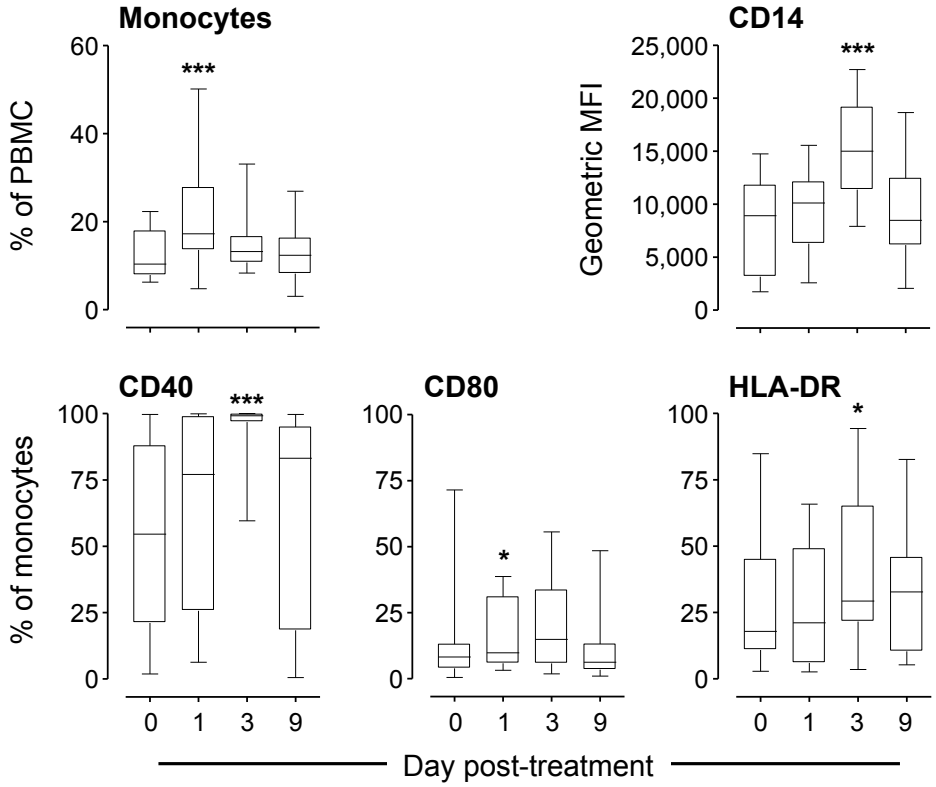

Figure 4.10 Activation of peripheral monocytes after Zometa treatment. Proportion of $CD14^+$ monocytes as percentage of all PBMCs as well as surface expression of CD14 (geometric mean fluorescence intensity [MFI]) and CD40, CD80, and HLA-DR on circulating $CD14^+$ monocytes following first-time infusion of 5mg intravenously Zometa (Aclasta). Differences were assessed using Wilcoxon's signed-rank tests for CD40 levels on day 3 and Student's t tests for all other parameters. Dr Joanne Welton processed the following samples with all statistical analysis performed by myself. N = 19. Data were analysed using a matched Friedman test with the reference group as day 0 and Dunn's correction for multiple comparisons

Taken together, it may be possible to exploit the ability of the safe, licenced drug Zometa to activate $V\gamma9^+$ T cell in sepsis patients with CARS. It can be argued that this would lead to a reprograming of sepsis monocytes into cells with a regained TNF-α responsiveness to LPS and a downregulated anti-inflammatory IL-10 profile reminiscent of normal monocytes.

4.3.4. Phenotypic changes in sepsis neutrophils

In order to resolve the existence of APC-like neutrophils in human infectious disease and determine a possible link with anti-microbial unconventional T cell responses, phenotypical and functional characterisation of neutrophils from culture-positive patients from our sepsis cohort described in Chapter 3 was performed.

Sepsis neutrophils displayed a strikingly altered phenotype compared with neutrophils from healthy individuals and patients with sterile SIRS who served as non-infected controls (Chapter 3, Figure 3.18, B and C). Sepsis neutrophils were characterized by markedly higher expression of CD40, CD64 (FcγRI) and CD86, consistent with an activated phenotype and with a potential APC function. Increased surface levels of CD83 and HLA-DR on circulating neutrophils in some sepsis patients has also been shown, although this was not significant across the cohort as a whole. Of note, there was a significant correlation between the expression of CD64 and HLA-DR on sepsis neutrophils, supporting a link between neutrophil activation and APC phenotype (Figure 4.11 A). This correlation was evidenced by higher levels of CD11b, CD40, and HLA-DR in patients with CD64hi neutrophils compared with those with CD64lo neutrophils (Figure 4.11 B). Vice versa, neutrophils expressed higher levels of CD64 in patients with HLA-DRhi neutrophils compared with HLA-DRlo neutrophils (Figure 4.11 B).

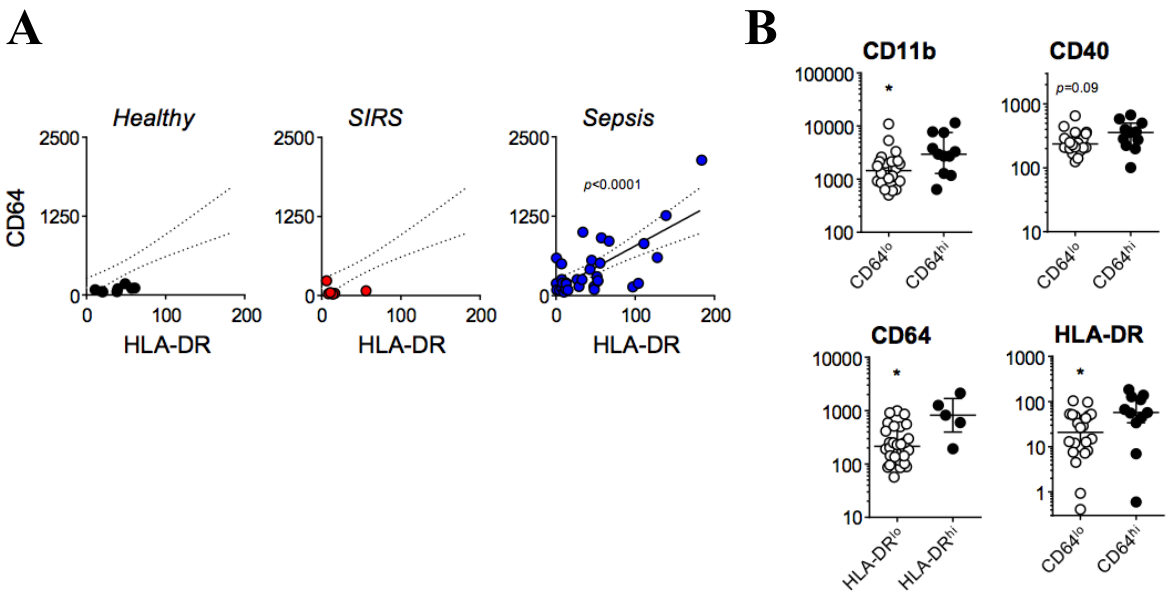

Figure 4.11 Neutrophils from patients with acute sepsis display an APC-like phenotype. (A) Surface expression of CD64 and HLA-DR on circulating neutrophils in healthy controls and in patients with SIRS or microbial sepsis. (B) Surface expression of CD11b, CD40, and HLA-DR on circulating neutrophils in sepsis patients with CD64 levels below (CD64lo) or above (CD64hi) a MFI of 500. Surface expression of CD64 on circulating neutrophils describes sepsis patients with HLA-DR levels below (HLA-DRlo) or above (HLA-DRhi) a MFI of 100. Each data point represents an individual patient. Each data point represents an individual patient; lines and error bars depict medians and interquartile ranges. Data were analysed using Kruskal-Wallis tests and Dunn's multiple comparison tests; comparisons were made with sepsis patients Lines in B depict linear regression and 95% confidence bands as calculated for sepsis neutrophils. SIRS (n = 8) or sepsis (n = 37) and in healthy controls (n = 10).

Sepsis patients often show signs of acute immune suppression, typically defined by a down modulation of HLA-DR expression on monocytes[71,158,188]. Therefore, the phenotype of circulating neutrophils in sepsis patients with and without presumed immune suppression was assessed. While circulating monocytes in healthy controls were uniformly HLA-DR^{+}, a proportion of patients with SIRS or with sepsis showed a significant reduction in HLA-DR expression levels on monocytes. In sepsis patients, there was a weak correlation of HLA-DR expression on monocytes with CD40 or CD64 expression on neutrophils (Figure 4.12 A and B). When splitting the sepsis cohort into patients with monocyte HLA-DR levels below and above 50% as a pre-determinant of presumed immune suppression, there was a higher expression of HLA-DR on circulating neutrophils in patients with HLA-DRhi monocytes (Figure 4.12 C). Yet, these differences were generally only very small, and most individuals showed classical signs of immune suppression (Figure 4.12 D).

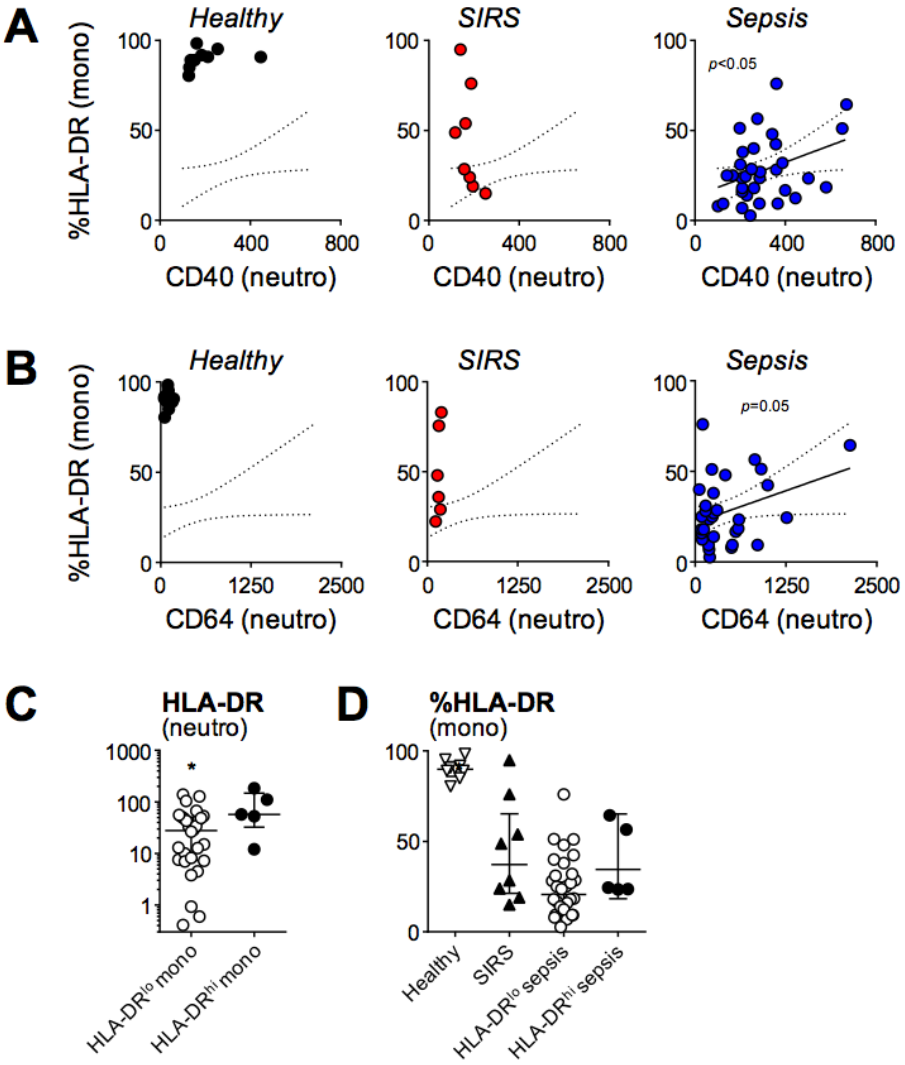

Figure 4.12 Correlation between monocyte HLA-DR suppression and APC-like phenotype of neutrophils from patients with acute sepsis. Surface expression of CD40 (A) and CD64 (B) on circulating neutrophils and frequency of HLA-DR$^+$ monocytes in healthy controls and in patients with SIRS or microbial sepsis. (C) Surface expression of HLA-DR on circulating neutrophils in sepsis patients with monocyte HLA-DR levels <50% (HLA-DRlo) or >50% (HLA-DRhi). (D) Frequency of HLA-DR$^+$ monocytes in healthy controls and SIRS patients, and in sepsis patients with HLA-DR levels on circulating neutrophils below (HLA-DRlo) or above (HLA-DRhi) a MFI of 100. Each data point represents an individual patient. Lines in A and B depict linear regression and 95% confidence bands as calculated for sepsis neutrophils. Lines and error bars in C depict medians and interquartile ranges; differences were analysed using Mann-Whitney tests. Lines and error bars in D depict geometric means and 95% confidence intervals. SIRS n = 8 or sepsis n = 37 and in healthy controls n = 10.

4.3.5. APC-like functions of sepsis neutrophils

It has not yet been established in human infections whether neutrophils are capable of triggering antigen-specific T cell responses. Here, isolated untouched neutrophils from the blood of sepsis patients were used in purities of 99.2-99.8% by negative selection, and advantage was taken of a well-established experimental readout based on HLA- A2 restricted responder T cell lines specific for M1(p58-66), the immunodominant epitope of the influenza M1 protein [44]. These experiments demonstrated that freshly isolated neutrophils from HLA-$A2^+$ patients with acute sepsis and neutrophils from HLA-$A2^+$ healthy controls had a similar capacity to activate M1(p58-66)-specific responder $CD8^+$ T cells when treated with the peptide itself, which can be readily pulsed onto cell surface-associated MHC class I molecules for direct presentation to $CD8^+$ T cells (Figure 4.13 A). Strikingly, sepsis neutrophils were also able to induce robust responses by M1(p58-66)-specific responder $CD8^+$ T cells when utilizing the full-length M1 protein, a 251 amino acid long viral antigen that requires uptake, processing and loading of M1(p58-66) onto intracellular MHC class I molecules for cross-presentation to $CD8^+$ T cells. Despite the clinical differences in the underlying disease and the phenotypical variability in the peripheral neutrophil population across the patient cohort, $CD8^+$ T cell responses were consistently induced by neutrophils from three HLA-$A2^+$ patients with culture-positive sepsis (Figure 4.13 B). Neutrophils from a further HLA-$A2^+$ patient presenting with non-viral pneumonia also induced substantial activation of $CD8^+$ T cells; yet this experiment was excluded from the analysis as the causative pathogen could not unambiguously be resolved for this individual (Figure 4.13 C). In contrast to sepsis patients, neutrophils from healthy controls were inactive even at the highest concentration of M1 protein, in agreement with their lack of APC marker expression (Figure 4.13 B). Taken together, these findings indicate that in acute sepsis neutrophils acquire an APC-like phenotype with the capacity to induce antigen-specific $CD8^+$ T cell responses.

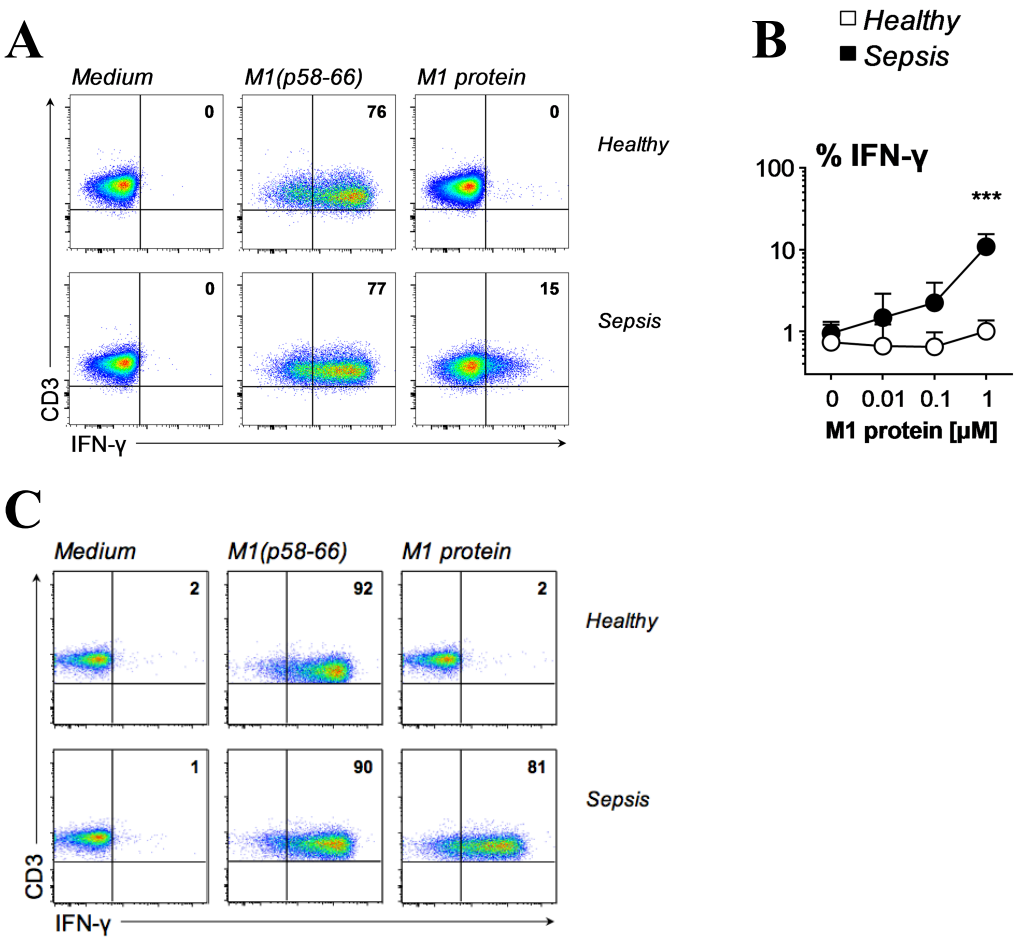

Figure 4.13 Neutrophils from patients with acute sepsis antigen cross-presenting capacity. (A) IFN-γ production by M1-specific $CD8^+$ T cells in response to freshly isolated neutrophils loaded with 0.1 μM synthetic M1(p58-66) peptide or 1 μM M1 protein. Data shown are representative of three HLA-$A2^+$ sepsis patients and three HLA-$A2^+$ healthy volunteers as controls. Sepsis patients recruited for these APC assays had confirmed infections as identified by positive culture results: *E. coli* (urine), *Klebsiella pneumoniae* (respiratory culture) and *Staphylococcus epidermidis* (blood), respectively. (B) Summary of all stimulation assays conducted, shown as percentage of IFN-γ positive $CD8^+$ T cells in response to freshly isolated neutrophils loaded with peptide or the indicated concentrations of M1 protein (means ± SD). Data were analysed by one-way ANOVA with Bonferroni's post-hoc testing. (C) IFN-γ production by M1-specific $CD8^+$ T cells in response to freshly isolated neutrophils loaded with 0.1 μM synthetic M1(p58-66) peptide or 1 μM M1 protein. The HLA- $A2^+$ sepsis patient analysed in this experiment was diagnosed with pneumonia and acute respiratory failure, and was negative for influenza A and B virus, parainfluenza virus, respiratory syncytial virus and adenovirus, yet did not allow a positive characterization of the causative pathogen due to no growth from blood and bronchoalveolar lavage samples. The sepsis neutrophils were tested alongside freshly isolated neutrophils from an HLA-$A2^+$ healthy volunteer as a control. Sepsis n = 3, healthy n = 3.

4.3.6. Cross-talk between neutrophils and unconventional T cells

Next, the potential involvement of unconventional T cells in the inflammatory response during acute sepsis was studied. Human Vγ9/Vδ2 T cells recognize the microbial metabolite (E)-4-hydroxy-3-methyl-but-2-enyl pyrophosphate (HMB-PP), an intermediate of the non-mevalonate pathway of isoprenoid biosynthesis shared by many Gram-negative and Gram-positive bacteria as well as malaria parasites[71,150,188] (Table 3.10). In analogy, Vα7.2$^+$ CD161$^+$ MAIT cells respond to a wide range of Gram-negative and Gram-positive bacteria as well as yeasts by sensing intermediates of the microbial vitamin B2 biosynthesis, such as the riboflavin precursor 6,7-dimethyl-8-D-ribityllumazine (from here on referred to as "lumazine") and its derivative, reduced 6-hydroxymethyl-8-D-ribityllumazine (rRL-6-CH_2OH)[139,150,188]. Based on genomic database searches, the vast majority of sepsis patients recruited to the present study, including those patients who provided samples for the cross-presentation experiments, were identified as being infected with organisms that utilize the non-mevalonate and/or riboflavin pathways and are hence capable of stimulating Vγ9/Vδ2 T cells and/or MAIT cells, respectively (Table 3.10).

Multi-colour flow cytometric analyses revealed a substantial activation of Vγ9/Vδ2 T cells as judged by expression of CD25 and CD69 in newly diagnosed sepsis patients but not in SIRS patients (Figure 3.20 B). It was also found that there were significant differences in the absolute counts and in the proportion of Vγ9/Vδ2 T cells among all circulating T cells between patients with microbiologically confirmed infections caused by HMB-PP producing pathogens including *E. coli*, *Klebsiella pneumoniae*, *Pseudomonas aeruginosa* and *Corynebacterium* spp., as opposed to HMB-PP deficient species like *Staphylococcus* spp. and *Streptococcus* spp. (Figure 3.28). In contrast, there was no difference in the proportion of CD4$^+$ and CD8$^+$ T cells between HMB-PP positive and HMB-PP negative infections (Figure 3.28). These clinical findings evoked earlier studies in patients with peritoneal dialysis-associated bacterial peritonitis[139,189] and further supported the notion of a differential responsiveness of Vγ9/Vδ2 T cells to defined pathogen subgroups.

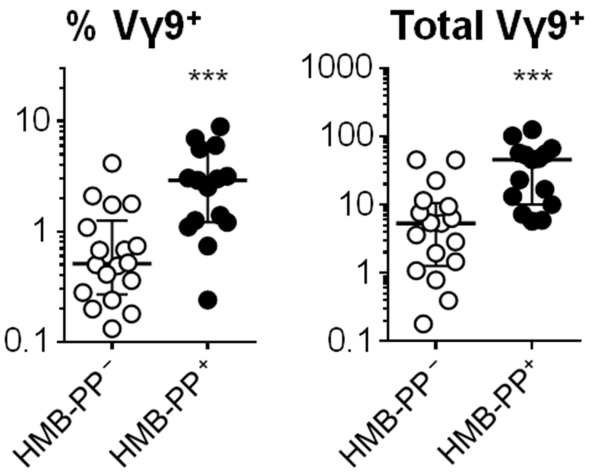

Figure 4.14 Activated Vγ9$^+$ T cells in patients with acute microbial sepsis. Proportion of Vγ9$^+$ T cells among all circulating T cells and absolute counts of circulating Vγ9$^+$ T cells (in cells/µl blood) in sepsis patients with microbiologically confirmed infections caused by HMB-PP producing or HMB-PP deficient bacteria. Data were analysed using Mann-Whitney tests. HMB-PP$^-$ n =18, HMB-PP$^+$ n = 19.

In the absence of specific staining reagents to unambiguously identify MAIT cells in biological samples such as MR1 tetramers, which were not available at the time of the clinical study, a similar analysis of circulating MAIT cells was not conducted. A recent study reported a systemic loss in peripheral MAIT cell counts in sepsis patients with non- streptococcal infections, suggesting a specific recruitment of activated MAIT cells to the site of inflammation in response to vitamin B2 producing pathogens[150,189]. Except for two cases of streptococcal infections, all bacterial and fungal pathogens identified in the present sepsis patient cohort in fact possessed the riboflavin pathway, i.e. were theoretically capable of interacting with MAIT cells (Table 3.10).

There is evidence that Vγ9$^+$ and MAIT cells exhort their influence on neutrophils via soluble mediators[102,150]. The particular requirement for TNF-α in the acquisition of the full APC phenotype is especially remarkable when considering the cytokine profiles found in acutely infected patients. In agreement with previous investigations[102,190], sepsis patients were characterized by elevated plasma levels of C-reactive protein (CRP), procalcitonin (PCT) and proadrenomedullin (proADM), confirming the presence of a strong systemic inflammatory response (Figure 3.23). Plasma cytokines that were highly elevated in sepsis patients included IL-6, CXCL8, and TNF-α. Moreover, although not being significant across the whole cohort, a proportion of sepsis patients

also had increased plasma levels of IL-1β, GM-CSF, and IFN-γ. Of note, there was a trend toward higher levels of TNF-α in patients with HMB-PP positive infections compared with patients with HMB-PP negative infections (p=0.09; data not shown). These findings confirmed that the blood of sepsis patients contains proinflammatory mediators that are implicated in driving survival and activation of neutrophils, including their differentiation into APCs.

4.3.7. Unconventional T cell primed neutrophils display a unique phenotype reminiscent of APC-like sepsis neutrophils.

Using data kindly contributed by Dr Martin Davey, these findings can be contextualized through additional in vitro experiments. Circulating neutrophils in healthy people do not express CD40, CD54 (ICAM-1), CD64 and CD83, yet all these molecules were significantly upregulated on neutrophils cultured in the presence of Vγ9/Vδ2 T cell or MAIT cell conditioned medium (Figure 4.15 A). Moreover, Vγ9/Vδ2 T cell and MAIT cell primed neutrophils also expressed high levels of HLA-DR (Figure 4.15 B), which is not found on circulating neutrophils in healthy people but in some sepsis patients, and showed a marked upregulation of surface HLA-ABC (Figure 4.15 B).

Neutrophils stimulated with defined microbial compounds on their own, in the absence of Vγ9/Vδ2 T cells or MAIT cells, failed to acquire a similar phenotype. Most notably, neutrophils cultured for 48 hours in the presence of bacterial LPS did not show increased levels of HLA-ABC, HLA-DR, CD40, CD64, and CD83 compared with neutrophils cultured in medium alone (data not shown), emphasizing the crucial and non-redundant contribution of unconventional T cells and their specific ligands in the differentiation process. Taken together, our data demonstrate that both types of unconventional T cells induce a pronounced survival of neutrophils and their acquisition of an unusual phenotype reminiscent of APC-like sepsis neutrophils.

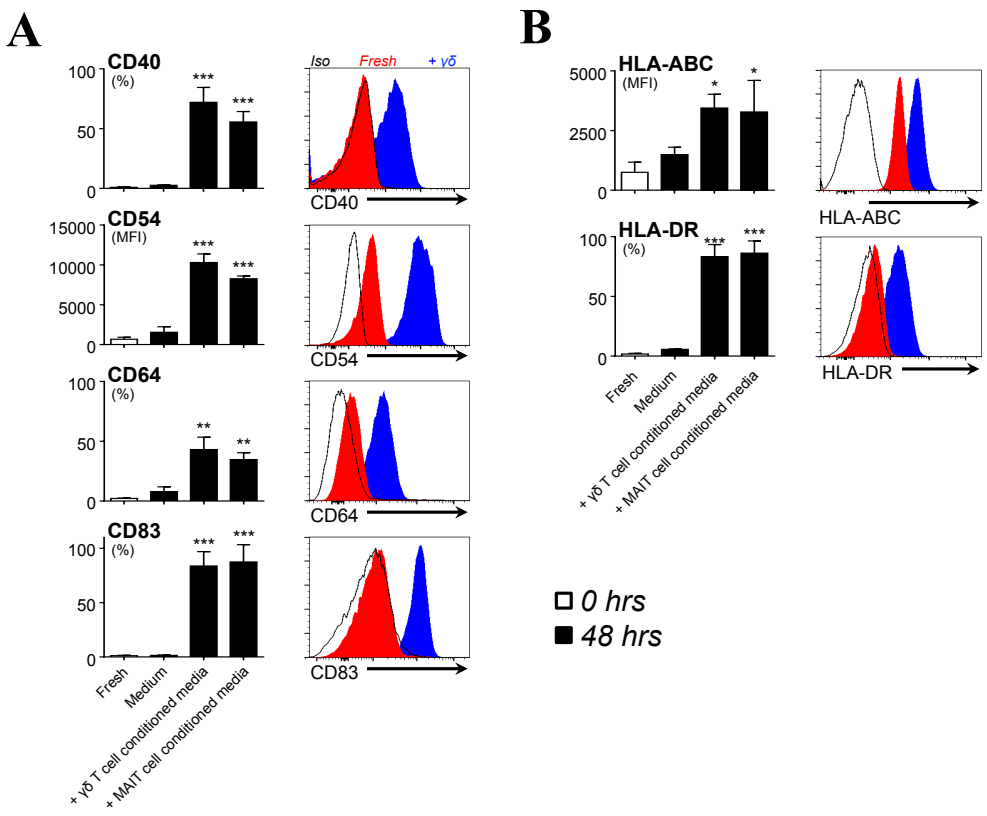

Figure 4.15 Vγ9/Vδ2 T cells and MAIT cells trigger expression of APC markers by neutrophils. (A, B) Expression of the indicated APC markers on freshly isolated neutrophils and CD16hi neutrophils after 48-hour culture in the absence or presence of $V\gamma9^{+}$ T cell or MAIT cell conditioned medium. Data shown are means ± SD and representative histograms from experiments using 3 individual donors. Data were analysed by one-way ANOVA with Dunnett's post-hoc testing; comparisons were made with medium controls. Data kindly contributed by Dr Martin Davey. N = 3.

4.3.8. Unconventional T cell-primed neutrophils process and cross-present MHC class I restricted antigens to CD8$^+$ T cells.

These experiments demonstrated a significant improvement of unconventional T cell primed neutrophils to present the cytomegalovirus (CMV) pp65(495-503) peptide to antigen-specific, HLA-A2-restricted responder CD8$^+$ T cells, in agreement with the elevated levels of HLA-ABC molecules on APC-like neutrophils. Importantly, unconventional T cell primed neutrophils but not freshly isolated neutrophils were able to induce CD8$^+$ T cell responses with the N-terminally extended CMV pp65(489-503) peptide, which requires cellular uptake and processing (Figure 4.16).

In analogy to the CMV system, unconventional T cell primed neutrophils pulsed with the M1(p58-66) peptide had a significantly improved capacity to prime M1(p58-66)-specific responder CD8$^+$ T cells, compared with freshly isolated neutrophils. Most importantly, only unconventional T cell primed neutrophils but not freshly isolated neutrophils were able to take up the full-length M1 protein and cross-present M1(p58-66) to responder CD8$^+$ T cells (Figure 4.16). The requirement for antigen uptake and processing was supported by control experiments confirming that potential degradation products present in the M1 protein preparation could not be pulsed directly onto neutrophils.

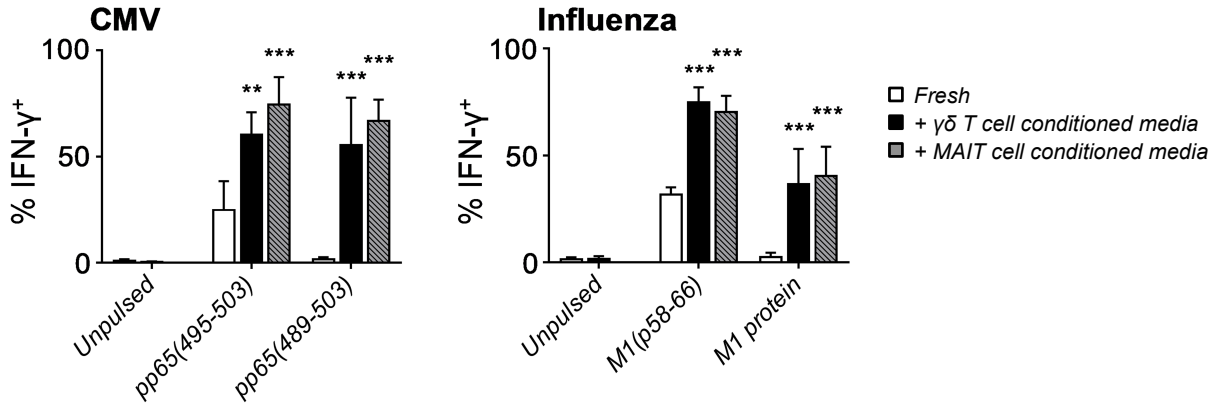

Figure 4.16 CD8$^+$ T cell responses to neutrophils cross-presenting viral antigens. IFN-γ production by antigen-specific CD8$^+$ T cells in response to neutrophils cultured for 48 hours in the presence of Vγ9$^+$ T cell or MAIT cell conditioned medium. Neutrophils were pulsed with 0.1 μM CMV pp65(495-503) or pp65(489-503) peptides, or with 0.1 μM influenza M1(p58-66) peptide or recombinant M1 protein (means + SD, n=3). Data were analysed by two-way ANOVA with Dunnett's post-hoc testing; comparisons were made with freshly isolated neutrophils. Data kindly contributed by Dr Martin Davey.

4.4. Discussion

Whilst it is accepted that the syndrome of CARS can be an important feature of sepsis, the ability of monocyte HLA-DR expression to function as an accurate means of diagnosis and monitoring for this condition is not certain. Despite having very low HLA-DR levels, many sepsis patients have preserved cytokine responsiveness to LPS. Whilst describing just one feature of a complex integrated immune response, LPS responses remain described as one of the key features that drive our defence to Gram-negative infection[182-184,190]. Other processes, such as a monocyte's ability to act as an APC, should equally be studied in relation to CARS and its relationship to a monocyte's HLA-DR expression level.

However, accepting the imperfect nature of HLA-DR as a marker, progress can still be made by investigating ways of reversing the monocyte reprogramming described in the literature. Whilst GM-CSF is a reasonable approach, the need to administer externally produced recombinant cytokines can be avoided. It may be possible to exploit the tendency of bisphosphonates to cause mild systemic inflammatory reactions through the activation of Vγ9$^+$ T cells to help reverse some elements of CARS. The reprogramming effects demonstrated when sepsis monocytes are cultured in the presence of Vγ9$^+$ T cell supernatant includes not only the promotion of a proinflammatory cytokine profile, but

importantly the reduction in the anti-inflammatory cytokine IL-10 indicative of CARS reversal. However, it is clear that the effect of Zometa on the PBMC response to LPS shows considerable donor-to-donor variation, likely due to its dependence on an adequate level of $V\gamma9^+$ T cells to be present as effector cells. To act on $V\gamma9^+$ T cells, Zometa depends on uptake by monocytes and other endocytic cell types, in which they inhibit farnesyl pyrophosphate synthase (FPPS), a key enzyme in the biosynthesis of sterols, ubiquinones, and other isoprenoids via the mevalonate pathway. Preferential uptake by osteoclasts and subsequent inhibition of FPPS is the prime mechanism of action in the aminobisphosphonate-mediated prevention of bone resorption. However, FPPS inhibition in osteoclasts, monocytes, and other cells also leads to intracellular accumulation of upstream metabolites including dimethylallyl pyrophosphate (DMAPP), isopentenyl pyrophosphate (IPP), and an ATP conjugate of IPP (ApppI), which function as ‘‘danger’’ signals and can be sensed by $V\gamma9^+$ T cells through the 30.2 intracellular domain of butyrophilin 3 (BTN3) although the exact details of this process remain unclear[191]. Therefore, if aminobisphosphonates were to be used in immunotherapy clinical trials of sepsis patients, identification of a subset of patients likely to respond through this mechanism would be a key requirement. The finding that a $V\gamma9^+$ T cell percentage above 3% is predictive of acute phase reactions in patients receiving aminobisphosphonates for the treatment of osteoporosis may act as a suitable marker to identify patients likely to benefit from this immunotherapy if considered in combination with monocyte HLA-DR levels below 30%. Using data from Figure 3.17 and Figure 3.19, the percentage of eligible patients in this cohort would be 25% of all patients with severe sepsis at day 1 of intensive care admission. However, if a later enrolment time point were to be used, further study would be needed to adequately plan trial recruitment.

Given that these cytokine changes seem not to be directly related to HLA-DR levels, but rather resulting from promotion of a CD16 high monocyte phenotype, other indices capable of monitoring CARS should be developed to allow therapeutic treatments to be directed towards the right patients at the right times.

This chapter is the first demonstration that human neutrophils can assume antigen cross-presenting properties both in vivo. Although this work does not formally demonstrate a causal link for the interaction of unconventional T cells and neutrophils in vivo, it does

provide a plausible scenario for the generation of neutrophils with APC-like properties during acute infection. Unconventional T cells such as Vγ9/Vδ2 T cells and MAIT cells are abundant in peripheral blood and inflamed tissues, and rapidly and uniformly respond to microbial compounds in a non-MHC restricted manner, thereby representing early and abundant sources of proinflammatory cytokines during infections with a broad range of pathogens[174,182-184,192-195]. In vitro this can be mimicked by exposing neutrophils to unconventional T cell-derived soluble factors, amongst which IFN-γ, GM-CSF, and TNF-α each makes key contributions. This observation is in accordance with earlier studies that identified crucial effects of those cytokines on neutrophils in vitro[174,177,192-197] and in vivo[179,196-198], albeit without disclosing their physiological source in acute inflammatory responses. Of note, plasma from sepsis patients was previously shown to induce some (upregulation of CD64) but not other features (upregulation of CD11b, loss of CD62L) that are characteristic for APC-like neutrophils, indicating that circulating cytokines alone do not confer APC properties[198,199]. In support of local cell-mediated processes at the site of inflammation, our findings evoke earlier descriptions of APC-like neutrophils that were characterized by surface expression of MHC class II molecules in infectious and non-infectious inflammatory scenarios including periodontitis[172,199] and tuberculosis pleuritis[172,200,201], in which locally activated Vγ9/Vδ2 T cells are present[200-202]. These associations lend further support to the existence of a peripheral immune surveillance network comprised of distinct types of unconventional T cells and their crosstalk with local immune and non-immune cells.

A population of CD16^{bright} CD62L^{dim} CD64^{neg} human neutrophils with hypersegmented nuclei was described recently in individuals receiving a systemic LPS challenge and in patients with severe trauma[163-165,202,203]. That population of neutrophils actively inhibited the non-specific activation of T cells through Mac-1 (CD11b/CD18) and the release of ROS. Here a population of neutrophils with a phenotype similar to T cell inhibitory neutrophils but that conversely also expresses high levels of MHC molecules and APC markers has been identified. APC-like human neutrophils as defined in the present study possess a CD16hi CD62L^{-} CD64^{+} MHC I^{hi} MHC II^{+} phenotype and readily present antigens to both CD4^{+} and CD8^{+} T cells. This evidence reinforces the emerging concept of diverse neutrophil populations that can assume specific effector and regulatory functions[163-165,170,203]. Although an antigen cross-presenting capacity was

previously reported for murine neutrophils[170,202], the ability of human neutrophils to process exogenous antigens for activation of $CD8^+$ T cells has only been speculated upon. Here conclusive evidence is provided that in sepsis neutrophils are primed to rapidly take up soluble proteins from the microenvironment and successfully present antigenic peptides to $CD8^+$ T cells in the context of MHC class I. In the absence of these unconventional T cell derived signals, such as during sterile inflammation induced by LPS administration[78,202], neutrophils may not become fully activated, in accordance with published failure to induce APC-like neutrophils using LPS alone.

The presence of cross-presenting neutrophils in patients with sepsis is intriguing and points to an essential role of APC-like neutrophils in acute disease. Sepsis patients who survive the primary infection often show signs of reduced surface expression of HLA-DR on monocytes and a relative tolerance of monocytes to LPS stimulation[78,204]. As a consequence of what is generally perceived as a loss of immune function, many patients are susceptible to subsequent nosocomial infections including reactivation of latent viruses that are associated with high mortality rates[84,204]. Trials specifically targeted at reversing this apparent monocyte deactivation have shown promising clinical results[84,205,206]. However, the present findings suggest that HLA-DR expression by circulating monocytes is a poor surrogate marker for a systemic immune suppression and rather indicate that, contrary to the proposed general loss-of-function, certain cells such as neutrophils actually assume APC properties under those conditions, as evidence of a gain of new function. Yet, with a complex and multi-layered clinical phenomenon such as sepsis it is challenging to dissect the relevance of APC-like neutrophils for infection resolution and clinical outcome.

APC-like neutrophils are likely to contribute to protective immune responses, by fighting the "first-hit" infection as a result of inducing antigen-specific $CD4^+$ and $CD8^+$ T cells and by harnessing the T cell compartment against potential "second-hit" infections. However, it is also perhaps plausible that such an early induction of cytotoxic $CD8^+$ T cells may add to the systemic inflammatory response and ultimately lead to tissue damage and organ failure. While it is expected that the generation of APC-like neutrophils to occur locally in the context of infected tissues and microbe-responsive unconventional T cells, in severe inflammatory conditions including sepsis such APC-like neutrophils may eventually leak into the circulation. Larger and stratified

approaches are clearly needed to define the role of APC-like neutrophils in different infectious scenarios, locally and systemically, in clinically and microbiologically well-defined patient subgroups.

While the present study focused on microbial infections, it is tempting to speculate that our findings may extend to viral infections and to non-infectious inflammatory events where certain unconventional T cells have been implicated[205-207]. Recent investigations also pointed toward the existence of a possible feedback regulation that may require the activation of unconventional T cells to reach a certain threshold to overcome the inhibitory effect of bystander neutrophils[207,208]. However, it is important to note that αβ T cell supernatant has not been used as controls in this series of experiments. Therefore, to explore the specific role of unconventional T cell activation further, it would be prudent to include additional controls to disentangle any functional similarities also present in conventional T cells.

Taken together with findings in Chapter 3, this present study provides evidence (i) that monocyte HLA-DR cannot be used in isolation as a reliable markers for sepsis-related CARS (ii) that activation of $V\gamma9^+$ T cells may be useful in attenuating sepsis-related CARS (iii) that circulating neutrophils from patients with acute sepsis are capable of cross-presenting soluble proteins to antigen-specific $CD8^+$ T cells; (iv) that Vγ9/Vδ2 T cells respond to microbial pathogens that produce the corresponding ligands in severe sepsis; (v) that once activated both Vγ9/Vδ2 T cells and MAIT cells trigger neutrophil survival, activation and differentiation; and (vi) that these surviving neutrophils acquire a phenotype reminiscent of APC-like neutrophils in sepsis patients and are capable of priming both $CD4^+$ and $CD8^+$ T cells.

These findings define a physiological context for the generation of APC- like neutrophils in response to a broad range of microbial pathogens, and have important implications for the understanding of neutrophil-driven inflammatory responses in acute infections. In extension of the recent demonstration that Vγ9/Vδ2 T cells readily engage with monocytes and drive the acute inflammation[208,209] the present data identify a unique and decisive role for human unconventional T cells in orchestrating local inflammatory events and in shaping the transition of the innate to the adaptive phase of the anti-microbial immune response. Overall, it adds to the concept that although loss-

of-function is an important concept in describing CARS, there may also be gain-of-function in other cell types.

CHAPTER 5

GENERAL DISCUSSION AND FUTURE WORK

Chapter 5 General discussion and future work

5.1. General discussion

Sepsis, as an encompassing entity, is finally being recognised as a major problem, not only in the developing world, but also more broadly across developed nations that have been so successful in battling other diseases such as cancer. However, this raising of the public consciousness has not been matched by similar scientific breakthroughs that have enabled the fight against cancer to be considered winnable. Health professionals are left with just three simple, yet difficult to apply, interventions that are considered by many to save lives and improve long-term outcomes. These interventions are good supportive critical care, early appropriate antibiotic use, and effective source control. Despite investment of many millions of pounds into new therapeutics for sepsis, these have universally failed to deliver on the promise of improved patient survival. This perhaps should not be surprising given that the complexity of this disease in trials is often reduced into one generic disease entity. Severe sepsis is a great deal more complex than simply being present or not. Such a one-size-fits-all approach is analogous to treating all cancers with a single chemotherapy agent. Baillie encapsulates this concept in his recent editorial where he argues that:

"Our immune system has evolved to fight a moving target. Whereas the job of the heart has changed little, and haemoglobin binds the same oxygen, and even the circuitry required to generate consciousness need not be different from that of our early ancestors, immunity must change rapidly, again and again, every time a new pathogen appears or an old pathogen mutates. By its very nature, the immune system is expected to be a mire of complexity, interdependence, and redundancy."[91,209]

When novel therapeutics are developed, the approach to clinical trials should instead concentrate on appropriate stratification and targeted treatment to patients that would benefit from the strategy that an intervention has been designed to attenuate. The intensive care community is now starting to implement this approach evidenced by the design of the most recent trial of GM-CSF in sepsis-related immunosuppression (ClinicalTrial.gov NCT01480479). This trial's design employs stratification by predicted eventual survival as well as by monocyte HLA-DR level, to allow targeted treatment of immune suppression to occur.

For now, strategies to maximise the effectiveness of the known evidence-based interventions should be pursued. Therefore, targeting the sickest patients with the correct antibiotic choice early and aggressively remains one hope for improving rates of patient survival from sepsis. In turn, for those that do survive, understanding the immunology involved may help prevent or treat ensuing second-hit infections that can lead to late sepsis mortality and morbidity.

There is some evidence demonstrating survival differences according to the Gram-status of the infecting organism causing sepsis. The only study controlling for appropriate antibiotic use shows an unadjusted hospital mortality rate of 50% in Gram-positive infections compared with a higher rate of 52.3% in Gram-negative infections[47]. However, the sites of these infections also need to be considered as cofounders. Therefore, it is difficult to accurately separate the attributable mortality due to Gram differences without new studies. However, there is now an emerging understanding that LPS is not solely responsible for the differing immune consequences and pathogenicity of Gram-negative infections. This avenue will play an important role in future research that may allow targeted interventions in patients with this infection type. Such interventions may include attenuating the effects of the intermediate metabolite HMB-PP that acts as a powerful stimulant to innate like $V\gamma9^+$ T cells. This finding also underlines the importance of further understanding of the pathophysiological consequences of Gram-negative infection to the patient.

If it is accepted that the Gram-status of an infecting organism can influence a patient's subsequent risk of death and direct appropriate treatment, it follows that a fast, reliable diagnostic test that can reveal Gram-status could impact on a patient's clinical course. Recent advances in technology that allow direct pathogen identification have reduced processing times and increased accuracy of these predictions. However, these technologies based upon PCR, microarrays or MALDI-TOF, all detect which microbes are actually present. This is appropriate in specimens that should remain sterile such as blood. However, with bacteraemia rates as low as 15% in the leading causes of sepsis in the Western world (community-acquired pneumonia), detecting pathogens directly will only help in a fraction of cases[91,210]. Furthermore, when testing specimens with high

non-pathogenic microbial loads, such as BAL fluid, positive species detection leads to difficult interpretation of what may be normal and what is pathogenic.

The approach of immune fingerprinting exploits a patient's own immune response to infection to identify not what microbes are present, but rather what microbes are causing disease. This can therefore avoid the issues surrounding low bacteraemia rates and simultaneously deal with specimens that have high commensal bacteria loads. Using statistical approaches such as neural networking, borrowed from diverse academic fields, immune fingerprinting can accurately and quickly separate patients into Gram-positive, Gram-negative or culture-negative groups. Hence, early appropriate targeted antibiotic treatment can be deployed without resorting to broad-spectrum empirical treatment that may contribute towards the controversial evidential basis of antibiotic use in sepsis. Furthermore, the identification of Gram-status may help focus antibiotic prescribing away from drugs that carry high risks of iatrogenic consequences including acute kidney injury. For example, identifying a Gram-negative infection in a recently hospitalised patient may allow the clinical team to avoid including Vancomycin as empirical MRSA cover thus reducing the associated side effects including acute kidney injury. Finally, early prediction of Gram-status may allow the diagnostic process to move towards source identification and hence source control more efficiently. For example, when trying to distinguish between bile-duct infection and lower respiratory tract infection as the main causative factor in a patient's presentation with sepsis, early identification of a Gram-negative organism may allow early focused investigation towards the former intra-abdominal source.

Although identification of Gram-status is a significant output from Chapter 3, immune fingerprinting is also helpful in differentiation between sepsis and SIRS as well as patient survival and non-survival. Again, attempting to form reliable predictions using a single marker is doomed to fail. However, the use of multiple markers in conjunction with new statistical modelling can capture the complexity of these outputs and form accurate predictions. The ability to differentiate sepsis from SIRS can allow not only sepsis to be treated appropriately, but more importantly may prompt treatment of alternative pathologies that may be responsible for a patient's presentation. Whilst early antibiotics are considered by many to be essential in a sepsis patient, those presenting with acute pancreatitis need equally early treatment of aetiological factors such as

gallstones. Interventions of this kind can be delayed when critically ill patients are labelled as having sepsis even when this subsequently is found not to be the case.

The final section of this thesis turns to more mechanistic studies of immune suppression in sepsis. Through exploration of monocyte responses to LPS, it is shown that monocyte HLA-DR, although inextricably associated with outcomes, is not an ideal surrogate for measuring sepsis-related immune suppression. This is of importance when considering studies now targeting sepsis-related immunosuppression with monocyte HLA-DR patient stratification. Furthermore, rescue of reprogrammed monocytes from a state of anergy, whilst possible with interventions such as GM-CSF, may relate more to monocyte subset changes rather than increases in HLA-DR levels. An alternative strategy to the extrinsic administration of recombinant cytokines may include using safe, licensed drugs such as aminobisphosphonates, shown in Chapter 4 to improve monocyte LPS responses ex vivo with early evidence of effectiveness in vitro. The chapter concludes by challenging the paradigm of sepsis-related immunosuppression being simply an application of immune system loss-of-function. Sepsis neutrophils actually display new gain-of-function abilities including a role as an APC despite published evidence of impaired functions including phagocytosis[38,210]. This somewhat questions the benefits of reversing sepsis-related immune suppression. Although if successful, such reversal may reduce the burden of second-hit infections that is currently seen, it may carry unexpected consequences if it also removes such gain-of-function abilities in other cell types. Reprogramming or reversing this process may simply change the nature of the threat that patients whom survive a first-hit sepsis insult will subsequently encounter.

Overall, this thesis uses small-scale yet complex basic science data, new statistical modelling techniques, and a new approach to microbe identification to shed light on the complexities of sepsis-related critical illness. It aims to ultimately improve patient care and improve scientific understanding through exploration of host-responses, microbe identification, and immunosuppression in a cohort of the sickest patients in hospital with this devastating disease. Its outputs include new concepts in risk stratification of first-hit infections, proof-of-concept for the development of a new technology to detect causative organisms and finally new insights into immunosuppression that may impact upon current and future clinical trials.

5.2. Future work

5.2.1. Immune fingerprints

When producing any predictive model, data used to form the predictive model should ideally be separated from that used to subsequently confirm the accuracy of the model. In this study, the relatively small number of unique patients made such a process not achievable. Therefore, future work should focus on confirming the findings of the three predictive models in Chapter 3 by applying their predictions to a second set of patients thus avoiding any over-fitting that may have occurred. In addition, whilst the ability to predict Gram-status of an infecting organism is important, if refined further to a species level of detail, the benefits would be significant. With a sufficiently large dataset, it may be possible to subdivide Gram-positive organisms into *Staphylococcal* and *Streptococcal* species for example. This would lead to important treatment consequences including the ability to exclude MRSA infection in suspected individuals and hence avoid antibiotics with poor side effect profiles.

5.2.2. Commercial translation of an immune fingerprinting strategy

Although the promise of immune fingerprinting is great, significant challenges remain to translate these findings into a sustainable, practical and accurate commercial solution to aid patients with sepsis. Whilst the use of a combination of markers heralds improvements in the sensitivity and specificity of predictions, this brings additional complexities to equipment manufacture and function. Firstly, any point-of-care or laboratory device would need to combine the abilities of flow cytometric and cytokine analysis in one unit. This would require differential sample preparation and division following patient sampling. Secondly, the steps outlined in 2.7.3.1 to ensure quality control of the flow cytometry analysis would be difficult, expensive and impractical to replicate in the commercial sector, although restricting measurement to different cell lineage percentages ($V\gamma9^+$ %) alone would reduce the complexity of this task. Thirdly, if specific cut-off values for the measured variables were required rather than a change compared with measured controls, the problems of inter-batch and calibration variability would be present. Finally, relying on complex models to predict outcomes poses not only interpretation issues for the clinician at the bedside, but regulatory and accreditation challenges. Where such technology impacts directly on patient care, the

relevant regulatory authorities and the producers of such diagnostics need to simplify the process of clinical decision making whilst ensuring that the underlying software architecture and modelling perform correctly across a diverse range of patients. Such patient groups not considered in this study include those that do not conform to the clean-cut nature of the studied population such as those with polymicrobial infections, pre-existing viral or fungal infections, and those with immunosuppression. Groups of this nature are an increasingly common occurrence in healthcare environments. Whilst these challenges are real, the advent of nanotechnology[211,212] and reductions in the costs associated with diagnostic technology development[213,214] may allow these issues to be overcome in the very near future. Point-of-care flow cytometric analysis has already been introduced with the CyFlow® miniPOC (Sysmex), the Pima™ CD4 Analyser (Alere) and multiplex cytokine analysis is likely to be commercially available soon[215].

5.2.3. Sepsis-related immunosuppression

Following the ability of bisphosphonates to rescue ex vivo sepsis monocytes, mechanisms replicated safely in healthy osteoporosis patients, a pilot study of Zometa in sepsis could be justified. Such a pilot should follow the design of the GM-CSF GRIP study (ClinicalTrial.gov NCT01480479) targeting those patients likely to survive, with a supressed monocyte HLA-DR level and a primary endpoint of second-hit infection rates. These clinical parameters could be accompanied by immunological data including pre and post treatment monocyte response analysis. However, another important outcome from Chapter 4 will be to question the ability of monocyte HLA-DR to act as a suitable stratifier in sepsis-related immune suppression. A dedicated study of the ability of HLA-DR low monocytes to act as competent immune cells is needed. This study should investigate their ability to act as APCs, respond appropriately to a range of bacterial pathogens and crosstalk with other immune cell types. Without confirmation that HLA-DR is a suitable surrogate for immunosuppression, yet more sepsis trials will fail due to the wrong patients being targeted, at the wrong times. Although Chapter 4 has demonstrated that sepsis neutrophils can act as APCs ex vivo, these findings could be brought one step closer to the bedside. Using isolated neutrophils from patients with confirmed influenza, the same $CD8^+$ M1 responder cells could be used in an APC assay to gauge responses directly from a patient's own acquired antigen. This would provide definitive, in vitro evidence that late sepsis brings not only loss-of-function abilities but

also heralds new roles for key immune cell types that may be of critical importance in dealing with the consequences of initial patient survival from severe sepsis.

Bibliography

1. Bryce, J., Boschi-Pinto, C., Shibuya, K. & Black, R. E. WHO estimates of the causes of death in children. *The Lancet* **365,** 1147–1152 (2005).
2. Newton, S., Cunningham, J. & Dobbin, J. *Sepsis and the NHS*. **2013/2014,** (All-Party Parliamentary Group on Sepsis).
3. Stevenson, E. K., Rubenstein, A. R., Radin, G. T., Wiener, R. S. & Walkey, A. J. Two Decades of Mortality Trends Among Patients With Severe Sepsis. *Critical Care Medicine* **42,** 625–631 (2014).
4. Angus, D. C. *et al.* Epidemiology of severe sepsis in the United States: analysis of incidence, outcome, and associated costs of care. *Critical Care Medicine* **29,** 1303–1310 (2001).
5. Schmid, A., Burchardi, H., Clouth, J. & Schneider, H. Burden of illness imposed by severe sepsis in Germany. *Eur J Health Econ* **3,** 77–82 (2002).
6. Longo, C. J. *et al.* A long-term follow-up study investigating health-related quality of life and resource use in survivors of severe sepsis: comparison of recombinant human activated protein C with standard care. *Crit Care* **11,** R128 (2007).
7. American College of Chest Physicians/Society of Critical Care Medicine Consensus Conference: Definitions for sepsis and organ failure and guidelines for the use of innovative therapies in sepsis. *Critical Care Medicine* **20,** (1992).
8. Dellinger, R. P. *et al.* Surviving Sepsis Campaign: international guidelines for management of severe sepsis and septic shock: 2008. in *Crit. Care Med.* **36,** 296–327 (2008).
9. Dellinger, R. P. *et al.* Surviving sepsis campaign: international guidelines for management of severe sepsis and septic shock: 2012. in *Crit. Care Med.* **41,** 580–637 (2013).
10. Vincent, J.-L., Opal, S. M., Marshall, J. C. & Tracey, K. J. Sepsis definitions: time for change. *Lancet* **381,** 774–775 (2013).
11. Vincent, J.-L. *et al.* International study of the prevalence and outcomes of infection in intensive care units. *JAMA* **302,** 2323–2329 (2009).
12. Tracey, K. *et al.* Shock and tissue injury induced by recombinant human cachectin. *Science* **234,** 470–474 (1986).
13. Dellinger, R. P. *et al.* Surviving Sepsis Campaign guidelines for management of severe sepsis and septic shock. *Intensive Care Med* **30,** 536–555 (2004).
14. Bernard, G. R. *et al.* Efficacy and safety of recombinant human activated protein C for severe sepsis. *N. Engl. J. Med.* **344,** 699–709 (2001).
15. Ranieri, V. M. *et al.* Drotrecogin alfa (activated) in adults with septic shock. *N. Engl. J. Med.* **366,** 2055–2064 (2012).
16. Opal, S. M. & LAROSA, S. P. Recombinant human activated protein C as a therapy for severe sepsis: lessons learned? *American Journal of Respiratory and Critical Care Medicine* **187,** 1041–1043 (2013).
17. Schmidt, G., Clardy, P. & Paarsons, P. Investigational and ineffective therapies for sepsis. *UpToDate* (2013). at <http://www.uptodate.com/contents/investigational-and-ineffective-therapies-for-sepsis>
18. Tomasz, A. The mechanism of the irreversible antimicrobial effects of

penicillins: how the beta-lactam antibiotics kill and lyse bacteria. *Annu. Rev. Microbiol.* **33,** 113–137 (1979).
19. Morgan, M. Neural networks offer many advantages over standard techniques in the field of biomarker prediction. (2014).
20. Kumar, A. *et al.* Initiation of inappropriate antimicrobial therapy results in a fivefold reduction of survival in human septic shock. *Chest* **136,** 1237–1248 (2009).
21. Vallés, J., Rello, J., Ochagavía, A., Garnacho, J. & Alcalá, M. A. Community-acquired bloodstream infection in critically ill adult patients: impact of shock and inappropriate antibiotic therapy on survival. *Chest* **123,** 1615–1624 (2003).
22. Ibrahim, E. H., Sherman, G., Ward, S., Fraser, V. J. & Kollef, M. H. The influence of inadequate antimicrobial treatment of bloodstream infections on patient outcomes in the ICU setting. *Chest* **118,** 146–155 (2000).
23. Weiss, S. L. *et al.* Delayed antimicrobial therapy increases mortality and organ dysfunction duration in pediatric sepsis. *Critical Care Medicine* **42,** 2409–2417 (2014).
24. Ferrer, R. *et al.* Empiric antibiotic treatment reduces mortality in severe sepsis and septic shock from the first hour: results from a guideline-based performance improvement program. *Critical Care Medicine* **42,** 1749–1755 (2014).
25. Garnacho-Montero, J. *et al.* Impact of adequate empirical antibiotic therapy on the outcome of patients admitted to the intensive care unit with sepsis. *Critical Care Medicine* **31,** 2742–2751 (2003).
26. Hranjec, T. *et al.* Aggressive versus conservative initiation of antimicrobial treatment in critically ill surgical patients with suspected intensive-care-unit-acquired infection: a quasi-experimental, before and after observational cohort study. *The Lancet Infectious Diseases* **12,** 774–780 (2012).
27. McGregor, J. C. *et al.* A systematic review of the methods used to assess the association between appropriate antibiotic therapy and mortality in bacteremic patients. *Clin Infect Dis* **45,** 329–337 (2007).
28. Marik, P. E. Early management of severe sepsis: concepts and controversies. *Chest* **145,** 1407–1418 (2014).
29. Bernhard, M., Lichtenstern, C., Eckmann, C. & Weigand, M. A. The early antibiotic therapy in septic patients - milestone or sticking point? *Crit Care* **18,** 1931–5 (2014).
30. Harbarth, S. *et al.* Inappropriate initial antimicrobial therapy and its effect on survival in a clinical trial of immunomodulating therapy for severe sepsis. *The American Journal of Medicine* **115,** 529–535 (2003).
31. Gaieski, D. F. *et al.* Impact of time to antibiotics on survival in patients with severe sepsis or septic shock in whom early goal-directed therapy was initiated in the emergency department. *Critical Care Medicine* **38,** 1045–1053 (2010).
32. Seifert, H. The clinical importance of microbiological findings in the diagnosis and management of bloodstream infections. *Clin Infect Dis* **48 Suppl 4,** S238–45 (2009).
33. Juknevicius, G., Balakumar, E. & Gratrix, A. Implementation of evidence-based care bundles in the ICU. *Crit Care* **16,** P524 (2012).
34. Rivers, E. *et al.* Early goal-directed therapy in the treatment of severe sepsis and septic shock. *N Engl J Med* **345,** 1368–1377 (2001).
35. ProCESS Investigators *et al.* A randomized trial of protocol-based care for early septic shock. *N Engl J Med* **370,** 1683–1693 (2014).

36. Alexiou, V. G., Ierodiakonou, V., Dimopoulos, G. & Falagas, M. E. Impact of patient position on the incidence of ventilator-associated pneumonia: a meta-analysis of randomized controlled trials. *J Crit Care* **24,** 515–522 (2009).
37. Li Bassi, G., Zanella, A., Cressoni, M., Stylianou, M. & Kolobow, T. Following tracheal intubation, mucus flow is reversed in the semirecumbent position: possible role in the pathogenesis of ventilator-associated pneumonia. *Critical Care Medicine* **36,** 518–525 (2008).
38. Delaney, A. P. *et al.* The Australasian Resuscitation in Sepsis Evaluation (ARISE) trial statistical analysis plan. *Crit Care Resusc* **15,** 162–171 (2013).
39. Chawla, S. & DeMuro, J. P. Current controversies in the support of sepsis. *Current Opinion in Critical Care* **20,** 681–684 (2014).
40. Yeh, R. W. *et al.* Population trends in the incidence and outcomes of acute myocardial infarction. *N Engl J Med* **362,** 2155–2165 (2010).
41. Friedman, G., Silva, E. & Vincent, J.-L. Has the mortality of septic shock changed with time? *Critical Care Medicine* **26,** 2078 (1998).
42. Kaukonen, K.-M., Bailey, M., Suzuki, S., Pilcher, D. & Bellomo, R. Mortality Related to Severe Sepsis and Septic Shock Among Critically Ill Patients in Australia and New Zealand, 2000-2012. *JAMA* **311,** 1308 (2014).
43. Iwashyna, T. J., ELY, E. W., Smith, D. M. & Langa, K. M. Long-term cognitive impairment and functional disability among survivors of severe sepsis. *JAMA* **304,** 1787–1794 (2010).
44. Rehabilitation After Critical Illness. (2009).
45. Alexandraki, I. & Palacio, C. Gram-negative versus Gram-positive bacteremia: what is more alarmin(g)? *Crit Care* **14,** 161 (2010).
46. Vincent, J.-L. *et al.* Sepsis in European intensive care units: results of the SOAP study. *Critical Care Medicine* **34,** 344–353 (2006).
47. Labelle, A. *et al.* The determinants of hospital mortality among patients with septic shock receiving appropriate initial antibiotic treatment. *Critical Care Medicine* **40,** 2016–2021 (2012).
48. Ani, C., Farshidpanah, S., Bellinghausen Stewart, A. & Nguyen, H. B. Variations in Organism-Specific Severe Sepsis Mortality in the United States: 1999-2008. *Critical Care Medicine* **Published Ahead of Print,** (2014).
49. Leligdowicz, A. *et al.* Association between Source of Infection and Hospital Mortality in Patients Who Have Septic Shock. *American Journal of Respiratory and Critical Care Medicine* **189,** 1204–1213 (2014).
50. Rossol, M. *et al.* LPS-induced cytokine production in human monocytes and macrophages. *Crit. Rev. Immunol.* **31,** 379–446 (2011).
51. Zanoni, I. *et al.* CD14 controls the LPS-induced endocytosis of Toll-like receptor 4. *Cell* **147,** 868–880 (2011).
52. Hagar, J. A., Powell, D. A., Aachoui, Y., Ernst, R. K. & Miao, E. A. Cytoplasmic LPS activates caspase-11: implications in TLR4-independent endotoxic shock. *Science* **341,** 1250–1253 (2013).
53. Belge, K.-U. *et al.* The proinflammatory CD14+CD16+DR++ monocytes are a major source of TNF. *J. Immunol.* **168,** 3536–3542 (2002).
54. Alves-Filho, J. C., Spiller, F. & Cunha, F. Q. Neutrophil paralysis in sepsis. *Shock* **34 Suppl 1,** 15–21 (2010).
55. Parlato, M. *et al.* CD24-triggered caspase-dependent apoptosis via mitochondrial membrane depolarization and reactive oxygen species production of human neutrophils is impaired in sepsis. *The Journal of Immunology* **192,** 2449–2459 (2014).

56. Grommes, J. & Soehnlein, O. Contribution of neutrophils to acute lung injury. *Mol. Med.* **17,** 293–307 (2011).
57. Wang, L. *et al.* Specific role of neutrophil inducible nitric oxide synthase in murine sepsis-induced lung injury in vivo. *Shock* **37,** 539–547 (2012).
58. Brown, K. A. *et al.* Neutrophils in development of multiple organ failure in sepsis. *Lancet* **368,** 157–169 (2006).
59. Yoshida, K., Kondo, R., Wang, Q. & Doerschuk, C. M. Neutrophil cytoskeletal rearrangements during capillary sequestration in bacterial pneumonia in rats. *American Journal of Respiratory and Critical Care Medicine* **174,** 689–698 (2006).
60. Tanaka, K. *et al.* In vivo characterization of neutrophil extracellular traps in various organs of a murine sepsis model. *PLoS ONE* **9,** e111888 (2014).
61. de Jong, H. K. *et al.* Neutrophil extracellular traps in the host defense against sepsis induced by Burkholderia pseudomallei (melioidosis). *Intensive Care Med Exp* **2,** 21 (2014).
62. Rendon, J. L. & Choudhry, M. A. Th17 cells: critical mediators of host responses to burn injury and sepsis. *Journal of Leukocyte Biology* **92,** 529–538 (2012).
63. Tang, L. *et al.* Active players in resolution of shock/sepsis induced indirect lung injury: immunomodulatory effects of Tregs and PD-1. *Journal of Leukocyte Biology* **96,** 809–820 (2014).
64. Cauvi, D. M., Williams, M. R., Bermudez, J. A., Armijo, G. & De Maio, A. Elevated expression of IL-23/IL-17 pathway-related mediators correlates with exacerbation of pulmonary inflammation during polymicrobial sepsis. *Shock* **42,** 246–255 (2014).
65. Kim, B.-J., Lee, S., Berg, R. E., Simecka, J. W. & Jones, H. P. Interleukin-23 (IL-23) deficiency disrupts Th17 and Th1-related defenses against Streptococcus pneumoniae infection. *Cytokine* **64,** 375–381 (2013).
66. Ma, C. S. *et al.* Deficiency of Th17 cells in hyper IgE syndrome due to mutations in STAT3. *Journal of Experimental Medicine* **205,** 1551–1557 (2008).
67. Cavaillon, J.-M., Eisen, D. & Annane, D. Is boosting the immune system in sepsis appropriate? *Crit Care* **18,** 216 (2014).
68. Mills, K. H. G. Regulatory T cells: friend or foe in immunity to infection? *Nat Rev Immunol* **4,** 841–855 (2004).
69. Huang, H. *et al.* High circulating CD39+ regulatory T cells predict poor survival for sepsis patients. *Int. J. Infect. Dis.* **Published Ahead of Print** (2014). doi:10.1016/j.ijid.2014.11.006
70. Kroca, M., Tärnvik, A. & Sjöstedt, A. The proportion of circulating γδ T cells increases after the first week of onset of tularaemia and remains elevated for more than a year. *Clin. Exp. Immunol.* **120,** 280–284 (2000).
71. Eberl, M. & Moser, B. Monocytes and gammadelta T cells: close encounters in microbial infection. *Trends in Immunology* **30,** 562–568 (2009).
72. Vavassori, S. *et al.* Butyrophilin 3A1 binds phosphorylated antigens and stimulates human γδ T cells. *Nature Immunology* **14,** 908–916 (2013).
73. Sandstrom, A. *et al.* The Intracellular B30.2 Domain of Butyrophilin 3A1 Binds Phosphoantigens to Mediate Activation of Human Vγ9Vδ2 T Cells. *Immunity* **40,** 490–500 (2014).
74. Davey, M. S. *et al.* Human neutrophil clearance of bacterial pathogens triggers anti-microbial γδ T cell responses in early infection. *PLoS Pathog* **7,** e1002040

(2011).
75. Payen, D., Monneret, G. & Hotchkiss, R. Immunotherapy - a potential new way forward in the treatment of sepsis. *Crit Care* **17,** 118 (2013).
76. Levin, J., Poore, T. E., Zauber, N. P. & Oser, R. S. Detection of Endotoxin in the Blood of Patients with Sepsis Due to Gram-Negative Bacteria. *N Engl J Med* **283,** 1313–1316 (1970).
77. Topalian, S. L. *et al.* Safety, activity, and immune correlates of anti-PD-1 antibody in cancer. *N Engl J Med* **366,** 2443–2454 (2012).
78. Hotchkiss, R. S., Monneret, G. & Payen, D. Sepsis-induced immunosuppression: from cellular dysfunctions to immunotherapy. *Nat Rev Immunol* **13,** 862–874 (2013).
79. Xiao, W. *et al.* A genomic storm in critically injured humans. *Journal of Experimental Medicine* **208,** 2581–2590 (2011).
80. Boomer, J. S. *et al.* Immunosuppression in patients who die of sepsis and multiple organ failure. *JAMA* **306,** 2594–2605 (2011).
81. Hotchkiss, R. S. & Karl, I. E. Medical progress: The pathophysiology and treatment of sepsis. *N Engl J Med* **348,** 138–150 (2003).
82. Hotchkiss, R. S., Monneret, G. & Payen, D. Immunosuppression in sepsis: a novel understanding of the disorder and a new therapeutic approach. *The Lancet Infectious Diseases* **13,** 260–268 (2013).
83. Deutschman, C. S. & Tracey, K. J. Sepsis: Current Dogma and New Perspectives. *Immunity* **40,** 463–475 (2014).
84. Meisel, C. *et al.* Granulocyte-macrophage colony-stimulating factor to reverse sepsis-associated immunosuppression: a double-blind, randomized, placebo-controlled multicenter trial. *American Journal of Respiratory and Critical Care Medicine* **180,** 640–648 (2009).
85. Chang, K. C. *et al.* Blockade of the negative co-stimulatory molecules PD-1 and CTLA-4 improves survival in primary and secondary fungal sepsis. *Crit Care* **17,** R85 (2013).
86. Chang, K. *et al.* Targeting the programmed cell death 1: programmed cell death ligand 1 pathway reverses T cell exhaustion in patients with sepsis. *Crit Care* **18,** R3 (2014).
87. Genser, B., Cooper, P. J., Yazdanbaksh, M., Barreto, M. L. & Rodrigues, L. C. A guide to modern statistical analysis of immunological data. *BMC Immunol* **8,** 27 (2007).
88. Scumpia, P. O. *et al.* Increased Natural CD4+CD25+ Regulatory T Cells and Their Suppressor Activity Do Not Contribute to Mortality in Murine Polymicrobial Sepsis. *The Journal of Immunology* **177,** 7943–7949 (2006).
89. Heuer, J. G. *et al.* Adoptive transfer of in vitro-stimulated CD4+CD25+ regulatory T cells increases bacterial clearance and improves survival in polymicrobial sepsis. *J. Immunol.* **174,** 7141–7146 (2005).
90. Shah, N. H. & Tenenbaum, J. D. The coming age of data-driven medicine: translational bioinformatics' next frontier. *J Am Med Inform Assoc* **19,** e2–4 (2012).
91. Afshar, N., Tabas, J., Afshar, K. & Silbergleit, R. Blood cultures for community-acquired pneumonia: are they worthy of two quality measures? A systematic review. *J Hosp Med* **4,** 112–123 (2009).
92. Tu, Y.-K., Kellett, M., Clerehugh, V. & Gilthorpe, M. S. Problems of correlations between explanatory variables in multiple regression analyses in the dental literature. *Br Dent J* **199,** 457–461 (2005).

93. Amato, F. *et al.* Artificial neural networks in medical diagnosis. *Journal of Applied Biomedicine* **11,** 47–58 (2013).
94. Zhang, F. & Chen, J. Y. A neural network approach to multi-biomarker panel development based on LC/MS/MS proteomics profiles: A case study in breast cancer. 1–6 (2009).
95. Meuter, S., Eberl, M. & Moser, B. Prolonged antigen survival and cytosolic export in cross-presenting human γδ T cells. *Proceedings of the National Academy of Sciences* **107,** 8730–8735 (2010).
96. Sallusto, F., Lenig, D., Förster, R., Lipp, M. & Lanzavecchia, A. Two subsets of memory T lymphocytes with distinct homing potentials and effector functions. *Nature* **401,** 708–712 (1999).
97. Dieli, F. *et al.* Differentiation of Effector/Memory Vδ2 T Cells and Migratory Routes in Lymph Nodes or Inflammatory Sites. *Journal of Experimental Medicine* **198,** 391–397 (2003).
98. Perfetto, S. P., Ambrozak, D., Nguyen, R., Chattopadhyay, P. & Roederer, M. Quality assurance for polychromatic flow cytometry. *Nat Protoc* **1,** 1522–1530 (2006).
99. Salluh, J. I. F. & Bozza, P. T. Biomarkers of sepsis: Lost in translation? *Critical Care Medicine* **36,** 2192–2194 (2008).
100. Trusheim, M. R., Berndt, E. R. & Douglas, F. L. Stratified medicine: strategic and economic implications of combining drugs and clinical biomarkers. *Nat Rev Drug Discov* **6,** 287–293 (2007).
101. Lynn, L. A. The diagnosis of sepsis revisited - a challenge for young medical scientists in the 21st century. *Patient Saf Surg* **8,** 1 (2014).
102. Andreola, B. *et al.* Procalcitonin and C-reactive protein as diagnostic markers of severe bacterial infections in febrile infants and children in the emergency department. *Pediatr. Infect. Dis. J.* **26,** 672–677 (2007).
103. Smith, R. C., Southwell-Keely, J. & Chesher, D. Should serum pancreatic lipase replace serum amylase as a biomarker of acute pancreatitis? *ANZ J Surg* **75,** 399–404 (2005).
104. Rahman, M. *et al.* Platelet shedding of CD40L is regulated by matrix metalloproteinase-9 in abdominal sepsis. *J. Thromb. Haemost.* **11,** 1385–1398 (2013).
105. Lekkou, A., Karakantza, M., Mouzaki, A., Kalfarentzos, F. & Gogos, C. A. Cytokine Production and Monocyte HLA-DR Expression as Predictors of Outcome for Patients with Community-Acquired Severe Infections. *Clinical and Vaccine Immunology* **11,** 161–167 (2004).
106. Woiciechowsky, C. *et al.* Diminished monocytic HLA-DR expression and ex vivo cytokine secretion capacity in patients with glioblastoma: effect of tumor extirpation. *J. Neuroimmunol.* **84,** 164–171 (1998).
107. Mokart, D. *et al.* HLA-DR and B7-2 (CD86) monocyte expressions after major cancer surgery: profile in sepsis. *Minerva Anestesiol* **77,** 522–527 (2011).
108. Williams, S. C. P. After Xigris, researchers look to new targets to combat sepsis. *Nature Publishing Group* **18,** 1001–1001 (2012).
109. Endo, S. *et al.* Two types of septic shock classified by the plasma levels of cytokines and endotoxin. *Circ. Shock* **38,** 264–274 (1992).
110. Meisner, M. Biomarkers of sepsis: clinically useful? *Current Opinion in Critical Care* **11,** 473–480 (2005).
111. Wipf, J. E. *et al.* Diagnosing pneumonia by physical examination: relevant or relic? *Arch. Intern. Med.* **159,** 1082–1087 (1999).

112. Lakatos, P. L., Fischer, S., Lakatos, L., Gal, I. & Papp, J. Current concept on the pathogenesis of inflammatory bowel disease-crosstalk between genetic and microbial factors: pathogenic bacteria and altered bacterial sensing or changes in mucosal integrity take 'toll' ? *World J. Gastroenterol.* **12,** 1829–1841 (2006).
113. Cochocki, A. & Unbehauen, R. Neural networks for optimization and signal processing. John Wiley & Sons, New York, USA (1993).
114. Kaastra, I. & Boyd, M. Designing a neural network for forecasting financial and economic time series. *Neurocomputing* **10,** 215–236 (1996).
115. Dony, T., Haykin, I. Neural network approaches to image compression. P*roc. IEEE*. 288-303 (1995).
116. Lee, S. W. Off-line recognition of totally unconstrained handwritten numerals using multilayer cluster neural network. *IEEE Transactions on Pattern Analysis and Machine Intelligence* **18,** 648–652 (1996).
117. Otto, G. P. *et al.* The late phase of sepsis is characterized by an increased microbiological burden and death rate. *Crit Care* **15,** R183 (2011).
118. Jack, C. R., Jr *et al.* Tracking pathophysiological processes in Alzheimer's disease: an updated hypothetical model of dynamic biomarkers. *The Lancet Neurology* **12,** 207–216 (2013).
119. Iba, T., Murai, M., Nagaoka, I. & Tabe, Y. Neutrophil extracellular traps (NETs), damage-associated molecular patterns (DAMPs) and cell-death during sepsis TI . *Nihon Kyukyu Igakukai Zasshi* **24,** 827–836 (2013).
120. Kellum, J. A. *et al.* Understanding the inflammatory cytokine response in pneumonia and sepsis: results of the Genetic and Inflammatory Markers of Sepsis (GenIMS) Study. *Arch. Intern. Med.* **167,** 1655–1663 (2007).
121. Remick, D. G., Bolgos, G. R., Siddiqui, J., Shin, J. & Nemzek, J. A. Six at six: interleukin-6 measured 6 h after the initiation of sepsis predicts mortality over 3 days. *Shock* **17,** 463–467 (2002).
122. Hack, C. E. *et al.* Increased plasma levels of interleukin-6 in sepsis. *Blood* **74,** 1704–1710 (1989).
123. Zolfaghari, P. S., Pinto, B., Dyson, A. & Singer, M. The metabolic phenotype of rodent sepsis: cause for concern? *Intensive Care Med Exp* **1,** 6 (2013).
124. Takeuchi, O. *et al.* Differential roles of TLR2 and TLR4 in recognition of gram-negative and gram-positive bacterial cell wall components. *Immunity* **11,** 443–451 (1999).
125. Hessle, C. C., Andersson, B. & Wold, A. E. Gram-positive and Gram-negative bacteria elicit different patterns of pro-inflammatory cytokines in human monocytes. *Cytokine* **30,** 311–318 (2005).
126. Opal, S. M. & Cohen, J. Clinical gram-positive sepsis: does it fundamentally differ from gram-negative bacterial sepsis? *Critical Care Medicine* **27,** 1608–1616 (1999).
127. Oda, S. *et al.* Sequential measurement of IL-6 blood levels in patients with systemic inflammatory response syndrome (SIRS)/sepsis. *Cytokine* **29,** 169–175 (2005).
128. Gibot, S. *et al.* Time-course of sTREM (soluble triggering receptor expressed on myeloid cells)-1, procalcitonin, and C-reactive protein plasma concentrations during sepsis. *Critical Care Medicine* **33,** 792–796 (2005).
129. Venet, F., Lukaszewicz, A.-C., Payen, D., Hotchkiss, R. & Monneret, G. Monitoring the immune response in sepsis: a rational approach to administration of immunoadjuvant therapies. *Curr. Opin. Immunol.* **25,** 477–483 (2013).

130. Rivers, E. P. *et al.* Early biomarker activity in severe sepsis and septic shock and a contemporary review of immunotherapy trials: not a time to give up, but to give it earlier. *Shock* **39,** 127–137 (2013).
131. Nguyen, H. B. *et al.* Implementation of a bundle of quality indicators for the early management of severe sepsis and septic shock is associated with decreased mortality. *Critical Care Medicine* **35,** 1105–1112 (2007).
132. Gao, F., Melody, T., Daniels, D. F., Giles, S. & Fox, S. The impact of compliance with 6-hour and 24-hour sepsis bundles on hospital mortality in patients with severe sepsis: a prospective observational study. *Crit Care* **9,** R764–70 (2005).
133. Almeida, M., Ribeiro, O., Aragão, I., Costa-Pereira, A. & Cardoso, T. Differences in compliance with Surviving Sepsis Campaign recommendations according to hospital entrance time: day versus night. *Crit Care* **17,** R79 (2013).
134. Ferri, L. E., Chia, S., Benay, C., Giannias, B. & Christou, N. V. L-selectin shedding in sepsis limits leukocyte mediated microvascular injury at remote sites. *Surgery* **145,** 384–391 (2009).
135. Hoffmann, J. J. M. L. Neutrophil CD64 as a sepsis biomarker. *Biochem Med (Zagreb)* **21,** 282–290 (2011).
136. White, M. *et al.* Post-operative infection and sepsis in humans is associated with deficient gene expression of **γc** cytokines and their apoptosis mediators. *Crit Care* **15(3)**,158 (2011).
137. Early activation of gammadelta T lymphocytes in patients with severe systemic inflammatory response syndrome. **22,** 11–15 (2004).
138. Eberl, M. *et al.* Microbial isoprenoid biosynthesis and human gammadelta T cell activation. *FEBS Letters* **544,** 4–10 (2003).
139. Lin, C. Y. *et al.* Pathogen-Specific Local Immune Fingerprints Diagnose Bacterial Infection in Peritoneal Dialysis Patients. *Journal of the American Society of Nephrology* **24,** 2002–2009 (2013).
140. Dransfield, I. *et al.* Neutrophil apoptosis is associated with a reduction in CD16 (Fc gamma RIII) expression. *J. Immunol.* **153,** 1254–1263 (1994).
141. Fialkow, L. *et al.* Neutrophil apoptosis: a marker of disease severity in sepsis and sepsis-induced acute respiratory distress syndrome. *Crit Care* **10,** R155 (2006).
142. Sakka, El, N. *et al.* Delayed neutrophil apoptosis in patients with multiple organ dysfunction syndrome. *Crit Care* **9,** 10 (2006).
143. Marshall, J. C. Neutrophils in the pathogenesis of sepsis. *Critical Care Medicine* **33,** S502–5 (2005).
144. Jia, S. H. *et al.* Pre–B cell colony–enhancing factor inhibits neutrophil apoptosis in experimental inflammation and clinical sepsis. *The Journal of Clinical Investigation* **113,** 1318–1327 (2004).
145. Tannahill, G. M. *et al.* Succinate is an inflammatory signal that induces IL-1β through HIF-1α. *Nature* **496,** 238–242 (2013).
146. Renaud, B. *et al.* Risk stratification of early admission to the intensive care unit of patients with no major criteria of severe community-acquired pneumonia: development of an international prediction rule. *Crit Care* **13,** R54 (2009).
147. Nelson, A. L., Dhimolea, E. & Reichert, J. M. Development trends for human monoclonal antibody therapeutics. *Nat Rev Drug Discov* **9,** 767–774 (2010).
148. Fraimow, H. S. Chipping away at unnecessary antibiotic use in the ICU, one day and one study at a time. *Critical Care Medicine* **41,** 2447–2448 (2013).
149. Nimmo, G. R. *et al.* Replacement of healthcare-associated MRSA by

community-associated MRSA in Queensland: confirmation by genotyping. *J. Infect.* **67,** 439–447 (2013).
150. Le Bourhis, L. *et al.* Antimicrobial activity of mucosal-associated invariant T cells. *Nature Immunology* **11,** 701–708 (2010).
151. Rello, J. *et al.* Survival in patients with nosocomial pneumonia: impact of the severity of illness and the etiologic agent. *Critical Care Medicine* **25,** 1862–1867 (1997).
152. Thermo Fisher Scientific PCT assay characteristics. *procalcitonin.com* at <http://www.procalcitonin.com/default.aspx?tree=_4_0_1&key=lumi3us>
153. Schuetz, P., Christ-Crain, M., Huber, A. R. & Müller, B. Long-term stability of procalcitonin in frozen samples and comparison of Kryptor and VIDAS automated immunoassays. *Clin. Biochem.* **43,** 341–344 (2010).
154. Forsström, J. J. & Dalton, K. J. Artificial neural networks for decision support in clinical medicine. *Ann. Med.* **27,** 509–517 (1995).
155. Tu, J. V. Advantages and disadvantages of using artificial neural networks versus logistic regression for predicting medical outcomes. *J Clin Epidemiol* **49,** 1225–1231 (1996).
156. Ward, N. S., Casserly, B. & Ayala, A. The compensatory anti-inflammatory response syndrome (CARS) in critically ill patients. *Clin. Chest Med.* **29,** 617–25– viii (2008).
157. Heininger, A. *et al.* Human cytomegalovirus infections in nonimmunosuppressed critically ill patients. *Critical Care Medicine* **29,** 541–547 (2001).
158. Almansa, R. *et al.* Immunological monitoring to prevent and treat sepsis. *Crit Care* **17,** 109 (2013).
159. Adib-Conquy, M. *et al.* Up-regulation of MyD88s and SIGIRR, molecules inhibiting Toll-like receptor signaling, in monocytes from septic patients. *Critical Care Medicine* **34,** 2377–2385 (2006).
160. Barnes, P. F. *et al.* Patterns of cytokine production by mycobacterium-reactive human T-cell clones. *Infection and Immunity* **61,** 197–203 (1993).
161. Chomarat, P., Kjeldsen-Kragh, J., Quayle, A. J., Natvig, J. B. & Miossec, P. Different cytokine production profiles of gamma delta T cell clones: relation to inflammatory arthritis. *Eur. J. Immunol.* **24,** 2087–2091 (1994).
162. Gold, R., Toyka, K. V. & Hartung, H. P. Synergistic effect of IFN-gamma and TNF-alpha on expression of immune molecules and antigen presentation by Schwann cells. *Cell. Immunol.* **165,** 65–70 (1995).
163. Mócsai, A. Diverse novel functions of neutrophils in immunity, inflammation, and beyond. *Journal of Experimental Medicine* **210,** 1283–1299 (2013).
164. Mantovani, A., Cassatella, M. A., Costantini, C. & Jaillon, S. Neutrophils in the activation and regulation of innate and adaptive immunity. *Nat Rev Immunol* **11,** 519–531 (2011).
165. Müller, I., Munder, M., Kropf, P. & Hänsch, G. M. Polymorphonuclear neutrophils and T lymphocytes: strange bedfellows or brothers in arms? *Trends in Immunology* **30,** 522–530 (2009).
166. Cerutti, A., Puga, I. & Magri, G. The B cell helper side of neutrophils. *Journal of Leukocyte Biology* **94,** 677–682 (2013).
167. Kesteman, N., Vansanten, G., Pajak, B., Goyert, S. M. & Moser, M. Injection of lipopolysaccharide induces the migration of splenic neutrophils to the T cell area of the white pulp: role of CD14 and CXC chemokines. *Journal of Leukocyte Biology* **83,** 640–647 (2008).

168. Puga, I. *et al.* B cell-helper neutrophils stimulate the diversification and production of immunoglobulin in the marginal zone of the spleen. *Nature Immunology* **13,** 170–180 (2012).
169. Chtanova, T. *et al.* Dynamics of neutrophil migration in lymph nodes during infection. *Immunity* **29,** 487–496 (2008).
170. Beauvillain, C. *et al.* Neutrophils efficiently cross-prime naive T cells in vivo. *Blood* **110,** 2965–2973 (2007).
171. Ostanin, D. V. *et al.* Acquisition of antigen-presenting functions by neutrophils isolated from mice with chronic colitis. *The Journal of Immunology* **188,** 1491–1502 (2012).
172. Aleman, M. *et al.* In tuberculous pleural effusions, activated neutrophils undergo apoptosis and acquire a dendritic cell-like phenotype. *J. Infect. Dis.* **192,** 399–409 (2005).
173. Iking-Konert, C. *et al.* Polymorphonuclear neutrophils in Wegener's granulomatosis acquire characteristics of antigen presenting cells. *Kidney Int.* **60,** 2247–2262 (2001).
174. Wagner, C. *et al.* Cellular inflammatory response to persistent localized Staphylococcus aureus infection: phenotypical and functional characterization of polymorphonuclear neutrophils (PMN). *Clin. Exp. Immunol.* **143,** 70–77 (2006).
175. Cross, A., Bucknall, R. C., Cassatella, M. A., Edwards, S. W. & Moots, R. J. Synovial fluid neutrophils transcribe and express class II major histocompatibility complex molecules in rheumatoid arthritis. *Arthritis Rheum.* **48,** 2796–2806 (2003).
176. Sandilands, G. P. *et al.* Cross-linking of neutrophil CD11b results in rapid cell surface expression of molecules required for antigen presentation and T-cell activation. *Immunology* **114,** 354–368 (2005).
177. Donor dependent, interferon-γ induced HLA-DR expression on human neutrophils in vivo. (2003). at <http://onlinelibrary.wiley.com/doi/10.1046/j.1365-2249.2003.02245.x/full>
178. Matsushima, H. *et al.* Neutrophil differentiation into a unique hybrid population exhibiting dual phenotype and functionality of neutrophils and dendritic cells. *Blood* **121,** 1677–1689 (2013).
179. Reinisch, W. *et al.* Donor dependent, interferon-gamma induced HLA-DR expression on human neutrophils in vivo. *Clin. Exp. Immunol.* **133,** 476–484 (2003).
180. Pillay, J., Tak, T., Kamp, V. M. & Koenderman, L. Immune suppression by neutrophils and granulocytic myeloid-derived suppressor cells: similarities and differences. *Cell. Mol. Life Sci.* **70,** 3813–3827 (2013).
181. Bonneville, M., O'Brien, R. L. & Born, W. K. Gammadelta T cell effector functions: a blend of innate programming and acquired plasticity. *Nat Rev Immunol* **10,** 467–478 (2010).
182. Vantourout, P. & Hayday, A. Six-of-the-best: unique contributions of γδ T cells to immunology. *Nat Rev Immunol* **13,** 88–100 (2013).
183. Brennan, P. J., Brigl, M. & Brenner, M. B. Invariant natural killer T cells: an innate activation scheme linked to diverse effector functions. *Nat Rev Immunol* **13,** 101–117 (2013).
184. Gold, M. C. & Lewinsohn, D. M. Co-dependents: MR1-restricted MAIT cells and their antimicrobial function. *Nat. Rev. Microbiol.* **11,** 14–19 (2012).

185. Welton, J. L. *et al.* Monocytes and γδ T cells control the acute-phase response to intravenous zoledronate: insights from a phase IV safety trial. *J Bone Miner Res* **28,** 464–471 (2013).
186. Davey, M. S. *et al.* Human neutrophil clearance of bacterial pathogens triggers anti-microbial γδ T cell responses in early infection. *PLoS Pathog* **7,** e1002040 (2011).
187. Kastenmüller, W., Torabi-Parizi, P., Subramanian, N., Lämmermann, T. & Germain, R. N. A spatially-organized multicellular innate immune response in lymph nodes limits systemic pathogen spread. *Cell* **150,** 1235–1248 (2012).
188. Morita, C. T., Jin, C., Sarikonda, G. & Wang, H. Nonpeptide antigens, presentation mechanisms, and immunological memory of human Vgamma2Vdelta2 T cells: discriminating friend from foe through the recognition of prenyl pyrophosphate antigens. *Immunol. Rev.* **215,** 59–76 (2007).
189. Grimaldi, D. *et al.* Specific MAIT cell behaviour among innate-like T lymphocytes in critically ill patients with severe infections. *Intensive Care Med* **40,** 192–201 (2014).
190. Abe, R. *et al.* Gram-negative bacteremia induces greater magnitude of inflammatory response than Gram-positive bacteremia. *Crit Care* **14,** R27 (2010).
191. Bonneville, M. *et al.* Chicago 2014 – 30 years of γδ T cells. *Cell. Immunol.* **Ahead of print** (2014). doi:http://dx.doi.org/10.1016/j.cellimm.2014.11.001
192. Gosselin, E. J., Wardwell, K., Rigby, W. F. & Guyre, P. M. Induction of MHC class II on human polymorphonuclear neutrophils by granulocyte/macrophage colony-stimulating factor, IFN-gamma, and IL-3. *J. Immunol.* **151,** 1482–1490 (1993).
193. Fanger, N. A. *et al.* Activation of human T cells by major histocompatability complex class II expressing neutrophils: proliferation in the presence of superantigen, but not tetanus toxoid. *Blood* **89,** 4128–4135 (1997).
194. Oehler, L. *et al.* Neutrophil granulocyte-committed cells can be driven to acquire dendritic cell characteristics. *J. Exp. Med.* **187,** 1019–1028 (1998).
195. Yamashiro, S. *et al.* Expression of CCR6 and CD83 by cytokine-activated human neutrophils. *Blood* **96,** 3958–3963 (2000).
196. Zarco, M. A. *et al.* Phenotypic changes in neutrophil granulocytes after G-CSF administration in patients with acute lymphoblastic leukemia under chemotherapy. *Haematologica* **83,** 573–575 (1998).
197. Mudzinski, S. P. *et al.* Expression of HLA-DR (major histocompatibility complex class II) on neutrophils from patients treated with granulocyte-macrophage colony-stimulating factor for mobilization of stem cells. *Blood* **86,** 2452–2453 (1995).
198. Lewis, S. M. *et al.* Plasma from patients with sepsis up-regulates the expression of CD49d and CD64 on blood neutrophils. *Am. J. Respir. Cell Mol. Biol.* **40,** 724–732 (2009).
199. Bisson-Boutelliez, C., Miller, N., Demarch, D. & Bene, M. C. CD9 and HLA-DR expression by crevicular epithelial cells and polymorphonuclear neutrophils in periodontal disease. *J. Clin. Periodontol.* **28,** 650–656 (2001).
200. Yokobori, N. *et al.* CD3 expression distinguishes two gammadeltaT cell receptor subsets with different phenotype and effector function in tuberculous pleurisy. *Clin. Exp. Immunol.* **157,** 385–394 (2009).
201. Lundqvist, C. & Hammarström, M. L. T-cell receptor gamma delta-expressing

intraepithelial lymphocytes are present in normal and chronically inflamed human gingiva. *Immunology* **79,** 38–45 (1993).
202. Pillay, J. *et al.* A subset of neutrophils in human systemic inflammation inhibits T cell responses through Mac-1. *Journal of Clinical Investigation* **122,** 327–336 (2012).
203. Nathan, C. Neutrophils and immunity: challenges and opportunities. *Nat Rev Immunol* **6,** 173–182 (2006).
204. Osawa, R. & Singh, N. Cytomegalovirus infection in critically ill patients: a systematic review. *Crit Care* **13,** R68 (2009).
205. Willcox, C. R. *et al.* Cytomegalovirus and tumor stress surveillance by binding of a human gamma delta T cell antigen receptor to endothelial protein C receptor. *Nature Immunology* **13,** 872–879 (2012).
206. Chiba, A. *et al.* Mucosal-associated invariant T cells promote inflammation and exacerbate disease in murine models of arthritis. *Arthritis Rheum.* **64,** 153–161 (2012).
207. Kalyan, S., Chandrasekaran, V., Quabius, E. S., Lindhorst, T. K. & Kabelitz, D. Neutrophil uptake of nitrogen-bisphosphonates leads to the suppression of human peripheral blood γδ T cells. *Cell. Mol. Life Sci.* **71,** 2335–2346 (2013).
208. Eberl, M. *et al.* A rapid crosstalk of human gammadelta T cells and monocytes drives the acute inflammation in bacterial infections. *PLoS Pathog* **5,** e1000308 (2009).
209. Baillie, J. K. Translational genomics. Targeting the host immune response to fight infection. *Science* **344,** 807–808 (2014).
210. Taneja, R., Sharma, A. P., Hallett, M. B., Findlay, G. P. & Morris, M. R. Immature circulating neutrophils in sepsis have impaired phagocytosis and calcium signaling. *Shock* **30,** 618–622 (2008).
211. Halo, T. L. *et al.* NanoFlares for the detection, isolation, and culture of live tumor cells from human blood. *Proc. Natl. Acad. Sci. U.S.A.* **111,** 17104–17109 (2014).
212. Galanzha, E. I., Kim, J.-W. & Zharov, V. P. Nanotechnology-based molecular photoacoustic and photothermal flow cytometry platform for in-vivo detection and killing of circulating cancer stem cells. *J Biophotonics* **2,** 725–735 (2009).
213. Sackmann, E. K., Fulton, A. L. & Beebe, D. J. The present and future role of microfluidics in biomedical research. *Nature* **507,** 181–189 (2014).
214. Nahavandi, S. *et al.* Microfluidic platforms for biomarker analysis. *Lab Chip* **14,** 1496–1514 (2014).
215. Spindel, S. & Sapsford, K. E. Evaluation of Optical Detection Platforms for Multiplexed Detection of Proteins and the Need for Point-of-Care Biosensors for Clinical Use. *Sensors (Basel)* **14,** 22313–22341 (2014).

Appendix 1: Scoring systems used in critical care

Acute Physiology and Chronic Health Evaluation II score

The Acute Physiology and Chronic Health Evaluation II (APACHE) score captures the worst value in twelve physiological parameters during the first 24-hours of critical care admission. It also considers a patient's age on admission, conditions present in the patient's medical history and whether the admission was following emergency surgery. Patients are excluded from recording or analysis of the mortality statistics if:

- The age at admission to the unit is less than 16 years old
- The length of stay in critical care is less than 8 hours
- The admission is:
    - for primary burns.
    - following coronary artery bypass graft surgery.
    - a transfer from another intensive care unit.
    - missing all twelve physiological variables.
    - a readmission within the same hospital.
    - missing an ultimate hospital outcome.

An example APACHE II scoring matrix is included on the following pages. Adapted from LeGall, J. R., Loirat, P. & Alpérovitch, A. APACHE II--a severity of disease classification system. *Critical Care Medicine* **14,** 754–755 (1986).

Sequential Organ Failure Assessment score

The Sequential Organ Failure Assessment (SOFA) score is based on a six component, organ-based calculation measured throughout a patient's stay calculated on multiple occasions. Both the average and the highest SOFA score can be used to predict mortality outcome. As with the APACHE score, the worst value in the last 24 hours is used to form the daily SOFA score

An example SOFA scoring matrix is included on the following pages along with a Glasgow Scoring System below. Adapted from Vincent, J. L. *et al.* The SOFA (Sepsis-related Organ Failure Assessment) score to describe organ dysfunction/failure. On behalf of the Working Group on Sepsis-Related Problems of the European Society of Intensive Care Medicine. *Intensive Care Med* **22,** 707–710 (1996).

.

Variable name	High abnormal range					Low abnormal range			
	+4	+3	+2	+1	0	+1	+2	+3	+4
Temperature (°C)	≥ 41	39 - 40.8		38.5 - 38.9	36 - 38.4	34 - 35.9	32 - 33.9	30 - 31.9	≤ 29.9
Mean arterial pressure (mmHg)	≥ 160	130 - 159	110 - 129		70 - 109		50 - 69		≤ 49
Heart rate (beats per minute)	≥ 180	140 - 179	110 - 139		70 - 109		55 - 69	40 - 54	≤ 39
Respiratory rate (rate per minute)	≥ 50	35 - 49		25 - 34	12 - 24	10 - 11	6 - 9		≤ 5
Oxygenation (mmHg)									
1. If FiO_2 > 0.5 use A-aDO_2	≥ 500	350 - 499	200 - 349		≤ 200				
2. Else use PaO_2					> 70	61 - 70		55 - 60	< 55
Arterial pH	≥ 7.7	7.6 - 7.69		7.5 - 7.59	7.33 - 7.49		7.15 - 7.32	7.15 - 7.24	< 7.15
Serum sodium (mMol/L)	≥ 180	160 - 179	155 - 159	150-154	130 - 149		120 - 129	111 - 119	≤ 110
Serum potassium (mMol/L)	≥ 7	6 - 6.9		5.5 - 5.9	3.5 - 5.4	3 - 3.4	2.5 - 2.9		< 2.5
Serum creatinine (mg/100 ml x 10^3)	≥ 3.5	2 - 3.4	1.5 - 1.9	0.6 - 1.4			≤ 0.6		
Hematocrit (%)	≥ 60		50 - 59.9	48 - 49.9	30 - 45.9		20-29.9		< 20
White blood count (total/mm^3 x 10^3)	≥ 40		20 - 39.9	15 - 19.9	3 - 14.9		1-2.9		< 1
Glasgow coma score (15- actual GCS score)									

Age (years)	Points
≤ 44	**0**
45 - 54	**2**
55 - 64	**3**
65 - 74	**5**
≥ 75	**6**

Total score:

Physiological + age + chronic health

Chronic health points

If the patient has a history of severe organ system deficiency or is immunocompromised before admission, assign points as follows:

a. For non-operative or emergency post-operative patients (**5** points)

b. for elective post-operative patients (**2** points)

Definitions

Liver: Biopsy proven cirrhosis and documented portal hypertension/episodes of past upper GI bleeding attributed to portal hypertension/prior episodes of hepatic failure/encephalopathy/coma.

Respiratory: Chronic restrictive, obstructive, or vascular disease resulting in severe exercise restriction.
Unable to climb stairs or perform household duties or documented chronic hypoxia, hypercapnia, secondary polycythemia, severe pulmonary hypertension (> 40mmHg), or respirator dependency.

Renal: Recurring chronic dialysis.

Immunocompromised The patient has received therapy that suppresses resistance to infection (e.g. immuno-suppresion, chemotherapy, radiation, long-term or recent high dose steroids) or has a disease that is sufficiently advanced to suppress resistance to infection (e.g. leukemia, lymphoma, AIDS).

SOFA Scoring System

Score	1	2	3	4
Respiration				
PaO_2/FiO_2 (mmHg)	<400	<300	<220	<100
SaO_2/FiO_2	221-301	142-220	67-141	<67
Coagulation				
Platelets x $103/mm^3$	<150	<100	<50	<20
Liver				
Bilirubin (mg/dL)	1.2-1.9	2.0-5.9	6.0-11.9	>12.0
Cardiovascular				
Hypotension (vasopressors in μmg/kg/min)	MAP <70	Dopamine ≤5 or dobutamine (any)	Dopamine >5 or norepinephrine ≤0.1	Dopamine >15 or norepinephrine >0.1
CNS				
Glasgow Coma Scale	13-14	10-12	6-9	<6
Renal				
Creatinine (mg/dL) or urine output (mL/d)	1.2-1.9	2.0-3.4	3.5-4.9 or <500	>5.0 or <200

Glasgow Coma Scale Scoring System

	Eyes		Verbal		Motor
				6	Obeys Commands
		5	Oriented, converses normally	5	Localizes painful stimuli
4	Opens eyes spontaneously	4	Confused, disoriented	4	Withdraws from pain stimuli
3	Opens eyes in response to voice	3	Utters inappropriate words	3	Decorticate posturing with pain painful stimuli
2	Opens eyes in response to painful stimuli	2	Incomprehensible sounds	2	Decerebrate posturing upon painful stimuli
1	Does not open eyes	1	Makes no sounds	1	Makes no movements

Appendix 2: Further data

5.3. Further details of clinical differences between survivors and non-survivors

Table 0.1 Day 1 clinical immune parameters in survivors and non-survivors.

	Survivor	Non-survivor	P value
Total leukocytes	18.1 ± 8.7	15.9 ± 7.5	-
Neutrophils	15.9 ± 8.2	13.6 ± 7.5	-
Lymphocytes	1.3 ± 1.0	0.9 ± 0.7	-
Eosinophils	0.3 ± 1.3	0.1 ± 0.2	-
Basophils	0.2 ± 1.3	0.5 ± 2.1	-
CRP	163.1 ± 134.6	190.3 ± 116.1	-

Whilst these measures often form the mainstay of immune monitoring in sepsis, no significant differences are shown between survivors and non-survivors.

Table 0.2 Day 5 clinical immune parameters in survivors and non-survivors.

	Survivor	Non-survivor	P value
Total leukocytes	14.9 ± 6.7	14.7 ± 7.0	-
Neutrophils	12.5 ± 6.2	13.0 ± 6.5	-
Lymphocytes	1.5 ± 0.8	1.1 ± 0.4	-
Eosinophils	0.02 ± 0.2	0.02 ± 0.2	-
Basophils	0.02 ± 0.04	0.03 ± 0.06	-
CRP	91.9 ± 90.2	117.1 ± 51.6	-

Whilst these measures often form the mainstay of immune monitoring in sepsis, no significant differences are shown between survivors and non-survivors.

Table 0.3 Day 1 clinical parameters recorded in ICU in survivors and non-survivors.

	Survivor	Non-survivor	P value
Heart rate	93.6 ± 20.5	88.5 ± 20.1	-
Systolic blood pressure	120.1 ± 25.1	120.3 ± 28.1	-
Diastolic blood pressure	61.2 ± 11.7	61.7 ± 13.1	-
Mean arterial pressure	80.2 ± 14	82.3 ± 18	-
Central venous pressure	13.1 ± 6.1	17.6 ± 8.6	-
Noradrenaline infusion rate	0.2 ± 0.3	0.1 ± 0.2	-
SpO_2	97.6 ± 3.5	96.2 ± 4.9	-
FiO_2	50.5 ± 20.1	55.2 ± 25.4	-
Tidal volume	507.3 ± 161.8	472.5 ± 194.0	-
Positive end expiratory pressure	7.1 ± 3	8 ± 3	-
Peak inspiratory pressure	20.5 ± 7	21.5 ± 6.3	-
Respiratory rate	18.1 ± 6.5	17.5 ± 3.5	-
$PaCO_2$	47.2 ± 11.6	37.3 ± 11.6	-
PaO_2	108.2 ± 41.5	104.2 ± 50.9	-
pH	7.31 ± 0.12	7.34 ± 0.08	-
Base excess	-3.26 ± 4.89	-4.41 ± 3.36	-
Alkaline phosphatase	95.4 ± 75.3	94.8 ± 62.3	-
Alanine transaminase	65.7 ± 74.4	60.6 ± 64.5	-
Albumin	22.7 ± 6.6	22.6 ± 6.4	-
Glucose day	8.2 ± 3.8	8.6 ± 3.3	-
Lactate day	2.1 ± 2.9	1.9 ± 1.7	-
Urea	10.8 ± 6.6	13.2 ± 8.7	-
Creatinine	153.3 ± 110.2	177.3 ± 128.3	-
Bicarbonate	18.4 ± 26.1	10.4 ± 6.6	-
Sodium	136.7 ± 5.4	137.4 ± 9.7	-
Potassium	4.4 ± 0.6	4.1 ± 0.7	-
Magnesium	0.9 ± 0.2	1 ± 0.3	-

Phosphate	1.6 ± 0.7	1.3 ± 0.6	-
Haemoglobin	11 ± 1.7	10.2 ± 1.8	-
Platelets	224.5 ± 116.1	229.5 ± 102.4	-
Prothrombin time	19.5 ± 9.7	19.8 ± 8.9	-
Activated partial prothrombin time	39.7 ± 7.3	39.9 ± 7.3	-
Fibrinogen	6.1 ± 2.5	5.6 ± 2	-

These measures form a key part of clinical decision-making in the critically ill patient despite the lack of significant differences between survivors and non-survivors.

Table 0.4 Day 5 clinical parameters recorded in ICU in survivors and non-survivors.

	Survivor	**Non-survivor**	**P value**
Heart rate	88.2 ± 15.9	95.5 ± 16.3	-
Systolic blood pressure	136.6 ± 23.9	120.3 ± 23.7	-
Diastolic blood pressure	71.9 ± 17.1	62.9 ± 9.7	-
Mean arterial pressure	93.8 ± 18.1	83.7 ± 15.1	-
Central venous pressure	14.3 ± 17.8	15.8 ± 9.4	-
Noradrenaline infusion rate	0.2 ± 0.1	0.1 ± 0.1	-
SpO_2	96.7 ± 3	95.1 ± 3.7	0.013
FiO_2	44.8 ± 18.1	47.6 ± 24.5	-
Tidal volume	573.6 ± 182.8	504.0 ± 130.7	-
Positive end expiratory pressure	8.3 ± 3.3	6.8 ± 1.6	-
Peak inspiratory pressure	22.1 ± 4.8	22.2 ± 6.6	-
Respiratory rate	19.4 ± 6.8	23.6 ± 9.3	-
$PaCO_2$	40.8 ± 8.6	42.2 ± 11.2	-
PaO_2	84.1 ± 20.7	79.7 ± 25.4	0.045
pH	7.42 ± 0.06	7.39 ± 0.09	-
Base excess	1.73 ± 3.95	-0.36 ± 6.35	-
Alkaline phosphatase	73 ± 84.2	88.5 ± 120.8	-
Alanine transaminase	22.5 ± 4.7	20.4 ± 5.7	-

Albumin	16.1 ± 2.3	16.5 ± 2.1	-
Glucose	8.5 ± 2.7	7.4 ± 2.8	-
Lactate	1.3 ± 1.4	2.4 ± 3.9	-
Urea	9.8 ± 5	11.6 ± 5.8	0.025
Creatinine	104.8 ± 58.6	147.3 ± 92.9	0.048
Bicarbonate	15.6 ± 15	11.9 ± 9.8	-
Sodium	139.1 ± 5.1	139.7 ± 7.5	-
Potassium	4.3 ± 0.5	4.6 ± 0.9	-
Magnesium	1 ± 0.2	0.9 ± 0.2	-
Phosphate	1 ± 0.3	1.3 ± 0.4	0.025
Haemoglobin	9.5 ± 1.5	9.5 ± 1.7	-
Platelets	214.8 ± 137.8	221 ± 157.1	-
Prothrombin time	16.1 ± 2.3	16.5 ± 2.1	-
Activated partial prothrombin time	36.6 ± 13	38.6 ± 7.4	-
Fibrinogen	6.2 ± 2.1	6 ± 1.7	-

By day 5, these parameters show signals of the common modes of ultimate death in severe sepsis, namely elevations in urea, creatinine and phosphate indicative of renal dysfunction and a low PaO_2 and SpO_2 related to respiratory failure.

5.4. Further detail of clinical differences between sepsis and SIRS

Table 0.5 Day 1 clinical immune parameters in sepsis and SIRS patients.

	Sepsis	SIRS	P value
Total leukocytes	18.1 ± 8.5	14.9 ± 8.8	-
Neutrophils	15.8 ± 8.4	12.6 ± 8	-
Lymphocytes	1.2 ± 1.6	1.5 ± 0.9	-
Monocytes	0.8 ± 0.6	0.7 ± 0.5	-
CRP	197.6 ± 122.6	44.8 ± 76.5	0.0003

Whilst these often form the mainstay of immune monitoring in sepsis, only a significant difference in CRP is shown between sepsis and SIRS patients.

Table 0.6 Day 5 clinical immune parameters in sepsis and SIRS patients.

	Sepsis	SIRS	P value
Total leukocytes	15.2 ± 6.8	13.1 ± 6.7	-
Neutrophils	13.1 ± 6.4	10.5 ± 5.7	-
Lymphocytes	1.4 ± 1	1.3 ± 0.7	-
Monocytes	0.8 ± 0.6	1 ± 0.8	-
CRP	94.9 ± 73.4	122.9 ± 112.6	-

Whilst these often form the mainstay of immune monitoring in sepsis, at day 5 no significant differences are seen.

Table 0.7 Day 1 clinical parameters recorded in ICU in sepsis and SIRS patients.

	Sepsis	SIRS	P value
Heart rate	93.1 ± 19	88.9 ± 25	-
Mean arterial pressure	78.9 ± 13.6	86.2 ± 17.4	-
Central venous pressure	17.2 ± 15.6	13.1 ± 6.9	-
Noradrenaline infusion rate	0.3 ± 0.4	0.1 ± 0.1	-
SpO_2	97 ± 3.7	97.5 ± 5.8	-
FiO_2	52.8 ± 21.6	46.9 ± 17.7	-
Tidal volume	498.2 ± 183.2	490.9 ± 160.6	-
Positive end expiratory pressure	7.5 ± 3.1	6.1 ± 2.3	-
Peak inspiratory pressure	21.6 ± 6.4	17.3 ± 6.7	-
Respiratory rate	17.4 ± 5	19.9 ± 8.2	-
$PaCO_2$	43.9 ± 12.2	53.1 ± 19.8	-
PaO_2	115.9 ± 62.5	131 ± 114.7	-
pH	7.3 ± 0.1	7.3 ± 0.1	-
Base excess	-4.1 ± 4.6	-1.5 ± 3.9	-
Alkaline phosphatase	97.5 ± 72	72.9 ± 61.3	0.06
Alanine transaminase	71.6 ± 91.5	73.6 ± 74.7	-
Albumin	22.4 ± 6.4	23.8 ± 6.5	-
Glucose day	7.9 ± 3.1	9.2 ± 5.6	-
Lactate day	1.8 ± 1.4	3.2 ± 5.3	-
Urea	12.6 ± 7.1	7.4 ± 4.7	0.05
Creatinine	173.9 ± 120.2	111.8 ± 63.6	-
Bicarbonate	18.5 ± 25.1	9.9 ± 4.7	-
Sodium	136.1 ± 6.5	139.7 ± 5.6	-
Potassium	4.4 ± 0.6	4.2 ± 0.8	-
Magnesium	0.9 ± 0.2	1.7 ± 1.6	-
Phosphate	1.5 ± 0.5	0.9 ± 0.3	-
Haemoglobin	10.7 ± 1.7	10.1 ± 2.5	-

Platelets	230.7 ± 111.7	251.1 ± 165.9	0.031
Prothrombin time	19.2 ± 7.1	17.2 ± 3.2	-
Activated partial prothrombin time	40.1 ± 7.4	39.3 ± 15.6	-
Fibrinogen	6 ± 2.3	4.3 ± 2	0.04

These form a key part of clinical decision making in the critically ill patient despite the lack of significant differences apart from minor significant differences in the parameters highlighted.

Table 0.8 Day 5 clinical parameters recorded in ICU in sepsis and SIRS patients.

	Sepsis	**SIRS**	**P value**
Heart rate	90.4 ± 16	98.2 ± 27.8	-
Mean arterial pressure	91.4 ± 17.9	90.4 ± 21.3	-
Central venous pressure	14.5 ± 15.3	20.5 ± 6.8	-
Noradrenaline infusion rate	0.1 ± 0.1	0.1 ± 0.1	-
SpO_2	96.3 ± 3.2	96.8 ± 3.9	-
FiO_2	46 ± 19.4	50 ± 19.5	-
Tidal volume	572.9 ± 183	492.9 ± 164.3	-
Positive end expiratory pressure	7.9 ± 3	6.9 ± 2.5	-
Peak inspiratory pressure	21.5 ± 5.8	19.6 ± 4.9	-
Respiratory rate	20.4 ± 7.3	16.7 ± 3.4	-
$PaCO_2$	41.3 ± 9.4	44.5 ± 10.5	-
PaO_2	82.5 ± 22.2	76.5 ± 19.5	-
pH	7.4 ± 0.1	7.4 ± 0.1	-
Base excess	1.2 ± 4.7	0.4 ± 3.8	-
Alkaline phosphatase	163.5 ± 115.5	101.2 ± 64.9	-
Alanine transaminase	77.1 ± 93.3	67.2 ± 87.2	-
Albumin	21.7 ± 5	23.8 ± 5.5	-
Glucose	8.2 ± 2.7	8.2 ± 3.2	-
Lactate	1.6 ± 2.4	1.5 ± 1.2	-

Urea	10.9 ± 5.8	6.3 ± 3.8	0.04
Creatinine	121.1 ± 74.8	97.1 ± 72.9	-
Bicarbonate	21.5 ± 38.8	11.4 ± 5	-
Sodium	139.3 ± 5.8	141.3 ± 6	-
Potassium	4.4 ± 0.6	4.3 ± 0.9	-
Magnesium	1 ± 0.2	0.9 ± 0.2	-
Phosphate	1.1 ± 0.3	1 ± 0.2	-
Haemoglobin	9.5 ± 1.5	10.4 ± 1.6	-
Platelets	215.6 ± 141.6	233.5 ± 156	-
Prothrombin time	16.3 ± 2.3	16.9 ± 4.1	-
Activated partial prothrombin time	37.3 ± 11.2	36.7 ± 7	-
Fibrinogen	6.1 ± 2	6.1 ± 2.1	-

These form a key part of clinical decision making in the critically ill patient despite the lack of significant differences apart from in urea.

5.5. Further detail of clinical differences between different infecting organism subtypes

Table 0.9 Day 1 clinical immune parameters in different infecting organism subtypes.

	Culture-negative	Gram-positive	Gram-negative	P value
Total leukocytes	18.9 ± 8.2	15.8 ± 7.6	19.4 ± 9.6	-
Neutrophils	16.6 ± 7.9	13.2 ± 7.6	17.3 ± 9.3	-
Lymphocytes	1.2 ± 1	1.3 ± 2.5	1.2 ± 0.8	-
Monocytes	1 ± 0.7	0.6 ± 0.6	0.8 ± 0.4	-
CRP	158.6 ± 130.2	214.8 ± 123.8	226.5 ± 105.5	-

Whilst these often form the mainstay of immune monitoring in sepsis, no significant difference are shown between these subgroups.

Table 0.10 Day 5 clinical immune parameters in different infecting organism subtypes.

	Culture-negative	Gram-positive	Gram-negative	P value
Total leukocytes	14 ± 4.9	17.9 ± 9	14 ± 5.7	-
Neutrophils	11.8 ± 5.1	15.8 ± 8.4	11.9 ± 4.7	-
Lymphocytes	1.2 ± 0.6	1.6 ± 1.5	1.5 ± 0.7	-
Monocytes	0.9 ± 0.4	0.8 ± 0.7	0.6 ± 0.6	-
CRP	71.4 ± 54.3	121.7 ± 94.6	95.4 ± 63.1	-

Whilst these often form the mainstay of immune monitoring in sepsis, no significant difference are shown between these subgroups.

Table 0.11 Day 1 clinical parameters recorded in ICU in different infecting organism subgroups.

	Culture-negative	Gram-positive	Gram-negative	P value
Heart rate	87.9 ± 16.7	100.9 ± 21.1	91.6 ± 17.9	-
Mean arterial pressure	78.8 ± 16.3	79.4 ± 13.7	78.5 ± 10.6	-
Central venous pressure	18.2 ± 17.7	20.9 ± 21	13.5 ± 5.3	-
Noradrenaline infusion rate	0.2 ± 0.2	0.4 ± 0.6	0.4 ± 0.5	-
SpO_2	97.1 ± 3.6	96.2 ± 4.8	97.8 ± 2.4	-
FiO_2	47.4 ± 20.3	60.1 ± 22.2	52.1 ± 21.8	-
Tidal volume	455 ± 216.3	573.5 ± 235.7	466.5 ± 96.5	-
Positive end expiratory pressure	6.8 ± 3.4	8.6 ± 3.3	7.5 ± 2.4	-
Peak inspiratory pressure	21.6 ± 9.2	23.1 ± 5.6	22.4 ± 6.7	-
Respiratory rate	17.8 ± 6.4	16.9 ± 4.1	17.3 ± 4	-
$PaCO_2$	48.4 ± 14	47 ± 13.3	38.6 ± 8.3	-
PaO_2	96.3 ± 30	133.2 ± 105.1	117.6 ± 33.6	-
pH	7.3 ± 0.1	7.3 ± 0.1	7.3 ± 0.1	-
Base excess	-2.8 ± 4.4	-4.7 ± 4.5	-4.8 ± 4.8	-
Alkaline phosphatase	87.1 ± 65.3	110.3 ± 84	97 ± 68.6	-
Alanine transaminase	42 ± 27.4	79.1 ± 108.2	100.6 ± 116	-
Albumin	25.5 ± 5.7*	19.2 ± 5.8*	22 ± 6.5	0.03
Glucose day	8 ± 2.3	8.1 ± 3.1	7.5 ± 3.8	-
Lactate day	1.6 ± 1.2	2 ± 1.6	1.9 ± 1.5	-
Urea	13.1 ± 8.5	12.1 ± 6.9	12.6 ± 5.7	-
Creatinine	189.5 ± 136.2	167.3 ± 120.5	160.6 ± 101.5	-
Bicarbonate	11.3 ± 6.3	15.6 ± 11.6	30.9 ± 42.1	-
Sodium	134.3 ± 9	136.6 ± 4.6	137.8 ± 4.1	-

Potassium	4.5 ± 0.7	4.3 ± 0.4	4.3 ± 0.6	-
Magnesium	1 ± 0.2	0.9 ± 0.3	0.9 ± 0.2	-
Phosphate	1.6 ± 0.6	1.5 ± 0.5	1.5 ± 0.4	-
Haemoglobin	10.7 ± 1.9	16 ± 21.5	16.1 ± 22.2	-
Platelets	254 ± 103	211.7 ± 82.2	222.2 ± 144.5	-
Prothrombin time	19 ± 8.1	20.4 ± 9	27.9 ± 38.2	-
Activated partial prothrombin time	38.4 ± 8.2	40.6 ± 6.1	41.6 ± 7.6	-
Fibrinogen				

These form a key part of clinical decision making in the critically ill patient despite the lack of significant differences in subgroups apart from albumin in the parameters highlighted.

Table 0.12 Day 5 clinical parameters recorded in ICU in different infecting organism subgroups.

	Culture-negative	Gram-positive	Gram-negative	P value
Heart rate	88.3 ± 20.4	95.6 ± 12.8	87.4 ± 13.2	
Mean arterial pressure	91.4 ± 20	91 ± 20.9	91.8 ± 12	
Central venous pressure	13.5 ± 10	16.2 ± 23.8	13.8 ± 6.8	
Noradrenaline infusion rate	0.2 ± 0.1	0.1 ± 0.1	0.2 ± 0.1	
SpO_2	96.4 ± 4.1	95.8 ± 3	96.5 ± 2.5	
FiO_2	44.3 ± 23.4	48.5 ± 19.4	44.3 ± 13	
Tidal volume	556.6 ± 94.8	598.4 ± 187.6	556.3 ± 255.5	
Positive end expiratory pressure	7.6 ± 2.3	7.6 ± 3	8.6 ± 4	
Peak inspiratory pressure	21.3 ± 6	19.3 ± 6.4	24.4 ± 4	
Respiratory rate	22 ± 3.5	17.4 ± 3.5	22.6 ± 12	
$PaCO_2$	40.1 ± 11.2	42.6 ± 10.6	41.4 ± 7.6	
PaO_2	92.8 ± 20.1	69.4 ± 15.2	83.6 ± 24.6	
pH	7.4 ± 0.1	7.4 ± 0.1	7.4 ± 0.1	

Base excess	1.6 ± 5	0 ± 5.8	1.8 ± 2.6	
Alkaline phosphatase	118.4 ± 80.3	187 ± 109.4	497.8 ± 1353.8	
Alanine transaminase	65.2 ± 111.9	70.1 ± 54	95.9 ± 106.4	
Albumin	22.9 ± 4.7	20.8 ± 4.7	21.4 ± 5.6	
Glucose day	8.5 ± 2.4	8.5 ± 2.8	7.4 ± 3	
Lactate day	1.2 ± 0.9	1.6 ± 2	2 ± 3.8	
Urea	8.6 ± 4.7*	14.2 ± 6.4*	9.6 ± 4.8	0.026
Creatinine	111.9 ± 79.7	144.7 ± 71.1	107.3 ± 72.5	
Bicarbonate	11.4 ± 9.2	21.6 ± 33.8	32.3 ± 57.9	
Sodium	138.6 ± 7.2	139.9 ± 5.7	139.4 ± 4.4	
Potassium	4.5 ± 0.8	4.4 ± 0.6	4.3 ± 0.4	
Magnesium	0.9 ± 0.1	1.1 ± 0.2	1 ± 0.3	
Phosphate	1.1 ± 0.2	1.2 ± 0.4	1.1 ± 0.4	
Haemoglobin	9.9 ± 1.7	15.6 ± 26.9	15.1 ± 22.7	
Platelets	252.5 ± 132.8	208.2 ± 119	188.7 ± 170.5	
Prothrombin time	16.2 ± 2.3	17.1 ± 2.7	15.7 ± 1.6	
Activated partial prothrombin time	35.2 ± 7.1	41.4 ± 16.3	35.1 ± 6.1	
Fibrinogen	6.2 ± 1.9	5.8 ± 2.3	6.3 ± 1.8	

These form a key part of clinical decision making in the critically ill patient despite the lack of significant differences apart from urea in the parameters highlighted.

Appendix 3: R scripts

The following script written in R studio Version 0.98.501 calculates and records an AUC value for every unique combination of x number of variables drawn from a pool of y possible variables using a neural network model:

```
require(RSNNS)
require(pROC)

#Read in the file as a csv from the filename below or from a finder window
#iris <- read.csv(file.choose(), fileEncoding="latin1")    # Select "master.csv"
iris <- read.csv('All sepsis_sirs signifigant immuted.csv', fileEncoding="latin1")    # Select "master.csv"
iris

#*****************************************************
#Set-up what variables are what and how many to combine
varibleColumns = 3:15
combinationNumber = 4:13
targetVarible = 2
hiddenNodes = 2
maximum iteration = 3000
#*****************************************************

#shuffle the vector before sampling for in- and out-of-sample sets
iris <- iris[sample(1:nrow(iris),length(1:nrow(iris))),1:ncol(iris)]
iris
oldIris = iris

# since the targets need to be dummy variables, need to translate text species values into 0/1 using the predictor column
irisTargets <- decodeClassLabels(iris[,targetVarible])
irisTargets
```

```
#Loop from lowest to highest number of combinations
for (n in combinationNumber) {

  cat("Calculating combinations of", n, "varibles","\n\n")

  #Make a list of variable combinations
  varibleCombinations <- combn(varibleColumns,n,simplify = TRUE)
  numberOfCombinations = ncol(varibleCombinations)

  #Make a object to store the AUC and combination values for this n of combinations
  output<-as.data.frame(matrix(0,nrow=numberOfCombinations,ncol=n+2))
  x=1

  #Loop through every combination with a total of n variables
  for (i in 1:numberOfCombinations){

    cat("Combination", i, "of", numberOfCombinations, "\n")
    iris = oldIris
    irisValues <- iris[,varibleCombinations[,i]]

    #Print the combinations being used currently
    cat(colnames(irisValues),"\n")



    # split into in- and out-of-sample sets - 15%  of cases are out-of-sample
    iris <- splitForTrainingAndTest(irisValues, irisTargets, ratio=0.15)

    # normalize to avoid very large weights and therefore avoid poor training
    iris <- normTrainingAndTestSet(iris)

    # set up model and do training based on the values selected at the top
    model <- mlp(iris$inputsTrain, iris$targetsTrain, size=c(hiddenNodes),
learnFuncParams=c(0.1),
```

```
        maxit=maximum iteration, inputsTest=iris$inputsTest,
targetsTest=iris$targetsTest)

   #Get an AUC for the training set
   trainingROC = roc(predictor=fitted.values(model)[,2], response=iris$targetsTrain[,2],
plot=TRUE)

   #Get an AUC for the test set (not done)***
   #roc(predictor=predictions[,2], response=iris$targetsTest[,2], plot=TRUE)

   #Print the AUC for this combination
   cat(auc(trainingROC),"\n\n")

   #Save the variable names used and AUC value to the output object
   output[i,] <- c(colnames(irisValues),auc(trainingROC),"to do")
  }

  #Print the output for n variables and save the output as a CSV file
  write.csv(output, paste0("Outcome_AUC_", n,".csv"), row.names=F)
  output = NULL
  cat("\n\n\n")
}

print("All combinations saved")
```

The following script written in R studio Version 0.98.501 produces a classification decision tree and the associated values for the calculation of sensitivity and specificity.

```
require(rpart)

#Load data
data = read.csv(file.choose(), fileEncoding="latin1")    # Select "master.csv"

data
attributes(data$outcome)
data$outcome

#Type in columns
varibleColumns = 3:21
targetVarible = 2
data[,targetVarible] <- as.factor(data[,targetVarible])

#Make formula
varibleColumnNames = names(data[varibleColumns])
targetVaribleName = names(data[targetVarible])
myFormula =
as.formula(paste(targetVaribleName,"~",paste(varibleColumnNames,collapse="+")))
myFormula

#Make tree
tree = rpart(myFormula, method="class", data=data)

#Info
printcp(tree) # display the results
plotcp(tree) # visualize cross-validation results
summary(tree) # detailed summary of splits

#Plots
plot(tree, use.n=TRUE, all=TRUE, cex=.8)
text(tree, use.n=TRUE, all=TRUE, cex=0.6)

#Info
printcp(ptree) # display the results
plotcp(ptree) # visualize cross-validation results
summary(ptree) # detailed summary of splits
```

Appendix 4: Published papers resulting from this work.

frontiers in
IMMUNOLOGY

OPINION ARTICLE
published: 13 November 2014
doi: 10.3389/fimmu.2014.00572

Pathogen-specific immune fingerprints during acute infection: the diagnostic potential of human γδ T-cells

***Matthias Eberl*[1]*, *Ida M. Friberg*[1], *Anna Rita Liuzzi*[1], *Matt P. Morgan*[1,2] *and Nicholas Topley*[3]**

[1] *Cardiff Institute of Infection and Immunity, School of Medicine, Cardiff University, Cardiff, UK*
[2] *Cardiff and Vale University Health Board, Cardiff, UK*
[3] *Institute of Translation, Innovation, Methodology and Engagement, School of Medicine, Cardiff University, Cardiff, UK*
**Correspondence: eberlm@cf.ac.uk*

Edited by:
Julie Dechanet-Merville, Centre National de la Recherche Scientifique, France

Reviewed by:
Bernhard Moser, Cardiff University, UK
Dieter Kabelitz, Christian-Albrechts University Kiel, Germany

Keywords: bacterial infection, point-of-care diagnosis, biomarkers, innate immunity, local inflammation

APOCALYPSE NOW: THE END OF MODERN MEDICINE AS WE KNOW IT

> Gentlemen, it is the microbes who will have the last word. [Messieurs, c'est les microbes qui auront le dernier mot]. – Louis Pasteur, 1822–1895

The last 200 years have seen a dramatic reduction in the prevalence and severity of microbial infections, due to the implementation of groundbreaking measures ranging from improved sanitation and hygiene and the introduction of aseptic techniques to the development of successful vaccines and the discovery of effective antibiotics. Devastating infections that were common until the late nineteenth century such as cholera, diphtheria, plague, syphilis, tuberculosis, and typhoid came into the reach of effective control, at least in developed countries, and with a minimized risk of wound infections surgical procedures began to revolutionize modern medicine. Antibiotics, in particular, radically transformed the treatment and prevention of microbial infections and have saved millions of lives since their introduction (1). However, antibiotic usage is invariably linked to the selective pressure it exerts on the target organism to develop escape strategies (2).

We are at present witnessing how the pendulum begins to swing backwards, with anti-microbial resistances developing on an unprecedented global scale. New classes of Gram-positive and Gram-negative "superbugs" are emerging and spreading at an alarming rate, some of which are virtually insusceptible to all available drugs (3–5). The once apocalyptic vision of a "post-antibiotic era" where common infections and minor injuries may result untreatable and eventually fatal is rapidly becoming a real possibility (1, 2, 6, 7), heralding what Margaret Chan, Director-General of the WHO, in 2012 called "the end of modern medicine as we know it." The appearance of multidrug-resistant bacteria has been identified by the WHO, the Centers for Disease Control and Prevention (CDC) in the USA and their European counterpart, the ECDC, as one of the major global health challenges humankind is facing in the twenty-first century (8–10). According to Sally Davies, the UK Chief Medical Officer, "there are few public health issues of greater importance than anti-microbial resistance in terms of impact on society" (11).

There is now an urgent call for anti-microbial stewardship programs that aim to prescribe antibiotics more prudently, and to tailor their use to defined patient groups who will benefit most. The fact that the prevalence of resistance appears to correlate directly with antibiotic consumption across different countries (12) argues in favor of the immediate effectiveness of such tightly controlled programs. As highlighted in a recent Outlook issue in *Nature*, "the potential to save lives with faster and more targeted diagnoses, decrease unnecessary and often incorrect prescriptions, and even help identify early on where bacterial resistance could occur, will have a drastic effect on the way patients are treated" (13).

MISSION IMPOSSIBLE: THE FUNDAMENTAL FLAWS OF CONVENTIONAL DIAGNOSIS

> When it concerns the search for pathogenic organisms suspected in the diseased body, in the first instance bacteria, then during conventional microscopic examination carried out without special preparations and artifices one encounters the most substantial, at times virtually insurmountable, obstacles. [Wenn es sich nun darum handelt, die im erkrankten Körper vermutheten pathogenen Organismen, zunächst Bacterien, aufzusuchen, so begegnet man bei der gewöhnlichen ohne besondere Vorbereitungen und Kunstgriffe ausgeführten mikroskopischen Untersuchung den erheblichsten, stellenweise geradezu unübersteiglichen Hindernissen]. – Robert Koch, 1843–1910 (14)

More than a century after Robert Koch's landmark discovery of the causative agents of anthrax, cholera, and tuberculosis, the diagnosis of suspected infections still depends largely on the definitive identification of the likely pathogen in biological samples. However, standard microbiological culture is inefficient and slow (typically >1–2 days, for a confirmed diagnosis of tuberculosis >4 weeks), and in many cases no organism can be grown despite

Abbreviation: HMB-PP, (*E*)-4-hydroxy-3-methyl-but-2-enyl pyrophosphate.

clinical signs of infection, indicating that conventional diagnostic methods are not specific and/or rapid enough to target therapy (15–17). Early management of patients with acute symptoms who require immediate medical intervention, including virtually all hospital-based infections, thus remains largely empirical. As direct consequence, the fundamental uncertainty about the real cause underlying the clinical signs observed leads to inappropriate and unnecessary treatments exposing patients to drug-related side effects; raising the risk of opportunistic, chronic, or recurrent infections; and contributing to the emergence and spread of multidrug resistance (1–7). This dilemma eventually results in potentially avoidable patient morbidity/mortality, and imposes a considerable burden on health care systems and societies (8–11). There remains an unmet clinical need for rapid and accurate diagnostic tests for patients with acute infections. According to Kessel and Sharland (18), "new technology focusing on rapid diagnosis of specific bacteria and resistance genes, along with combination biomarkers indicating bacterial or viral infections, especially if adapted to near patient testing, could have a major impact on targeting appropriate antibiotic treatment."

In order to circumvent the almost insurmountable obstacles of a rapid and accurate identification of the causative pathogen by traditional microbiological techniques, efforts are being made to utilize state-of-the-art molecular methods. Approaches based on the detection of microbial nucleic acids, cell wall constituents, or other unique features of distinct pathogens by PCR, chromatography, or mass spectrometry certainly complement culture-based tests and speed up microbial identification, yet they require considerable resources and may not be applicable to primary care or home settings (19–23). Moreover, they do not provide information about the pathogenicity of the identified species and its interaction with the host. Of note, neither microbiological nor molecular methods discriminate between pathogens causing disease, asymptomatic carriage, and sample contaminants, and thus even positive test results require extensive interpretation by the treating physician (24–26).

There is a plethora of disease-related markers that are commonly assessed by clinicians to aid a correct diagnosis, ranging from basic blood and urine parameters to indicators of tissue damage, tumor progression and autoimmunity, among others. However, there is a conspicuous paucity of biomarkers for accurate diagnosis of microbial disease. Current biomarkers of inflammation such as C-reactive protein (CRP) or procalcitonin (PCT) are often not sensitive or specific enough and are only poor surrogates for acute infections (22, 27, 28). The vast majority of research on novel diagnostics has so far focused on identifying individual factors and assessing their performance in isolation. Yet, it may come as no surprise that none of these proposed parameters have reached sufficient discriminatory power on their own, given the complex and multifactorial processes underlying local and systemic inflammatory responses to a broad range of pathogens (29, 30). As a result, neither the direct identification of the causative pathogen nor the measurement of currently used biomarkers of inflammation is sufficiently accurate or rapid for a reliable point-of-care diagnosis of acute microbial infection.

QUANTUM OF SOLACE: EXPLOITATION OF PATHOGEN-SPECIFIC HOST RESPONSES FOR NOVEL DIAGNOSTICS

> The immune system appears to have originated as a set of effector cells having multiple distinct receptors that discriminate self from infectious non-self by recognition of patterns found exclusively on microorganisms. – Charles A. Janeway, Jr., 1943–2003 (31)

Key to developing better and stratified approaches to treating infection is a detailed understanding of the intricate host–pathogen relationships in disease, in order to exploit the unique sophistication of the human immune system for diagnostic and therapeutic purposes (32, 33). In a radical departure from current practice, our research is based upon the premise that each type of infection evokes a distinct pathogen-specific host response – what we refer to as "immune fingerprint." A patient's early anti-microbial response itself is likely to provide far more detailed insight into the true cause and severity of acute infections than conventional methods, independently of the subsequent clinical course of the disease (34). The human immune system is a highly complex network of interdependent cellular and humoral players that has evolved over millions of years in order to survey the body for potentially hazardous structures and initiate an appropriate defense. The communication with invading micro-organisms thus occurs at multiple levels, giving rise to a plethora of biomarkers of potential relevance for diagnostic purposes. Different pathogens interact uniquely with different components of the innate immune system due to the efficient self/non-self discrimination based on conserved microbial signals such as non-methylated bacterial DNA, bacterial flagella, and cell wall constituents. These structures are typically recognized by members of the Toll-like receptor family and/or other pattern recognition receptors expressed by sentinel cells (35–37). However, there is also emerging evidence that certain types of innate or "unconventional" T-cells such as γδ T-cells and mucosal-associated invariant T (MAIT) cells are able to detect common microbial metabolites through their T-cell receptors, by sensing intermediates of the non-mevalonate and riboflavin biosynthesis pathways that are unique to certain types of microorganisms (38, 39).

Vγ9/Vδ2 T-cells represent a unique subpopulation of human T-cells (40, 41) that appears to have a particularly crucial role in contributing to immune fingerprints of diagnostic relevance (34). This is due to their exquisite responsiveness to the microbial isoprenoid precursor (*E*)-4-hydroxy-3-methyl-but-2-enyl pyrophosphate (HMB-PP) that is produced by the majority of Gram-negative pathogens and a large proportion of Gram-positive species such as *Clostridium difficile*, *Listeria monocytogenes*, and *Mycobacterium tuberculosis*, while it is not found in other bacteria including staphylococci and streptococci as well as fungi (42–44). The rapid and sensitive response of Vγ9/Vδ2 T-cells to a broad range of pathogens evokes Janeway's criteria for a "pathogen-associated molecular pattern" in that HMB-PP is an invariant metabolite in many different species that is essential in the microbial physiology but absent from the human

host (43, 45). Bacterial extracts prepared from HMB-PP producing species typically activate Vγ9/Vδ2 T-cells much stronger than extracts prepared from HMB-PP deficient micro-organisms (42, 44, 46), and peripheral and/or local Vγ9/Vδ2 T-cell levels are often elevated in patients infected with defined HMB-PP producing pathogens (43, 47). Elegant proof of concept for this responsiveness comes from the demonstration that HMB-PP producing wildtype *L. monocytogenes* activate Vγ9/Vδ2 T-cells far better, both *in vitro* (48) and in primate models *in vivo* (49), than genetically engineered *L. monocytogenes* that are identical to the parental strain except for an inability to produce HMB-PP. Similarly, overexpression of HMB-PP synthase through genetic manipulation increases the stimulatory potential of bacteria such as *E. coli*, *L. monocytogenes*, *M. tuberculosis*, and *Salmonella enterica* on Vγ9/Vδ2 T-cells *in vitro* (42, 46, 48, 50, 51) and *in vivo* (52). Our own data demonstrate that even in heterogeneous patient cohorts infected with a whole spectrum of diverse bacteria, differences in Vγ9/Vδ2 T-cell frequencies between patients with microbiologically confirmed infections caused by HMB-PP producing and HMB-PP deficient species remain apparent. This is true both for peritoneal dialysis patients with acute peritonitis as an exemplar of localized immune responses restricted to the peritoneal cavity (34, 46, 53), as well as on a systemic level in the peripheral blood of critically ill patients with severe sepsis (54). Most importantly, studies in patients with acute peritonitis suggest that a diagnostic test measuring local Vγ9/Vδ2 T-cells on the first day of presentation with acute symptoms may not only indicate the presence of Gram-negative (predominantly HMB-PP producing) bacteria but also identify patients at an increased risk of inflammation-related downstream complications (34).

The exquisite responsiveness of Vγ9/Vδ2 T-cells and other unconventional T-cells to microbial metabolites shared by certain pathogens but not by others identifies these cell types as key constituent of diagnostically relevant immune fingerprints at the point of care. This is especially the case when Vγ9/Vδ2 T-cell levels are assessed locally and when they are combined with other powerful discriminators such as peritoneal proportions of neutrophils, monocytes, and $CD4^+$ T-cells in the inflammatory infiltrate as well as intraperitoneal concentrations of certain soluble immune mediators (34) (**Figure 1**). Such a combination with further parameters provides additional information as to the precise nature of the causative pathogen, for instance to distinguish between immune responses induced by Gram-negative (LPS producing) and Gram-positive (LPS deficient) bacteria, and is also likely to help increase sensitivity owing to the age and gender-dependent variability of Vγ9/Vδ2 T-cell levels (55). Pathogen-specific immune fingerprints that discriminate between certain subgroups of patients (e.g., with Gram-negative vs. Gram-positive bacterial infections) can be determined within hours of presentation with acute symptoms, long before traditional culture results become available, and by guiding early patient

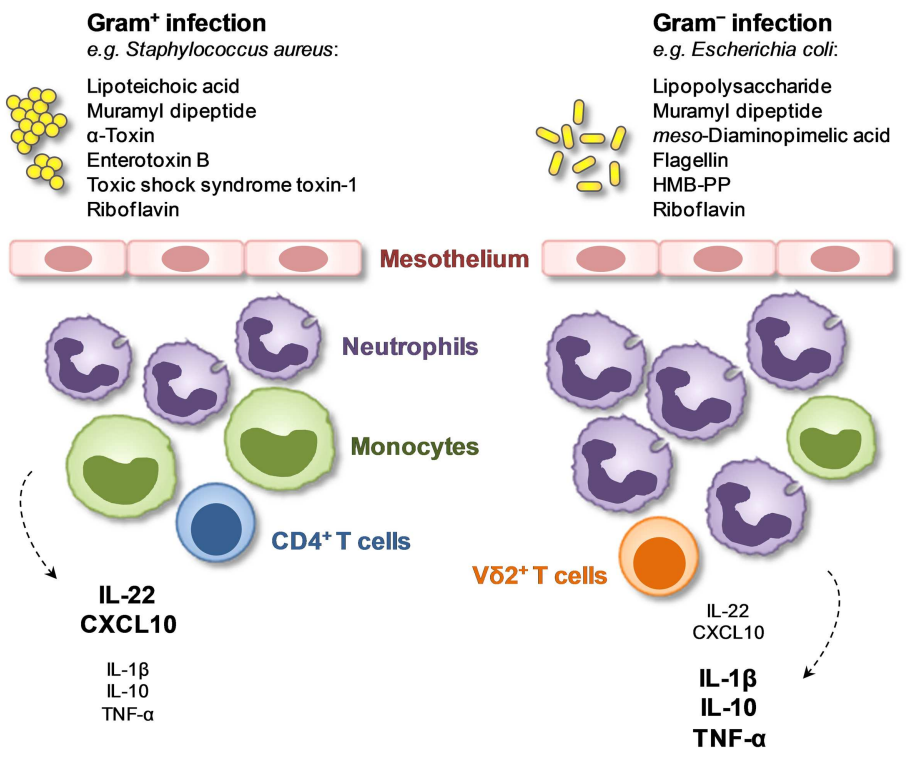

FIGURE 1 | Local immune fingerprints in peritoneal dialysis patients on the day of presentation with acute peritonitis. Shown are cellular and humoral biomarkers that are associated with the presence of Gram-positive or Gram-negative bacteria and that may be exploited for novel diagnostic tests (34).

management and optimizing targeted treatment will contribute to improving outcomes and advancing antibiotic stewardship. It remains to be investigated how much these findings on diagnostic immune fingerprints in peritoneal dialysis patients can be extended to other local or systemic scenarios to diagnose infections at the point of care, and whether they can also be applied to monitoring the course of the disease and the response to treatment.

Applied research on γδ T-cells has so far focused predominantly on their use for novel immunotherapies against different types of cancers (56–58). Thirty years after the unexpected cloning of the TCRγ chain (59, 60) and 20 years after the first description of microbial "phosphoantigens" as specific activators of human Vγ9/Vδ2 T-cells (61, 62), the diagnostic potential of γδ T-cells is only beginning to unfold (34, 47, 63, 64).

ACKNOWLEDGMENTS

The work described has received support from the UK Clinical Research Network Study Portfolio, NISCHR/Wellcome Trust Institutional Strategic Support Fund, NIHR Invention for Innovation Programme, Baxter Healthcare Renal Discoveries Extramural Grant Programme, SARTRE/SEWAHSP Health Technology Challenge Scheme, MRC Confidence in Concept scheme, and EU-FP7 Initial Training Network "European Training & Research in Peritoneal Dialysis" (EuTRiPD).

REFERENCES

1. Fauci AS, Morens DM. The perpetual challenge of infectious diseases. *N Engl J Med* (2012) **366**(5):454–61. doi:10.1056/nejmra1108296
2. Hede K. Antibiotic resistance: an infectious arms race. *Nature* (2014) **509**(7498):S2–3. doi:10.1038/509S2a
3. Kumarasamy KK, Toleman MA, Walsh TR, Bagaria J, Butt F, Balakrishnan R, et al. Emergence of a new antibiotic resistance mechanism in India, Pakistan, and the UK: a molecular, biological, and epidemiological study. *Lancet Infect Dis* (2010) **10**(9):597–602. doi:10.1016/S1473-3099(10)70143-2
4. Davey MS, Tyrrell JM, Howe RA, Walsh TR, Moser B, Toleman MA, et al. A promising target for treatment of multidrug-resistant bacterial infections. *Antimicrob Agents Chemother* (2011) **55**(7):3635–6. doi:10.1128/aac.00382-11
5. Edelstein MV, Skleenova EN, Shevchenko OV, D'Souza JW, Tapalski DV, Azizov IS, et al. Spread of extensively resistant VIM-2-positive ST235 *Pseudomonas aeruginosa* in Belarus, Kazakhstan, and Russia: a longitudinal epidemiological and clinical study. *Lancet Infect Dis* (2013) **13**(10):867–76. doi:10.1016/S1473-3099(13)70168-3
6. Livermore DM. Has the era of untreatable infections arrived? *J Antimicrob Chemother* (2009) **64**(Suppl 1):i29–36. doi:10.1093/jac/dkp255
7. Arias CA, Murray BE. Antibiotic-resistant bugs in the 21st century – a clinical super-challenge. *N Engl J Med* (2009) **360**(5):439–43. doi:10.1056/nejmp0804651
8. Antimicrobial Resistance: Global Report on Surveillance 2014. *World Health Organisation.* (2014). Available from: http://www.who.int/drugresistance
9. Annual Epidemiological Report 2012 – Reporting on 2010 Surveillance Data and 2011 Epidemic Intelligence Data. *European Centre for Disease Prevention and Control.* Stockholm: ECDC (2013).
10. Antibiotic Resistance Threats in the United States, 2013. *Centers for Disease Control and Prevention.* (2013). Available from: http://www.cdc.gov/drugresistance/threat-report-2013
11. UK Five Year Antimicrobial Resistance Strategy2013 to 2018. *UK Department of Health.* (2013). Available from: https://www.gov.uk/government/publications/uk-5-year-antimicrobial-resistance-strategy-2013-to-2018
12. van de Sande-Bruinsma N, Grundmann H, Verloo D, Tiemersma E, Monen J, Goossens H, et al. Antimicrobial drug use and resistance in Europe. *Emerg Infect Dis* (2008) **14**(11):1722–30. doi:10.3201/eid1411.070467
13. Kanthor R. Diagnostics: detection drives defence. *Nature* (2014) **509**(7498):S14–5. doi:10.1038/509S14a
14. Koch R. Zur Untersuchung von pathogenen Organismen. *Mittheilungen aus dem Kaiserlichen Gesundheitsamte* (1881) **1**:1–48.
15. Shafazand S, Weinacker AB. Blood cultures in the critical care unit: improving utilization and yield. *Chest* (2002) **122**(5):1727–36. doi:10.1378/chest.122.5.1727
16. Richards D, Toop L, Chambers S, Fletcher L. Response to antibiotics of women with symptoms of urinary tract infection but negative dipstick urine test results: double blind randomised controlled trial. *BMJ* (2005) **331**(7509):143. doi:10.1136/bmj.38496.452581.8F
17. Fahim M, Hawley CM, McDonald SP, Brown FG, Rosman JB, Wiggins KJ, et al. Culture-negative peritonitis in peritoneal dialysis patients in Australia: predictors, treatment, and outcomes in 435 cases. *Am J Kidney Dis* (2010) **55**(4):690–7. doi:10.1053/j.ajkd.2009.11.015
18. Kessel AS, Sharland M. The new UK antimicrobial resistance strategy and action plan. *BMJ* (2013) **346**:f1601. doi:10.1136/bmj.f1601
19. Leggieri N, Rida A, François P, Schrenzel J. Molecular diagnosis of bloodstream infections: planning to (physically) reach the bedside. *Curr Opin Infect Dis* (2010) **23**(4):311–9. doi:10.1097/qco.0b013e32833bfc44
20. Gubala V, Harris LF, Ricco AJ, Tan MX, Williams DE. Point of care diagnostics: status and future. *Anal Chem* (2012) **84**(2):487–515. doi:10.1021/ac2030199
21. Bissonnette L, Bergeron MG. Infectious disease management through point-of-care personalized medicine molecular diagnostic technologies. *J Pers Med* (2012) **2**(2):50–70. doi:10.3390/jpm2020050
22. Caliendo AM, Gilbert DN, Ginocchio CC, Hanson KE, May L, Quinn TC, et al. Better tests, better care: improved diagnostics for infectious diseases. *Clin Infect Dis* (2013) **57**(Suppl 3):S139–70. doi:10.1093/cid/cit578
23. Fournier PE, Drancourt M, Colson P, Rolain JM, La Scola B, Raoult D. Modern clinical microbiology: new challenges and solutions. *Nat Rev Microbiol* (2013) **11**(8):574–85. doi:10.1038/nrmicro3068
24. Casadevall A, Pirofski LA. Host-pathogen interactions: basic concepts of microbial commensalism, colonization, infection, and disease. *Infect Immun* (2000) **68**(12):6511–8. doi:10.1128/IAI.68.12.6511-6518.2000
25. Trautner BW. Asymptomatic bacteriuria: when the treatment is worse than the disease. *Nat Rev Urol* (2011) **9**(2):85–93. doi:10.1038/nrurol.2011.192
26. Yu VL. Guidelines for hospital-acquired pneumonia and health-care-associated pneumonia: a vulnerability, a pitfall, and a fatal flaw. *Lancet Infect Dis* (2011) **11**(3):248–52. doi:10.1016/S1473-3099(11)70005-6
27. Tang BM, Eslick GD, Craig JC, McLean AS. Accuracy of procalcitonin for sepsis diagnosis in critically ill patients: systematic review and meta-analysis. *Lancet Infect Dis* (2007) **7**(3):210–7. doi:10.1016/S1473-3099(07)70052-X
28. Lam MF, Leung JC, Lam CW, Tse KC, Lo WK, Lui SL, et al. Procalcitonin fails to differentiate inflammatory status or predict long-term outcomes in peritoneal dialysis-associated peritonitis. *Perit Dial Int* (2008) **28**(4):377–84.
29. Pierrakos C, Vincent JL. Sepsis biomarkers: a review. *Crit Care* (2010) **14**(1):R15. doi:10.1186/cc8872
30. Kibe S, Adams K, Barlow G. Diagnostic and prognostic biomarkers of sepsis in critical care. *J Antimicrob Chemother* (2011) **66**(Suppl 2):ii33–40. doi:10.1093/jac/dkq523
31. Janeway CA Jr. Approaching the asymptote? Evolution and revolution in immunology. *Cold Spring Harb Symp Quant Biol* (1989) **54**(1):1–13. doi:10.1101/SQB.1989.054.01.003
32. Ramilo O, Allman W, Chung W, Mejias A, Ardura M, Glaser C. Gene expression patterns in blood leukocytes discriminate patients with acute infections. *Blood* (2007) **109**(5):2066–77. doi:10.1182/blood-2006-02-002477
33. Mejias A, Suarez NM, Ramilo O. Detecting specific infections in children through host responses: a paradigm shift. *Curr Opin Infect Dis* (2014) **27**(3):228–35. doi:10.1097/QCO.0000000000000065
34. Lin CY, Roberts GW, Kift-Morgan A, Donovan KL, Topley N, Eberl M. Pathogen-specific local immune fingerprints diagnose bacterial infection in peritoneal dialysis patients. *J Am Soc Nephrol* (2013) **24**(12):2002–9. doi:10.1681/asn.2013040332
35. Blander JM, Sander LE. Beyond pattern recognition: five immune checkpoints for scaling the microbial threat. *Nat Rev Immunol* (2012) **12**(3):215–25. doi:10.1038/nri3167
36. Stuart LM, Paquette N, Boyer L. Effector-triggered versus pattern-triggered immunity: how

animals sense pathogens. *Nat Rev Immunol* (2013) **13**(3):199–206. doi:10.1038/nri3398
37. Broz P, Monack DM. Newly described pattern recognition receptors team up against intracellular pathogens. *Nat Rev Immunol* (2013) **13**(8):551–65. doi:10.1038/nri3479
38. Sandstrom A, Peigné CM, Léger A, Crooks JE, Konczak F, Gesnel MC, et al. The intracellular B30.2 domain of butyrophilin 3A1 binds phosphoantigens to mediate activation of human Vγ9Vδ2 T cells. *Immunity* (2014) **40**(4):490–500. doi:10.1016/j.immuni.2014.03.003
39. Corbett AJ, Eckle SB, Birkinshaw RW, Liu L, Patel O, Mahony J, et al. T-cell activation by transitory neo-antigens derived from distinct microbial pathways. *Nature* (2014) **509**(7500):361–5. doi:10.1038/nature13160
40. Bonneville M, O'Brien RL, Born WK. γδ T cell effector functions: a blend of innate programming and acquired plasticity. *Nat Rev Immunol* (2010) **10**(7):467–78. doi:10.1038/nri2781
41. Vantourout P, Hayday A. Six-of-the-best: unique contributions of γδ T cells to immunology. *Nat Rev Immunol* (2013) **13**(2):88–100. doi:10.1038/nri3384
42. Altincicek B, Moll J, Campos N, Foerster G, Beck E, Hoeffler JF, et al. Human γδ T cells are activated by intermediates of the 2-*C*-methyl-D-erythritol 4-phosphate pathway of isoprenoid biosynthesis. *J Immunol* (2001) **166**(6):3655–8. doi:10.4049/jimmunol.166.6.3655
43. Morita CT, Jin C, Sarikonda G, Wang H. Nonpeptide antigens, presentation mechanisms, and immunological memory of human Vγ2Vδ2 T cells: discriminating friend from foe through the recognition of prenyl pyrophosphate antigens. *Immunol Rev* (2007) **215**(1):59–76. doi:10.1111/j.1600-065x.2006.00479.x
44. Eberl M, Moser B. Monocytes and γδ T cells: close encounters in microbial infection. *Trends Immunol* (2009) **30**(12):562–8. doi:10.1016/j.it.2009.09.001
45. Riganti C, Massaia M, Davey MS, Eberl M. Human γδ T-cell responses in infection and immunotherapy: common mechanisms, common mediators? *Eur J Immunol* (2012) **42**(7):1668–76. doi:10.1002/eji.201242492
46. Davey MS, Lin CY, Roberts GW, Heuston S, Brown AC, Chess JA, et al. Human neutrophil clearance of bacterial pathogens triggers anti-microbial γδ T cell responses in early infection. *PLoS Pathog* (2011) **7**(5):e1002040. doi:10.1371/journal.ppat.1002040
47. Bank I, Marcu-Malina V. Quantitative peripheral blood perturbations of γδ T cells in human disease and their clinical implications. *Clin Rev Allergy Immunol* (2014). doi:10.1007/s12016-013-8391-x
48. Begley M, Gahan CG, Kollas AK, Hintz M, Hill C, Jomaa H, et al. The interplay between classical and alternative isoprenoid biosynthesis controls γδ T cell bioactivity of *Listeria monocytogenes*. *FEBS Lett* (2004) **561**(1–3):99–104. doi:10.1016/S0014-5793(04)00131-0
49. Frencher J, Shen H, Yan L, Wilson JO, Freitag NE, Rizzo AN, et al. HMBPP-deficient *Listeria* mutant induces altered pulmonary/systemic responses, effector functions and memory polarization of Vγ2Vδ2 T cells. *J Leukoc Biol* (2014). doi:10.1189/jlb.6HI1213-632R
50. Puan KJ, Wang H, Dairi T, Kuzuyama T, Morita CT. *fldA* is an essential gene required in the 2-*C*-methyl-D-erythritol 4-phosphate pathway for isoprenoid biosynthesis. *FEBS Lett* (2005) **579**(17):3802–6. doi:10.1016/j.febslet.2005.05.047
51. Brown AC, Eberl M, Crick DC, Jomaa H, Parish T. The nonmevalonate pathway of isoprenoid biosynthesis in *Mycobacterium tuberculosis* is essential and transcriptionally regulated by Dxs. *J Bacteriol* (2010) **192**(9):2424–33. doi:10.1128/JB.01402-09
52. Workalemahu G, Wang H, Puan KJ, Nada MH, Kuzuyama T, Jones BD, et al. Metabolic engineering of *Salmonella* vaccine bacteria to boost human Vγ2Vδ2 T cell immunity. *J Immunol* (2014) **193**(2):708–21. doi:10.4049/jimmunol.1302746
53. Eberl M, Roberts GW, Meuter S, Williams JD, Topley N, Moser B. A rapid crosstalk of human γδ T cells and monocytes drives the acute inflammation in bacterial infections. *PLoS Pathog* (2009) **5**(2):e1000308. doi:10.1371/journal.ppat.1000308
54. Davey MS, Morgan MP, Liuzzi AR, Tyler CJ, Khan MWA, Szakmany T, et al. Microbe-specific unconventional T cells induce human neutrophil differentiation into antigen cross-presenting cells. *J Immunol* (2014) **193**:3704–16. doi:10.4049/jimmunol.1401018
55. Caccamo N, Dieli F, Wesch D, Jomaa H, Eberl M. Sex-specific phenotypical and functional differences in peripheral human Vγ9/Vδ2 T cells. *J Leukoc Biol* (2006) **79**(4):663–6. doi:10.1189/jlb.1105640
56. Gomes AQ, Martins DS, Silva-Santos B. Targeting γδ T lymphocytes for cancer immunotherapy: from novel mechanistic insight to clinical application. *Cancer Res* (2010) **70**(24):10024–7. doi:10.1158/0008-5472.can-10-3236
57. Moser B, Eberl M. γδ T-APCs: a novel tool for immunotherapy? *Cell Mol Life Sci* (2011) **68**(14):2443–52. doi:10.1007/s00018-011-0706-6
58. Fisher JP, Heuijerjans J, Yan M, Gustafsson K, Anderson J. γδ T cells for cancer immunotherapy: a systematic review of clinical trials. *Oncoimmunology* (2014) **3**(1):e27572. doi:10.4161/onci.27572
59. Saito H, Kranz DM, Takagaki Y, Hayday AC, Eisen HN, Tonegawa S. Complete primary structure of a heterodimeric T-cell receptor deduced from cDNA sequences. *Nature* (1984) **309**(5971):757–62. doi:10.1016/0092-8674(85)90140-0
60. Hayday AC, Saito H, Gillies SD, Kranz DM, Tanigawa G, Eisen HN, et al. Structure, organization, and somatic rearrangement of T cell gamma genes. *Cell* (1985) **40**(2):259–69. doi:10.1016/0092-8674(85)90140-0
61. Constant P, Davodeau F, Peyrat MA, Poquet Y, Puzo G, Bonneville M, et al. Stimulation of human γδ T cells by nonpeptidic mycobacterial ligands. *Science* (1994) **264**(5156):267–70. doi:10.1126/science.8146660
62. Tanaka Y, Morita CT, Tanaka Y, Nieves E, Brenner MB, Bloom BR. Natural and synthetic non-peptide antigens recognized by human γδ T cells. *Nature* (1995) **375**(6527):155–8. doi:10.1038/375155a0
63. Welton JL, Morgan MP, Martí S, Stone MD, Moser B, Sewell AK, et al. Monocytes and γδ T cells control the acute-phase response to intravenous zoledronate: insights from a phase IV safety trial. *J Bone Miner Res* (2013) **28**(3):464–71. doi:10.1002/jbmr.1797
64. Welton JL, Martí S, Mahdi MH, Boobier C, Barrett-Lee PJ, Eberl M. γδ T cells predict outcome in zoledronate-treated breast cancer patients. *Oncologist* (2013) **18**(8):e22–3. doi:10.1634/theoncologist.2013-0097

Conflict of Interest Statement: The authors declare that the research was conducted in the absence of any commercial or financial relationships that could be construed as a potential conflict of interest. The Specialty Chief Editor Bernhard Moser declares that, despite being affiliated to the same department as authors Matthias Eberl, Ida M. Friberg, Anna Rita Liuzzi, Matt P. Morgan and being affiliated to the same institution as Nicholas Topley, and despite having collaborated on publications in the last 2 years with Matthias Eberl, Anna Rita Liuzzi, Matt P. Morgan and Nicholas Topley, the review process was handled objectively.

Received: 19 July 2014; accepted: 26 October 2014; published online: 13 November 2014.
*Citation: Eberl M, Friberg IM, Liuzzi AR, Morgan MP and Topley N (2014) Pathogen-specific immune fingerprints during acute infection: the diagnostic potential of human γδ T-cells. Front. Immunol. **5**:572. doi: 10.3389/fimmu.2014.00572*
This article was submitted to T Cell Biology, a section of the journal Frontiers in Immunology.

Published August 27, 2014, doi:10.4049/jimmunol.1401018

Microbe-Specific Unconventional T Cells Induce Human Neutrophil Differentiation into Antigen Cross-Presenting Cells

Martin S. Davey,*[,1,2] Matt P. Morgan,*[,†,1] Anna Rita Liuzzi,* Christopher J. Tyler,* Mohd Wajid A. Khan,* Tamas Szakmany,*[,‡] Judith E. Hall,* Bernhard Moser,* and Matthias Eberl*

The early immune response to microbes is dominated by the recruitment of neutrophils whose primary function is to clear invading pathogens. However, there is emerging evidence that neutrophils play additional effector and regulatory roles. The present study demonstrates that human neutrophils assume Ag cross-presenting functions and suggests a plausible scenario for the local generation of APC-like neutrophils through the mobilization of unconventional T cells in response to microbial metabolites. Vγ9/Vδ2 T cells and mucosal-associated invariant T cells are abundant in blood, inflamed tissues, and mucosal barriers. In this study, both human cell types responded rapidly to neutrophils after phagocytosis of Gram-positive and Gram-negative bacteria producing the corresponding ligands, and in turn mediated the differentiation of neutrophils into APCs for both $CD4^+$ and $CD8^+$ T cells through secretion of GM-CSF, IFN-γ, and TNF-α. In patients with acute sepsis, circulating neutrophils displayed a similar APC-like phenotype and readily processed soluble proteins for cross-presentation of antigenic peptides to $CD8^+$ T cells, at a time when peripheral Vγ9/Vδ2 T cells were highly activated. Our findings indicate that unconventional T cells represent key controllers of neutrophil-driven innate and adaptive responses to a broad range of pathogens. ***The Journal of Immunology*****, 2014, 193: 000–000.**

Neutrophils are the first cells that are recruited to sites of microbial infection. Although classically viewed as terminally differentiated cells, there is emerging evidence that neutrophils represent key components of the effector and regulatory arms of the innate and adaptive immune system (1–3). As such, neutrophils regulate the recruitment and function of various cell types and interact with immune and nonimmune cells. Intriguingly, neutrophils directly affect Ag-specific responses by facilitating monocyte differentiation and dendritic cell maturation, and by interacting with T cells and B cells (4–10). Murine neutrophils have been shown to present Ags to both $CD4^+$ and $CD8^+$ T cells (11–13), and to differentiate into neutrophil–dendritic cell hybrids in vitro and in vivo (14, 15). In humans, neutrophils with a phenotype consistent with a possible APC function, including expression of MHC class II, have been found in diverse inflammatory and infectious conditions (16–22). This notwithstanding, direct Ag presentation by neutrophils has to date not been demonstrated in patients, especially with respect to an induction of Ag-specific $CD8^+$ T cell responses upon cross-presentation of exogenous proteins.

The physiological context underlying the differentiation of neutrophils into APCs and the implications for Ag-specific immune responses remain unclear. Unconventional T cells such as human γδ T cells, NKT cells, and mucosal-associated invariant T (MAIT) cells represent unique sentinel cells with a distinctive responsiveness to low m.w. compounds akin to pathogen and danger-associated molecular patterns (23–25). Such unconventional T cells represent a substantial proportion of all T cells in blood and mucosal epithelia, accumulate in inflamed tissues, and constitute an efficient immune surveillance network in inflammatory and infectious diseases as well as in tumorigenesis. Besides orchestrating local responses by engaging with other components of the inflammatory infiltrate (26–29), unconventional T cells are also ideally positioned in lymphoid tissues to interact with freshly recruited monocytes and neutrophils (30–32). We previously showed that human γδ T cells enhance the short-term survival of neutrophils but did not characterize these surviving neutrophils on a phenotypical and functional level (28). In this work, we studied the outcome of such a crosstalk of human neutrophils with both γδ T cells and MAIT cells in vitro and translated our findings to patients with severe sepsis. We demonstrate that neutrophils with APC-like features can be found in blood during acute infection,

*Cardiff Institute of Infection and Immunity, School of Medicine, Cardiff University, Cardiff CF14 4XN, United Kingdom; †Cardiff and Vale University Health Board, Cardiff CF14 4XW, United Kingdom; and ‡Cwm Taf University Health Board, Llantrisant CF72 8XR, United Kingdom

[1]M.S.D. and M.P.M. contributed equally to this study.

[2]Current address: Birmingham Cancer Research UK Centre, School of Cancer Sciences, University of Birmingham, Birmingham, U.K.

Received for publication April 21, 2014. Accepted for publication July 28, 2014.

This work was supported by the United Kingdom Clinical Research Network Study Portfolio, the National Institute for Social Care and Health Research (NISCHR), the NISCHR/Wellcome Trust Institutional Strategic Support Fund, the Severnside Alliance for Translational Research/South East Wales Academic Health Science Partnership Health Technology Challenge Scheme, the European Union-Framework Programme 7 Marie Curie Initial Training Network "European Training and Research in Peritoneal Dialysis," a Medical Research Council Ph.D. studentship (to C.J.T.), and Cancer Research UK.

Address correspondence and reprint requests to Dr. Matthias Eberl, Cardiff Institute of Infection and Immunity, Henry Wellcome Building, School of Medicine, Cardiff University, Heath Park, Cardiff CF14 4XN, U.K. E-mail address: eberlm@cf.ac.uk

The online version of this article contains supplemental material.

Abbreviations used in this article: DMRL, 6,7-dimethyl-8-D-ribityllumazine; HMB-PP, (*E*)-4-hydroxy-3-methyl-but-2-enyl pyrophosphate; MAIT, mucosal-associated invariant T; MR1, MHC-related protein 1; PPD, *Mycobacterium tuberculosis* purified protein derivate; SIRS, systemic inflammatory response syndrome; sTNFR, soluble TNFR; TSST-1, *Staphylococcus aureus* toxic shock syndrome toxin-1.

and that the phenotype and ex vivo function of circulating sepsis neutrophils was replicated in vitro upon priming of neutrophils by human γδ T cells and MAIT cells. Our findings thus provide a possible physiological context and propose a cellular mechanism for the local generation of neutrophils with APC functions, including their potential to cross-present soluble Ags to $CD8^+$ T cells, in response to a broad range of microbial pathogens.

Materials and Methods

Subjects

This study was approved by the South East Wales Local Ethics Committee under reference numbers 08/WSE04/17 and 10/WSE04/21 and conducted according to the principles expressed in the Declaration of Helsinki and under local ethical guidelines. Sampling of adult patients with sterile systemic inflammatory response syndrome (SIRS) or with acute sepsis (defined as patients with SIRS in conjunction with a proven or suspected infection) was carried out within the United Kingdom Clinical Research Network under study portfolio UKCRN ID 11231, "Cellular and Biochemical Investigations in Sepsis." All study participants provided written informed consent for the collection of samples and their subsequent analysis. A waiver of consent system was used when patients were unable to provide prospective informed consent due to the nature of their critical illness or therapeutic sedation at the time of recruitment. In all cases, retrospective informed consent was sought as soon as the patient recovered and regained capacity. In cases in which a patient died before regaining capacity, the initial consultee's approval would stand.

Sepsis patients had a proven infection as confirmed by positive culture of at least one relevant sample according to the local microbiology laboratory overseen by Public Health Wales, and developed at least three of the four following SIRS criteria over the previous 36 h: 1) temperature from any site >38˚C or core <36˚C; 2) heart rate of >90 beats/min (unless individual had a medical condition or was receiving treatment preventing tachycardia); 3) respiratory rate of >20 breaths/min, arterial $PaCO_2$ <32 mmHg, or mechanical ventilation for an acute process; and 4) total WBC >12,000 cells/mm^3 or <4,000 cells/mm^3 or differential WBC count showing >10% immature (band) forms (n = 37; age range 35–82 y, median 63 y; 51% female). Patients with sterile SIRS developed at least three of the four SIRS criteria but had no suspected or proven microbial infection (n = 14; age range 26–70 y, median 48 y; 21% female). All patients with sepsis or SIRS had at least one documented organ failure on recruitment to the study and were either mechanically ventilated, on inotropic support, or received acute renal replacement therapy. Healthy donors served as controls for the patient cohorts (n = 10; age range 31–68 y, median 59 y; 20% female). Individuals were excluded from the study if pregnant or breastfeeding; suffering from documented severe immune deficiency or severe liver failure; admitted postcardiac arrest; treated with high-dose steroids or immunosuppressant drugs for the last 6 mo; or unlikely to survive for the duration of the study period regardless of treatment.

Media, reagent, and Abs

Culture medium was RPMI 1640 medium supplemented with 2 mM L-glutamine, 1% sodium pyruvate, 50 μg/ml penicillin/streptomycin, and 10% FCS (Invitrogen). Synthetic (*E*)-4-hydroxy-3-methyl-but-2-enyl pyrophosphate (HMB-PP) was provided by H. Jomaa (Justus-Liebig University Giessen); synthetic 6,7-dimethyl-8-D-ribityllumazine (DMRL) was provided by B. Illarionov (Hamburg School of Food Science). *Staphylococcus aureus* toxic shock syndrome toxin-1 (TSST-1) was purchased from Toxin Technology; *Mycobacterium tuberculosis* purified protein derivate (PPD) was purchased from Statens Serum Institut (Copenhagen, Denmark). *Salmonella abortus equi* LPS, brefeldin A, and BSA-FITC were purchased from Sigma-Aldrich. Recombinant IFN-γ, TNF-α, and GM-CSF was purchased from Miltenyi Biotec. Human T-activator CD3/CD28 Dynabeads, CFSE, and 10-kDa dextran-FITC were purchased from Life Technologies.

The following mAbs were used for surface labeling: anti-CD3 (UCHT1, SK7, HIT3a), anti-CD4 (SK3, RPA-T4), anti-CD8 (SK1, HIT8a, RPA-T8), anti-CD11c (S-HCL-3), anti-CD14 (M5E2, MOP9), anti-CD15 (HI98), anti-CD16 (3G8), anti-CD25 (M-A251), anti-CD27 (M-T271), anti-CD31 (WM-59), anti-CD32 (FLI8.26), anti-CD45RO (UCHL1), anti-CD49d (9F10), anti-CD50 (TU41), anti-CD54 (HA58), anti-CD56 (B159), anti-CD62L (DREG-56), anti-CD64 (10.1), anti-CD69 (FN50), anti-CD70 (Ki24), anti-CD71 (M-A712), anti-CD72 (J4-112), anti-CD83 (HB15e), anti-CD86 (2331), anti-CD209 (DCN46), anti–HLA-DR (L243), anti–TCR-Vδ2 (B6.1), anti-CCR4 (1G1), anti-CCR5 (2D7), anti-CCR7 (3D12), and anti-CXCR3 (1C6) from BD Biosciences; anti–TCR-Vβ2 (MPB2D5), anti–TCR-Vγ9 (Immu360), and anti-CD40 (mAB89) from Beckman Coulter; anti-CD11a (HI111), anti-CD66b (G10F5), anti-CD154 (24-31), anti-CD161 (HP-3G10), anti–HLA-ABC (w6/32), and anti–TCR-Vα7.2 (3C10) from BioLegend; anti-CD11b (ICRF44), anti-CD14 (61D3), anti-CD19 (SJ25C1), anti-CD25 (BC96), anti-CD45RA (HI100), and anti-CD80 (2D10.4) from eBioscience; anti–HLA-A2 (BB7.2) from Serotec; and anti-CCR9 (248601) and anti-CCR10 (314305) from R&D Systems; together with appropriate isotype controls. Intracellular cytokines were detected using anti–IFN-γ (B27, BD Biosciences; 4S.B3, eBioscience) and anti–TNF-α (6401.1111, BD Biosciences; 188, Beckman Coulter). Blocking reagents used included anti-Vα7.2 (3C10; BioLegend); anti–TCR-Vγ9 (Immu360; Beckman Coulter); anti-TLR4 (HTA125; eBioscience); anti-CD277 (103.2; D. Olive, Université de la Méditerranée, Marseille, France); anti–MHC-related protein 1 (MR1) (26.5; T. Hansen, Washington University School of Medicine, St. Louis, MO); anti–IFN-γ (25718) and anti–GM-CSF (3209) (BioLegend); and soluble TNFR (sTNFR) p75-IgG1 fusion protein (etanercept/Enbrel; Amgen).

Cells

Total leukocytes from healthy donors and patients were isolated from heparinized blood by mixing with HetaSep (StemCell Technologies), followed by sedimentation of RBCs (Supplemental Fig. 1A). Neutrophils were purified from whole blood or Lymphoprep (Axis-Shield) separated granulocytes by HetaSep sedimentation, followed by negative selection using the EasySep neutrophil enrichment kit (StemCell Technologies) (33), resulting in purities of >99.2% $CD14^-CD66b^+CD15^+$ and <0.1% contaminating monocytes (Supplemental Fig. 1B). Total $CD3^+$ T cells (>98%) were isolated from PBMC using the pan T cell isolation kit II (Miltenyi Biotec); $CD4^+$ and $CD8^+$ T cells (>98%) were obtained using the corresponding EasySep kits (StemCell Technologies). $Vγ9^+$ T cells (>98%) were purified using anti–Vγ9-PE-Cy5 (Immu360; Beckman Coulter) and anti-PE microbeads (Miltenyi Biotec); $Vα7.2^+$ T cells (>98%) were purified using anti–Vα7.2-PE (3C10; BioLegend) and anti-PE microbeads. Alternatively, $Vγ9^+$ $CD3^+$ γδ T cells or $Vα7.2^+$ $CD161^+$ $CD3^+$ MAIT cells were sorted to purities >99% using a FACSAria II (BD Biosciences).

Bacteria

Clinical isolates of *Enterobacter cloacae*, *Enterococcus faecalis*, *Klebsiella pneumoniae*, and *S. aureus* (28) were grown in liquid Luria-Bertani broth and on solid Columbia blood agar (Oxoid). The distribution of the nonmevalonate and riboflavin pathways across microbial species was determined based on the absence or presence of the enzymes HMB-PP synthase (EC 1.17.7.1) and DMRL synthase (EC 2.5.1.78) in the corresponding genomes, according to the Kyoto Encyclopedia of Genes and Genomes (http://www.genome.jp/kegg).

T cell culture

PBMC were stimulated with 0.1–100 nM HMB-PP or 0.1–100 μM DMRL. $Vγ9^+$ T cells or $Vα7.2^+$ T cells were cocultured with autologous monocytes at a ratio of 1:1, in the presence of 25% (v/v) cell-free supernatants from neutrophils that had phagocytosed live bacteria, as described previously (28). For blocking experiments, anti–TCR-Vα7.2, anti–TCR-Vγ9, anti-CD277, and anti-MR1 were used at 1–20 μg/ml.

Neutrophil culture

Freshly isolated neutrophils were cultured for up to 48 h in the absence or presence of autologous Vγ9/Vδ2 T cells or MAIT cells at a ratio of 10:1, and 10 nM HMB-PP or anti-CD3/CD28 dynabeads (1 bead per T cell). Alternatively, neutrophils were cultured with 25–50% (v/v) conditioned medium obtained from purified Vγ9/Vδ2 T cells or MAIT cells stimulated for 24 h with anti-CD3/CD28 dynabeads (1 bead per cell) or 100 nM HMB-PP. Other stimuli included 100 ng/ml LPS and 100 U/ml recombinant IFN-γ, TNF-α, and/or GM-CSF. sTNFR p75-IgG1 fusion protein, anti–IFN-γ, and anti–GM-CSF were used at 10 μg/ml. Neutrophil survival and activation were assessed by flow cytometry, after gating on $CD15^+$ cells and exclusion of $Vγ9^+$ or $Vα7.2^+$ cells where appropriate. For morphological analyses, neutrophils were centrifuged onto cytospin slides, stained with May-Grünwald-Giemsa solution, and analyzed by light microscopy.

Functional assays

Endocytosis and APC functions were assessed as before (34–38). Freshly purified neutrophils and neutrophils cultured for 24 h in the presence or absence of unconventional T cell–conditioned medium were incubated with 500 μg/ml 10-kDa dextran-FITC or BSA-FITC for up to 60 min at 4˚C or 37˚C. Endocytic uptake was measured immediately by flow cytom-

etry; the specific uptake of each reagent was calculated by subtracting the background MFI at 4°C from the MFI obtained at 37°C.

For MHC class II–restricted presentation of Ags, activated neutrophils were generated by 48-h culture with a combination of IFN-γ, GM-CSF, and/or TNF-α, or with unconventional T cell–conditioned medium. Neutrophils were pulsed with 10 ng/ml TSST-1 for 1 h. After extensive washing, neutrophils were mixed with autologous $CD4^+$ T cells at a ratio of 1:1; 1 h later 10 μg/ml brefeldin A was added and cultures were incubated for an additional 4 h. Activation of TSST-1–responsive $V\beta2^+$ $CD4^+$ T cells was assessed by intracellular cytokine staining and analysis by flow cytometry (35). To assess $CD4^+$ and $CD8^+$ T cell responses to complex Ag preparations, neutrophils were pulsed with 1–10 μg/ml PPD for the last 18 h of the 48-h culture phase. After extensive washing, neutrophils were mixed with CFSE-labeled autologous $CD3^+$ T cells at a ratio of 1:1 and incubated for 7 d. CFSE dilution in the $CD4^+$ and $CD8^+$ T cell populations was assessed by flow cytometry, after exclusion of $CD66b^+$ cells.

For MHC class I–restricted Ag presentation, Ag-specific HLA-A2–restricted $CD8^+$ T cell lines were generated using the immunodominant peptide of influenza matrix protein, M1(p58–66) (GILGFVFTL), as described before (37, 38). M1(p58–66)-specific responder $CD8^+$ T cells used in APC assays were >95% pure, as confirmed by tetramer staining (data not shown). Activated neutrophils from HLA-$A2^+$ donors were generated as above, using unconventional T cell–conditioned medium or recombinant cytokines, and pulsed for 1 h with 0.1 μM peptide. For cross-presentation assays, 0.01–1 μM recombinant influenza M1 protein was added during the last 18 h of the 48-h neutrophil culture period. Fresh neutrophils from HLA-$A2^+$ sepsis patients were incubated with 0.01–1 μM recombinant influenza M1 protein for 18 h or cultured in medium for 17 h prior to addition of 0.1 μM M1(p58–66) peptide for an additional 1 h. In each case, following extensive washing, neutrophils were incubated with HLA-$A2^+$ peptide-specific $CD8^+$ T cells at a ratio of 1:1; after 1 h, 10 μg/ml brefeldin was added and cultures were incubated for an additional 4 h. Activation of $CD8^+$ T cells was assessed by intracellular cytokine staining and analyzed by flow cytometry, after exclusion of $CD66b^+$ cells.

Flow cytometry

Cells were acquired on an eight-color FACSCanto II (BD Biosciences) and analyzed with FlowJo (Tree Star). Single cells of interest were gated based on their appearance in side and forward scatter area/height, exclusion of live/dead staining (fixable Aqua; Invitrogen), and surface staining. Apoptotic cells were identified using annexin-V (BD Biosciences).

ELISA

Cell culture supernatants were analyzed on a Dynex MRX II reader, using ELISA kits for IL-17A (R&D Systems) as well as IFN-γ and TNF-α (eBioscience). Cell-free plasma samples and unconventional T cell–conditioned media were analyzed on a SECTOR Imager 6000 using the ultrasensitive human proinflammatory 9-plex kit (Meso Scale Discovery).

Statistics

Data were analyzed using two-tailed Student *t* tests for normally distributed data and Mann–Whitney tests for nonparametric data (GraphPad Prism). Differences between groups were analyzed using one-way ANOVA with Bonferroni's posttests or with Kruskal–Wallis and Dunn's posttests; two-way ANOVA was used when comparing groups with independent variables.

Results

Unconventional human T cells respond to neutrophil-released microbial metabolites

$V\gamma9/V\delta2^+$ γδ T cells recognize the isoprenoid precursor HMB-PP, which is produced via the nonmevalonate pathway by a broad range of Gram-negative and Gram-positive bacteria (27, 39). $V\alpha7.2^+$ $CD161^+$ MAIT cells show a very similar responsiveness to an overlapping, but distinct spectrum of microorganisms by sensing intermediates of the microbial vitamin B2 biosynthesis (Table I) (40–43). We therefore sought to investigate the antimicrobial responses of these two types of unconventional T cells side by side. In this study, Vγ9/Vδ2 T cells, but not MAIT cells, responded to HMB-PP, as judged by induction of CD69 expression (Fig. 1A). In contrast, the riboflavin precursor DMRL induced a dose-dependent activation of MAIT cells, but not Vγ9/Vδ2 T cells. Blocking experiments confirmed a requirement for butyrophilin 3A/CD277 for Vγ9/Vδ2 T cells and the MHC-related protein MR1 for MAIT cells (Fig. 1B), in support of current models of Ag recognition (41–45).

We previously identified a crucial role for neutrophils in facilitating access to HMB-PP by Vγ9/Vδ2 T cells (28). As control, purified $V\gamma9^+$ T cells readily responded to neutrophils after phagocytosis of clinically relevant bacteria, in accordance with the distribution of the nonmevalonate pathways across the different pathogens (Table I). Strikingly, purified $V\alpha7.2^+$ T cells showed very similar responses depending on the utilization of the riboflavin biosynthesis pathway by the phagocytosed species. Activated $V\gamma9^+$ T cells and $V\alpha7.2^+$ T cells upregulated CD69 (Fig. 1C) and secreted IFN-γ (Fig. 1D), but not IL-17A (data not shown). The response of $V\alpha7.2^+$ T cells to microbial compounds was confined to the $CD161^+$ bona fide MAIT cell population (Fig. 1C, 1D). Both Vγ9/Vδ2 T cells and MAIT cells failed to respond to neutrophil-released microbial compounds in the presence of anti-CD277 and anti-MR1, respectively (Fig. 1D), and in the absence of autologous monocytes (Fig. 1E), highlighting a requirement for presentation by accessory cells. These findings reveal a remarkable similarity in the responsiveness of Vγ9/Vδ2 T cells and MAIT cells to microbial metabolites.

Patients with acute sepsis caused by HMB-PP–producing pathogens display elevated levels of activated γδ T cells

To resolve the existence of APC-like neutrophils in human infectious disease and determine a possible link with antimicrobial unconventional T cell responses, we recruited adult patients with newly diagnosed severe sepsis and characterized their circulating leukocytes phenotypically and functionally. As proof of principle for the involvement of unconventional T cells in early inflammatory responses, patients with acute sepsis revealed a substantial activation of Vγ9/Vδ2 T cells, as judged by CD69 expression, but not SIRS patients who served as noninfected controls (Fig. 1F, Supplemental Fig. 1A). Of note, we found a significant increase in the absolute counts and the proportion of Vγ9/Vδ2 T cells among all circulating T cells between patients with microbiologically confirmed infections caused by HMB-PP–producing as opposed to HMB-PP–deficient species (Fig. 1F). These clinical findings evoke earlier studies in patients with acute peritonitis (28) and further support the notion of a differential responsiveness of unconventional T cells to defined pathogen groups that can be detected both locally at the site of infection (46) and systemically in blood (Fig. 1F).

Unconventional human T cells induce prolonged neutrophil survival and activation

We recently showed that Vγ9/Vδ2 T cells trigger short-term (<20 h) survival of autologous neutrophils (28). In this study, highly purified neutrophils cocultured for extended periods with activated Vγ9/Vδ2 T cells or MAIT cells displayed a prolonged survival, as judged by exclusion of amine reactive dyes and retention of surface CD16 (FcγRIII) for at least 48 h (Fig. 2A). A similar effect was observed when incubating purified neutrophils with Vγ9/Vδ2 T cell or MAIT cell–conditioned culture supernatants, indicating a significant contribution of soluble factors in mediating the observed effects (Fig. 2B). In contrast to the highly active metabolite HMB-PP as specific activator of Vγ9/Vδ2 T cells, the MAIT cell activator used in the current study, DMRL, only possesses a relatively modest bioactivity. The true MAIT cell activator is far more potent than DMRL and active at subnanomolar concentrations, but not commercially available and difficult to synthesize chemically (41, 43). Most stimulation experiments with purified MAIT cells were therefore conducted with anti-CD3/CD28–coated beads. Importantly, use of either anti-CD3/CD28 beads or HMB-PP to

Table I. Distribution across clinically relevant microbial pathogens of key biosynthetic pathways that produce metabolites targeted by human unconventional T cells

	Nonmevalonate Pathway (Vγ9/Vδ2 T Cell Activation)	Vitamin B2 Synthesis (MAIT Cell Activation)
Gram-negative bacteria		
Acinetobacter baumannii	+	+
Chryseobacterium gleum	−	+
Enterobacter cloacae	+	+
Escherichia coli	+	+
Haemophilus influenzae	+	+
Helicobacter pylori	+	+
Klebsiella pneumoniae	+	+
Legionella pneumophila	−	+
Neisseria meningitidis	+	+
Pseudomonas aeruginosa	+	+
Shigella dysenteriae	+	+
Gram-positive bacteria		
Bacillus anthracis	+	+
Clostridium difficile	+	+
Corynebacterium diphtheriae	+	+
Enterococcus faecalis	−	−
Listeria monocytogenes	+	−
Mycobacterium tuberculosis	+	+
Propionibacterium acnes	+	+
Staphylococcus aureus	−	+
Streptococcus pyogenes	−	−
Other bacteria		
Borrelia burgdorferi	−	−
Leptospira interrogans	+	+
Mycoplasma genitalium	−	−
Mycoplasma penetrans	+	−
Treponema pallidum	−	−
Yeasts, fungi		
Aspergillus fumigatus	−	+
Candida albicans	−	+
Crytococcus neoformans	−	+
Saccharomyces cerevisiae	−	+

activate Vγ9/Vδ2 T cells elicited identical neutrophil responses (Fig. 2A–C and data not shown). Surviving neutrophils possessed a highly activated morphology, as judged by the presence of hypersegmented nuclei (Fig. 2C). The antiapoptotic effect of unconventional T cells was confirmed by the preservation of the total number of neutrophils present after 48 h of culture and the lack of annexin-V binding (Fig. 2D). As confirmation of their activated status, surviving neutrophils showed pronounced upregulation of CD11b and CD66b expression and complete loss of CD62L (Fig. 2E).

Unconventional T cell–primed neutrophils have a unique APC-like phenotype

Circulating neutrophils in healthy people do not express CD40, CD64 (FcγRI), CD83, or HLA-DR, yet all these surface markers were found on unconventional T cell–primed neutrophils (Fig. 2F). Moreover, these neutrophils also showed a marked upregulation of CD54 (ICAM-1) and HLA-ABC (Fig. 2F), suggestive of a possible function of unconventional T cell–primed neutrophils as APCs for both $CD4^+$ and $CD8^+$ T cells.

The chemokine receptors CCR7, CCR9, and CCR10 remained undetectable under those culture conditions (data not shown), arguing against trafficking of APC-like neutrophils to noninflamed lymph nodes, the intestine, or the skin. In contrast, APC-like neutrophils displayed enhanced expression levels of CXCR3 and CCR4 (data not shown), indicative of an increased responsiveness to inflammatory chemokines and supporting a local role during acute inflammation.

Neutrophils stimulated with defined microbial compounds on their own, in the absence of Vγ9/Vδ2 T cells or MAIT cells, failed to acquire a similar phenotype. Most notably, neutrophils cultured for 48 h in the presence of LPS did not show increased levels of HLA-ABC, HLA-DR, CD40, CD64, or CD83 compared with neutrophils cultured in medium alone (data not shown), emphasizing the crucial and nonredundant contribution of unconventional T cells and their specific ligands to the acquisition of APC characteristics by neutrophils.

Circulating neutrophils in sepsis patients display an APC-like phenotype

To resolve the existence of APC-like neutrophils in human infectious disease, we characterized circulating leukocytes in sepsis patients as a means to access neutrophils that had recently been activated in different infected tissues. Sepsis neutrophils displayed a strikingly altered phenotype compared with neutrophils from healthy individuals and SIRS patients and were characterized by markedly higher expression of CD40, CD64, and CD86 (Fig. 3A). We also found increased surface levels of CD83 and HLA-DR on circulating neutrophils in some patients with sepsis, although this was not significant across the cohort as a whole. Of note, there was a correlation between the expression of CD64 and HLA-DR on sepsis neutrophils, supporting a link between neutrophil activation and APC phenotype (Fig. 3B). These findings indicate the presence of APC-like neutrophils in sepsis patients, despite the generally presumed immune suppression in those individuals, as judged by reduced HLA-DR expression levels on monocytes (data not shown) (47).

Neutrophil survival and APC marker expression are mediated via unconventional T cell–secreted cytokines

To identify the unconventional T cell–derived factor(s) exerting the observed effects on neutrophils, we quantified proinflammatory

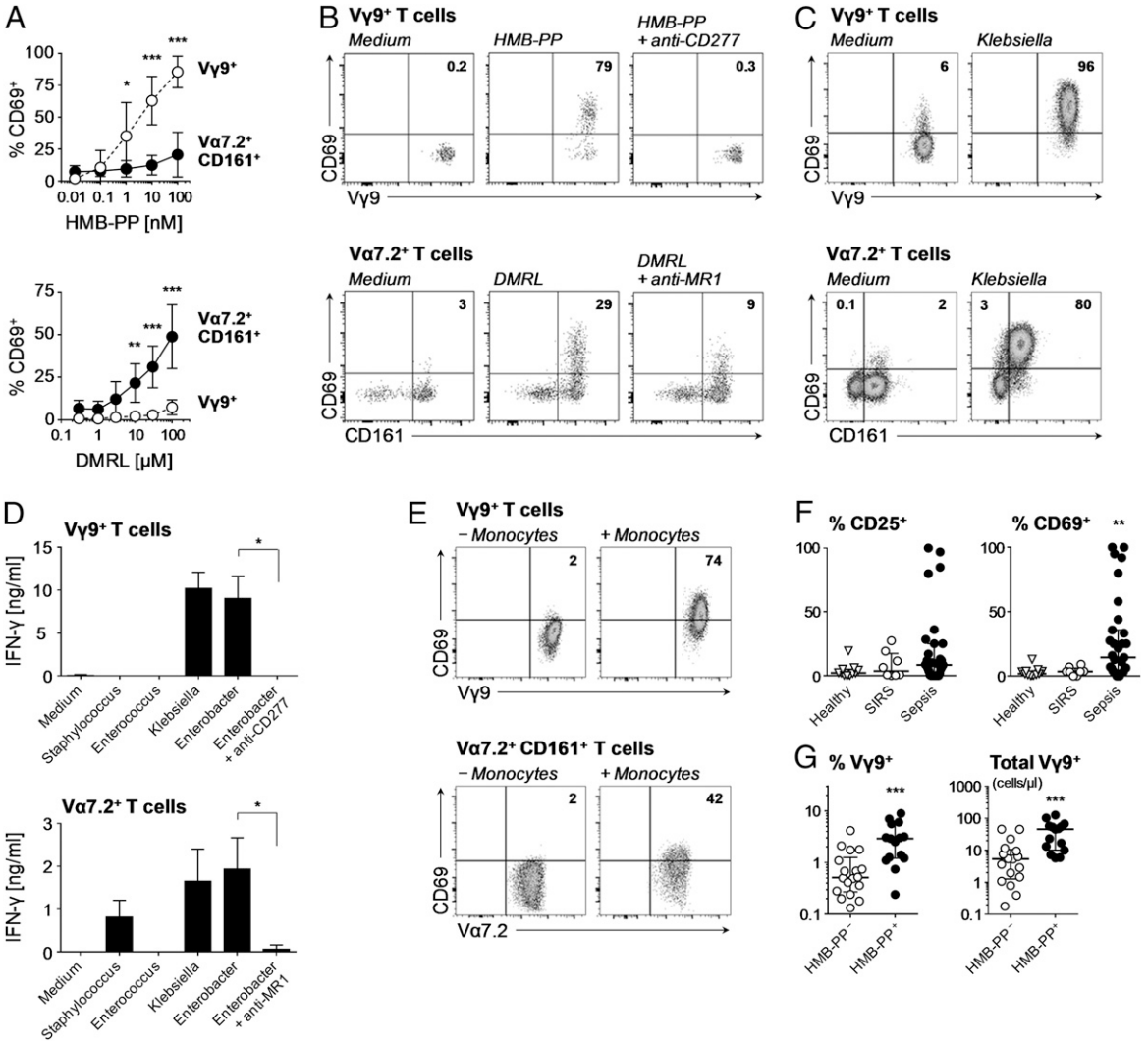

FIGURE 1. Unconventional human T cell responses to microbial metabolites in vitro and in vivo. (**A**) CD69 surface expression by Vγ9$^+$ T cells and Vα7.2$^+$ CD161$^+$ T cells in PBMC stimulated overnight with HMB-PP or DMRL (means ± SD, $n = 5$). Data were analyzed by two-way ANOVA with Bonferroni's post hoc tests. (**B**) Representative FACS plots of two donors showing CD69 expression by Vγ9$^+$ T cells and Vα7.2$^+$ T cells in PBMC stimulated overnight with 100 nM HMB-PP or 100 μM DMRL, in the absence or presence of anti-CD277 or anti-MR1 mAb. (**C**) CD69 expression by MACS-purified Vγ9$^+$ T cells or Vα7.2$^+$ T cells cocultured overnight with autologous monocytes in the presence of supernatants from neutrophils after phagocytosis of *Klebsiella pneumoniae* (representative of three donors). (**D**) IFN-γ secretion by MACS-purified Vγ9$^+$ T cells or Vα7.2$^+$ T cells cocultured overnight with autologous monocytes in the presence of supernatants from neutrophils after phagocytosis of different bacteria: HMB-PP$^-$ DMRL$^+$, *Staphylococcus aureus*; HMB-PP$^-$ DMRL$^-$, *Enterococcus faecalis*; and HMB-PP$^+$ DMRL$^+$, *Enterobacter cloacae* and *K. pneumoniae* (means ± SD, $n = 3$–4 donors). Differences between mAb-treated and untreated cultures were analyzed using Mann–Whitney tests. (**E**) CD69 expression by FACS-sorted Vγ9$^+$ T cells or Vα7.2$^+$ CD161$^+$ T cells cocultured overnight with or without autologous monocytes in the presence of supernatants from neutrophils after phagocytosis of *E. cloacae* (representative of two donors). (**F**) Surface expression by CD25 and CD69 on circulating Vγ9$^+$ T cells in healthy controls and in patients with SIRS or sepsis. Each data point represents an individual; lines and error bars depict medians and interquartile ranges. Data were analyzed using Kruskal–Wallis tests and Dunn's multiple comparison tests; comparisons were made with sepsis patients. (**G**) Proportion of Vγ9$^+$ T cells among all circulating T cells and absolute counts of circulating Vγ9$^+$ T cells (in cells/μl blood) in sepsis patients with microbiologically confirmed infections caused by HMB-PP–producing (*E. coli*, *Enterobacter aerogenes*, *Haemophilus influenzae*, *K. pneumoniae*, *Pseudomonas aeruginosa*, *Stenotrophomonas maltophilia*, anaerobic Gram-negative bacilli, diphtheroid bacteria) or HMB-PP–deficient organisms (*Aspergillus fumigatus*, *Candida spp.*, *Staphylococcus spp.*, *Streptococcus pneumoniae*). Data were analyzed using Mann–Whitney tests. Differences were considered significant as indicated: $*p < 0.05$, $**p < 0.01$, $***p < 0.001$.

mediators in the culture supernatants. These experiments revealed a dominant production (>1000 pg/ml on average) of GM-CSF, IFN-γ, and TNF-α by activated Vγ9/Vδ2 T cells and MAIT cells, but only very low levels (<25 pg/ml) of IL-1β, IL-6, and CXCL8, indicating that both unconventional T cell populations share a similar cytokine profile (Fig. 4A). Experiments using blocking reagents identified an involvement of GM-CSF, IFN-γ, and TNF-α in promoting neutrophil survival by both Vγ9/Vδ2 T cells and MAIT cells (Fig. 4B). Whereas neutralization of each individual cytokine on its own had a partial effect, combined blocking of GM-CSF and IFN-γ was most effective in inhibiting neutrophil survival, with blocking of TNF-α having little additive effect. In contrast, CD66b upregulation was mainly triggered by TNF-α (Fig. 4B). Of note, the effect of unconventional T cells on neutrophils could be mimicked in part by using recombinant GM-CSF, IFN-γ, and TNF-α. In this respect, only neutrophils cultured with a combination of all three cytokines exhibited a morphology characterized by hypersegmented nuclei (Fig. 4C). TNF-α was particularly important for the induction of CD40, CD54, CD66b, and MHC class I expression (Fig. 4D). Taken together,

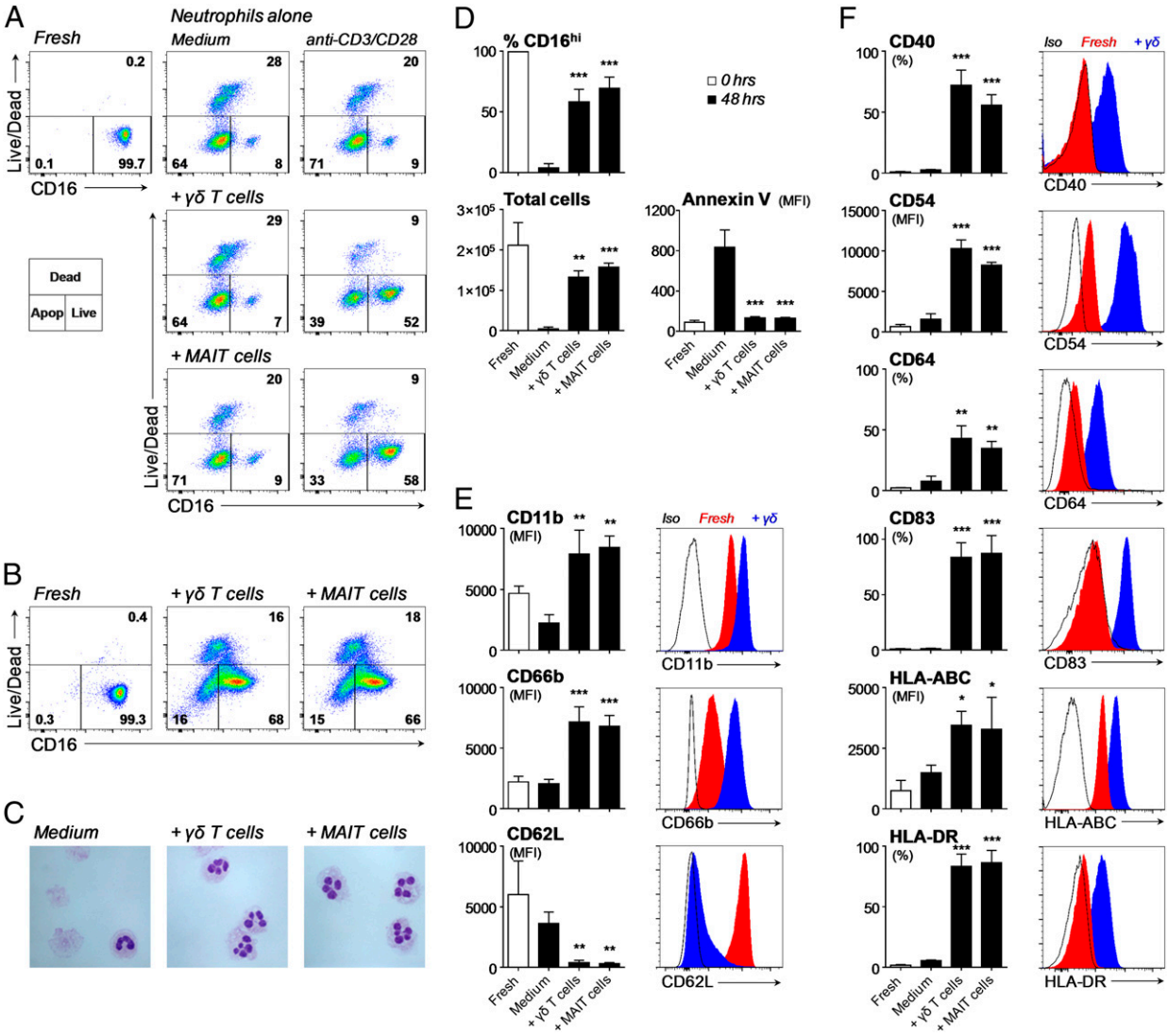

FIGURE 2. Survival, activation, and expression of APC markers by unconventional T cell–primed neutrophils. (**A**) Neutrophil survival judged by retention of CD16 expression and exclusion of live/dead staining after 48-h coculture with FACS-sorted Vγ9/Vδ2 T cells or MAIT cells, in the absence or presence of anti-CD3/CD28 beads. FACS plots are representative of three donors and depict total neutrophils after gating on $CD15^+$ $V\gamma9^-$ or $CD15^+$ $V\alpha7.2^-$ cells. (**B**) Neutrophil survival after 48-h culture in the presence of HMB-PP–activated Vγ9/Vδ2 T cell or anti-CD3/CD28–activated MAIT cell–conditioned medium (representative of three donors). (**C**) Morphological analysis of surviving neutrophils after 48-h culture in the absence or presence of HMB-PP–activated Vγ9/Vδ2 T cell or anti-CD3/CD28–activated MAIT cell–conditioned medium (representative of two donors). Original magnification ×400. (**D**) Neutrophil survival after 48-h culture in the absence or presence of HMB-PP–activated Vγ9/Vδ2 T cell or anti-CD3/CD28–activated MAIT cell–conditioned medium. Shown are means ± SD for the proportion of $CD16^{high}$ cells (n = 9–10), the total number of neutrophils (n = 3), and annexin V staining on $CD16^{high}$ neutrophils (n = 3). Expression of (**E**) activation markers and (**F**) APC markers on freshly isolated neutrophils and $CD16^{high}$ neutrophils after 48-h culture in the absence or presence of HMB-PP–activated Vγ9/Vδ2 T cell– or anti-CD3/CD28–activated MAIT cell–conditioned medium. Data shown are means ± SD and representative histograms from three individual donors. Data were analyzed by one-way ANOVA with Bonferroni's post hoc tests; comparisons were made with medium controls. Differences were considered significant as indicated: $*p < 0.05$, $**p < 0.01$, $***p < 0.001$.

these experiments identify microbe-responsive unconventional T cells as a rapid physiological source of GM-CSF, IFN-γ, and TNF-α and imply that the unique combination of cytokines secreted by unconventional T cells is key for the observed impact on neutrophils.

The particular requirement for TNF-α in the acquisition of the full APC phenotype is especially noteworthy when considering the cytokine/chemokine profiles in acutely infected patients. Plasma proteins that were highly elevated in sepsis patients included TNF-α as well as IL-6 and CXCL8 (Fig. 4E). Of note, there was a trend toward higher levels of TNF-α in patients with HMB-PP–positive infections (p = 0.09; data not shown). A proportion of individuals with sepsis also had increased plasma levels of GM-CSF, IFN-γ, and IL-1β, although this was not significant across the whole cohort (Fig. 4E). These findings confirm that the blood of sepsis patients contains proinflammatory mediators implicated in driving survival and activation of neutrophils, including their differentiation into APCs.

Unconventional T cell–primed neutrophils readily take up soluble Ags

We next tested the capacity of APC-like neutrophils to take up soluble Ags. Although freshly isolated neutrophils were not very efficient at endocytosing FITC-labeled BSA and dextran (10,000 Da) as model compounds, short-term exposure to Vγ9/Vδ2 T cell–conditioned medium led to a greatly enhanced uptake (Fig. 5A). With unconventional T cell–primed neutrophils kept in culture for 24 h before addition of BSA-FITC, Ag endocytosis was confined

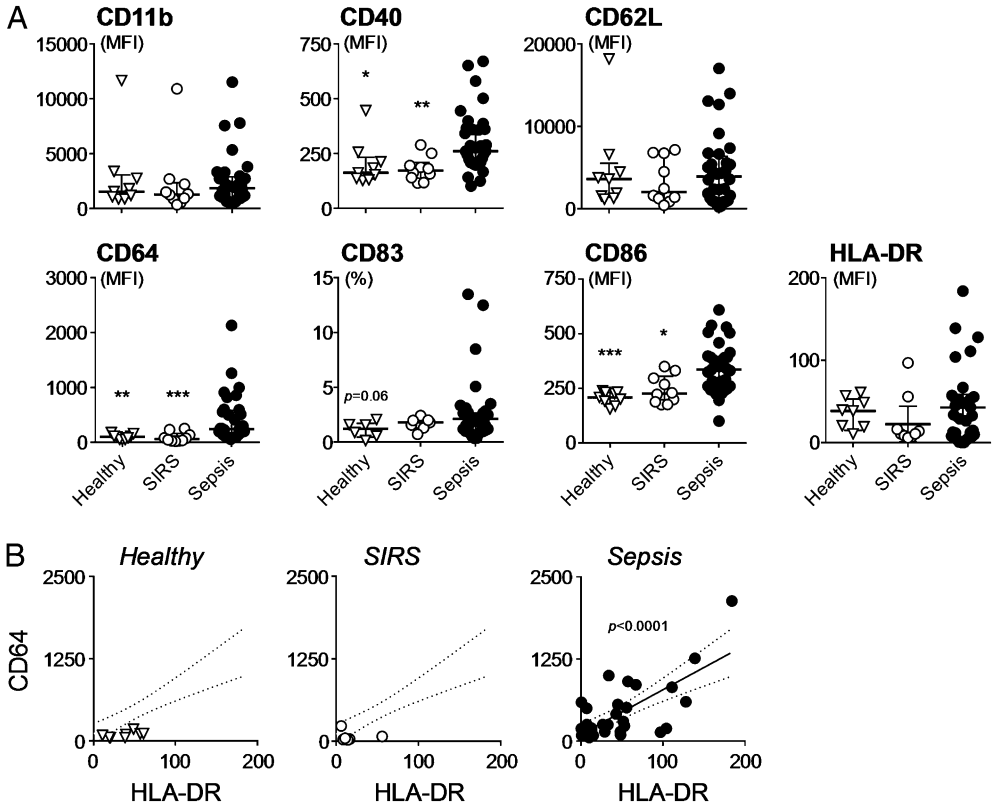

FIGURE 3. APC-like phenotype of circulating neutrophils during acute sepsis. (**A**) Surface expression of the indicated markers on circulating neutrophils in patients with SIRS (n = 14) or sepsis (n = 37) and in healthy controls (n = 10). Each data point represents an individual; lines and error bars depict medians and interquartile ranges. Data were analyzed using Kruskal–Wallis tests and Dunn's multiple comparison tests; comparisons were made with sepsis patients. (**B**) Correlation between surface expression of CD64 and HLA-DR on circulating neutrophils in healthy controls and in patients with SIRS or sepsis. Lines depict linear regression and 95% confidence bands as calculated for sepsis neutrophils. Differences were considered significant as indicated: $*p < 0.05$, $**p < 0.01$, $***p < 0.001$.

to the $CD16^{high}$ APC-like population, whereas no such uptake was seen in the apoptotic $CD16^{low}$ population (Fig. 5B). In contrast, neutrophils cultured in medium alone showed no specific uptake of BSA in the $CD16^{high}$ population. These data indicate that unconventional T cells promote the uptake of exogenous Ags as a prerequisite for Ag processing and presentation by neutrophils.

Unconventional T cell–primed neutrophils are efficient APCs for $CD4^+$ and $CD8^+$ T cells

The functionality of cell surface–expressed HLA-DR on activated neutrophils was confirmed using the *S. aureus* superantigen, TSST-1, which cross-links MHC class II molecules with the TCR of $CD4^+$ T cells expressing a Vβ2 chain (35). Neutrophils exposed to Vγ9/Vδ2 T cell–conditioned medium or to a combination of GM-CSF, IFN-γ, and TNF-α were both capable of presenting TSST-1 to autologous $V\beta2^+$ $CD4^+$ T cells (Fig. 5C). When using the complex *M. tuberculosis* Ag, PPD, which requires intracellular processing, unconventional T cell–primed neutrophils displayed a striking capacity to trigger proliferation of both $CD4^+$ and $CD8^+$ T cells (Fig. 5D). Sequestration of TNF-α during the neutrophil-priming period by addition of sTNFR diminished both $CD4^+$ and $CD8^+$ T cell responses (Fig. 5E) as further confirmation of the key role for unconventional T cell–derived TNF-α in the acquisition of APC features by neutrophils.

Unconventional T cell–primed neutrophils cross-present Ags to $CD8^+$ T cells

Following up from the striking induction of PPD-specific $CD4^+$ and $CD8^+$ T cell responses, we assessed the potential of APC-like neutrophils to trigger $CD8^+$ T cell responses, by taking advantage of HLA-A2–restricted responder T cell lines specific for M1(p58–66), the immunodominant epitope of the influenza M1 protein (36–38). Using the M1(p58–66) peptide, which can be pulsed readily onto cell surface–associated MHC class I molecules for direct presentation to $CD8^+$ T cells, unconventional T cell–primed neutrophils showed a significantly improved Ag presentation, compared with freshly isolated neutrophils (Fig. 6A) and in agreement with the elevated levels of MHC class I molecules on APC-like neutrophils. Importantly, only unconventional T cell–primed neutrophils, but not freshly isolated neutrophils, were also able to induce robust responses by M1(p58–66)-specific responder $CD8^+$ T cells when utilizing the full-length M1 protein (Fig. 6A), a 251-aa–long Ag that requires uptake, processing, and loading of M1(p58–66) onto intracellular MHC class I molecules for cross-presentation to $CD8^+$ T cells (36–38). Control experiments supported the need for Ag uptake and processing, as recombinant M1 protein could not be pulsed directly onto neutrophils, demonstrating the absence of potential degradation products in the M1 protein preparation that might be able to bind directly to cell surface–associated MHC class I molecules on neutrophils or $CD8^+$ T cells (Fig. 6B). Neutrophils cultured for 48 h in the presence of GM-CSF and IFN-γ were also capable of enhanced presentation of M1(p58–66) peptide to M1-specific $CD8^+$ T cells. However, only neutrophils generated by incubation with a combination of GM-CSF, IFN-γ, and TNF-α readily processed the full-length M1 protein (Fig. 6A), demonstrating that TNF-α plays a pivotal role in the acquisition of a fully competent APC phenotype and function by neutrophils.

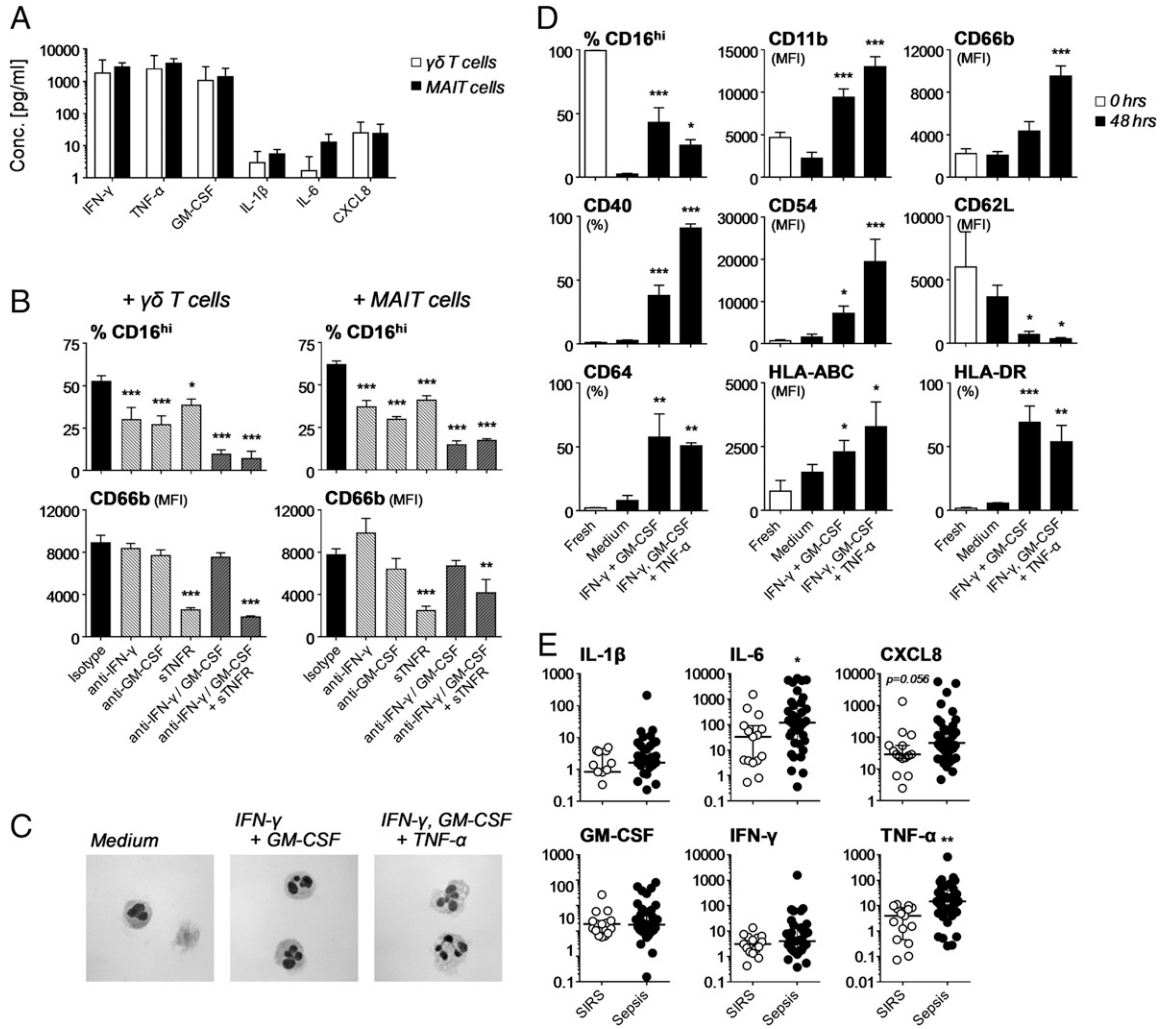

FIGURE 4. Effect of unconventional T cell–derived cytokines on neutrophil survival and APC marker expression. (**A**) Secretion of the indicated mediators into the culture supernatant by FACS-sorted Vγ9/Vδ2 T cells or MAIT cells stimulated overnight in the presence of HMB-PP or anti-CD3/CD28 beads, respectively, as detected using multiplex ELISA (means + SD, n = 2–3). (**B**) Neutrophil survival (as proportion of $CD16^{high}$ cells) and CD66b expression on $CD16^{high}$ neutrophils after 48-h culture in the presence of HMB-PP–activated Vγ9/Vδ2 T cell– or anti-CD3/CD28 MAIT cell–conditioned medium and neutralizing agents against GM-CSF, IFN-γ, and/or TNF-α (means + SD, n = 3). Data were analyzed by one-way ANOVA with Bonferroni's post hoc tests; comparisons were made with isotypes. (**C**) Morphological analysis of surviving neutrophils after 48-h culture in the absence or presence of GM-CSF, IFN-γ, and/or TNF-α (representative of two donors). Original magnification ×400. (**D**) Neutrophil survival and expression of the indicated markers on $CD16^{high}$ neutrophils after 48-h culture in the absence or presence of recombinant GM-CSF, IFN-γ, and/or TNF-α (means + SD, n = 3). Data were analyzed by one-way ANOVA with Bonferroni's post hoc tests; comparisons were made with medium controls. (**E**) Plasma levels of IL-1β, IL-6, CXCL8, GM-CSF, IFN-γ, and TNF-α in SIRS and sepsis patients (in pg/ml). Each data point represents an individual; lines and error bars depict medians and interquartile ranges. Differences between the two groups were analyzed using Mann–Whitney tests. Differences were considered significant as indicated: $*p < 0.05$, $**p < 0.01$, $***p < 0.001$.

Circulating neutrophils from sepsis patients are capable of cross-presenting Ags to $CD8^+$ T cells

It has not yet been established whether neutrophils are capable of triggering Ag-specific T cell responses in vivo. To translate our findings on APC-like neutrophils to the situation in acute infections, we isolated untouched neutrophils from sepsis patients to purities of 99.2–99.8%. Our experiments show that sepsis neutrophils and control neutrophils had a similar capacity to activate M1-specific responder $CD8^+$ T cells when pulsed with the peptide itself (Fig. 6C). Strikingly, only sepsis neutrophils, but not control neutrophils, were also able to take up the full-length M1 protein and cross-present the M1(p58–66) peptide to responder $CD8^+$ T cells (Fig. 6C, 6D), consistent with the differences in APC marker expression between patients and healthy individuals. These findings indicate that in acute sepsis neutrophils acquire an APC-like phenotype with the capacity to induce Ag-specific $CD8^+$ T cell responses that is reminiscent of neutrophils primed by unconventional T cells (Fig. 7).

Discussion

To our knowledge, the present study is the first demonstration that human neutrophils can assume Ag cross-presenting properties. Although our work does not formally demonstrate a causal link for the interaction of unconventional T cells and neutrophils in vivo, it does suggest a plausible scenario for the generation of APC-like neutrophils during acute infection. Our data support a model in which different types of unconventional T cells respond rapidly to neutrophils after phagocytosis of a broad range of bacteria at the site of infection, and in turn mediate the local differentiation of bystander neutrophils into APCs for both $CD4^+$ and $CD8^+$ T cells (Fig. 7). APC-like neutrophils may be particularly relevant for local responses by tissue-resident memory and/or freshly recruited

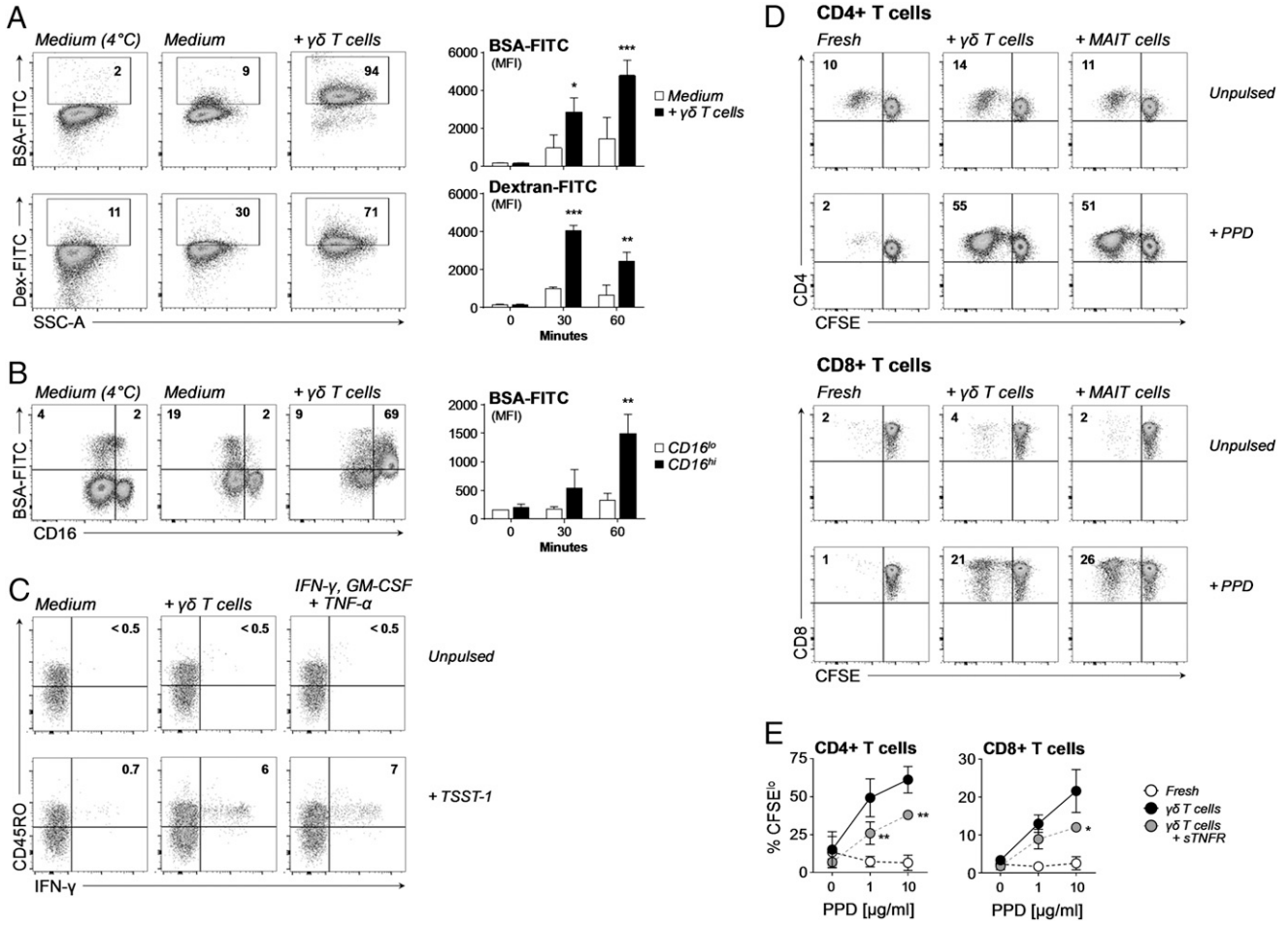

FIGURE 5. Efficient endocytosis of exogenous molecules and presentation of microbial Ags by unconventional T cell–primed neutrophils. (**A**) Endocytosis of FITC-labeled BSA and 10-kDa dextran by freshly isolated neutrophils incubated for 60 min at 4°C or at 37°C in the absence or presence of HMB-PP–activated γδ T cell supernatant. FACS plots are representative of two to three donors; specific uptake of FITC-labeled BSA and dextran by freshly isolated neutrophils was determined over 30 and 60 min (means + SD, $n = 2–3$). (**B**) Endocytosis of FITC-labeled BSA over 60 min by neutrophils that had been cultured overnight in the absence or presence of HMB-PP–activated γδ T cell supernatant. FACS plots are representative of three healthy donors; specific uptake of FITC-labeled BSA by γδ T cell–primed neutrophils was determined over 30 and 60 min (means + SD, $n = 2–3$). Data were analyzed by two-way ANOVA with Bonferroni's post hoc tests; comparisons were made with (A) medium controls or (B) $CD16^{low}$ cells. (**C**) IFN-γ production by superantigen-specific $CD4^+$ $Vβ2^+$ T cells in response to autologous neutrophils cultured for 48 h in medium or in the absence or presence of HMB-PP–activated Vγ9/Vδ2 T cell–conditioned medium or a combination of IFN-γ, GM-CSF, and TNF-α prior to pulsing with 10 ng/ml TSST-1 (representative of two donors). (**D**) Proliferation of $CD4^+$ and $CD8^+$ T cells in response to freshly isolated neutrophils and neutrophils cultured for 48 h in the presence of HMB-PP–activated Vγ9/Vδ2 T cell– or anti-CD3/CD28–activated MAIT cell–conditioned medium. Neutrophils were pulsed with 10 μg/ml PPD for 18 h prior to addition of CFSE-labeled bulk $CD3^+$ T cells; CFSE dilution of responder T cells was assessed after 7 d of coculture (representative of three donors). (**E**) Proliferation of CFSE-labeled $CD4^+$ and $CD8^+$ T cells in response to PPD-pulsed freshly isolated neutrophils and neutrophils cultured for 48 h in the presence of HMB-PP–activated Vγ9/Vδ2 T cell–conditioned medium with and without sTNFR. CFSE dilution of responder T cells was assessed after 7 d of coculture (means + SD, $n = 3$). Data were analyzed by one-way ANOVA with Bonferroni's post hoc tests; comparisons were made with Vγ9/Vδ2 T cell + sTNFR–treated neutrophils. Differences were considered significant as indicated: $*p < 0.05$, $**p < 0.01$, $***p < 0.001$.

effector $CD4^+$ and $CD8^+$ T cells at the site of infection, rather than the priming of naive $CD4^+$ and $CD8^+$ T cells in secondary lymphoid tissues. Expression of the lymph node homing receptor CCR7 by activated neutrophils was reported before (30) but could not be confirmed in the current study (data not shown). Still, APC-like neutrophils may also gain access to inflamed draining lymph nodes through the action of inflammatory chemokines (7–10). Irrespective of the anatomical context, APC-like neutrophils may contribute to protective immune responses, by fighting the "first hit" infection as a result of inducing Ag-specific $CD4^+$ and $CD8^+$ T cells and by harnessing the T cell compartment against potential "second hit" infections. However, it is also thinkable that such an early induction of cytotoxic $CD8^+$ T cells may add to the systemic inflammatory response and ultimately lead to tissue damage and organ failure. Whereas the generation of APC-like neutrophils is likely to occur locally in the context of infected tissues, in severe inflammatory conditions, including sepsis, such APC-like neutrophils may eventually leak into the circulation and become detectable in blood. Larger stratified approaches are clearly needed to define the role of APC-like neutrophils in different infectious scenarios, locally and systemically, in clinically and microbiologically well-defined patient subgroups.

The presence of cross-presenting neutrophils in patients with sepsis is intriguing and may point to an essential role of APC-like neutrophils in acute disease. Sepsis patients who survive the primary infection often show signs of reduced surface expression of HLA-DR on monocytes and a relative tolerance of monocytes to LPS stimulation (47). As consequence of what is generally perceived as a loss of immune function, many patients are susceptible to subsequent nosocomial infections, including reactivation of

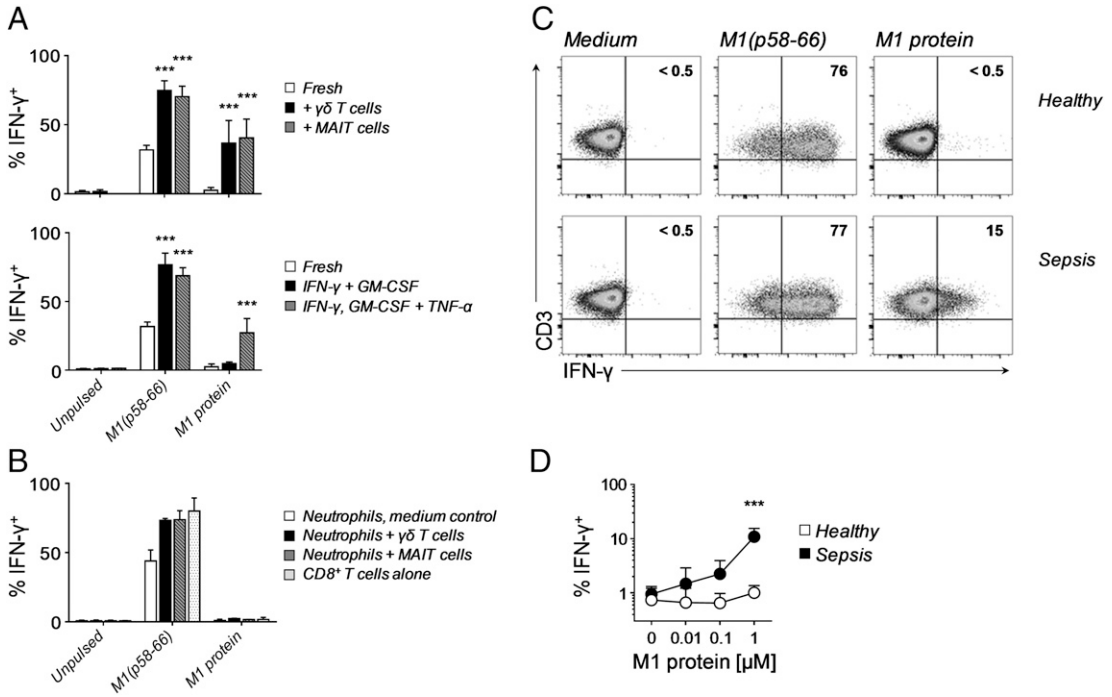

FIGURE 6. Cross-presentation of exogenous Ags by unconventional T cell–primed neutrophils and sepsis neutrophils. (**A**) IFN-γ production by Ag-specific $CD8^+$ T cells in response to neutrophils cultured for 48 h in the presence of HMB-PP–activated Vγ9/Vδ2 T cell– or anti-CD3/CD28–activated MAIT cell–conditioned medium (*top*), or neutrophils cultured for 48 h with the recombinant cytokines indicated (*bottom*). Neutrophils were pulsed for 1 h with 0.1 μM influenza M1(p58–66) peptide or for 18 h with recombinant M1 protein (means + SD, $n = 3$). Data were analyzed by two-way ANOVA with Bonferroni's post hoc tests; comparisons were made with freshly isolated neutrophils. (**B**) Failure of M1 protein to be pulsed directly onto neutrophils, as judged by IFN-γ production of Ag-specific $CD8^+$ T cells alone or in response to neutrophils cultured for 48 h in the absence or presence of HMB-PP–activated Vγ9/Vδ2 T cell– or anti-CD3/CD28–activated MAIT cell–conditioned medium. Neutrophils were pulsed for 1 h with either 0.1 μM influenza M1 (p58–66) peptide or 1 μM recombinant M1 protein; $CD8^+$ T cells were incubated directly with the peptide or M1 protein (means + SD, $n = 2$). (**C**) IFN-γ production by M1-specific $CD8^+$ T cells in response to freshly isolated neutrophils loaded with 0.1 μM synthetic M1(p58–66) peptide or 1 μM M1 protein. Data shown are representative of three $HLA\text{-}A2^+$ sepsis patients and three $HLA\text{-}A2^+$ healthy volunteers as controls. Sepsis patients recruited for these APC assays had confirmed infections as identified by positive culture results: *Escherichia coli* (urine), *Klebsiella pneumoniae* (respiratory culture), and *Staphylococcus epidermidis* (blood), respectively. (**D**) Summary of all stimulation assays conducted, shown as percentage of IFN-γ–positive $CD8^+$ T cells in response to freshly isolated neutrophils loaded with peptide or the indicated concentrations of M1 protein (means ± SD, $n = 3$). Data were analyzed by two-way ANOVA with Bonferroni's post hoc tests. Differences were considered significant as indicated: $*p < 0.05$, $**p < 0.01$, $***p < 0.001$.

latent viruses that are associated with high mortality rates (48, 49). Trials specifically targeted at reversing this apparent monocyte deactivation have shown promising clinical results (50). However, our present findings suggest that HLA-DR expression by circulating monocytes is a poor surrogate marker for a systemic immune suppression and rather indicate that, contrary to the proposed general loss of function, certain cells such as neutrophils may actually assume APC properties under such conditions, as evidence of a gain of new function. Yet, with a complex and multilayered clinical phenomenon such as sepsis it is challenging to dissect the relevance of APC-like neutrophils for infection resolution and clinical outcome in vivo.

With their unique ability to recognize microbial metabolites in a non-MHC–restricted manner, unconventional T cells such as Vγ9/Vδ2 T cells and MAIT cells greatly outnumber Ag-specific conventional $CD4^+$ and $CD8^+$ T cells at the site of infection and represent early and abundant sources of proinflammatory cytokines (23, 27), among which GM-CSF, IFN-γ, and TNF-α each make key contributions. Although conventional T cells may produce a similar combination of cytokines and provide similar signals to neutrophils, preliminary findings in our laboratory indicate that Vγ9/Vδ2 T cells and MAIT cells represent together up to 50% of all TNF-α–producing T cells among peritoneal cells stimulated with bacterial extracts, suggesting that these two cell types are indeed major producers of proinflammatory cytokines in response to microbial stimulation (A. Liuzzi and M. Eberl, unpublished observations). Although we cannot rule out a further contribution of contact-dependent mechanisms, this observation builds upon earlier studies describing the generation of human neutrophils expressing MHC class II through the action of recombinant cytokines in vitro (22, 51–56) and in vivo (57–59). Previous investigations reported an upregulation of MHC class II on activated neutrophils under the control of GM-CSF and IFN-γ, albeit the physiological source of those mediators during acute infection was not defined. Most importantly, in this study, we describe a direct role for TNF-α in the efficient induction of MHC class I–restricted $CD8^+$ T cell responses by neutrophils. Of note, plasma from sepsis patients was previously shown to induce some (upregulation of CD64), but not other features (upregulation of CD11b, loss of CD62L) (60) that are characteristic for unconventional T cell–primed neutrophils, indicating that circulating cytokines alone do not confer APC properties. In support of local cell-mediated processes at the site of inflammation, our findings evoke earlier descriptions of APC-like neutrophils characterized by MHC class II expression in infectious and noninfectious inflammatory scenarios such as periodontitis (17) and tuberculous pleuritis (20), in which locally activated Vγ9/Vδ2 T cells were found (61–63). These associations lend further support to the existence of a peripheral immune surveillance network comprised of distinct types of unconventional T cells and their crosstalk with

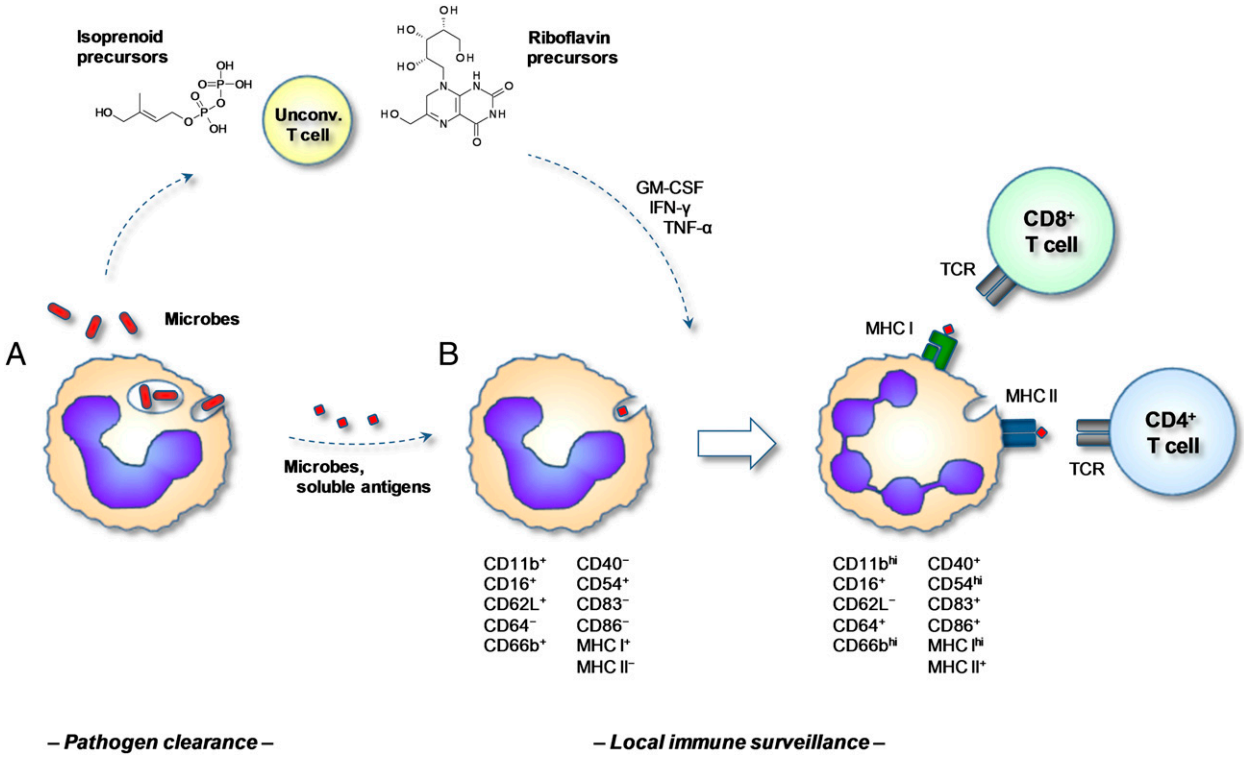

FIGURE 7. Proposed model for the local induction of APC-like neutrophils under the influence of microbe-responsive unconventional T cells. (**A**) Upon pathogen clearance, neutrophils release microbial metabolites into the microenvironment, where they stimulate local or freshly recruited unconventional T cells to release proinflammatory cytokines. (**B**) In the presence of unconventional T cell–derived mediators such as GM-CSF, IFN-γ, and TNF-α, bystander neutrophils acquire the capacity to act as APCs for tissue-resident and/or newly arriving effector and memory $CD4^+$ and $CD8^+$ T cells. Activated neutrophils may also gain access to inflamed draining lymph nodes and prime T cell responses in secondary lymphoid tissues (not depicted).

local immune and nonimmune cells. In the absence of unconventional T cell–derived signals, such as during sterile inflammation induced by LPS administration (64), neutrophils may not become fully primed, in accordance with our failure to induce APC-like neutrophils using LPS alone. Of note, a possible feedback regulation may require the activation of unconventional T cells to reach a certain threshold to overcome the inhibitory effect of bystander neutrophils (65–67).

Our present data demonstrate that both isoprenoid and riboflavin precursors are released by human neutrophils upon phagocytosis of live bacteria and depend on uptake by monocytes and loading onto butyrophilin 3A and MR1, respectively. The surprising similarities between Vγ9/Vδ2 T cells and MAIT cells illustrate their overlapping, yet distinct roles. Given the broad distribution of the nonmevalonate and riboflavin pathways across pathogenic, opportunistic, and commensal species, the vast majority of invading microbes is likely to be detected by either Vγ9/Vδ2 T cells or MAIT cells, or both. Our analysis of sepsis patients identified a systemic mobilization of Vγ9/Vδ2 T cells in response to HMB-PP–producing species, in support of their differential responsiveness to distinct groups of bacteria (28, 46). Because the present clinical study was conceived before information about the responsiveness of MAIT cells for riboflavin metabolites became available in the literature, we did not conduct a differential analysis for MAIT cells during acute sepsis. Of note, except for two cases of streptococcal infections, all bacterial and fungal pathogens identified in this patient cohort in fact possessed the riboflavin pathway, that is, were theoretically capable of stimulating MAIT cells. Intriguingly, Grimaldi et al. (68) recently reported a specific depletion of peripheral MAIT cells in sepsis patients with nonstreptococcal (i.e., riboflavin-producing) bacteria compared with infections caused by riboflavin-deficient species, which may indicate differences in the recruitment and retention of different types of unconventional T cells at sites of infection, depending on the nature of the causative pathogen and the underlying pathology (69–72). The contribution of tissue-resident and freshly recruited unconventional T cells to acute inflammatory responses has implications for clinical outcome and for the development of novel diagnostics and therapeutic interventions (46).

Taken together, our present study provides evidence 1) that Vγ9/Vδ2 T cells and MAIT cells respond similarly to microbial pathogens that produce the corresponding ligands when phagocytosed by human neutrophils, 2) that, once activated, both types of unconventional T cells trigger longer-term survival and differentiation of neutrophils into APC-like cells, 3) that unconventional T cell–primed neutrophils readily process exogenous Ags and prime both $CD4^+$ and $CD8^+$ T cells, and 4) that circulating neutrophils from patients with acute sepsis possess a similar APC-like phenotype and are capable of cross-presenting soluble proteins to Ag-specific $CD8^+$ T cells ex vivo. These findings define a possible physiological context for the generation of APC-like neutrophils in response to a broad range of microbial pathogens and imply a unique and decisive role for human unconventional T cells in orchestrating local inflammatory events and in shaping the transition of the innate to the adaptive phase of the antimicrobial immune response, with implications for diagnosis, therapy, and vaccination.

Acknowledgments

We are grateful to all patients and volunteers for participating in this study and we thank the clinicians and nurses for cooperation. We also thank Mark Toleman for clinical pathogens, Hassan Jomaa and Boris Illarionov for HMB-PP and DMRL, Andrew Thomas for recombinant M1 protein and

HLA-A2 tetramers, Ted Hansen and Daniel Olive for mAbs, Ann Kift-Morgan for multiplex ELISA measurements, Catherine Naseriyan for cell sorting, Chia-Te Liao for help with cytospins, and Marco Cassatella, Adrian Hayday, Ian Sabroe, and Phil Taylor for stimulating discussion.

Disclosures

The authors have no financial conflicts of interest.

References

1. Nathan, C. 2006. Neutrophils and immunity: challenges and opportunities. *Nat. Rev. Immunol.* 6: 173–182.
2. Mantovani, A., M. A. Cassatella, C. Costantini, and S. Jaillon. 2011. Neutrophils in the activation and regulation of innate and adaptive immunity. *Nat. Rev. Immunol.* 11: 519–531.
3. Mócsai, A. 2013. Diverse novel functions of neutrophils in immunity, inflammation, and beyond. *J. Exp. Med.* 210: 1283–1299.
4. Müller, I., M. Munder, P. Kropf, and G. M. Hänsch. 2009. Polymorphonuclear neutrophils and T lymphocytes: strange bedfellows or brothers in arms? *Trends Immunol.* 30: 522–530.
5. Pillay, J., T. Tak, V. M. Kamp, and L. Koenderman. 2013. Immune suppression by neutrophils and granulocytic myeloid-derived suppressor cells: similarities and differences. *Cell. Mol. Life Sci.* 70: 3813–3827.
6. Cerutti, A., I. Puga, and G. Magri. 2013. The B cell helper side of neutrophils. *J. Leukoc. Biol.* 94: 677–682.
7. Kesteman, N., G. Vansanten, B. Pajak, S. M. Goyert, and M. Moser. 2008. Injection of lipopolysaccharide induces the migration of splenic neutrophils to the T cell area of the white pulp: role of CD14 and CXC chemokines. *J. Leukoc. Biol.* 83: 640–647.
8. Puga, I., M. Cols, C. M. Barra, B. He, L. Cassis, M. Gentile, L. Comerma, A. Chorny, M. Shan, W. Xu, et al. 2012. B cell-helper neutrophils stimulate the diversification and production of immunoglobulin in the marginal zone of the spleen. *Nat. Immunol.* 13: 170–180.
9. Abadie, V., E. Badell, P. Douillard, D. Ensergueix, P. J. Leenen, M. Tanguy, L. Fiette, S. Saeland, B. Gicquel, and N. Winter. 2005. Neutrophils rapidly migrate via lymphatics after *Mycobacterium bovis* BCG intradermal vaccination and shuttle live bacilli to the draining lymph nodes. *Blood* 106: 1843–1850.
10. Chtanova, T., M. Schaeffer, S. J. Han, G. G. van Dooren, M. Nollmann, P. Herzmark, S. W. Chan, H. Satija, K. Camfield, H. Aaron, et al. 2008. Dynamics of neutrophil migration in lymph nodes during infection. *Immunity* 29: 487–496.
11. Beauvillain, C., Y. Delneste, M. Scotet, A. Peres, H. Gascan, P. Guermonprez, V. Barnaba, and P. Jeannin. 2007. Neutrophils efficiently cross-prime naive T cells in vivo. *Blood* 110: 2965–2973.
12. Abi Abdallah, D. S., C. E. Egan, B. A. Butcher, and E. Y. Denkers. 2011. Mouse neutrophils are professional antigen-presenting cells programmed to instruct Th1 and Th17 T-cell differentiation. *Int. Immunol.* 23: 317–326.
13. Ostanin, D. V., E. Kurmaeva, K. Furr, R. Bao, J. Hoffman, S. Berney, and M. B. Grisham. 2012. Acquisition of antigen-presenting functions by neutrophils isolated from mice with chronic colitis. *J. Immunol.* 188: 1491–1502.
14. Matsushima, H., S. Geng, R. Lu, T. Okamoto, Y. Yao, N. Mayuzumi, P. F. Kotol, B. J. Chojnacki, T. Miyazaki, R. L. Gallo, and A. Takashima. 2013. Neutrophil differentiation into a unique hybrid population exhibiting dual phenotype and functionality of neutrophils and dendritic cells. *Blood* 121: 1677–1689.
15. Geng, S., H. Matsushima, T. Okamoto, Y. Yao, R. Lu, K. Page, R. M. Blumenthal, N. L. Ward, T. Miyazaki, and A. Takashima. 2013. Emergence, origin, and function of neutrophil-dendritic cell hybrids in experimentally induced inflammatory lesions in mice. *Blood* 121: 1690–1700.
16. Iking-Konert, C., S. Vogt, M. Radsak, C. Wagner, G. M. Hänsch, and K. Andrassy. 2001. Polymorphonuclear neutrophils in Wegener's granulomatosis acquire characteristics of antigen presenting cells. *Kidney Int.* 60: 2247–2262.
17. Bisson-Boutelliez, C., N. Miller, D. Demarch, and M. C. Bene. 2001. CD9 and HLA-DR expression by crevicular epithelial cells and polymorphonuclear neutrophils in periodontal disease. *J. Clin. Periodontol.* 28: 650–656.
18. Cross, A., R. C. Bucknall, M. A. Cassatella, S. W. Edwards, and R. J. Moots. 2003. Synovial fluid neutrophils transcribe and express class II major histocompatibility complex molecules in rheumatoid arthritis. *Arthritis Rheum.* 48: 2796–2806.
19. Iking-Konert, C., B. Ostendorf, O. Sander, M. Jost, C. Wagner, L. Joosten, M. Schneider, and G. M. Hänsch. 2005. Transdifferentiation of polymorphonuclear neutrophils to dendritic-like cells at the site of inflammation in rheumatoid arthritis: evidence for activation by T cells. *Ann. Rheum. Dis.* 64: 1436–1442.
20. Alemán, M., S. S. de la Barrera, P. L. Schierloh, L. Alves, N. Yokobori, M. Baldini, E. Abbate, and M. C. Sasiain. 2005. In tuberculous pleural effusions, activated neutrophils undergo apoptosis and acquire a dendritic cell-like phenotype. *J. Infect. Dis.* 192: 399–409.
21. Sandilands, G. P., J. McCrae, K. Hill, M. Perry, and D. Baxter. 2006. Major histocompatibility complex class II (DR) antigen and costimulatory molecules on in vitro and in vivo activated human polymorphonuclear neutrophils. *Immunology* 119: 562–571.
22. Wagner, C., C. Iking-Konert, F. Hug, S. Stegmaier, V. Heppert, A. Wentzensen, and G. M. Hänsch. 2006. Cellular inflammatory response to persistent localized *Staphylococcus aureus* infection: phenotypical and functional characterization of polymorphonuclear neutrophils (PMN). *Clin. Exp. Immunol.* 143: 70–77.
23. Gold, M. C., and D. M. Lewinsohn. 2013. Co-dependents: MR1-restricted MAIT cells and their antimicrobial function. *Nat. Rev. Microbiol.* 11: 14–19.
24. Brennan, P. J., M. Brigl, and M. B. Brenner. 2013. Invariant natural killer T cells: an innate activation scheme linked to diverse effector functions. *Nat. Rev. Immunol.* 13: 101–117.
25. Vantourout, P., and A. Hayday. 2013. Six-of-the-best: unique contributions of γδ T cells to immunology. *Nat. Rev. Immunol.* 13: 88–100.
26. Bonneville, M., R. L. O'Brien, and W. K. Born. 2010. Gammadelta T cell effector functions: a blend of innate programming and acquired plasticity. *Nat. Rev. Immunol.* 10: 467–478.
27. Eberl, M., and B. Moser. 2009. Monocytes and gammadelta T cells: close encounters in microbial infection. *Trends Immunol.* 30: 562–568.
28. Davey, M. S., C. Y. Lin, G. W. Roberts, S. Heuston, A. C. Brown, J. A. Chess, M. A. Toleman, C. G. Gahan, C. Hill, T. Parish, et al. 2011. Human neutrophil clearance of bacterial pathogens triggers anti-microbial γδ T cell responses in early infection. *PLoS Pathog.* 7: e1002040.
29. Welton, J. L., M. P. Morgan, S. Martí, M. D. Stone, B. Moser, A. K. Sewell, J. Turton, and M. Eberl. 2013. Monocytes and γδ T cells control the acute-phase response to intravenous zoledronate: insights from a phase IV safety trial. *J. Bone Miner. Res.* 28: 464–471.
30. Beauvillain, C., P. Cunin, A. Doni, M. Scotet, S. Jaillon, M. L. Loiry, G. Magistrelli, K. Masternak, A. Chevailler, Y. Delneste, and P. Jeannin. 2011. CCR7 is involved in the migration of neutrophils to lymph nodes. *Blood* 117: 1196–1204.
31. Kastenmüller, W., P. Torabi-Parizi, N. Subramanian, T. Lämmermann, and R. N. Germain. 2012. A spatially-organized multicellular innate immune response in lymph nodes limits systemic pathogen spread. *Cell* 150: 1235–1248.
32. Barral, P., M. D. Sánchez-Niño, N. van Rooijen, V. Cerundolo, and F. D. Batista. 2012. The location of splenic NKT cells favours their rapid activation by blood-borne antigen. *EMBO J.* 31: 2378–2390.
33. Davey, M. S., N. Tamassia, M. Rossato, F. Bazzoni, F. Calzetti, K. Bruderek, M. Sironi, L. Zimmer, B. Bottazzi, A. Mantovani, et al. 2011. Failure to detect production of IL-10 by activated human neutrophils. *Nat. Immunol.* 12: 1017–1018, author reply 1018–1020.
34. Brandes, M., K. Willimann, and B. Moser. 2005. Professional antigen-presentation function by human gammadelta T cells. *Science* 309: 264–268.
35. Eberl, M., G. W. Roberts, S. Meuter, J. D. Williams, N. Topley, and B. Moser. 2009. A rapid crosstalk of human gammadelta T cells and monocytes drives the acute inflammation in bacterial infections. *PLoS Pathog.* 5: e1000308.
36. Brandes, M., K. Willimann, G. Bioley, N. Lévy, M. Eberl, M. Luo, R. Tampé, F. Lévy, P. Romero, and B. Moser. 2009. Cross-presenting human gammadelta T cells induce robust CD8+ alphabeta T cell responses. *Proc. Natl. Acad. Sci. USA* 106: 2307–2312.
37. Meuter, S., M. Eberl, and B. Moser. 2010. Prolonged antigen survival and cytosolic export in cross-presenting human gammadelta T cells. *Proc. Natl. Acad. Sci. USA* 107: 8730–8735.
38. Khan, M. W. A., S. M. Curbishley, H.-C. Chen, A. D. Thomas, H. Pircher, D. Mavilio, N. M. Steven, M. Eberl, and B. Moser. 2014. Expanded human blood-derived γδ T cells display potent antigen-presentation functions. *Front. Immunol.* 5: 344.
39. Morita, C. T., C. Jin, G. Sarikonda, and H. Wang. 2007. Nonpeptide antigens, presentation mechanisms, and immunological memory of human Vgamma2Vdelta2 T cells: discriminating friend from foe through the recognition of prenyl pyrophosphate antigens. *Immunol. Rev.* 215: 59–76.
40. Le Bourhis, L., E. Martin, I. Péguillet, A. Guihot, N. Froux, M. Coré, E. Lévy, M. Dusseaux, V. Meyssonnier, V. Premel, et al. 2010. Antimicrobial activity of mucosal-associated invariant T cells. *Nat. Immunol.* 11: 701–708.
41. Kjer-Nielsen, L., O. Patel, A. J. Corbett, J. Le Nours, B. Meehan, L. Liu, M. Bhati, Z. Chen, L. Kostenko, R. Reantragoon, et al. 2012. MR1 presents microbial vitamin B metabolites to MAIT cells. *Nature* 491: 717–723.
42. López-Sagaseta, J., C. L. Dulberger, A. McFedries, M. Cushman, A. Saghatelian, and E. J. Adams. 2013. MAIT recognition of a stimulatory bacterial antigen bound to MR1. *J. Immunol.* 191: 5268–5277.
43. Corbett, A. J., S. B. Eckle, R. W. Birkinshaw, L. Liu, O. Patel, J. Mahony, Z. Chen, R. Reantragoon, B. Meehan, H. Cao, et al. 2014. T-cell activation by transitory neo-antigens derived from distinct microbial pathways. *Nature* 509: 361–365.
44. Harly, C., Y. Guillaume, S. Nedellec, C. M. Peigné, H. Mönkkönen, J. Mönkkönen, J. Li, J. Kuball, E. J. Adams, S. Netzer, et al. 2012. Key implication of CD277/butyrophilin-3 (BTN3A) in cellular stress sensing by a major human γδ T-cell subset. *Blood* 120: 2269–2279.
45. Sandstrom, A., C. M. Peigné, A. Léger, J. E. Crooks, F. Konczak, M. C. Gesnel, R. Breathnach, M. Bonneville, E. Scotet, and E. J. Adams. 2014. The intracellular B30.2 domain of butyrophilin 3A1 binds phosphoantigens to mediate activation of human Vγ9Vδ2 T cells. *Immunity* 40: 490–500.
46. Lin, C. Y., G. W. Roberts, A. Kift-Morgan, K. L. Donovan, N. Topley, and M. Eberl. 2013. Pathogen-specific local immune fingerprints diagnose bacterial infection in peritoneal dialysis patients. *J. Am. Soc. Nephrol.* 24: 2002–2009.
47. Hotchkiss, R. S., G. Monneret, and D. Payen. 2013. Sepsis-induced immunosuppression: from cellular dysfunctions to immunotherapy. *Nat. Rev. Immunol.* 13: 862–874.
48. Angus, D. C., and T. van der Poll. 2013. Severe sepsis and septic shock. *N. Engl. J. Med.* 369: 840–851.
49. Osawa, R., and N. Singh. 2009. Cytomegalovirus infection in critically ill patients: a systematic review. *Crit. Care* 13: R68.
50. Meisel, C., J. C. Schefold, R. Pschowski, T. Baumann, K. Hetzger, J. Gregor, S. Weber-Carstens, D. Hasper, D. Keh, H. Zuckermann, et al. 2009. Granulocyte-

macrophage colony-stimulating factor to reverse sepsis-associated immunosuppression: a double-blind, randomized, placebo-controlled multicenter trial. *Am. J. Respir. Crit. Care Med.* 180: 640–648.
51. Gosselin, E. J., K. Wardwell, W. F. Rigby, and P. M. Guyre. 1993. Induction of MHC class II on human polymorphonuclear neutrophils by granulocyte/macrophage colony-stimulating factor, IFN-gamma, and IL-3. *J. Immunol.* 151: 1482–1490.
52. Smith, W. B., L. Guida, Q. Sun, E. I. Korpelainen, C. van den Heuvel, D. Gillis, C. M. Hawrylowicz, M. A. Vadas, and A. F. Lopez. 1995. Neutrophils activated by granulocyte-macrophage colony-stimulating factor express receptors for interleukin-3 which mediate class II expression. *Blood* 86: 3938–3944.
53. Fanger, N. A., C. Liu, P. M. Guyre, K. Wardwell, J. O'Neil, T. L. Guo, T. P. Christian, S. P. Mudzinski, and E. J. Gosselin. 1997. Activation of human T cells by major histocompatibility complex class II expressing neutrophils: proliferation in the presence of superantigen, but not tetanus toxoid. *Blood* 89: 4128–4135.
54. Oehler, L., O. Majdic, W. F. Pickl, J. Stöckl, E. Riedl, J. Drach, K. Rappersberger, K. Geissler, and W. Knapp. 1998. Neutrophil granulocyte-committed cells can be driven to acquire dendritic cell characteristics. *J. Exp. Med.* 187: 1019–1028.
55. Yamashiro, S., J. M. Wang, D. Yang, W. H. Gong, H. Kamohara, and T. Yoshimura. 2000. Expression of CCR6 and CD83 by cytokine-activated human neutrophils. *Blood* 96: 3958–3963.
56. Radsak, M., C. Iking-Konert, S. Stegmaier, K. Andrassy, and G. M. Hänsch. 2000. Polymorphonuclear neutrophils as accessory cells for T-cell activation: major histocompatibility complex class II restricted antigen-dependent induction of T-cell proliferation. *Immunology* 101: 521–530.
57. Mudzinski, S. P., T. P. Christian, T. L. Guo, E. Cirenza, K. R. Hazlett, and E. J. Gosselin. 1995. Expression of HLA-DR (major histocompatibility complex class II) on neutrophils from patients treated with granulocyte-macrophage colony-stimulating factor for mobilization of stem cells. *Blood* 86: 2452–2453.
58. Zarco, M. A., J. M. Ribera, N. Villamor, A. Balmes, A. Urbano Ispizua, and E. Feliu. 1998. Phenotypic changes in neutrophil granulocytes after G-CSF administration in patients with acute lymphoblastic leukemia under chemotherapy. *Haematologica* 83: 573–575.
59. Reinisch, W., C. Lichtenberger, G. Steger, W. Tillinger, O. Scheiner, A. Gangl, D. Maurer, and M. Willheim. 2003. Donor dependent, interferon-gamma induced HLA-DR expression on human neutrophils in vivo. *Clin. Exp. Immunol.* 133: 476–484.
60. Lewis, S. M., D. F. Treacher, L. Bergmeier, S. D. Brain, D. J. Chambers, J. D. Pearson, and K. A. Brown. 2009. Plasma from patients with sepsis up-regulates the expression of CD49d and CD64 on blood neutrophils. *Am. J. Respir. Cell Mol. Biol.* 40: 724–732.
61. Yokobori, N., P. Schierloh, L. Geffner, L. Balboa, M. Romero, R. Musella, J. Castagnino, G. De Stéfano, M. Alemán, S. de la Barrera, et al. 2009. CD3 expression distinguishes two gammadeltaT cell receptor subsets with different phenotype and effector function in tuberculous pleurisy. *Clin. Exp. Immunol.* 157: 385–394.
62. Kawahara, K., M. Fukunaga, T. Takata, M. Kawamura, M. Morishita, and Y. Iwamoto. 1995. Immunohistochemical study of γ δ T cells in human gingival tissues. *J. Periodontol.* 66: 775–779.
63. Gemmell, E., and G. J. Seymour. 1995. γ δ T lymphocytes in human periodontal disease tissue. *J. Periodontol.* 66: 780–785.
64. Pillay, J., V. M. Kamp, E. van Hoffen, T. Visser, T. Tak, J. W. Lammers, L. H. Ulfman, L. P. Leenen, P. Pickkers, and L. Koenderman. 2012. A subset of neutrophils in human systemic inflammation inhibits T cell responses through Mac-1. *J. Clin. Invest.* 122: 327–336.
65. Wingender, G., M. Hiss, I. Engel, K. Peukert, K. Ley, H. Haller, M. Kronenberg, and S. von Vietinghoff. 2012. Neutrophilic granulocytes modulate invariant NKT cell function in mice and humans. *J. Immunol.* 188: 3000–3008.
66. Sabbione, F., M. L. Gabelloni, G. Ernst, M. S. Gori, G. Salamone, M. Oleastro, A. Trevani, J. Geffner, and C. C. Jancic. 2014. Neutrophils suppress γδ T-cell function. *Eur. J. Immunol.* 44: 819–830.
67. Kalyan, S., V. Chandrasekaran, E. S. Quabius, T. K. Lindhorst, and D. Kabelitz. 2014. Neutrophil uptake of nitrogen-bisphosphonates leads to the suppression of human peripheral blood γδ T cells. *Cell. Mol. Life Sci.* 71: 2335–2346.
68. Grimaldi, D., L. Le Bourhis, B. Sauneuf, A. Dechartres, C. Rousseau, F. Ouaaz, M. Milder, D. Louis, J. D. Chiche, J. P. Mira, et al. 2014. Specific MAIT cell behaviour among innate-like T lymphocytes in critically ill patients with severe infections. *Intensive Care Med.* 40: 192–201.
69. Matsushima, A., H. Ogura, K. Fujita, T. Koh, H. Tanaka, Y. Sumi, K. Yoshiya, H. Hosotsubo, Y. Kuwagata, T. Shimazu, and H. Sugimoto. 2004. Early activation of gammadelta T lymphocytes in patients with severe systemic inflammatory response syndrome. *Shock* 22: 11–15.
70. Venet, F., J. Bohé, A. L. Debard, J. Bienvenu, A. Lepape, and G. Monneret. 2005. Both percentage of gammadelta T lymphocytes and CD3 expression are reduced during septic shock. *Crit. Care Med.* 33: 2836–2840.
71. Andreu-Ballester, J. C., C. Tormo-Calandín, C. Garcia-Ballesteros, J. Pérez-Griera, V. Amigó, A. Almela-Quilis, J. Ruiz del Castillo, C. Peñarroja-Otero, and F. Ballester. 2013. Association of γδ T cells with disease severity and mortality in septic patients. *Clin. Vaccine Immunol.* 20: 738–746.
72. Heffernan, D. S., S. F. Monaghan, C. S. Chung, W. G. Cioffi, S. Gravenstein, and A. Ayala. 2014. A divergent response of innate regulatory T-cells to sepsis in humans: circulating invariant natural killer T-cells are preserved. *Hum. Immunol.* 75: 277–282.

SUPPLEMENTAL INFORMATION

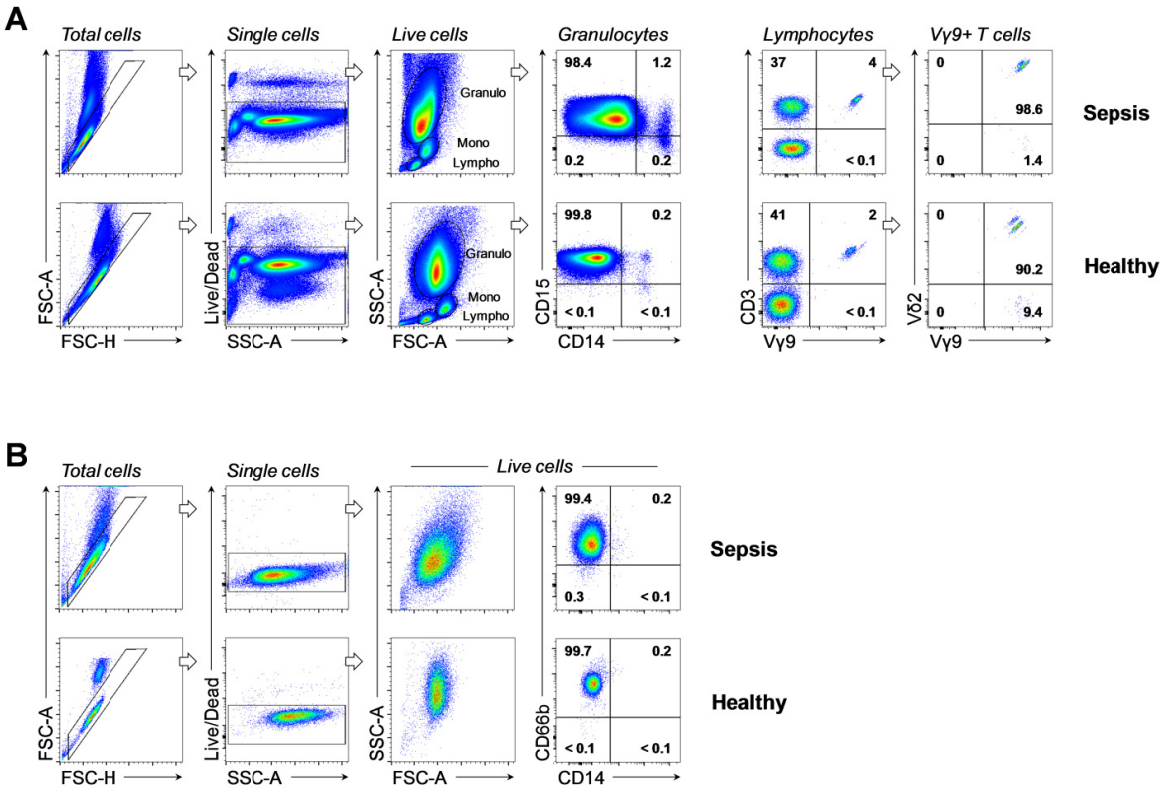

SUPPLEMENTAL FIGURE 1. Flow cytometric gating strategies for human neutrophils and Vγ9/Vδ2 T cells. (***A***) For immunophenotyping of peripheral leukocytes, whole white blood cells were isolated from healthy donors or patients with sepsis. Cells were gated on single live cells and segregated by their appearance in forward and side scatter. Neutrophils were positively identified by their surface expression of CD15 and lack of CD14. Vγ9/Vδ2 T cells were positively identified by their surface expression of CD3, TCR-Vγ9 and TCR-Vδ2. FACS plots are representative of 37 sepsis patients and 10 healthy donors. (***B***) For functional assays, neutrophils were isolated by negative selection from the blood of healthy donors or patients with sepsis, using the EasySep neutrophil enrichment kit that depletes all other human blood cells by specifically targeting CD2, CD3, CD9, CD19, CD36, CD56 and glycophorin A (StemCell Technologies). Purities were confirmed by the percentage of cells expressing CD66b but lacking CD14. FACS plots are representative of 5 sepsis patients and 15 healthy donors.

ORIGINAL ARTICLE

JBMR

Monocytes and γδ T Cells Control the Acute-Phase Response to Intravenous Zoledronate: Insights From a Phase IV Safety Trial

Joanne L Welton,[1] Matt P Morgan,[1] Salvador Martí,[1] Michael D Stone,[2] Bernhard Moser,[1] Andrew K Sewell,[1] Jane Turton,[2] and Matthias Eberl[1]

[1]Cardiff Institute of Infection and Immunity, School of Medicine, Cardiff University, Cardiff, United Kingdom
[2]Bone Research Unit, Cardiff University Academic Centre, Llandough Hospital, Penarth, United Kingdom

ABSTRACT

Aminobisphosphonates (NBPs) are used widely against excessive bone resorption in osteoporosis and Paget's disease as well as in metastatic bone disease and multiple myeloma. Intravenous NBP administration often causes mild to severe acute-phase responses (APRs) that may require intervention with analgesics and antipyretics and lead to treatment noncompliance and nonadherence. We here undertook a phase IV safety trial in patients with osteoporosis to investigate the APR of otherwise healthy individuals to first-time intravenous treatment with the NBP zoledronate. This study provides unique insight into sterile acute inflammatory responses in vivo, in the absence of confounding factors such as infection or cancer. Our data show that both peripheral γδ T cells and monocytes become rapidly activated after treatment with zoledronate, which ultimately determines the clinical severity of the APR. Our study highlights a key role for IFN-γ in the zoledronate-induced APR and identifies pretreatment levels of monocytes and central/memory Vγ9/Vδ2 T cells as well as their responsiveness to zoledronate in vitro as predictive risk factors for the occurrence of subclinical and clinical symptoms. These findings have diagnostic and prognostic implications for patients with and without malignancy and are relevant for Vγ9/Vδ2 T-cell–based immunotherapy approaches. © 2013 American Society for Bone and Mineral Research.

KEY WORDS: AMINOBISPHOSPHONATES; γδ T CELLS; ACUTE-PHASE RESPONSE; OSTEOPOROSIS; IMMUNOTHERAPY

Introduction

There is increasing evidence that γδ T cells play a key role in orchestrating and regulating immune responses in humans and in animal models.[1] Our own recent findings demonstrate that a rapid crosstalk of human γδ T cells and monocytes drives acute inflammatory responses, which may contribute to pathogen clearance and protective immunity but may also lead to tissue damage and poor clinical outcome.[2,3] For reasons not yet understood, human γδ T cells differ fundamentally from those found in nonprimate species, and hence no small animal model replicates the complex interactions between γδ T cells and other immune and nonimmune cells in the human body.[4,5]

Nitrogen-containing bisphosphonates, or aminobisphosphonates (NBPs), are effective drugs against excessive bone resorption in osteoporosis, Paget's disease, metastatic bone disease, and multiple myeloma. Despite their overall safety, NBP therapy is frequently associated with mild to severe inflammatory events, which may require intervention with analgesics and antipyretics and lead to treatment noncompliance and nonadherence.[6,7] Treatment with intravenous NBPs such as pamidronate (Aredia; Novartis, Basel, Switzerland) and zoledronate (Aclasta/Zometa; Novartis) may cause systemic acute-phase responses (APRs) characterized by fever, pain, nausea, and fatigue in up to 50% of all patients within 48 hours after administration. These flu-like symptoms are typically transient, resolve spontaneously, and are accompanied by decreased lymphocyte counts and elevated levels of the pro-inflammatory cytokines IL-6, IFN-γ, and TNF-α.[8–11] The APR upon intravenous treatment with NBPs is most severe in first-time treated patients, whereas subsequent further administration induces no APR

Received in original form June 11, 2012; revised form October 2, 2012; accepted October 8, 2012. Accepted manuscript online Ocober 16, 2012.
Address correspondence to: Jane Turton, MB, ChB, Cardiff and Vale University Health Board, Bone Research Unit, Cardiff University Academic Centre, Llandough Hospital, Penlan Road, Penarth, Vale of Glamorgan CF64 2XX, United Kingdom. E-mail: turtonj@cf.ac.uk. Matthias Eberl, PhD, Cardiff Institute of Infection and Immunity, Henry Wellcome Building, School of Medicine, Cardiff University, Heath Park, Cardiff CF14 4XN, United Kingdom. E-mail: eberlm@cf.ac.uk
JT and ME contributed equally to this work.
Additional Supporting Information may be found in the online version of this article.

Journal of Bone and Mineral Research, Vol. 28, No. 3, March 2013, pp 464–471
DOI: 10.1002/jbmr.1797

symptoms at all or an APR with much milder outcome than at first exposure. For instance, in the HORIZON trial, net APR rates were 30%, 7%, and 3% after zoledronate (ZOL) infusions 1 to 3, respectively.[11,12] The immunological basis for this "tolerance" to repeated treatment with NBPs is not known.

Kunzmann and colleagues were the first to ascribe a role for γδ T cells in the NBP-induced APR.[13] Subsequent cell culture–based studies have elegantly demonstrated that NBPs are potent stimulators of Vγ9/Vδ2$^+$ γδ T cells in vitro.[14–18] To act on Vγ9/Vδ2 T cells, NBPs depend on uptake by monocytes and other endocytically active cell types, in which they inhibit farnesyl pyrophosphate synthase (FPPS), a key enzyme in the biosynthesis of sterols, ubiquinones, and other isoprenoids via the mevalonate pathway. Preferential uptake by osteoclasts and subsequent inhibition of FPPS is the prime mechanism of action in the NBP-mediated prevention of bone resorption. However, FPPS inhibition in osteoclasts, monocytes, and other cells also leads to intracellular accumulation of upstream metabolites including dimethylallyl pyrophosphate (DMAPP), isopentenyl pyrophosphate (IPP), and an ATP conjugate of IPP (Apppl), which may function as "danger" signals and be sensed by Vγ9/Vδ2 T cells via a largely unknown mechanism.[19]

Despite the wealth of data from in vitro experiments, there has been a paucity of studies addressing the cellular events in vivo in NBP-treated patients. We here wished to study the physiological consequences of the human γδ T-cell interaction with monocytes in vivo and provide unique insight into purely γδ T cell–mediated responses in the absence of confounding factors, by investigating the immune response of otherwise healthy individuals with osteoporosis to first-time administration of intravenous ZOL. During the revision process of the present study, Kalyan and colleagues reported the presence of circulating monocytes with increased forward scatter in ZOL-treated osteoporosis patients, yet did not characterize these cells further nor give any indication as to the time frame of this response.[20] Our own findings show that both γδ T cells and monocytes become rapidly activated after treatment with ZOL, thus providing proof-of-concept for the crosstalk of both cell types in vivo. Moreover, our study highlights a key role for IFN-γ in the NBP-induced APR and identifies pretreatment levels of monocytes and Vγ9/Vδ2 T cells as well as the proportion of central/memory T_{CM} cells within the Vγ9/Vδ2 T-cell population and their in vitro responsiveness to ZOL as predictive risk factors.

Materials and Methods

Patients

This study was approved by the South East Wales Local Ethics Committee under reference number 10/WSE04/52, EudraCT number 2009-017369-47, and conducted according to the principles expressed in the Declaration of Helsinki and under local ethical guidelines. All patients provided written informed consent. The study cohort comprised 19 healthy nonsmoking adult females with postmenopausal osteoporosis and a bone density *T*-score of −2.5 or worse at either total spine, total hip, or neck of femur when measured by dual-energy X-ray absorptiometry (DXA). The mean age was 68 years (range 57 to 79 years). All study participants were NBP naïve and attended outpatient appointments at Cardiff Royal Infirmary for first-time infusion of 5 mg ZOL (Aclasta). Inclusion criteria included no contraindications to treatment with intravenous NBPs; normal creatinine clearance levels of >35 mL/min; and normal vitamin D levels of 30 to 100 μg/L. Exclusion criteria included a body temperature >38.5°C at first visit; participation in another therapeutic trial within 20 days of consent; history of illness that might compromise participation such as drug or alcohol abuse; hypocalcaemia (<2.2 mmol/L corrected); and current use of oral steroids or other immunosuppressive agents. Vital signs such as resting pulse, resting blood pressure, and oral temperature and APR symptoms were recorded before treatment (day 0) and on days 1, 3, and 9 post infusion; cumulative APR scores (0 to 4) comprised one or several of the following symptoms for at least 24 hours after treatment: fatigue, muscle pain, headache, and/or joint pain. Blood parameters recorded included white blood cell (WBC) counts, erythrocyte sedimentation rates (ESR), and plasma levels of C-reactive protein (CRP) as markers of inflammation. From all patients, 15 mL of blood were drawn on each visit; PBMCs were isolated using Lymphoprep (Axis-Shield, Dundee, United Kingdom) and used directly for multicolor flow cytometric analyses or stored in liquid nitrogen for later stimulation assays.

Flow cytometry

Freshly isolated PBMCs were stained using monoclonal antibodies against CD3 (SK7 and UCHT1), CD4 (SK3), CD8 (HIT8a), CD25 (M-A251), CD27 (M-T271), CD56 (B159), CD69 (FN50), and HLA-DR (L243) from BD Biosciences, Oxford, United Kingdom; Vγ9 (Immu360) and CD40 (MAB89) from Beckman Coulter, High Wycombe, United Kingdom; NKG2D (1D11), CD14 (61D3), CD19 (SJ25C1), CD45RA (HI100), and CD80 (2D10.4) from eBioscience, Hatfield, United Kingdom, together with appropriate isotype controls. Cells were acquired on an eight-color FACSCanto II (BD Biosciences) and analyzed with FloJo 7.6 (TreeStar, Ashland, OR, USA). Leukocyte populations were identified based on their appearance in side scatter and forward scatter area/height, exclusion of live/dead staining (fixable Aqua; Invitrogen, Paisley, United Kingdom), and surface staining: CD3$^-$CD56$^+$ NK cells, CD3$^-$CD14$^+$ monocytes, CD3$^-$CD19$^+$ B cells, and CD3$^+$ T cells. T-cell subsets were identified as CD3$^+$CD4$^+$CD8$^-$Vγ9$^-$ helper T cells, CD3$^+$CD4$^-$CD8$^+$Vγ9$^-$ cytotoxic T cells, CD3$^+$CD56$^+$Vγ9$^-$ NKT cells, and CD3$^+$Vγ9$^+$ γδ T cells.

Plasma analysis

Plasma samples were collected before PBMC separation and stored at −80°C. At the end of the study, all samples were analyzed together on a SECTOR Imager 600 (Meso Scale Discovery, Rockville, MD, USA) for IL-1β, IL-2, IL-6, IL-10, IL-12p70, CXCL8, GM-CSF, IFN-γ, and TNF-α (Human Pro-Inflammatory 9-Plex Assay Ultra-Sensitive Kit; Meso Scale Discovery). In addition, CXCL10 and IL-17 were measured on a Dynex MRX II reader, using conventional ELISA kits (R&D Systems, Abingdon, United Kingdom).

Cell culture

The medium used was RPMI-1640 with 2 mM L-glutamine, 1% non-essential amino acids, 50 μg/mL penicillin/streptomycin, and 10% fetal calf serum (Invitrogen). Frozen PBMC samples were defrosted and cultured for 24 hours in medium or with 10 μM ZOL (Zometa). Activation of Vγ9/Vδ2 T cells was analyzed by flow cytometry using antibodies against CD3, Vγ9, and CD69; levels of IFN-γ were measured on a Dynex MRX II reader, using conventional ELISA kits (R&D Systems).

Statistical analysis

Differences between groups were analyzed using paired Student's *t* tests for normally distributed data or Wilcoxon signed-rank matched pairs for nonparametric data using GraphPad Prism 4.03 software. Advanced statistical analyses were performed using SPSS 18.0. Differences between IFN-γ levels in groups with pretreatment frequencies of Vγ9/Vδ2 T cells above or below the mean were analyzed using independent *t* tests. Pearson's correlations were used to assess any relationships between variables; nonparametric variables not passing the Shapiro-Wilk test were log-transformed as done for plasma levels of IFN-γ and TNF-α on day 1 and all IL-6 levels. Predictive biomarkers were assessed using linear regression; statistically significant ($p < 0.05$) variables from univariate analyses were included in multiple regression analyses based on backward selection. All statistical tests were two-tailed. Box-and-whisker plots depict minimum, 25th percentile, median, 75th percentile, and maximum values; arrows in Fig. 5 and Supplemental Figs. S1 and S2 depict significant correlations as assessed by Pearson's correlations and/or regression analyses as specified in the figure legends. Asterisks indicate statistically significant differences to pretreatment values as indicated in the table and the figures: $^{*}p < 0.05$; $^{**}p < 0.01$; $^{***}p < 0.001$.

Results

First-time intravenous administration of ZOL causes APRs in osteoporosis patients

Upon first-time intravenous treatment with ZOL, the majority of patients experienced at least one APR symptom on day 1 (12/19) and day 3 (15/19) after treatment, two-thirds of which experienced at least two APR symptoms on day 1 (7/19) and day 3 (10/19). Nine days after treatment, 7/19 patients still had an APR score of ≥ 1. In line with the occurrence of APR symptoms, oral temperatures and pulse rates of patients were elevated on day 1 (Fig. 1). These changes were accompanied by a temporary drop in WBC ($p < 0.05$) and a concomitant rise in ESR ($p < 0.01$) on day 3 compared with baseline (not shown). Plasma levels of CRP were elevated on days 1 and 3 but returned to baseline by day 9 in most patients. Of note, all patients (19/19) showed considerable increases in CRP levels by day 3, and increases in CRP levels from baseline to days 1 and 3 correlated well with cumulative APR scores on days 1 and 3 (Table 1). These findings indicate not only that plasma CRP accurately reflected the severity of the APR but also that all patients showed an objective response to ZOL, albeit in many cases subclinically.

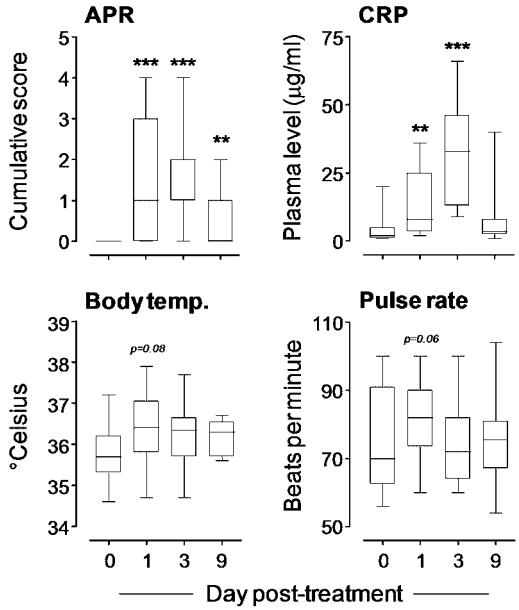

Fig. 1. Acute-phase response to intravenous ZOL in female osteoporosis patients. Cumulative APR scores, CRP plasma levels, resting body temperatures, and pulse rates immediately before and 1, 3, and 9 days after intravenous ZOL administration. Differences were assessed using Student's *t* tests.

ZOL treatment induces systemic activation of γδ T cells

To investigate the immunological basis of the APRs in our patient cohort and to be able to identify biomarkers that may correlate with, or even predict, the increase in CRP levels or the extent of the clinical symptoms experienced, we measured a comprehensive range of humoral and cellular immune parameters of possible relevance in the APR. On the cellular level, we detected a temporary drop in peripheral Vγ9/Vδ2 T cells (measured as proportion of all circulating T cells) from 2.9 ± 0.8% (mean ± SEM) down to 2.1 ± 0.7% on day 3 ($p < 0.05$); these frequencies returned to baseline levels by day 9 (Fig. 2*A*). In contrast, proportions of $CD4^+$ and $CD8^+$ T cells were not affected (data not shown). This transient ~30% decrease in Vγ9/Vδ2 T cells was similar to the findings by Thompson and colleagues[18] in ZOL-treated osteoporosis patients and confirms the specificity of ZOL for Vγ9/Vδ2 T cells. Direct evidence for activation of Vγ9/Vδ2 T cells was obtained by measuring surface expression of CD25, CD69, HLA-DR, and NKG2D. Although CD25 levels remained low throughout the study period, CD69, HLA-DR, and NKG2D showed a significant upregulation on Vγ9/Vδ2 T cells after treatment (Fig. 2*B*). Moreover, the distribution of Vγ9/Vδ2 T-cell memory subsets changed significantly in that the proportion of $CD27^+CD45RA^-$ central memory (T_{CM}) cells dropped, whereas $CD27^-CD45RA^-$ effector/memory (T_{EM}) cells and $CD27^-CD45RA^+$ terminally differentiated effector/memory (T_{EMRA}) cells increased after treatment (Fig. 2*C*). These changes in the distribution of memory subsets were detectable for at least 9 days after treatment and indicated a longer-lasting systemic effect of ZOL on the Vγ9/Vδ2 T-cell compartment beyond the initial APR.

Table 1. Correlations of CRP Values With APR Scores and Immune Biomarkers

		CRP increase	
Parameter		Day 1	Day 3
APR	Day 1	0.510*	0.690*
	Day 3	0.532*	0.806**
IFN-γ	Day 1	0.654**	*0.508*
	Day 3	*0.452*	*0.245*
IL-6	Day 1	0.595*	*–0.135*
	Day 3	*–0.471*	*–0.154*
% Vγ9$^+$	Day 0	0.637**	*0.325*
	Day 1	0.588*	0.706*
	Day 3	*0.400*	*0.464*
	Day 9	0.632**	*0.365*

Note: CRP increases above baseline were calculated by subtracting day 0 values. APR scores were expressed as cumulative symptoms on day 1 (score 0 to 4) or days 1 and 3 (score 0 to 8). Biomarkers analyzed before treatment (day 0) and on days 1, 3, and 9 after ZOL administration included plasma levels of IFN-γ and IL-6 (in pg/mL), and the frequency of Vγ9$^+$ cells within the peripheral T-cell population. Values shown are Pearson's coefficients (*r*). Numbers in italics indicate nonsignificant correlations.

*$p < 0.05$.

**$p < 0.01$.

ZOL treatment induces systemic activation of monocytes

Vγ9/Vδ2 T cells only respond to NBPs after uptake by monocytes or other endocytically active cells.[17,19,21] Because Vγ9/Vδ2 T cells stimulate monocyte survival and activation in vitro,[2,4] we next examined the effects of ZOL administration on the circulating monocyte population in vivo. Of note, we detected a pronounced increase in the proportion of monocytes among total PBMCs on day 1 (Fig. 3). However, it is not clear whether this constituted a specific expansion of monocytes, as we detected a similar increase in B cells and a parallel drop in T cells (data not shown). This notwithstanding, there was a significant increase in the surface expression of CD14, CD40, CD80, and HLA-DR at 1 to 3 days after treatment, indicative of a considerable but transient activation of monocytes in vivo (Fig. 3) and evoking our earlier demonstration of an intimate crosstalk between γδ T cells and monocytes in vitro.[2]

The ZOL-induced APR is characterized by elevated plasma cytokine levels

We next measured a range of soluble mediators in patient plasma, especially those that are associated with Vγ9/Vδ2 T-cell and/or monocyte responses. Among these, a sharp peak on day 1 was observed for IFN-γ, with an average increase of ~50-fold over baseline (Fig. 4). Less pronounced but nevertheless significant changes on day 1 were also detected for TNF-α and IL-6, in accordance with earlier studies.[8,18,22] In addition, changes were seen for IL-2, IL-10, and GM-CSF (Fig. 4) as well as CXCL10 (data not shown). To our knowledge, the latter four factors have not been implicated in the APR to NBPs before. In contrast to these effects, plasma levels of IL-1β, IL-12p70, and CXCL8 (Fig. 4) as well as IL-17 (data not shown) did not change upon treatment with ZOL. These findings suggest that the APR to ZOL, evidenced by the occurrence of clinical symptoms and elevated CRP levels peaking at day 3, is preceded by a rapid and transient production of a distinct set of inflammatory mediators on day 1. Many of these factors were previously shown to play a role in the crosstalk between activated Vγ9/Vδ2 T cells and monocytes (IFN-γ, TNF-α, GM-CSF, IL-6, CXCL10).[2]

IFN-γ takes center stage in the APR to ZOL

In an attempt to delineate the molecular and cellular events after systemic ZOL administration leading to the development of APR symptoms, we performed a detailed statistical analysis of a large range of humoral and cellular parameters, including the proportions of monocytes, B cells, NK cells, Vγ9/Vδ2 T cells, CD4 and CD8 T cells, and their expression of markers associated with activated cells (CD25, CD69, NKG2D), antigen-presenting

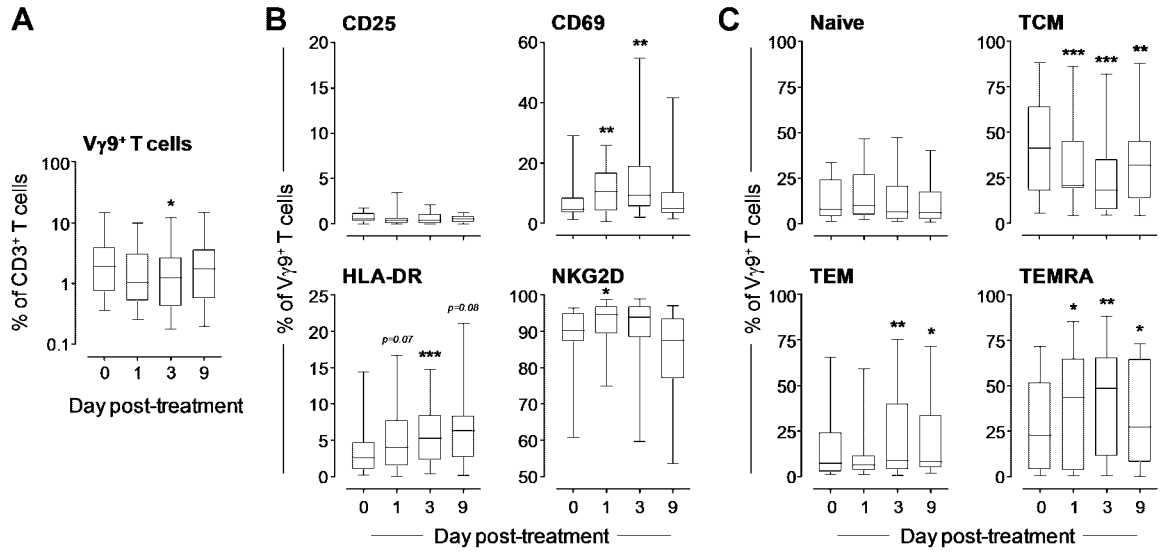

Fig. 2. Activation of peripheral γδ T cells after ZOL treatment. Proportion of Vγ9$^+$ T cells as percentage of all circulating CD3$^+$ T cells (*A*); their surface expression of CD25, CD69, HLA-DR, and NKG2D (*B*); and the relative proportion of CD27$^+$CD45RA$^+$ naive cells, CD27$^+$CD45RA$^-$ T_{CM} cells, CD27$^-$CD45RA$^-$ T_{EM} cells, and CD27$^-$CD45RA$^+$ T_{EMRA} cells amongst circulating Vγ9$^+$CD3$^+$ T cells (*C*). Differences were assessed using Student's *t*-tests.

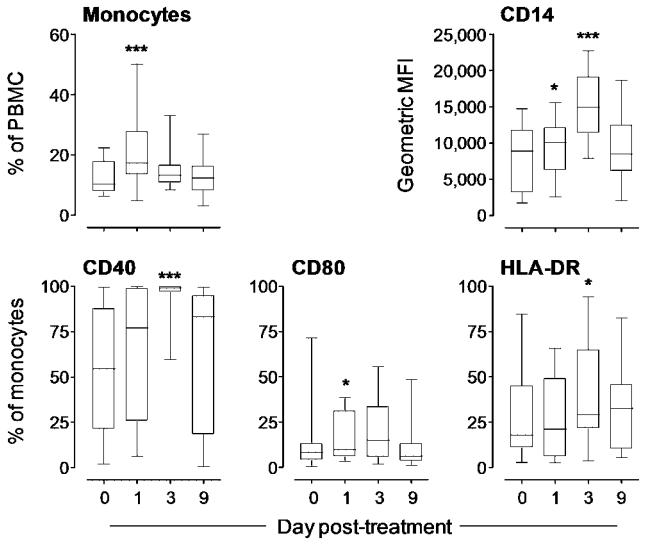

Fig. 3. Activation of peripheral monocytes after ZOL treatment. Proportion of $CD14^+$ monocytes as percentage of all PBMCs as well as surface expression of CD14 (geometric mean fluorescence intensity [MFI]) and CD40, CD80, and HLA-DR on circulating $CD14^+$ monocytes. Differences were assessed using Wilcoxon's signed-rank tests for CD40 levels on day 3 and Student's *t* tests for all other parameters.

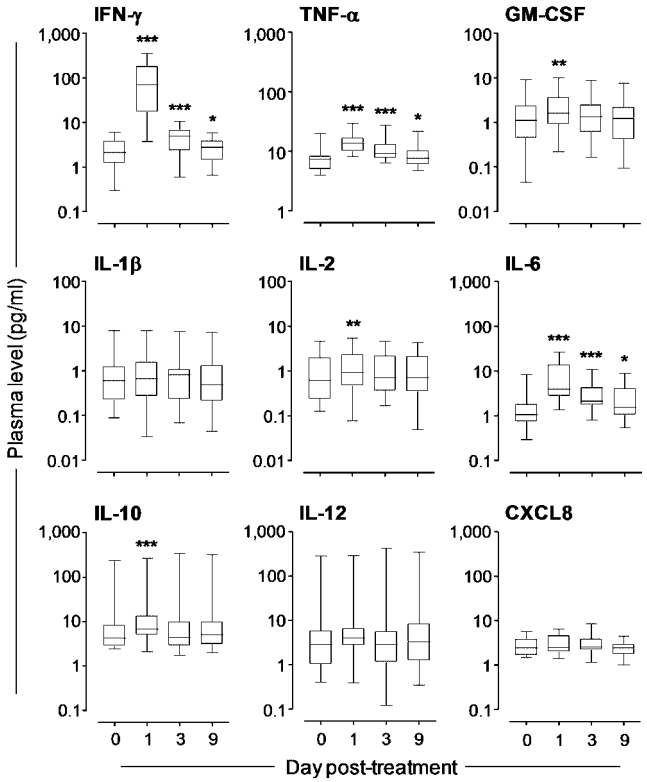

Fig. 4. Increased plasma cytokines and chemokines after ZOL treatment. Plasma levels of the markers indicated as determined by multiplex ELISA. Differences were assessed using Wilcoxon's signed-rank tests for IL-1β, IL-6, IL-10, and IL-12 levels and Student's *t* tests for all other soluble mediators.

cells (CD40, CD80, HLA-DR), and/or memory cells (CD27, CD45RA). Amongst these parameters, we identified a positive correlation between IFN-γ levels on either day 1 or day 3 and the expression of CD69 on Vγ9/Vδ2 T cells on day 1 or day 3 (Supplemental Fig. S1*A–D*). CD69 expression on Vγ9/Vδ2 T cells on day 3 also correlated moderately with plasma TNF-α levels on day 3 (Supplemental Fig. S1*D*). Moreover, pretreatment frequencies of Vγ9/Vδ2 T cells ultimately determined IFN-γ levels on day 1 (Supplemental Fig. S1*A*), and pretreatment proportions of T_{CM} cells within the Vγ9/Vδ2 T-cell population accurately predicted the levels of IFN-γ (Supplemental Fig. S1*A*) as well as TNF-α (Supplemental Fig. S1*E*) detected on day 1. No further post-treatment correlations were found between other cellular parameters and plasma cytokine/chemokine levels, except for a correlation between IFN-γ levels on day 1 and activation on NK cells on day 1 (Pearson's coefficient, $r = 0.640^{**}$) or day 3 ($r = 0.766^{**}$), measured as CD69 expression on $CD56^+$ $CD3^-$ cells (not shown). Taken together, these findings are consistent with the view that activated Vγ9/Vδ2 T cells are the prime source of the elevated levels of IFN-γ in the circulation, and that activated Vγ9/Vδ2 T cells may also induce IFN-γ production by other cell types such as NK cells.[23] A proposed model incorporating the described correlations is shown in Fig. 5. Of note, the depicted associations do not represent the result of a comprehensive path analysis or causal modeling but are derived from nonindependent regression models (individual Pearson's correlations and separate multivariate analyses by backward selection as summarized in Table 1 and Supplemental Figs. S1 and S2) and should thus be interpreted with caution because of the potential inclusion of type I errors.

The occurrence of a specific monocyte-γδ T-cell crosstalk in ZOL-treated patients was supported by the demonstration that pretreatment frequencies of monocytes in PBMCs but no other pretreatment parameters correlated directly with the activation levels of Vγ9/Vδ2 T cells on day 1, day 3, and day 9, expressed as proportion of $CD69^+$ cells (Supplemental Fig. S1*F*). Vice versa, there was a modest correlation between the frequency of Vγ9/Vδ2 T cells on day 1 and the activation status of monocytes on day 1 (Pearson's coefficient, $r = 0.495^*$) and day 3 ($r = 0.557^*$), expressed as CD40 surface levels (not shown).

Of all humoral parameters measured, day 1 levels of IFN-γ (and IL-6) correlated with increased CRP levels on day 1 (Table 1) (Supplemental Fig. S2*A, B*). Using linear regression, only IFN-γ levels on day 1 were predictive of total APR symptoms (Supplemental Fig. S2*A*). No further correlations were found between other plasma cytokines/chemokines and CRP levels or APR symptoms. Taken together, these data emphasize a crucial and previously underestimated role for IFN-γ in the development of a ZOL-induced APR. Of note, CRP levels also correlated with pre- and post-treatment frequencies of Vγ9/Vδ2 T cells, indicating that the extent of the APR upon ZOL administration is influenced by the number of ZOL-responsive Vγ9/Vδ2 T cells (Table 1). In accordance with previous findings,[24] high Vγ9/Vδ2 T-cell frequencies were indeed associated with an increased risk of APRs. Patients with pretreatment Vγ9/Vδ2 T-cell percentages greater than the median of 3% had significantly higher levels of IFN-γ on day 1, with a mean difference of 127 pg/mL (confidence interval 31 to 223 pg/mL; $p < 0.05$).

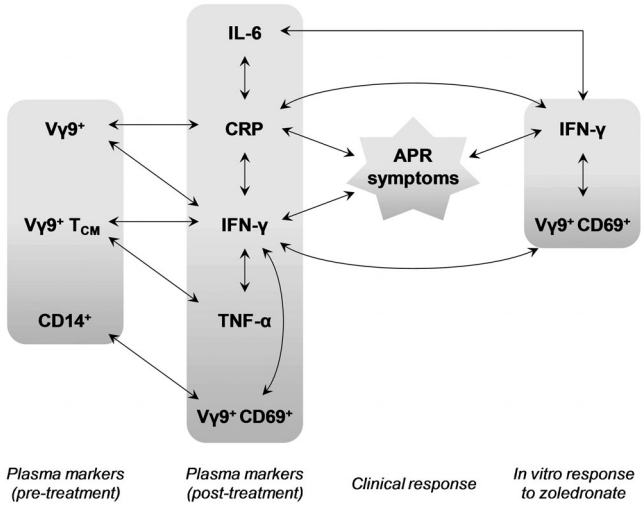

Fig. 5. Proposed relationships of pre- and post-treatment immune parameters, in vitro biomarkers, and clinical response. Biomarkers analyzed before treatment (day 0) and on days 1, 3, and 9 after ZOL administration included plasma levels of IFN-γ, TNF-α, IL-6, and CRP; the proportion of $CD14^+$ monocytes among PBMCs; the frequency of $V\gamma9^+$ cells within the peripheral T-cell population; and the percentage of $CD27^+CD45RA^-$ T_{CM} cells and $CD69^+$ cells within the $V\gamma9^+$ T-cell population. In vitro parameters determined included concentrations of IFN-γ secreted into the culture supernatant and the percentage of $CD69^+$ Vγ9/Vδ2 T cells after overnight stimulation of pretreatment PBMCs with ZOL. APR scores were calculated as cumulative APR symptoms on days 1 and 3 after ZOL administration.

The in vitro responsiveness of pretreatment PBMCs to ZOL predicts the APR in patients receiving intravenous ZOL

Having established the crucial role of Vγ9/Vδ2 T cells, monocytes, and IFN-γ in the APR to ZOL, we finally tested whether the response of pretreatment PBMCs to ZOL in vitro could predict the APR in vivo. Activation markers determined included the expression of CD69 on Vγ9/Vδ2 T cells and levels of IFN-γ in the culture supernatants after overnight stimulation with ZOL. Statistical analyses demonstrated that the in vitro responsiveness of PBMCs before treatment indeed predicted the development of clinical symptoms and the levels of certain blood biomarkers. As such, CD69 expression on Vγ9/Vδ2 T cells after ZOL stimulation in vitro correlated with the IFN-γ concentrations in the culture supernatant of ZOL-stimulated PBMCs as well as with plasma levels of IFN-γ on day 1 in treated patients (Supplemental Fig. S2*C*). Moreover, the IFN-γ production by ZOL-stimulated PBMCs correlated with plasma levels of IL-6 and CRP on day 1 as well as with cumulative APR scores by day 3. These associations between in vitro and in vivo parameters remained significant in multiple regression analyses (Supplemental Fig. S2*D*) and are summarized in the proposed model depicted in Fig. 5. Taken together, our findings demonstrate that a simple screening test to help identify individuals at risk of severe side effects upon intravenous NBP treatment may be feasible.

Discussion

The present phase IV safety trial is the most comprehensive study so far on the cellular immune response after intravenous NBP administration and provides evidence that both Vγ9/Vδ2 T cells and monocytes are involved in mediating the APR in vivo. Moreover, our study identifies a key role for IFN-γ in the NBP-induced APR, which may be of diagnostic and prognostic value and have implications for patient management. Given the proven efficacy of NBPs to reduce the risk of fractures that are associated with high mortality, a simple test predicting the likelihood of a severe APR would allow the attending clinician to tailor medication to the individual and improve adherence to intravenous NBPs.

Our findings identify pretreatment frequencies of peripheral monocytes and Vγ9/Vδ2 T cells as well as the proportion of $CD27^+CD45RA^-$ T_{CM} cells within the Vγ9/Vδ2 T-cell population and their responsiveness to ZOL in vitro as important predictors of the extent of pro-inflammatory cytokine production 24 hours after treatment. Incidentally, the cut-off value of >3% Vγ9/Vδ2 T cells identified by us above which patients showed considerably elevated IFN-γ levels at day 1 is in remarkable agreement with the failure of Rossini and colleagues to observe an APR in ZOL-treated osteoporosis patients who had pretreatment frequencies below 3% γδ T cells.[24] These observations imply that the age and sex bias in peripheral Vγ9/Vδ2 T cells, which are higher in younger individuals and in women, is an important determinant of the APR incidence in different patient groups.[24,25]

Our study also shows that ZOL administration caused a significant (albeit transient) drop in peripheral Vγ9/Vδ2 T cells and a longer-lasting reduction in the percentage of T_{CM} cells among them. Earlier studies reported a similar drop in circulating Vγ9/Vδ2 T cells in osteoporosis patients after receiving a single dose of ZOL[18] and a loss of T_{CM} cells in cancer patients treated repeatedly with ZOL.[26–28] As the loss of T_{CM} cells occurring after a single administration of ZOL may last for at least a year,[29] the qualitative and quantitative long-term effects of NBPs on the Vγ9/Vδ2 T-cell compartment appear to be the underlying basis for the general absence of adverse events in patients receiving repeat treatments.[11,24] However, this correlation between the numbers of T_{CM} cells in the circulation, the plasma levels of IFN-γ reached shortly after ZOL treatment, and the occurrence of APR symptoms is seemingly at odds with the present paradigm in Vγ9/Vδ2 T-cell biology.[30] T_{CM} cells are generally perceived as cells with high proliferative capacity but only modest cytokine production, as opposed to T_{EM} and T_{EMRA} cells, which proliferate poorly but produce copious amounts of cytokines upon restimulation. Our findings suggest that, in fact, activated T_{CM} cells are the major source of the IFN-γ detected in the circulation after ZOL treatment, emphasizing the importance of in vivo studies in patients.

It is known from cell culture experiments that NBP-driven Vγ9/Vδ2 T-cell responses are sensitive to statins.[16] By inhibiting 3-hydroxy-3-methyl-glutaryl-CoA (HMG-CoA) reductase, the rate-limiting enzyme of the mevalonate pathway, statins lower the synthesis of all downstream isoprenoids including cholesterol, which is exploited in the clinic to prevent cardiovascular diseases. Through the same mechanism, statins also counteract

the NBP-induced intracellular accumulation of IPP, DMAPP, and ApppI, and thus inhibit the activation of Vγ9/Vδ2 T cells in vitro.[19] However, studies investigating the efficacy of statins in preventing the APR to intravenous NBPs have failed to demonstrate a clinical benefit,[11,18,22,31,32] most likely because the plasma concentrations required for effective inhibition of IPP/DMAPP/ApppI accumulation may not be reached pharmacologically. Our present findings suggest that interference with key players in the NBP-dependent γδ T cell-monocyte crosstalk such as IFN-γ might be an alternative therapeutic approach to manipulate the APR in patients at risk of severe reactions.

The present study has implications beyond the APR in osteoporosis patients. Recently, a transient drop in Vγ9/Vδ2 T-cell levels was interpreted as extravasation of activated cells into peripheral tissues,[18] evoking similar findings in primate studies upon intravenous treatment with Vγ9/Vδ2 T-cell agonists.[33,34] It is interesting to note that in primates activated Vγ9/Vδ2 T cells accumulate in the lung where they may confer some degree of protection against subsequent infection, which may be mirrored by reports showing that intravenous ZOL treatment has a largely unexplained beneficial effect in reducing pneumonia-related mortality.[35]

Our findings also have implications for current attempts to utilize NBP-based treatment regimes for targeted therapy of cancer patients. Large cohort studies have shown that ZOL has beneficial effects beyond improving bone health and may prolong disease-free and/or overall survival in patients with breast cancer[36] and multiple myeloma.[37] The underlying reason for these direct antitumor properties is not clear but may involve γδ T-cell–mediated effects. ZOL and other NBPs are, therefore, increasingly moving into the focus of novel immunotherapeutic approaches, especially in combination with low-dose IL-2 to boost the expansion and cytotoxicity of Vγ9/Vδ2 T cells.[27,28,38,39] Previous studies identified possible "responders" and "nonresponders" based on the proliferative capacity of a patient's Vγ9/Vδ2 T cells to NBP stimulation in vitro.[14,40,41] However, it remains to be investigated whether the severity of the APR or levels of early immune biomarkers such as those described here correlate with long-term clinical outcomes after administration of NBPs with or without IL-2.

Taken together, our data are consistent with a model in which intravenously administered ZOL is taken up by monocytes, which thereby acquire the ability to "present" isoprenoid metabolites or related structures to Vγ9/Vδ2 T cells.[17,19] Through mutual crosstalk, both monocytes and Vγ9/Vδ2 T cells undergo a series of activation and differentiation steps that ultimately determine the severity of the APR and replicate similar events taking place in acute infection.[2,4] Although the effects on circulating monocytes appear to be only transient (be it because of rapid inactivation, extravasation and/or replenishment from the bone marrow), the Vγ9/Vδ2 T-cell pool shows longer-term changes in that T_{CM} cells disappear and T_{EM} cells and T_{EMRA} cells become more prominent. Our findings imply that the gradual loss of T_{CM} cells and their inability to produce IFN-γ is a major determinant of the reduced risk of experiencing APR symptoms in patients repeatedly treated with NBPs. Future studies will reveal whether the immediate response to first-time NBPs determines clinical outcome in patients with and without malignancy and whether it has diagnostic and/or prognostic value for Vγ9/Vδ2 T-cell–based immunotherapy approaches.

Disclosures

All authors state that they have no conflicts of interest.

Acknowledgments

We are grateful to all patients for their participation in this study and to our nurses Roz Broadbent, Cheryl Culley, Jacqui Dickens, and Sue Day for their help. We thank Sarah James for CRP measurements; Ann Kift-Morgan for technical assistance; Antony Wilkes for statistical advice; and Martin Davey, Francesco Dieli, Keith Thompson, and Massimo Massaia for the stimulating discussion. This research was in part supported by the Cardiff CR-UK Centre Development Fund and CR-UK project grant C28524/A9497.

Authors' roles: Study design: AKS, JT, and ME. Study conduct and data collection: JLW and JT. Data analysis and interpretation: JLW, MPM, JT, and ME. Experimental methods: SMP. Study support and intellectual input: MDS and BM. Drafting manuscript: ME. Approving final version of manuscript: all authors. JT and ME take responsibility for the integrity of the data analysis.

References

1. Bonneville M, O'Brien RL, Born WK. γδ T cell effector functions: a blend of innate programming and acquired plasticity. Nat Rev Immunol. 2010;10:467–78.
2. Eberl M, Roberts GW, Meuter S, Williams JD, Topley N, Moser B. A rapid crosstalk of human γδ T cells and monocytes drives the acute inflammation in bacterial infections. PLoS Pathog. 2009;5:e1000308.
3. Davey MS, Lin CY, Roberts GW, Heuston S, Brown AC, Chess JA, Toleman MA, Gahan CG, Hill C, Parish T, Williams JD, Davies SJ, Johnson DW, Topley N, Moser B, Eberl M. Human neutrophil clearance of bacterial pathogens triggers anti-microbial γδ T cell responses in early infection. PLoS Pathog. 2011;7:e1002040.
4. Eberl M, Moser B. Monocytes and γδ T cells: close encounters in microbial infection. Trends Immunol. 2009;30:562–8.
5. Moser B, Eberl M. γδ T-APCs: a novel tool for immunotherapy?. Cell Mol Life Sci. 2011;68:2443–52.
6. Tanvetyanon T, Stiff PJ. Management of the adverse effects associated with intravenous bisphosphonates. Ann Oncol. 2006;17:897–07.
7. Cramer JA, Gold DT, Silverman SL, Lewiecki EM. A systematic review of persistence and compliance with bisphosphonates for osteoporosis. Osteoporosis Int. 2007;18:1023–31.
8. Thiébaud D, Sauty A, Burckhardt P, Leuenberger P, Sitzler L, Green JR, Kandra A, Zieschang J, Ibarra de Palacios P. An in vitro and in vivo study of cytokines in the acute-phase response associated with bisphosphonates. Calcif Tissue Int. 1997;61:386–92.
9. Buckler HM, Mercer SJ, Davison CE, Hollis S, Richardson PC, Anderson DG. Evaluation of adverse experiences related to pamidronate infusion in Paget's disease of bone. Ann Rheum Dis. 1998;57:572.
10. Dicuonzo G, Vincenzi B, Santini D, Avvisati G, Rocci L, Battistoni F, Gavasci M, Borzomati D, Coppola R, Tonini G. Fever after zoledronic acid administration is due to increase in TNF-α and IL-6. J Interferon Cytokine Res. 2003;23(11):649–54.

11. Reid IR, Gamble GD, Mesenbrink P, Lakatos P, Black DM. Characterization of and risk factors for the acute-phase response after zoledronic acid. J Clin Endocrinol Metab. 2010;95:4380–7.
12. Black DM, Delmas PD, Eastell R, Reid IR, Boonen S, Cauley JA, Cosman F, Lakatos P, Leung PC, Man Z, Mautalen C, Mesenbrink P, Hu H, Caminis J, Tong K, Rosario-Jansen T, Krasnow J, Hue TF, Sellmeyer D, Eriksen EF, Cummings SR. HORIZON Pivotal Fracture Trial. Once-yearly zoledronic acid for treatment of postmenopausal osteoporosis. N Engl J Med. 2007;356:1809–22.
13. Kunzmann V, Bauer E, Wilhelm M. γ/δ T-cell stimulation by pamidronate. N Engl J Med. 1999;340:737–8.
14. Kunzmann V, Bauer E, Feurle J, Weissinger F, Tony HP, Wilhelm M. Stimulation of γδ T cells by aminobisphosphonates and induction of antiplasma cell activity in multiple myeloma. Blood. 2000;96:384–92.
15. Gober HJ, Kistowska M, Angman L, Jenö P, Mori L, De Libero G. Human T cell receptor γδ cells recognize endogenous mevalonate metabolites in tumor cells. J Exp Med. 2003;197:163–8.
16. Hewitt RE, Lissina A, Green AE, Slay ES, Price DA, Sewell AK. The bisphosphonate acute phase response: rapid and copious production of proinflammatory cytokines by peripheral blood γδ T cells in response to aminobisphosphonates is inhibited by statins. Clin Exp Immunol. 2005;139:101–11.
17. Roelofs AJ, Jauhiainen M, Mönkkönen H, Rogers MJ, Mönkkönen J, Thompson K. Peripheral blood monocytes are responsible for γδ T cell activation induced by zoledronic acid through accumulation of IPP/DMAPP. Br J Haematol. 2009;144:245–50.
18. Thompson K, Keech F, McLernon DJ, Vinod K, May RJ, Simpson WG, Rogers MJ, Reid DM. Fluvastatin does not prevent the acute-phase response to intravenous zoledronic acid in post-menopausal women. Bone. 2011;49:140–5.
19. Riganti C, Massaia M, Davey MS, Eberl M. Human γδ T-cell responses in infection and immunotherapy: common mechanisms, common mediators?. Eur J Immunol. 2012;42:1668–76.
20. Kalyan S, Quabius ES, Wiltfang J, Mönig H, Kabelitz D. Can peripheral blood γδ T cells predict osteonecrosis of the jaw? An immunological perspective on the adverse drug-effects of aminobisphosphonate therapy. J Bone Miner Res. 2012 Sep 18. [Epub ahead of print].
21. Miyagawa F, Tanaka Y, Yamashita S, Minato N. Essential requirement of antigen presentation by monocyte lineage cells for the activation of primary human γδ T cells by aminobisphosphonate antigen. J Immunol. 2001;166:5508–14.
22. Silverman SL, Kriegman A, Goncalves J, Kianifard F, Carlson T, Leary E. Effect of acetaminophen and fluvastatin on post-dose symptoms following infusion of zoledronic acid. Osteoporos Int. 2011;22:2337–45.
23. Maniar A, Zhang X, Lin W, Gastman BR, Pauza CD, Strome SE, Chapoval AI. Human γδ T lymphocytes induce robust NK cell-mediated antitumor cytotoxicity through CD137 engagement. Blood. 2010;116:1726–33.
24. Rossini M, Adami S, Viapiana O, Ortolani R, Vella A, Fracassi E, Gatti D. Circulating γδ T cells and the risk of acute-phase response after zoledronic acid administration. J Bone Miner Res. 2012;27:227–30.
25. Caccamo N, Dieli F, Wesch D, Jomaa H, Eberl M. Sex-specific phenotypical and functional differences in peripheral human Vγ9/Vδ2 T cells. J Leukoc Biol. 2006;79:663–6.
26. Dieli F, Gebbia N, Poccia F, Caccamo N, Montesano C, Fulfaro F, Arcara C, Valerio MR, Meraviglia S, Di Sano C, Sireci G, Salerno A. Induction of γδ T-lymphocyte effector functions by bisphosphonate zoledronic acid in cancer patients in vivo. Blood. 2003;102:2310–1.
27. Dieli F, Vermijlen D, Fulfaro F, Caccamo N, Meraviglia S, Cicero G, Roberts A, Buccheri S, D'Asaro M, Gebbia N, Salerno A, Eberl M, Hayday AC. Targeting human γδ T cells with zoledronate and interleukin-2 for immunotherapy of hormone-refractory prostate cancer. Cancer Res. 2007;67:7450–7.
28. Meraviglia S, Eberl M, Vermijlen D, Todaro M, Buccheri S, Cicero G, La Mendola C, Guggino G, D'Asaro M, Orlando V, Scarpa F, Roberts A, Caccamo N, Stassi G, Dieli F, Hayday AC. In vivo manipulation of Vγ9Vδ2 T cells with zoledronate and low-dose interleukin-2 for immunotherapy of advanced breast cancer patients. Clin Exp Immunol. 2010;161:290–7.
29. Santini D, Martini F, Fratto ME, Galluzzo S, Vincenzi B, Agrati C, Turchi F, Piacentini P, Rocci L, Manavalan JS, Tonini G, Poccia F. In vivo effects of zoledronic acid on peripheral γδ T lymphocytes in early breast cancer patients. Cancer Immunol Immunother. 2009;58:31–8.
30. Dieli F, Poccia F, Lipp M, Todaro M, Buccheri S, Cicero G, La Mendola C, Guggino G, D'Asaro M, Orlando V, Scarpa F, Roberts A, Caccamo N, Stassi G, Dieli F, Hayday AC. Differentiation of effector/memory Vδ2 T cells and migratory routes in lymph nodes or inflammatory sites. J Exp Med. 2003;198:391–7.
31. Srivastava T, Haney CJ, Alon US. Atorvastatin may have no effect on acute phase reaction in children after intravenous bisphosphonate infusion. J Bone Miner Res. 2009;24:334–7.
32. Makras P, Anastasilakis AD, Polyzos SA, Bisbinas I, Sakellariou GT, Papapoulos SE. No effect of rosuvastatin in the zoledronate-induced acute-phase response. Calcif Tissue Int. 2011;88:402–8.
33. Sicard H, Ingoure S, Luciani B, Serraz C, Fournié JJ, Bonneville M, Tiollier J, Romagné F. In vivo immunomanipulation of Vγ9Vδ2 T cells with a synthetic phosphoantigen in a preclinical nonhuman primate model. J Immunol. 2005;175:5471–80.
34. Ali Z, Shao L, Halliday L, Reichenberg A, Hintz M, Jomaa H, Chen ZW. Prolonged (E)-4-hydroxy-3-methyl-but-2-enyl pyrophosphate-driven antimicrobial and cytotoxic responses of pulmonary and systemic Vγ2Vδ2 T cells in macaques. J Immunol. 2007;179:8287–96.
35. Colón-Emeric CS, Mesenbrink P, Lyles KW, Pieper CF, Boonen S, Delmas P, Eriksen EF, Magaziner J. Potential mediators of the mortality reduction with zoledronic acid after hip fracture. J Bone Miner Res. 2010;25:91–7.
36. Gnant M, Mlineritsch B, Stoeger H, Luschin-Ebengreuth G, Heck D, Menzel C, Jakesz R, Seifert M, Hubalek M, Pristauz G, Bauernhofer T, Eidtmann H, Eiermann W, Steger G, Kwasny W, Dubsky P, Hochreiner G, Forsthuber EP, Fesl C, Greil R. Austrian Breast and Colorectal Cancer Study Group, Vienna, Austria. Adjuvant endocrine therapy plus zoledronic acid in premenopausal women with early-stage breast cancer: 62-month follow-up from the ABCSG-12 randomised trial. Lancet Oncol. 2011;12:631–41.
37. Morgan GJ, Davies FE, Gregory WM, Cocks K, Bell SE, Szubert AJ, Navarro-Coy N, Drayson MT, Owen RG, Feyler S, Ashcroft AJ, Ross F, Byrne J, Roddie H, Rudin C, Cook G, Jackson GH, Child JA. National Cancer Research Institute Haematological Oncology Clinical Study Group. First-line treatment with zoledronic acid as compared with clodronic acid in multiple myeloma (MRC Myeloma IX): a randomised controlled trial. Lancet. 2010;376:1989–99.
38. Wilhelm M, Kunzmann V, Eckstein S, Reimer P, Weissinger F, Ruediger T, Tony HP. γδ T cells for immune therapy of patients with lymphoid malignancies. Blood. 2003;102:200–6.
39. Lang JM, Kaikobad MR, Wallace M, Staab MJ, Horvath DL, Wilding G, Liu G, Eickhoff JC, McNeel DG, Malkovsky M. Pilot trial of interleukin-2 and zoledronic acid to augment γδ T cells as treatment for patients with refractory renal cell carcinoma. Cancer Immunol Immunother. 2011;60:1447–60.
40. Mariani S, Muraro M, Pantaleoni F, Fiore F, Nuschak B, Peola S, Foglietta M, Palumbo A, Coscia M, Castella B, Bruno B, Bertieri R, Boano L, Boccadoro M, Massaia M. Effector γδ T cells and tumor cells as immune targets of zoledronic acid in multiple myeloma. Leukemia. 2005;19:664–70.
41. Coscia M, Vitale C, Peola S, Foglietta M, Rigoni M, Griggio V, Castella B, Angelini D, Chiaretti S, Riganti C, Guarini A, Drandi D, Ladetto M, Bosia A, Foà R, Battistini L, Boccadoro M, Fournié JJ, Massaia M. Dysfunctional Vγ9Vδ2 T cells are negative prognosticators and markers of dysregulated mevalonate pathway activity in chronic lymphocytic leukemia cells. Blood. 2012 Aug 29. [Epub ahead of print].

CRITICAL CARE

LETTER

Duration of antibiotic therapy in bacteraemia

Matt P Wise[1]*, Matt PG Morgan[2] and Anton G Saayman[1]

See related research by Havey *et al.*, http://ccforum.com/content/15/6/R267

Reducing duration of antibiotic therapy without a diminution in efficacy decreases cost, side effects, antibiotic related diarrhoea, and bacterial resistance. Havey and colleagues [1] reported the results of a systematic review and meta-analysis of antibiotic duration in bacteraemia and deduced short course therapy (<7 days) might be as effective as longer treatments. It is surprising given the obvious benefits and the frequency with which bacteraemia is documented in critically ill patients that there is such a paucity of randomised clinical trials (RCTs) comparing duration of therapy. Only one RCT, in neonates, had been performed in patients solely with bacteraemia. Accordingly, Havey and colleagues concluded that duration of antibiotic therapy in bacteraemia is poorly studied and would benefit from a large RCT.

Daneman and colleagues [2] performed a survey of Canadian infectious disease and critical care specialists to gauge the optimal duration of therapy in bacteraemic critically ill patients. Considerable variability existed amongst clinicians and undoubtedly reflects the lack of robust data to guide best practice. However, length of treatment is only one aspect of optimising outcomes from antibiotic use. Future RCTs need to take into account whether adequate source control has been achieved, as this will bias duration of therapy. Moreover, it is clear that since many antibiotics deployed in critical care demonstrate time-dependent killing, inadequate doses are frequently used, which increases treatment failure and the emergence of resistance [3,4]. Pharmacokinetic optimisation that ensures adequate time above minimum inhibitory concentration should therefore be an integral component of any trial that compares duration of antibiotic therapy [5].

Abbreviations
RCT, randomised clinical trial.

Competing interests
The authors declare that they have no competing interests.

Author details
[1]Adult Critical Care, University Hospital of Wales, Cardiff, CF14 4XW, UK.
[2]Department of Anaesthesia, University Hospital of Wales, Cardiff, CF14 4XW, UK.

Published: 9 January 2012

References

1. Havey TC, Fowler R, Daneman N: **Duration of antibiotic therapy for bacteremia: a systematic review and meta-analysis.** *Crit Care* 2011, **15:**R267.
2. Daneman N, Shore K, Pinto R, Fowler R: **Antibiotic treatment duration for bloodstream infections in critically ill patients: a national survey of Canadian infectious diseases and critical care specialists.** *Int J Antimicrob Agents* 2011, **38:**480-485.
3. Taccone FS, Laterre PF, Dugernier T, Spapen H, Delattre I, Wittebole X, De Backer D, Layeux B, Wallemacq P, Vincent JL, Jacobs F: **Insufficient β-lactam concentrations in the early phase of severe sepsis and septic shock.** *Crit Care* 2010, **14:**R126.
4. Seyler L, Cotton F, Taccone FS, De Backer D, Macours P, Vincent JL, Jacobs F: **Recommended β-lactam regimens are inadequate in septic patients treated with continuous renal replacement therapy.** *Crit Care* 2011, **15:**R137.
5. Roberts JA: **Using PK/PD to optimize antibiotic dosing for critically ill patients.** *Curr Pharm Biotechnol* 2011 [Epub ahead of print].

doi:10.1186/cc10590
Cite this article as: Wise MP, *et al.*: Duration of antibiotic therapy in bacteraemia. *Critical Care* 2012, **16:**403.

*Correspondence: mattwise@doctors.org.uk
[1]Adult Critical Care, University Hospital of Wales, Cardiff, CF14 4XW, UK
Full list of author information is available at the end of the article